



Provided by the author(s) and University of Galway in accordance with publisher policies. Please cite the published version when available.

Title	In vitro, pre-clinical and commercial evaluation of a novel xeno- and serum-free culture system for production of human bone marrow derived mesenchymal stem cells for bone regeneration
Author(s)	Gaynard, Sean
Publication Date	2016-10-21
Item record	<a href="http://hdl.handle.net/10379/6090">http://hdl.handle.net/10379/6090</a>

Downloaded 2024-05-14T05:27:16Z

Some rights reserved. For more information, please see the item record link above.



***In vitro*, Pre-Clinical & Commercial Evaluation of  
a Novel Xeno- & Serum-free Culture System for  
Production of Human Bone Marrow Derived  
Mesenchymal Stem Cells for  
Bone Regeneration**



*A thesis submitted to the National University of Ireland as  
fulfilment of the requirement for the degree of*

***Doctor of Philosophy***

***By***

***Seán Gaynard***

Regenerative Medicine Institute (REMEDI),  
College of Medicine, Nursing & Health Sciences,  
National University of Ireland, Galway

**Thesis Supervisor:**

**Dr. Mary Murphy**

Thesis Co-Supervisors:

Prof. Frank Barry & Dr. Jessica Hayes

Date of Submission: 05<sup>th</sup> September 2016



## Table of Contents

<i>Declaration</i> .....	ix
<i>Abstract</i> .....	x
<i>List of Tables</i> .....	xii
<i>List of Figures</i> .....	xiii
<i>Abbreviations</i> .....	xviii
<i>Acknowledgements</i> .....	xxiii
Chapter 1 .....	1
Introduction .....	1
1.1 Regenerative Medicine .....	2
1.2 Stem cells .....	2
1.2.1 Embryonic Stem Cells .....	3
1.2.2 Induced Pluripotent Stem cells .....	3
1.2.3 Mesenchymal stem cells .....	4
1.2.3.1 Therapeutic Potential of MSCs .....	8
1.2.3.2 Identifying the MSC .....	9
1.2.3.3 Markers for the Identification of MSCs .....	10
1.3 Foetal Bovine Serum .....	12
1.3.1 The Beginning of the Story .....	12
1.3.2 Peak Serum – A looming global shortage .....	14
1.3.3 Insufficient Regulation of FBS Industry .....	14
1.3.4 Concerns over safety .....	15
1.3.5 FBS Replacement .....	18
1.4 Alternatives to FBS .....	18
1.4.1 Human Platelet Lysate .....	18
1.4.2 Development of Serum-free Media .....	20
1.5 PurSTEM – A Novel Medium for the Culture of MSCs .....	22
1.6 Aims and Objectives .....	25
Hypothesis: .....	25
Aims: .....	25
Chapter 2 .....	29
2.0 Materials & Methods .....	30

2.1 Isolation of Serum-Free (SF)/ Serum-Containing (SC) MSCs from Human Bone Marrow .....	30
2.1.1 Isolation of Serum-Free MSCs from Bone Marrow with Commercially Available Serum-free Media .....	31
2.2 Coating of Tissue Culture Plastic with Fibronectin .....	32
2.2.1 Coating of Tissue Culture Plastic for Use with Commercial Serum-Free Media .....	32
2.3 Colony Forming Unit-fibroblast (CFU-f) Assay .....	32
2.3.1 CFU-f assays for Commercial media .....	33
2.4 Sub-culturing of MSCs.....	33
2.4.1 Subculture of Mesencult-cultured MSCs.....	34
2.5 Cumulative Population Doublings .....	34
2.6 Seeding, Maintaining & Subculturing MSCs in GE Xuri™ Adherent Cell Expansion System Macrocarriers .....	35
2.7 Osteogenic Differentiation .....	36
2.7.1 Alizarin Red S Staining.....	36
2.7.2 Quantitative Calcium Assay .....	37
2.7.3 <i>In situ</i> osteogenesis on Xuri bioreactor waffles.....	37
2.8 Adipogenic Differentiation.....	37
2.8.1 Oil Red O staining.....	38
2.8.2 Extraction/Quantification of Oil Red O staining .....	38
2.8.3 <i>In situ</i> adipogenesis on Xuri bioreactor waffle .....	38
2.9 Chondrogenic Differentiation .....	39
2.9.1 Dimethylmethylene Blue (DMMB) Analysis .....	39
2.9.2 PicoGreen Assay.....	40
2.9.3 Safranin O Staining.....	40
2.9.4 <i>In situ</i> chondrogenesis on Xuri waffle and Safranin O staining .....	41
2.10 Safranin O staining of Xuri™ ‘Waffles’ .....	42
2.11 Surface Marker Expression Analysis .....	42
2.12 Immunogenicity/Immunosuppression Assays.....	43
2.12.1 Preparation of MSCs .....	44
2.12.2 Isolation and Preparation of Peripheral Blood Mononuclear Cells .....	44
2.12.3 Preparation of T-cell stimulant .....	45

2.12.4 CD4 Staining and Flow Cytometry Preparation .....	45
2.13 <i>In vitro</i> Assessment of Angiogenesis by Matrigel assay .....	45
2.14 Preparation of Cell Implants for Ectopic Analysis of Bone Forming Ability of MSCs in Mice.....	46
2.14.1 Assessment of Viability and Loading Efficiency of MSCs in MBCP/Tyseel Constructs .....	47
2.14.2 Preparation of Cell Implants for Orthotopic Analysis of Bone Forming Ability of MSCs in Rats .....	47
2.14.3 Subcutaneous implantation of constructs.....	48
2.15 Fixation and Decalcification of Cell Implants from Mouse Ectopic Bone Formation Assay.....	49
2.16 Fixation and Decalcification and Histological Preparation of Cell Implants from Rat Femur CSD Model .....	49
2.17 Histological Preparation of Transplants.....	49
2.18 Mallory’s Trichrome Stain & Scoring .....	50
2.19 Preparation of Immunosuppression cocktail of FK506 and SEW2871 .....	50
2.20 Generation of Rat Critical Size Defect (CSD) Model .....	51
2.21 Micro-Computed Tomography ( $\mu$ CT) Imaging of Bone Formation.....	54
2.21.1 $\mu$ CT of Mouse Constructs.....	54
2.21.2 $\mu$ CT Rat Femur CSD .....	54
2.22 Photoacoustic Imaging of Blood Vessel Infiltration of Rat Femur CSD .....	54
2.23 Blood Vessel Staining using Ulex Europaeus Agglutinin (UEA-1).....	56
2.24 Movat’s Pentachrome staining.....	57
2.25 statistical analysis.....	58
Chapter 3.....	59
3.1 Introduction .....	60
3.2 Methods .....	65
3.3 Results.....	69
3.3.1 Serum-free medium isolates CFU-fs with distinct size and shape similar to serum-containing isolated CFU-fs.....	69
3.3.2 Growth kinetics of SF and SC cells isolated and cultured in hypoxia and normoxia .....	71
3.3.3 Serum-free isolated cells have morphology distinct from serum-containing isolated cells.....	73

3.3.4 Normoxia cultured cells have increased osteogenic potential compared to hypoxia cultured cells.....	74
3.3.5 Adipogenic potential of MSCs is reduced by hypoxia and is unaffected by use of SF or SC media .....	76
3.3.6 Chondrogenic potential of SF cultured cells is increased in hypoxia .....	78
3.3.7 Flow cytometry evaluation of bone marrow-derived MSCs.....	80
3.3.8 Increased expression of CD271 and CD146 on serum-free MSCs .....	81
3.3.9 Serum-free MSCs display increased pro-angiogenic potential.....	83
3.3.10 Flow cytometry gating strategies to assess the immunosuppressive & immunogenic potential of MSCS .....	86
3.3.11 Immunosuppressive effect of MSCs is unaffected by use of serum-free medium .....	88
3.3.12 Immunogenicity of MSCs cultured in SF and SC media .....	89
3.4 Discussion.....	92
Chapter 4.....	100
4.1 Introduction .....	101
4.2 Methods.....	107
4.3 Results.....	110
4.3.1 Cells were retained in MBCP <sup>+</sup> following encapsulation and remained metabolically active .....	110
4.3.2 MSCs retained metabolic activity following encapsulation.....	111
4.3.3 Implanted constructs were successfully retrieved at 8 weeks.....	112
4.3.4 Micro-computed ( $\mu$ CT) tomography of retrieved constructs 8-weeks post implantation.....	114
4.3.5 Representative images of Mallory’s modified Trichrome stain defining various observed tissues.....	117
4.3.6 Bone and cartilage tissue observed in all implanted groups.....	119
4.4 Discussion.....	122
Chapter 5.....	129
5.1 Introduction .....	130
5.2 Methods.....	132
5.3 Results.....	134
5.3.1 Histological staining control using Movat’s Pentachrome stain of goat knee .....	137

5.3.3 Histological analysis of bone repair superior regeneration of defect by SC MSCs.....	138
5.3.4 Optimisation of <i>in vivo</i> visualisation of angiogenesis by photoacoustic imaging (PA) .....	147
5.3.5 Oxygen saturation levels of CSD does not change over time .....	150
5.3.6 Haemoglobin saturation levels of CSD do not statistically change over time .....	152
5.3.7 Histological analysis of neovascularisation indicate low levels of vascularisation in all groups .....	154
5.4 Discussion.....	156
Chapter 6.....	161
6.1 Introduction .....	162
6.2 Methods .....	166
6.3 Results .....	168
6.3.1 Assessment of various commercial serum-free media for ability to isolate MSCs from bone marrow with and without the support of 2% serum .....	168
6.3.2 Serum-free and commercial media isolate equivalent CFU-fs in hypoxia and normoxia .....	169
6.3.3 Growth kinetics MSCs in SF and commercial media cells isolated and cultured in hypoxia and normoxia .....	171
6.3.4 Morphology of MSCs is unaffected by use of commercial media in either hypoxia or normoxia .....	173
6.3.5 Commercial media isolated MSCs have superior osteogenic potential compared to SF cultured MSCs .....	174
6.3.6 Adipogenic potential of MSCs is increased in cells cultured in commercial media and inhibited by hypoxia.....	176
6.3.7 Chondrogenic potential of SF cultured cells is increased in hypoxia.....	177
6.3.8 Assessment of MSCs Surface marker expression .....	180
6.3.9 Serum-free MSCs display increased pro-angiogenic potential.....	181
6.3.10 Immunosuppressive effect of MSCs is unaffected by use of commercial media .....	184
6.3.11 Immunogenicity of MSCs cultured in SF and commercial media .....	186
6.4 Discussion.....	188
Chapter 7.....	193

7.1 Introduction .....	194
7.2 Methods.....	196
7.3 Results.....	198
7.3.1 Growth kinetics of SF and SC MSCs cultured in a 3D Bioreactor with Xuri microcarriers (“Waffles”).....	198
7.3.2 Morphology of MSCs is altered when cultured on Xuri Waffles .....	201
7.3.3 Culture of MSCs in Xuri bioreactor increases their osteogenic potential ..	202
7.3.4 Culture of MSCs on bioreactor increases adipogenic potential of MSCs ...	206
7.3.5 Chondrogenic potential of MSCs cultured on the Xuri bioreactor .....	210
7.3.6 Surface marker phenotype of SF and SC MSCS is unaffected by culture in the Xuri bioreactor.....	214
7.3.7 Production of pro-angiogenic factors by MSCs is unaffected by culture in the Xuri bioreactor.....	215
7.4 Discussion.....	218
Chapter 8.....	221
Discussion.....	221
Appendix I .....	229
Publications and Achievements.....	229
Appendix II .....	233
Permissions .....	233
Appendix III .....	239
Bibliography .....	239
Links .....	240
References .....	240

# ***Declaration***

I declare that all the work in this thesis was performed personally with the assistance of other stated individuals where appropriate. No part of this work has been submitted for consideration as part of any other degree or award

# ***Abstract***

The therapeutic potential of mesenchymal stem cells (MSCs) is recognised in treating a wide range of debilitating diseases. For clinical-scale manufacturing, serum-free and xenogenic-free media formulations have been proposed as alternatives to the use of foetal bovine serum (FBS), an undefined product with significant safety concerns. Previously, the orthobiologics laboratory had developed a novel xeno- and serum-free media formulation for the isolation of bone marrow-derived MSCs. The overall goal of this project was to identify the optimal cell culture conditions for both the isolation and expansion of bone marrow derived mesenchymal stem cells for orthopaedic use. This included assessing the effect of varying the oxygen tension during culture and the use of the novel xeno- and serum-free (SF) medium. Specifically, this was determined by assessing the efficacy of SF medium-isolated and cultured bone marrow-derived MSCs for their ability to contribute to bone repair in pre-clinical orthotopic models of bone regeneration namely a mouse ectopic model of bone formation and a rat femoral critical size bone defect model. These cells were compared to conventional FBS-isolated cells to determine if the novel SF medium was a suitable alternative for the manufacture of MSCs. Subsequently, evaluation of the SF medium in comparison to commercially available serum-free media was performed and the medium's functionality in a 3D macrocarrier bioreactor system for the manufacture of MSCs was also performed. The specific aims of this PhD were as follows;

*In vitro* characterisation of xeno and serum-free MSCs (MSC-SF) and serum-cultured MSCs (MSC-SC) in hypoxia (2% O<sub>2</sub>) and normoxia (21% O<sub>2</sub>) were assessed in chapter 3. SF MSCs isolated and cultured in hypoxia underwent increased proliferation in comparison to their SC counterparts while maintaining their tri-lineage differentiation potential. In addition, hypoxia-cultured SF MSCs demonstrated an increased chondrogenic potential in comparison to normoxia-cultured SF MSCs which had an increased osteogenic phenotype. These data indicated differences in the phenotype of the cells that may alter the efficacy of these cells to repair bone.

In chapter 4, SF and SC MSCs cultured in either hypoxia or normoxia were implanted subcutaneously on an osteoconductive biomaterial in CD1-nude mice for 8 weeks and bone formation was assessed. No difference was observed between the various treatment groups. In addition, no difference in level of bone tissue was observed between treatment groups and vehicle control which received a cell-free material. This data indicated that bone formed was due to recruitment of endogenous cells to the implants.

To assess the ability of SF MSCs to repair bone in a clinically relevant model of bone repair, MSCs were implanted into a rat femoral critical size bone defect model for 8 weeks and their bone repair ability was assessed *in vivo* and *ex vivo* (Chapter 5). Micro-computed tomography ( $\mu$ CT) analysis of bone regeneration was assessed at 4 and 8 weeks. Subsequently, histological analysis of bone repair was also assessed. These data indicated superior bone repair in groups which received SC MSCs cultured in normoxia with minimal repair in groups which received SF MSCs.

Consequently to this, *in vitro* comparison of the SF media with commercially available media was performed (Chapter 6). Here, equivalent growth kinetics were observed in all media formulations. Increased differentiation potential was observed in commercial media groups, specifically Xuri produced by GE Healthcare and Mesencult produced by Stemcell Therapeutics. Superior production of pro-angiogenic factors were observed in SF medium groups. SF and Xuri media met the international society for cell therapy (ISCT) guidelines for surface marker profile of MSCs while Mesencult-MSCs maintained expression of HLA-DR.

The ultimate success of the SF media will depend on its ability to function in scalable processes for large scale production of cell therapies. In chapter 7, the function of the SF medium in a 3D spinner-flask bioreactor system was assessed and demonstrated that SF MSCs maintained their growth kinetics in addition to maintaining their tri-lineage differentiation potential when cultured in the bioreactor system.

Together, these data suggest that the SF medium is a suitable alternative to the large scale production of bone marrow-derived MSCs for cell based therapies.

# ***List of Tables***

<b>Table</b>	<b>Description</b>	<b>Page</b>
1	Potential limitations associated with the use of FBS in cell product preparation.	13
2	Presence /Absence of viruses of concern to Recipients of FBS-based products from the 30 global FBS supplying countries.	17
2.1	Bone marrow donor details	30
2.11	Antibody details for MSC surface marker expression	42
6.1.1	Various commercially available serum-free, xeno-free media.	162

# *List of Figures*

<b>Figure</b>	<b>Description</b>	<b>Page</b>
1	Caplan's proposed hypothesis of mesengenic process from mesenchymal stem cells to terminally differentiated tissue	6
2	Known paracrine factors produced by cultured MSCs	9
3	Platelet granule cargo. Platelet lysate contains a variety of factors released from platelets including chemokines, adhesion molecules, growth factor and immunological factors	20
4	Hierarchical importance of serum-free medium components for the specific chemically defined medium.	22
5	Distribution of markers expressed on MSCs under previously described culture conditions.	23
2.14.2	Preparation of MSC-MBCP <sup>+</sup> constructs for In vivo implantation into rat femur	46
2.3	Surgical procedure for generation of rat femoral critical size defect model	51
2.22	Experimental setup for PA imaging of rat defect.	54
3.2.1	Schematic representation of the approach taken for the in vitro characterisation of bone marrow-derived mesenchymal stem cells isolated in serum-containing (SC) or serum-free (SF) culture medium.	64
3.3.1	CFU-fs isolated using serum-free medium are equivalent to serum-containing medium.	67

3.3.2	Growth kinetics of serum-free (SF) and serum-containing (SC) isolated cells in normoxia (21% O <sub>2</sub> ) compared to hypoxia (2% O <sub>2</sub> ).	68
3.3.3	Morphology of MSCs was altered by culture of MSCs in SF and SC medium.	69
3.3.4	Osteogenic potential of cells was enhanced in normoxia cultured cells and was maintained in all conditions.	70
3.3.5	Adipogenic potential of cells was enhanced in normoxia cultured cells and was maintained in all conditions.	72
3.3.6	Chondrogenic potential of SF cells was enhanced in hypoxia cultured cells and was maintained in all conditions.	74
3.3.7	Gating strategy for flow cytometry analysis of surface marker expression of bone marrow-derived MSCs.	76
3.3.8	Surface marker characterisation of bone marrow-derived MSCs.	78
3.3.9	Angiogenic potential of human umbilical vein epithelial cells (HUVEC) cells cultured in the presence of MSC conditioned medium.	80
3.3.10	Gating strategy for flow cytometry analysis of T-lymphocyte expression.	82
3.3.11	Immunosuppressive effect of MSCs on CD28/CD3 antibody stimulated peripheral blood T-lymphocytes.	84
3.3.12	Immunogenic potential of MSCs on unstimulated peripheral blood T-lymphocytes.	86
4.2.1	Schematic representation of experimental design to assess the effect of hypoxic/normoxic priming on bone marrow-derived MSCs isolated in serum-containing and serum-free media.	104

4.3.1	Efficient loading of MSCs onto MBCP+/Tyseel scaffolds prior to implantation.	103
4.3.2	Cells remain metabolically viable following encapsulation.	104
4.3.3	Implanted constructs were clearly visible 8 weeks following implantation.	105
4.3.4	Micro-computed tomography ( $\mu$ CT) analysis of bone formation in implants 8 weeks following transplantation.	108
4.3.5	Representative images of Mallory's Trichrome stain.	110
4.3.6	Histological analysis of bone, cartilage and bone marrow present in implanted constructs.	113
4.4	Proposed Mechanism of MSC migration to injured tissue in comparison to leukocyte migration to inflammation.	119
5.2.1	Schematic representation of the experimental design used to assess the in vivo ability of SF and SC MSCs to repair bone in a rat femoral critical size bone defect model.	125
5.3.1	Serum-containing MSCs cultured in normoxia are superior at in vivo bone formation.	128
5.3.2	Representative staining control for Movat's Pentachrome using healthy goat knee. Bone is indicated by yellow, cartilage by green and bone marrow by purple.	129
5.3.2a	Representative histological analysis of bone, cartilage and bone marrow present in implanted constructs.	132
5.3.3b	Representative "Empty defect" group staining.	133
5.3.3c	Representative "Empty scaffold" group staining.	134
5.3.3d	Representative "Serum-free normoxia" group staining.	135

5.3.3e	Representative “Serum-free hypoxia” group staining.	136
5.3.3f	Representative “Serum-containing normoxia” group staining.	137
5.3.3g	Representative “Serum-containing hypoxia” group staining.	138
5.3.4	Optimisation of PA imaging of neovascularisation.	141
5.3.5	Assessment of sO <sub>2</sub> levels of CSD over time.	144
5.3.6	Assessment of HbT levels of the CSD region over time.	146
5.3.7	Lectin staining detects the presence of blood vessels in groups that received normoxia-cultured MSCs.	148
6.2.1	Schematic representation of the approach taken for the in vitro characterisation of bone marrow-derived mesenchymal stem cells isolated in serum-free (SF), Xuri and Mesencult (MC) culture media.	158
6.3.2	CFU-f size and number are affected by the culture medium.	161
6.3.3	Growth kinetics of serum-free (SF), Xuri (X) and Mesencult (MC) isolated cells in normoxia (21% O <sub>2</sub> ) compared to hypoxia (2% O <sub>2</sub> ).	162
6.3.4	Morphology of MSCs was altered by culture of MSCs in SF, Xuri and MC medium irrespective of oxygen levels.	163
6.3.5	Commercial media isolated MSCs demonstrate increased osteogenic potential in hypoxia and normoxia.	165
6.3.6	Adipogenic potential of cells was enhanced in normoxia cultured cells and was maintained in all conditions.	167
6.3.7	Chondrogenic potential of SF cells was enhanced in hypoxia cultured cells and was maintained in all conditions.	169
6.3.8	Surface marker characterisation of bone marrow derived MSCs	171

isolated in SF and commercially available media.

6.3.9	Angiogenic potential of human umbilical vein epithelial cells (HUVEC) cells cultured in the presence of MSC conditioned medium.	174
6.3.10	Immunosuppressive effect of MSCs on CD28/CD3 stimulated peripheral blood T-lymphocytes.	175
6.3.11	Immunogenic potential of MSCs on unstimulated peripheral blood T-lymphocytes.	177
7.2.1	Schematic representation of the approach taken to assess the ability of serum-free (SF) and serum-containing (SC) MSCs to proliferate and differentiate in the Xuri scalable bioreactor.	187
7.3.1	Growth kinetics of serum-free (SF) and serum-containing (SC) cultured in Xuri bioreactor and in 2D culture	189
7.3.2	Morphology of MSCs on Waffles is more rounded indicating stress	190
7.3.3	Osteogenic potential of SF and SC MSCs cultured on 2D TC plastic and the 3D bioreactor system.	194
7.3.4	Adipogenic potential of SF and SC MSCs was enhanced when differentiated on bioreactor waffles	198
7.3.5	Chondrogenic potential of SF and SC MSCs was unaltered by culture or differentiation the on bioreactor waffles	202
7.3.6	Surface marker characterisation of bone marrow-derived MSCs.	203
7.3.7	Angiogenic potential of human umbilical vein epithelial cells (HUVEC) cells cultured in the presence of MSC conditioned medium from SF and SC MSCs cultured on 2D TC plastic and in 3D Xuri bioreactor.	205

# ***Abbreviations***

°C	Degrees Celsius
μCT	Micro-computed tomography
μg	Micrograms
μL	Micro litres
μm	Micron
2D	2 Dimensional
3D	3 Dimensional
AT	Adipose tissue
BAV	Bovine adenovirus
BM	Bone marrow
BMP-2	Bone morphogenic protein 2
BPV	Bovine paravirus
BRSV	Bovine respiratory syncytial virus
BSA	Bovine serum albumin
BT	Blue tongue
BV	Bone volume
BVD	Bovine viral diarrhoea
Ca <sup>++</sup>	Calcium ion
CCM	Complete chondrogenic medium
CFD	Compliment factor D
CFSE	Carboxyfluorescein succinimidyl ester
CFU-f	Colony forming unit-fibroblastic
cm	Centimetre
CO <sub>2</sub>	Carbon dioxide
Col	Collagen
ColII	Collagen type 2
ColX	Collagen type 10
CSD	Critical size defect

CTI	Cell therapy industry
DAPI	4'-Diamidino-2-phenylindole
ddH <sub>2</sub> O	Distilled, deionised water
dH <sub>2</sub> O	Distilled water
DMEM	Dulbecco's modified Eagle's medium
DMEM-HG	Dulbecco's Modified Eagle Medium, high glucose
DMEM-LG	Dulbecco's Modified Eagle Medium, low glucose
DMMB	1,9-dimethylmethylene blue
DMSO	Dimethyl sulfoxide
DNA	Deoxyribonucleic acid
DPX	Distyrene plasticizer/xylene
dsDNA	Double stranded DNA
EC	European commission
EDTA	Ethylenediamine tetraacetic acid
EGF	Epidermal growth factor
ES	Embryonic stem cell
ETOH	Ethanol
EU	European union
FACS	Fluorescence-activated cell sorting
FBS	Foetal bovine serum
FDA	Food and Drug administration
FGF	Fibroblast growth factor
FMD	Foot and Mouth disease
g	Grams
g	Relative centripetal force
GMP	Good manufacturing practice
hrs	Hours
HA	Hydroxyapatite
HCl	Hydrochloric acid
HEPES	4-(2-hydroxyethyl)-1-piperazineethanesulfonic acid
HIF	Hypoxia inducible factor

HIG2	Hypoxia inducible gene 2
HLA-DR	Human Leukocyte Antigen – Antigen D related
HPL	Human platelet lysate
HSA	Human serum albumin
HSCs	Haematopoietic stem cells
HUVEC	Human umbilical cord vein epithelial cells
IBR	Infectious bovine rhinotracheitis
ICM	Incomplete chondrogenic medium
IGF	Insulin-like growth factor
IgG	Immunoglobulin G
IPSC	Induced pluripotent stem cell
ISCT	International Society for Cell Therapy
ITS	Insulin, Transferrin, Selenium
KLF4	Kruppel-like factor 4
kVp	Peak kilo Voltage
L	Litres
LIF	Leukaemia inhibitory factor
LNGFR	Low affinity nerve growth factor receptor
LPL	Lipoprotein lipase
M	Molar
MCAM	Melanoma cell adhesion molecule
MEF	Mouse embryonic fibroblast
mg	Milligrams
Mg <sup>++</sup>	Magnesium ion
min	Minutes
mL	Millilitres
mm	Millimetre
mM	Millimolar
MNCs	Mononuclear cells
MSC	Mesenchymal stem cell
NaCl	Sodium chloride

NaOH	Sodium hydroxide
ng	Nanograms
NG2	Neuronal glial antigen 2
NGF	Nerve growth factor
nm	Nanometre
OC	Osteocalcin
OCT4	Octomer-binding transcription factor 4
P/S	Penicillin/Streptomycin
PA	Photoacoustic
PBS	Phosphate buffered saline
PDGFR $\beta$	Platelet derived growth factor receptor – beta
PE	Phycoerythrin
PI3	Parainfluenza 3
REO3	Reovirus
RM	Regenerative Medicine
rpm	Rotations per minute
RPMI	Roswell park memorial Institute
RT	Room temperature
Runx2	Runt-related transcription factor 2
SC	Serum-containing
SCID	Severe combined immunodeficiency
SD	Standard deviation
SDF-1	Stromal cell derived factor 1
SEM	Standard error of the Mean
SF	Serum-free
SOX2	Sex determining region-Y-box2
TCP	Tricalcium phosphate
TE	Tris-EDTA
TGF- $\beta$	Transforming growth factor beta
TRITC	Tetramethylrhodamine
TV	Tissue volume

TWIST	TWIST related protein
U	Units
UC	Umbilical cord
US	Ultrasound
USDA	United States Department of Agriculture
v/v	Volume/volume
VCAM-1	Vascular cell adhesion protein 1
w/v	Weight/volume
αMEM	Alpha modified Minimum essential medium Eagle

# ***Acknowledgements***

Firstly, I would like to sincerely thank Dr. Mary Murphy for all her help and guidance over the years. There are no words that would sufficiently describe how appreciative I am for everything you have done for me. The time and dedication you give to your students is second to none. It was truly a privilege to study under you and I look forward to continuing to work with you in the future.

I would also like to thank Frank Barry for all his help and direction throughout the project and as we continue into Autostem.

I'd like to thank the entire Orthobiologics group, both past and present. In particular I would like to acknowledge the assistance of Ms. Yvonne Dooley, Mr. Patrizio Mancuso, Ms. Swarna Raman, Ms. Claire Dooley and of course Ms. Tatiana Doroshenkova. It was never boring working with you all! I would like to especially acknowledge Ms. Georgina Shaw for all her help and training over the years. You were a constant pillar of support throughout my time at REMEDI and I am extremely grateful! Thank you also to Dr. Siobhan Gaughan for the literally countless things you do around the lab that keeps us from killing ourselves every day!

Thank you to Dr. Cathal O'Flatharta, Mr. Dave Connelly and Dr. Haroon Zafar for your assistance with the *in vivo* imaging study. Thank you to all in REMEDI, past and present, for everything over the years. There are just too many to mention! Although I do have to acknowledge Ms. Serika Naicker, my writing buddy, who has made the last hurdle of actually writing the PhD a lot easier to endure.

I would also like to thank my GRC committee members, Prof. Matthew Griffin, Dr. Faisal Sharif and Dr. Linda Howard for your help and direction along the way. I'd like to especially acknowledge all the time and support Dr. Howard provided throughout my time at REMEDI.

Thank you to all the friends I have made throughout my Master's and PhD for all the great memories made... although some of them may be a bit blurry! Thank you to all of the amazing housemates I've had over the years in Snipe Lawn, especially to my current housemates for putting up with me for the last few months. Smurf, Becky, Deirdre and Yvonne (Again!) you absolute legends!

Finally I'd like to thank my family. Thank you to my sister Aisling and my brothers Martin and Richie (wedding pending) for everything over the years. I couldn't have asked for a better family who I'm sure have had to struggle through my absence in their lives lately.

Finally, to my parents for encouraging me throughout my life and studies! I swear there isn't as much money in "them stem cells" as you seem to think but I'll try and look after you anyway! I dedicate this to you!

# **Chapter 1**

## **Introduction**

### **1.1 Regenerative Medicine**

Regenerative medicine (RM) is a rapidly developing field tasked with the repair, replacement and regeneration of cells, organs and tissues (Bajada et al., 2008). Although the term has been around for a long time, RM is still very much in its infancy in terms of how far research has progressed into mainstream clinical use. Although some of this may be due to issues in terms of our understanding of the biology of stem cells, the interactions with biomaterials and their mechanism of action, another major hurdle for the transition of regenerative medicine from the bench to the bedside is a poorly defined translational route consisting of a number of practical hurdles that must be overcome. These include a lack of large-scale, economically-viable cell therapy manufacturing processes. Currently, the majority of cell culture is done in 2D monolayer and is extremely labour intensive. In addition, the current dependence on foetal bovine serum (FBS) is a major hurdle to the translation of cell therapies with fluctuating costs and issues with availability (Brindley et al., 2012). To address this need, a major effort has been made by those in the industry to progress past 2D culture into larger 3D, ultimately scalable, bioreactor systems for the production of cells for therapies. Additionally, increasing our understanding of cell biology to replace conventionally used foetal bovine serum for the production of stem cell products towards more chemically defined, large scale systems of manufacturing is also essential to realise the clinical potential of stem cell therapy. Finally, standardisation of the cells used needs to be achieved. Ideally this would be by the identification of novel cell specific markers.

### **1.2 Stem cells**

Towards the end of the 19<sup>th</sup> century the concept of stem cells as a mechanism by which organs and tissues of the body could repair itself was first proposed (Bianco et al., 2008). Unlike other cells in the body, stem cells possess the unique ability to differentiate into specialised cells when stimulated to do so by their environment such as injury to a tissue (Wan et al., 2012, Rennert et al., 2012). Otherwise these cells remain in a quiescent stem cell state. Stem cells can also be recruited to other tissues to contribute to the repair of that tissue (Sasaki et al., 2008, Chen et al.,

2010, Kitaori et al., 2009a). They can also produce factors which direct other cells for the repair of tissues. Based on this ability, the therapeutic application of stem cells is enormous and has been explored in great detail (Aziz et al., 2007, Picinich et al., 2007). Of all the stem cell types within the body, there are three types which have been given particular attention. These are embryonic stem cells (ES), adult mesenchymal stem or stromal cells (MSCs) and induced pluripotent stem cells (iPS). All of these cells have a number of advantages and limitations but have been considered as either a direct therapeutic tool, as is the case with many adult stem cells such as MSCs, or as a means of disease modelling which is more typically the case with iPS cells. These stem cells are also being investigated with clinical applications in mind.

### **1.2.1 Embryonic Stem Cells**

ES cells were first identified in murine models over 30 years ago after they were isolated from developing blastocysts and successfully grown in culture (Evans and Kaufman, 1981). Although these cells are short lived *in vivo*, they can be propagated in an undifferentiated state indefinitely when cultured in the presence of leukaemia inhibitory factor (LIF) on a feeder layer of murine embryonic fibroblasts (MEF) for example (Williams et al., 1988, Smith et al., 1988). ES cells have the potential to differentiate into the three embryonic germ layers; endoderm, mesoderm and ectoderm and thus can ultimately give rise to every tissue of the embryo. Therapeutically, ES cells have been given much attention due to their pluripotency (Martin, 1981). However, ethical issues with obtaining these cells have greatly hampered their use with many countries making the use of these cells for research illegal (Robertson, 2001). Even in countries where the use of these cells is legal, generation of ES cells purely for research is often restricted and thus supply becomes an issue, often relying solely on discarded material from *in vitro* fertilisation (IVF) treatment.

### **1.2.2 Induced Pluripotent Stem cells**

Despite the issues limiting ES cell research, understanding the basic biology of these cells and advancements in technologies resulted in the generation of induced pluripotent stem (iPS) cells. These are embryonic like cells derived from adult

somatic cells and were first generated by Shinya Yamanaka's group in Kyoto, Japan and would result in him being awarded the Nobel prize for this work (Takahashi and Yamanaka, 2006). iPS cells are generated by introducing four transcription factors; octamer-binding transcription factor 4 (OCT4), sex determining region-Y-Box2 (SOX2), Kruppel-like factor 4 (KLF4) and c-MYC. Over-expression of these four factors in mouse embryonic fibroblasts resulted in generation of colonies of cells, morphologically similar to that of ES cells (Takahashi and Yamanaka, 2006). Initially, 24 factors were tested and by a process of elimination, these four factors were shown to be sufficient for the process. These cells share similar characteristics to ES cells in their self-renewal capacity, morphology, surface marker phenotype and gene expression. Additionally, iPS cells have been shown to be capable to differentiate into tissues of all three germ layers; the mesoderm, endoderm and ectoderm in both *in vitro* assays as well as the *in vivo* formation of teratomas (Abad et al., 2013). These cells are now being used largely for research purposes, specifically the development of *in vitro* models of disease and drug discovery with particular focus given to diseases where isolation of the primary cells is not possible due to the anatomical location e.g. neural cells (Cai et al., 2014).

### **1.2.3 Mesenchymal stem cells**

Bone marrow was first reported to contain two distinct populations of stem cells (Ford et al., 1956). The first population was haematopoietic stem cells (HSCs) which give rise to the various blood cell types of both lymphoid and myeloid lineages (Muller-Sieburg et al., 2002). The second population were MSCs which were originally investigated for their role in the maintenance of the haematopoietic stem cell niche. More recently, they were suggested to act as a source of cells that could contribute to tissue repair of a number of secondary tissues (Prockop, 1998). Since then, vast arrays of studies have, and continue to, investigate their basic biology, therapeutic potential and possible mechanism of action for a variety of disease types. MSCs were first described by Friedenstien *et al* as plastic adherent cells capable of differentiation towards the osteogenic lineage (Friedenstein et al., 1976, Friedens.Aj et al., 1966). Subsequently, the ability of MSCs to differentiate towards the chondrogenic lineage was shown, identifying a role of the cells in cartilage as

well as endochondral bone formation (Johnstone et al., 1998, Mackay et al., 1998). Similarly, the osteogenic differentiation of MSCs facilitates direct bone formation via intramembranous ossification. This ability to form bone via multiple lineages has led to extensive research into these cells for orthopaedic tissue engineering applications as well as many other areas. Theoretically these cells can differentiate down each of the mesenchymal lineages as proposed by Arnold Caplan (Figure 1)(da Silva Meirelles et al., 2008). Since their discovery in bone marrow, MSCs have been identified in virtually every tissue within the body including adipose tissue (De Ugarte et al., 2003), synovium (De Bari et al., 2001b, Djouad et al., 2005), skeletal muscle (Bujan et al., 2006), umbilical cord (Bieback et al., 2004) and placenta (Prather et al., 2009).

Interestingly, the location of MSCs within each tissue seems to affect their physiological function and differentiation capabilities. Nowhere is this more evident than within bone and bone marrow where MSCs occupy two distinct stem cell niches.

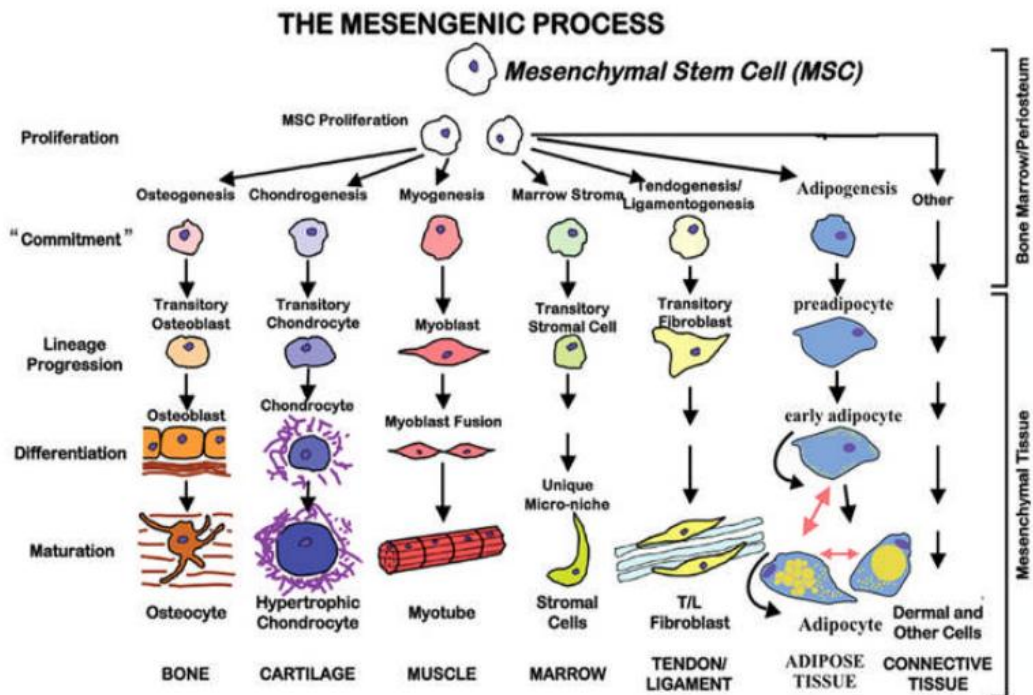


Figure 1: Caplan's proposed hypothesis of mesengenic process from mesenchymal

***stem cells to terminally differentiated tissue*** (Reprinted with permission from (Caplan, 1990), see appendix II)

The perivascular niche where MSC precursors known as pericytes exist in association with blood vessels (Shi and Gronthos, 2003) and the endosteal or bone lining niche where MSCs are found on the surface of bone (Mitsiadis et al., 2007, Sacchetti et al., 2007b, da Silva Meirelles et al., 2008). MSC progeny such as osteoblasts and fibroblasts are found at the endosteal niche (da Silva Meirelles et al., 2008). Additionally, lining the surface of bone is a thin layer of connective tissue known as the periosteum which has also been identified as a source of MSCs (Nakahara et al., 1991, Yoshimura et al., 2007, Chang and Knothe Tate, 2012). It is unclear which endogenous cell population contributes towards tissue repair post-fracture with no literature to date definitively identifying the fraction of MSCs responsible for bone repair. A comprehensive review on post-natal fracture healing by Gerstenfeld *et al.* highlighted this issue (Gerstenfeld and Einhorn, 2003). During fracture healing, bone repair is initiated in distinct crescent-shaped cartilaginous centres. Two centres develop symmetrically to the fracture line with intramembranous bone formation occurring concurrently at separate centres proximally and distally. These two distinct bone healing responses initiated upon injury may be induced by different cells located in the surrounding tissue. The bone marrow itself, and the surrounding periosteum and soft tissue may all be sources of these reparative cells (Gerstenfeld and Einhorn, 2003). The periosteum is believed to be the primary source of stem cells required to form the callus (Murao et al., 2013), with removal of the periosteum resulting in incomplete fracture callus formation (Gerstenfeld and Einhorn, 2003). The periosteum has also been proposed as a novel source of progenitor cells capable of contributing to bone regeneration (Chang and Knothe Tate, 2012). In a direct comparison, periosteal-derived rat MSCs produced 100-fold more colonies than bone marrow-derived MSCs and had higher proliferative and tri-lineage differentiation potential [20]. Periosteal cells also maintained *in vitro* chondrogenic differentiation potential after prolonged culture (De Bari et al., 2001a). Human studies on the periosteum as a source of stem cells

have also identified this tissue as being superior to other sites based on *in vitro* differentiation and proliferation potential (Sakaguchi et al., 2005). Skeletal muscle is also being explored as a potential source of osteoprogenitors that contribute to bone formation. Ectopic bone formation can occur within muscle (Bosch et al., 2000) and a subpopulation of muscle progenitor cells, identified by expression of alkaline phosphatase (ALP) after exposure to BMP-2, was observed in lacunae of newly formed bone matrix when injected into the hind limb of severe combined immunodeficiency (SCID) mice. These cells co-localised with osteocalcin (OC)-producing cells indicating potential differentiation to osteoblasts and osteocytes (Bosch et al., 2000).

However, identification of a definitive cell source for endochondral ossification in fracture callus has not been described. Notwithstanding, a number of MSC populations within the bone marrow which may contribute to bone repair have been identified based on expression of surface markers. Sacchetti *et al* identified a population of osteoprogenitors based on CD146, melanoma cell adhesion molecule (MCAM) expression (Sacchetti et al., 2007b). These cells were deemed to be *bona fide* stem cells after subcutaneous transplantation into nude mice resulted in formation of bone and induced the haematopoietic stem cell niche (Sacchetti et al., 2007b). Prior to this, CD271, also known as low affinity nerve growth factor receptor (LNGFR) was shown to select for the entire fibroblastic colony-forming unit (CFU-f) population, or MSC fraction, within bone marrow (Jones et al., 2002). CD271-positive cells were subsequently shown to reside in the intramedullary cavity of long bones (Cox et al., 2012). Combining both CD146 and CD271 expression resulted in the identification of the two distinct MSC niches described above, the endosteal niche and the perivascular niche with CD271+ CD146+ cells residing in the perivascular niche and CD271+ CD146- residing in the endosteal niche (Tormin et al., 2011a). The presence of MSCs at a bone lining niche and their osteogenic potential suggests a role for these cells in maintaining bone homeostasis.

### **1.2.3.1 Therapeutic Potential of MSCs**

MSCs have been deemed to have a high therapeutic potential since they were first discovered. To date, both autologous and allogeneic MSCs from a variety of sources have been delivered to a multitude of tissues or also systemically due to their ability to home to sites of injury (Barry and Murphy, 2013, Pers et al., 2016, Zhao et al., 2010, Wagner et al., 2005, Dai et al., 2005, Bang et al., 2005, Tang et al., 2004). Original studies were based on their reported potential to be able to differentiate into cell types along the mesenchymal lineage i.e. the ability to differentiate into chondrocytes, adipocytes and osteocytes. Since then, a far wider therapeutic potential of these cells has been identified since the discovery of paracrine factors produced by these cells having effects on immune cells (Singer and Caplan, 2011, Beggs et al., 2006, Devine et al., 2001, Aggarwal and Pittenger, 2005). A number of key mechanisms of action of MSCs can be clearly identified. They include direct differentiation or support of differentiation of local stem/progenitor cells, chemoattraction, immunomodulation, angiogenesis, anti-apoptosis and anti-scarring (Figure 2) (Singer and Caplan, 2011). Indeed, the ability of MSCs to modulate the immune system has been given particular focus with several studies reporting the ability of MSCs to modulate T-cell activation and proliferation (Beyth et al., 2005, Duffy et al., 2011, Griffin et al., 2010, Keyser et al., 2007, Le Blanc and Ringden, 2005, Le Blanc et al., 2003, Uccelli et al., 2006). Based on this ability of MSCs to suppress T-cells, the use of MSCs in inflammatory diseases such as graft-versus-host disease and organ transplantation are being explored (Ely et al., 2008).

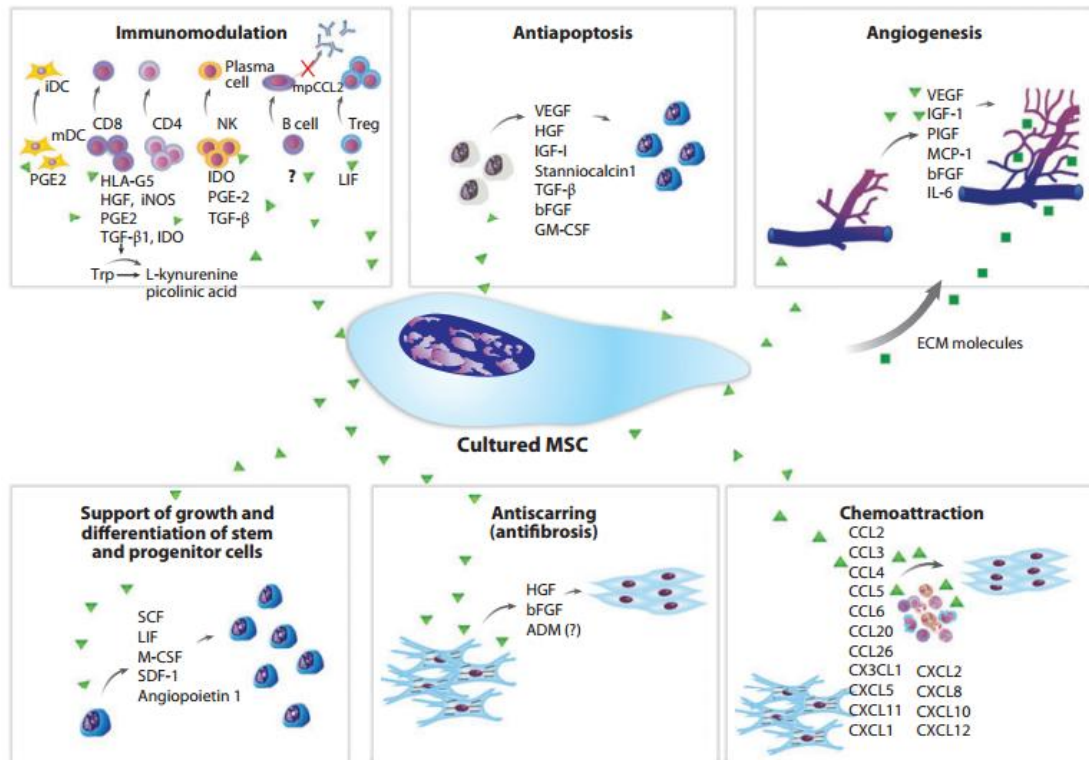


**Figure 2: Known paracrine factors produced by cultured MSCs** (Reprinted with permission from (Singer and Caplan, 2011), see appendix II)

### 1.2.3.2 Identifying the MSC

A large variation between MSC preparations remains one of the largest issues with the translation of these cells into the clinic. Factors that contribute to this include alterations in isolation and expansion methods which include the use of various media, culturing cells at various oxygen tensions and huge variation in criteria used by different groups to define an MSC. Overcoming the problems associated with each of these issues is incredibly challenging. However, as MSCs progress ever closer to clinical use, increased efforts have been taken to unify what MSCs are and how we use them. In 2006, the International Society for Cell Therapy (ISCT) published a definition of MSCs which they described as the minimal criteria a cell must pass to be deemed a MSC (Dominici et al., 2006a). The first criterion was the ability for the cells to adhere to uncoated tissue culture plastic under standard culture conditions i.e. medium containing 10% FBS. Secondly, the cells must express CD105, CD73, and CD90 while also not expressing CD45, CD34, CD14 (or CD11b), CD19 (or CD79 $\alpha$ ) and HLA-DR. Finally, MSCs must be capable of tri-lineage differentiation, namely being able to differentiate into osteoblasts, chondrocytes

and adipocytes. These criteria were based on characteristics of the cells during *in vitro* culturing and thus may not be a true representative of the cell phenotype *in vivo*. However, many studies have reported high levels of heterogeneity in cells that have met this ISCT standard (Phinney, 2012, Tormin et al., 2009). This heterogeneity appears to be indicative of MSCs with even single-cell derived colonies resulting in three morphologically distinct populations of cells (Colter et al., 2001, Prockop et al., 2001). The first cell type visible is a small rapidly dividing cell, an elongated spindle-like fibroblastic cells and a larger, slower replicating flattened cell. The smaller sized cell displays greater tri-lineage potential and proliferation. This population also had increased migratory and engraftment potential. Prolonged culturing of the cells resulted in a loss of this population (Lee et al., 2006, Prockop et al., 2001, Colter et al., 2001). Another factor which may contribute to the heterogeneity of MSCs could be due to variations in isolation processes which have been shown to affect the differentiation potential of these cells (Lane et al., 2014, Jiang et al., 2002, Kuroda et al., 2010). This heterogeneity within batches of MSCs may lead to discrepancies between studies and thus result in false reporting of efficacy or lack thereof of the cells themselves (Phinney, 2012). Two key ways to overcome this heterogeneity which is impeding the progression of MSC therapies would be the identification of a cell specific marker universally accepted for the selection of MSCs. The second would be the standardisation of the *in vitro* culture conditions of these cells which includes standardisation of the isolation process, culture medium used and physical and chemical factors such as oxygen tension, and type of culture vessel used. Although this would not entirely remove the donor variation typically observed currently.

### **1.2.3.3 Markers for the Identification of MSCs**

As outlined previously, due to the lack of markers specific to MSCs, the identification and selection of these cells is difficult and leads to inconsistencies. A number of antigens have been found on the surface of MSCs; unfortunately, none of them are specific to MSCs (Lv et al., 2014, Rostovskaya and Anastassiadis, 2012). CD271 was originally reported by Jones *et al* (Jones et al., 2002) as a marker capable of selecting the entire CFU-f fraction of bone marrow-derived MSCs. CD271

is present on other bone marrow cells such as HSC but since these cells are non-plastic adherent, they result in only minimal contamination of isolated MSC populations (Iso et al., 2012, Cuthbert et al., 2012). CD271+ MSCs also have an increased osteogenic and chondrogenic differentiation capacity compared to plastic adherent MSCs (Cuthbert et al., 2015, Churchman et al., 2012, Mifune et al., 2013). They have also shown improved therapeutic efficacy in a rat chondral repair model (Mifune et al., 2013) and a mouse cardiac infarct model (Noort et al., 2012). CD146 has also previously been identified as a marker for the selection of MSCs (Shi and Gronthos, 2003). CD146+ MSCs are considered to be pericytes due to being located around capillaries and sinusoids in many tissues such as bone marrow, adipose tissue, muscle and placenta (Crisan et al., 2008). CD146+ cells are capable of tri-lineage differentiation and also co-express neuronal glial antigen 2 (NG2) and platelet derived growth factor beta (PDGFR $\beta$ ) further supporting their perivascular origin (Crisan et al., 2008, Sacchetti et al., 2007b). Therapeutically in a model of inflammatory arthritis, CD146+ MSCs offered greater cartilage protection and increased immunosuppression compared to CD146- cells indicating a potential role of these cells in the treatment of immune-mediated diseases (Wu et al., 2016). Stro-1 was one of the first markers to identify MSCs in bone marrow (Ning et al., 2011, Simmons and Torok-Storb, 1991). Stro-1 identifies a population of MSCs with a high CFU-f efficiency and is expressed on 11.2% of unfractionated mononuclear cells and 6% of cultured MSCs (Psaltis et al., 2010, Bensidhoum et al., 2004). These cells are deemed therapeutically appealing due to their enhanced trafficking and engraftment ability. Stro-1+ cells showed greater trafficking ability to the bone marrow, kidneys, liver, muscles and spleen compared to Stro-1- cells with a reduction in the number of cells trapped in the lungs (Bensidhoum et al., 2004). Other markers being tested for the enrichment of a MSC population are CD106 (Vascular cell adhesion protein 1, VCAM-1) which is expressed highly in bone marrow and placenta and at lower levels in umbilical cord and adipose tissue (Yang et al., 2013b, Arufe et al., 2010, Alon et al., 1995, Schaffler and Buchler, 2007). CD106 has been reported to enrich for cells with increased multipotent potential (Mo et al., 2016). CD106 in combination with CD271 select a bone marrow MSC with faster proliferation, tri-lineage differentiation and migratory potential

compared to the CD271+CD106- population (Mabuchi et al., 2013). In addition CD106+ MSCs have an increased immunoregulatory phenotype which has been associated with the higher expression of COX-2 suggesting a role for immune diseases (Yang et al., 2013b). There are many other MSC markers which have also been identified which all select for MSCs with a specific phenotype above that set out by the ISCT (Mo et al., 2016). Although, the pursuit of a definitive marker for the identification is key to the standardisation of batches of MSCs, some of the inherent heterogeneity in MSCs may be due to the heterogeneity in the components used to culture the cells, for example foetal bovine serum. For this reason, to truly define MSCs the combination of both a defined population with a defined culture system is essential.

### **1.3 Foetal Bovine Serum**

#### **1.3.1 The Beginning of the Story**

In 1955, Henry Eagle first showed that the substitution of medium with animal sera could be used to improve cell proliferation (Eagle, 1955). Over 60 years later, the use of animal serum, namely foetal bovine serum (FBS), is still considered the gold standard for cell culture of most mammalian cells. However, there is increasing pressure on those involved in the translation of cell therapy into the clinic to move away from the use of animal products for a number of reasons. These include ethical concerns related to the process of FBS production, health and safety concerns for recipients who receive products manufactured using FBS and an ever increasing global shortage which threatens to bring the cell therapy industry (CTI) to a grinding halt (Table 1). There are also practical limitations with the use of FBS including the requirement to perform a serum screen to determine the most suitable serum for use with specific cell types due to the batch-to-batch variation between serum lots (van der Valk et al., 2004, Jayme and Smith, 2000).

	<b>Disadvantages/Limitations</b>	<b>Reference</b>
<b>1</b>	High and increasing cost of FBS due to global shortage of supply and increased demand	(van der Valk et al., 2004, Brindley et al., 2012)
<b>2</b>	Undefined composition with lot-to-lot variation	(Jayme and Smith, 2000)
<b>3</b>	High contamination risk i.e. bacteria, viruses and mycoplasma	(Levings and Wessman, 1991)
<b>4</b>	Need for serum screening – some lots incapable of MSC isolation, proliferation and differentiation	(van der Valk et al., 2004)
<b>5</b>	FBS internalisation by MSCs and risk of disease transmission	(Dimarakis and Levicar, 2006)
<b>6</b>	Ability of non-MSC cells to attach and proliferate due to presence of FBS at isolation stage	(Tekkatte et al., 2011, Shahdadfar et al., 2005)
<b>7</b>	FBS cultured cells undergo senescence with progressive loss of differentiation capacity	(Bieback et al., 2012)
<b>8</b>	Bovine protein attachment to cells triggers xenogenic immune response affecting the viability efficacy and safety of transplanted MSCs	(Heiskanen et al., 2007)
<b>9</b>	Requirement for adventitious agent testing of raw material and final product	(Erickson et al., 1991)

***Table 1: Potential limitations associated with the use of FBS in cell product preparation.***

### **1.3.2 Peak Serum – A looming global shortage**

The driving force for FBS production is not demand for FBS but rather is dependent on the state of the cattle industry (Brindley et al., 2012). The majority of FBS used for research purposes is not primarily derived from dedicated manufacturers of FBS but rather as a by-product of the beef industry and so inherent instability in the supply of FBS is an issue which ultimately leads to fluctuations in the cost of FBS, a major barrier to the ultimate translation of cell therapies manufactured using this component into the clinic. FBS may be considered a renewable resource in that it can be constantly produced. However despite this, a constant low level of serum has been produced for the last number of years. It is estimated that 600,000L of serum are produced annually, a number which we can consider 'Peak Serum', the maximal level of serum produced based per year (Festen, 2007, Brindley et al., 2012) based on limiting factors such as cattle being used for other purposes such as beef manufacturing. An estimated mere one third of that volume is produced at a grade suitable for GMP manufacture and thus for use in cell therapies. Currently all GMP-grade FBS is produced in either Australia or New Zealand as these countries have not been exposed to bovine spongiform encephalopathy (BSE) like most of Europe and America. There are currently 30 major countries in the world (Table 2) that produce FBS and there is a global misconception that Australia and New Zealand produce FBS with a reduced viral load and thus are safer for clinical use than these countries, which will be discussed later (Hawkes, 2015). In fact, sera originating in Australia have on average one of the higher viral loads compared to some European countries which have been excluded from distributing sera since the BSE outbreak (Table 2). These safety concerns will be discussed in greater detail later.

### **1.3.3 Insufficient Regulation of FBS Industry**

For the vast majority of its existence, the FBS industry has been largely unregulated and this has led to a number of abuses by companies which have potentially devastating consequences for the cell therapy industry (CTI). In 1994, an estimated 30,000L of FBS from New Zealand were sold globally (Hodgson, 1995). This was despite the fact that only 15,000L of FBS were produced there in this same time

period. To this day, the identity of the components used to supplement the FBS supply has never been disclosed. This is an inexcusable breach of industry ethics which has been mirrored more recently in 2011 when GE healthcare acquired PAA laboratories. After an internal audit, GE issued an Urgent Field Safety Notice (GEHC Ref #90200) indicating that batches of FBS sold between 2003 and 2011 may have been supplemented with bovine serum albumin (BSA), water or cell growth promoting additives. This diluting or modifying of the FBS product which was being sold as clinical grade FBS exposed countless people around the world to a variety of unknown effects and highlights the utter lack of effective regulation of this industry considering two major breaches of industry standards occurred in two separate companies within the same decade.

### **1.3.4 Concerns over safety**

Currently, only FBS supplied from either Australia or New Zealand is allowed for use in clinical production for cell therapies. This is due to misconceptions over the safety status of these countries and those deemed to produce FBS of a lower quality (Siegel W, 2013). Not every country is permitted to export FBS due to the presence of certain diseases in the cattle population and as a consequence restrictions are imposed on these countries due to the viral content (Table 2) (Hawkes, 2015). Viruses of concern are those which are known to be capable of passing the placental barrier and infecting the calf. Current exporting rules are in place due to the presence of various viruses in the supplying country's cattle stock and a perceived concern of the potential effect of these viruses by the receiving countries. Considering that the two largest markets for FBS are Europe and the United States of America (USA), the standards set out by both the US department of Agriculture (USDA) and the European commission (EC) have become the standards for the global FBS industry (Hawkes, 2015). The EU (EMEA-CPMP-BWP-1793-02) and the USDA (USDA 9 CFR 113.46-53) regulations require that FBS from all sources/countries be tested for eight viruses of adventitious concern (Hawkes, 2015). All samples must be either heat-treated or gamma-irradiated to insure absence of these viruses in imported FBS batches. The eight viruses are; rabies, bovine viral diarrhoea (BVD), parainfluenza 3 (PI3), infectious bovine rhinotracheitis

## Chapter One

(IBR), reovirus (REO3), bovine paravirus (BPV), bovine adenovirus (BAV) and bovine respiratory syncytial virus (BRSV). Although these viruses are assumed to be present in essentially every region, Scandinavian countries have made progress in recent years eliminating their presence (Figure 4)(Hawkes, 2015). Also of concern are viruses of importation concern. These are viruses not globally distributed. There have been six such infectious agents identified by the USDA (Veterinary Services Notice 1998) and EU (Regulation EC No. 294-2013): the human form of BSE, Foot and Mouth disease (FMD), Vesicular Stomatitis, Blue Tongue (BT), Akabane, Aino and Schmallenberg (Hawkes, 2015). These are all insect vectored diseases except for BSE. In all 30 countries are currently listed as being free of FMD, with some eradicating the virus more recently (Table 2). Of the remaining viruses on this list, Scandinavian countries are deemed free of all except Schmallenberg virus but are still not granted permission to produce GMP grade FBS. Conversely Australia, one of the two only global suppliers of GMP-grade FBS is positive for BT, Akabane and Aino virus raising concerns over its eligibility as a supplier of GMP grade FBS. This could put major pressure on New Zealand to meet global demand and may further increase the cost of FBS for clinical use. Even if permission were to be granted to Scandinavian countries to produce GMP grade FBS, it is unclear whether their production rates could replace that lost by exclusion of Australia as a producer. This of course, makes the state of the GMP supply for clinical use even more unpredictable and could be crippling for translation of cell therapies into the clinic.

	Adventitious Viruses of Concern								Total adventitious viruses	Imported Viruses of Concern						Total Imported viruses of Concern	Total viruses of FBS Concern
	Para influenza 3	Reovirus 3	Bovine adenoviruses	Bovine parvoviruses	Bovine respiratory syncytial virus	Bovine viral diarrhea (BVD)	Infectious bovine rhinotracheitis (IBR)	Rabies		Foot and mouth disease (FMD)	Vesicular stomatitis (VS)	Bluetongue (BT)	Akabane	Aino virus	Schmallenberg virus		
Finland	+	+	+	+	+	2010	1994	2007	5	1959	-	-	-	-	+	1	6
Norway	+	+	+	+	+	2005	1992	2011	5	1952	-	2010	-	-	+	1	6
Sweden	+	+	+	+	+	2011	1995	1886	5	1966	-	2009	-	-	+	1	6
Denmark	+	+	+	+	+	+	2005	2002	6	1983	-	2009	-	-	+	1	7
New Zealand	+	+	+	+	+	+	+	-	7	-	-	-	-	-	-	0	7
Belgium	+	+	+	+	+	+	+	2008	7	1976	-	2008	-	-	+	1	8
Chile	+	+	+	+	+	+	+	+	8	1987	-	-	-	-	-	0	8
Germany	+	+	+	+	+	+	+	2005	7	1988	-	2009	-	-	+	1	8
Ireland	+	+	+	+	+	+	+	1903	7	2001	-	-	-	-	+	1	8
Uruguay	+	+	+	+	+	+	+	+	8	2001	-	-	-	-	-	0	8
Argentina	+	+	+	+	+	+	+	+	8	2006	1986	+	-	-	-	1	9
Canada	+	+	+	+	+	+	+	+	8	1952	1949	+	-	-	-	1	9
Colombia	+	+	+	+	+	+	+	+	8	2009	+	2007	-	-	-	1	9
Dominican Republic	+	+	+	+	+	+	+	+	8	-	-	+	-	-	-	1	9
El Salvador	+	+	+	+	+	+	+	+	8	-	+	1997	-	-	-	1	9
Guatemala	+	+	+	+	+	+	+	+	8	-	+	1998	-	-	-	1	9
Honduras	+	+	+	+	+	+	+	+	8	-	+	2004	-	-	-	1	9
Holland	+	+	+	+	+	+	+	+	8	2001	-	2009	-	-	+	1	9
Mexico	+	+	+	+	+	+	+	+	8	1954	+	2010	-	-	-	1	9
Nicaragua	+	+	+	+	+	+	+	+	8	-	+	2009	-	-	-	1	9
Panama	+	+	+	+	+	+	+	+	7	-	+	+	-	-	-	2	9
Paraguay	+	+	+	+	+	2007	+	+	8	2012	-	-	-	-	-	1	9
Peru	+	+	+	+	+	+	+	+	8	2004	+	2004	-	-	-	1	9
Poland	+	+	+	+	+	+	+	+	8	1971	-	-	-	-	+	1	9
Australia	+	+	+	+	+	+	+	1867	7	1871	-	+	+	+	-	3	10
Brazil	+	+	+	+	+	+	+	+	8	2006	+	+	-	-	-	2	10
Costa Rica	+	+	+	+	+	+	+	+	8	-	+	+	-	-	-	2	10
France	+	+	+	+	+	+	+	+	8	2001	-	+	-	-	+	2	10
Spain	+	+	+	+	+	+	+	+	8	1986	-	+	-	-	+	2	10
United States	+	+	+	+	+	+	+	+	8	1929	+	+	-	-	-	2	10

**Table 2:**

**Presence /Absence of viruses of concern to Recipients of FBS-based products from the 30 global FBS supplying countries. (+) indicates the continued detection of virus in FBS preparations. (-) indicates the absence of detection of virus in the designated country. (Year) indicates the last year the virus was detected within each country (Modified from open access source (Hawkes, 2015)).**

### **1.3.5 FBS Replacement**

For many years, there has been much effort focused on replacing the use of FBS with alternatives that wouldn't pose such a potential health risk to patients and would be more suitable for large scale production and thus ultimately far cheaper than relying on the expensive, unstable and volatile supply of FBS. These included replacing FBS with alternatives such as human platelet lysate, human autologous serum and the development of chemically defined serum-free and xeno-free media capable of supporting the isolation and long term propagation of stem cells, specifically MSCs. Despite this, making the transition away from FBS appears to be very slow with over 80% of MSC clinical trials submitted to the FDA describing the use of FBS in their manufacturing process (Mendicino et al., 2014). Although there is a global perception that efforts are being made to move away from the use of FBS, such a change is not being observed at a clinical level or in fact even at a research level where the majority of papers describing MSC work still utilise FBS for their cultures. This slow progression towards FBS alternatives may be due to some pressing practical reasons including excessive costs of alternatives such as platelet lysate in addition to concerns specific to the alternatives.

## **1.4 Alternatives to FBS**

### **1.4.1 Human Platelet Lysate**

Human platelet-derived products have emerged as the most heavily investigated alternative to the use of FBS. Human platelet lysate (HPL) has been previously shown to promote growth of MSCs as well as other cells types (Gruber et al., 2004). This is due to the presence of a whole cohort of growth factors (Figure 3) contained within platelets which contain essential growth factors such as FGF, attachment factors such as fibronectin and many more factors including chemokines. Platelet releasate is one such platelet derived product that contains all the factors released by platelets upon activation by calcium and thrombin (Kilian et al., 2004, Gruber et al., 2004). HPL, however, contains all the factors contained within platelets than can be obtained upon mechanical destruction of the cell itself. Where platelet releasate requires chemical activation of cells, HPL is easier to produce as it only requires

## Chapter One

mechanical lysis of the cells (Bieback, 2013). There are a number of advantages to the use of platelet lysate compared to FBS. These include a lack of ethical concerns associated with the harvesting of HPL as it can be donated by willing volunteers negating any animal rights issues. As a result of it being a human product, there is no possibility of xenogenic transmission of viruses or prions (Walenda et al., 2012). HPL has also been used in clinical trials without adverse effects being reported (Kuznetsov et al., 2000). HPL was first reported in 2005 for the expansion of MSCs (Doucet et al., 2005). Since then a number of papers have reported data indicating HPL is equivalent or even superior to the use of FBS in terms of proliferation, differentiation and genetic stability (Chen et al., 2012a, Doucet et al., 2005, Abdelrazik et al., 2011, Crespo-Diaz et al., 2011). The key limitation of HPL is the batch-to batch variability associated with batches as they come from different pools of donors (Burnouf et al., 2016). This pooling of HPL donors also increases the risk of transmission of unknown viruses. With each additional donor used to generate a pool, the risk of transmission of untested viruses increases. This lack of definition of the constituents of HPL is similar to that observed in FBS. Although HPL is a welcome step forward from FBS, this variation in batches may continue to contribute to the heterogeneity observed in MSCs. With that in mind, progress should be made to work towards a chemically defined cell culture medium.

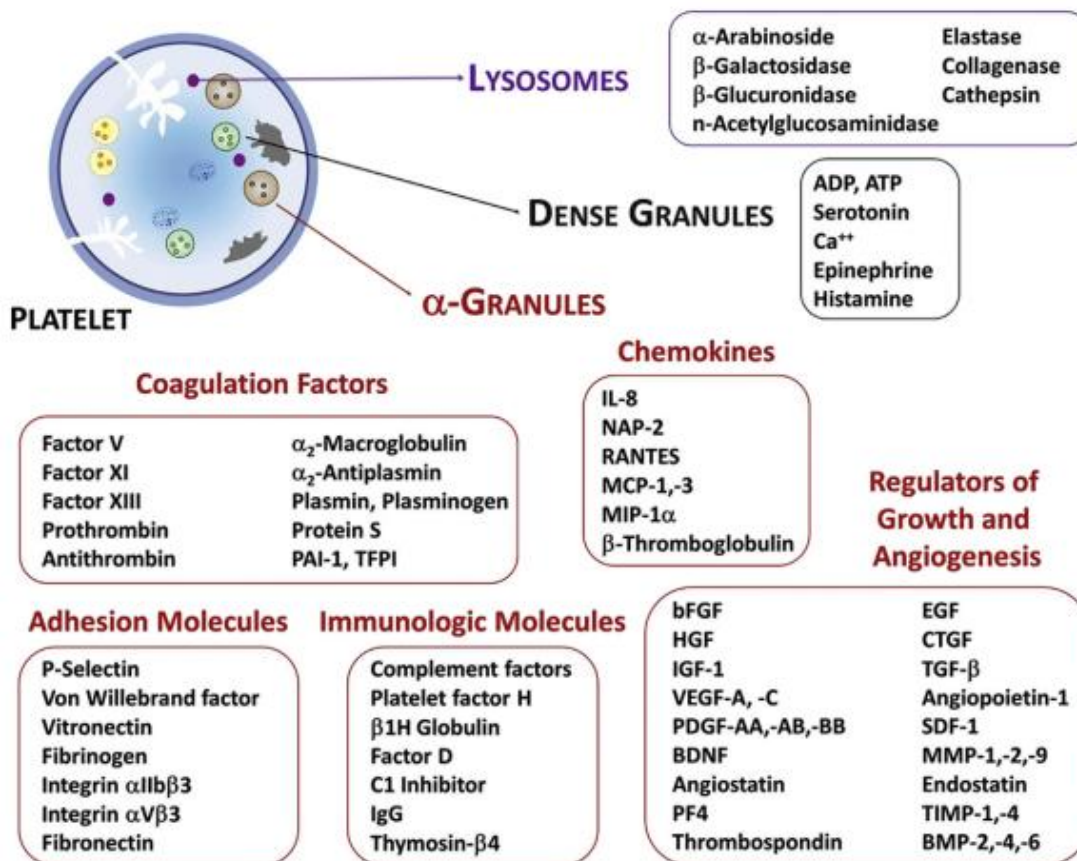


**Figure 3: Platelet granule cargo.** Platelet lysate contains a variety of factors released from platelets including chemokines, adhesion molecules, growth factor and immunological factors (Published with copyright permission from (Burnouf *et al.*, 2016), see appendix II)

### 1.4.2 Development of Serum-free Media

A number of commercially available serum-free media are now available and will be discussed and evaluated in chapter 6. To develop a chemically defined serum-free medium, it is essential to understand the components within FBS which make it, to this day, the gold standard in cell culture. This involves the identification of the hormones, lipids, growth factors and proteins within FBS and their involvement with the cell type of interest. This is well described by Van der Valk *et al* (van der Valk *et al.*, 2010) and attempts to develop a serum-free medium by understanding the key components of FBS essential for cell culture are not recent. However, until the last decade, there has been limited progression in the development of functional serum-free media for the expansion of mammalian cells in culture. A

modular process for the development of a serum-free medium was proposed (van der Valk et al., 2010) outlining a stepwise system whereby one begins with a non cell-specific basal medium (Figure 4), attachment factors, vitamins and lipids. As the medium becomes more refined the focus moved to cell-specific components such as growth factors and hormones (van der Valk et al., 2010). Selection of the correct basal medium is a vital component for insuring cell health. This requires an understanding of the development of these basal medium. For example Roswell Park Memorial Institute (RPMI) 1640 medium was originally developed for use with lymphoid cells (Moore et al., 1967) and is distinctly different from most other mammalian cell culture basal media in that it has a high pH of 8. Dulbecco modified Eagle's minimal essential medium (DMEM) on the other hand has a high vitamin and amino acid content and a higher glucose content. This makes DMEM more robust and suitable for use with multiple cell types from multiple species. All basal media for FBS-free culture must be supplemented with ITS (Insulin, transferrin, selenium) supplement (Moore et al., 1967). Insulin has been known to be essential for all cell culture for its function in the uptake of glucose by cells since the 1920s (Gey and Thalhimer, 1924). The function of transferrin is the transfer of iron into the cells (Bjare, 1992), whereas selenium protects against oxidative stress (Helmy et al., 2000). The next consideration for the development of a serum-free medium is the use of hormones. Hormones are found in serum in varying amounts and thus have to be considered for use in a serum-free formulation (Barnes and Sato, 1980). Apart from insulin, other hormones such as glucocorticoids are also important components for serum-free media. Common examples of these include hydrocortisone or dexamethasone, which inhibit apoptosis of cells (Bailly-Maitre et al., 2001). All of these components are not cell-specific and can act as a basal medium for many cell types. Where particular consideration needs to be given to the cell type is evident in the growth factors being added to the medium. FGF-2 is a commonly used growth factor as it has been shown to pro-mitogenic for a number of cell types (Shihabuddin et al., 1997). Similarly, TGF- $\beta$  is involved in a number of cellular pathways and so is also often considered (Stewart et al., 2010). The most commonly reported growth factor to be used in serum-free media is epidermal growth factor (EGF) due to its ability to induce cell proliferation (Herbst, 2004). The

requirement for these growth factors is entirely dependent on the cell type and the addition of other growth factors may also be required depending on the cells. For example, nerve growth factor (NGF) is a growth factor typically added to neuron cultures (Honegger and Lenoir, 1982). For this reason, a comprehensive understanding of the biology of the cell type of interest is essential in attempting to develop a chemically defined, serum-free medium.

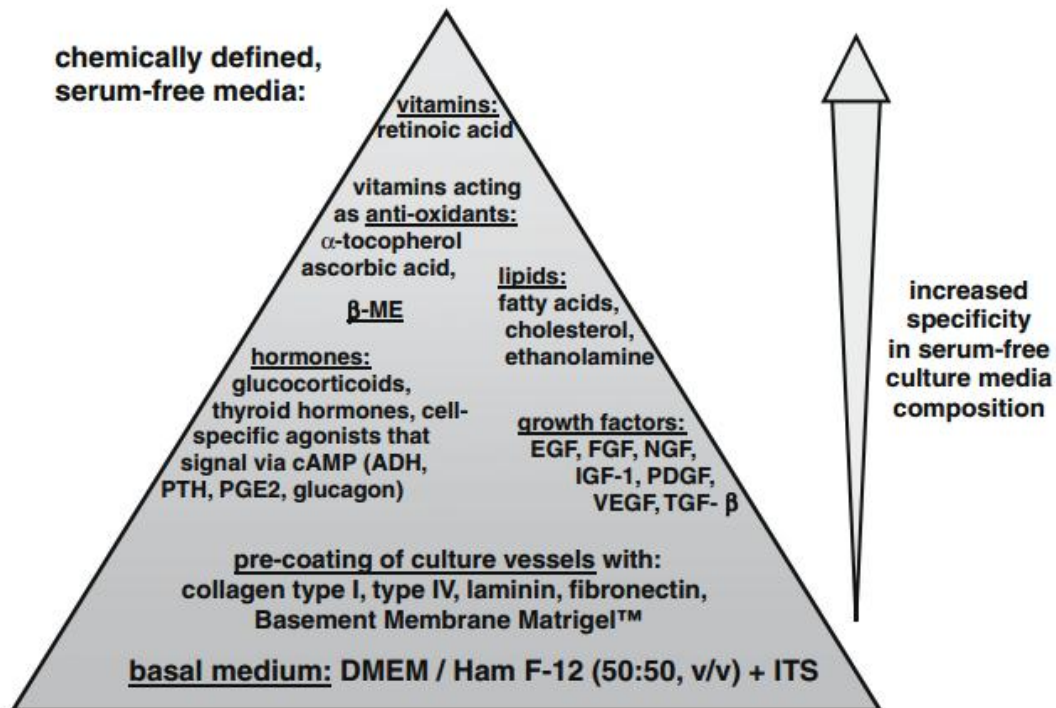


**Figure 4: Hierarchical importance of serum-free medium components for the development of a cell-specific chemically defined medium.** (Published with copyright permission from (van der Valk et al., 2010), see appendix II)

### 1.5 PurSTEM – A Novel Medium for the Culture of MSCs

Prior to the undertaking of this PhD, a European wide consortium ‘PurStem’ was established and coordinated through the Regenerative Medicine Institute (REMEDI) in the National University of Ireland, Galway (NUIG) with one of its goals being the development of a novel serum-free, xeno-free medium for the isolation and proliferation of bone marrow-derived MSCs that would ultimately be able to provide an alternative to the crippling dependence of the cell therapy industry on the highly variable FBS supply. To achieve this, bone marrow aspirates were taken at University Hospital Galway (UHG) with ethical approval and split into three equal

parts. The bone marrow samples were then shipped to partners in Genoa, Italy and Leeds in the UK. MSCs were then isolated within NUIG and these two partner institutes in accordance with their isolation methods at the time. These varied in percentage FBS used and seeding density. Ultimately three isolation conditions were tested; isolation in 10% FBS at a seeding density of  $5 \times 10^4$  mononuclear cells/cm<sup>2</sup>, isolation in 10% FBS at a seeding density of  $1 \times 10^4$  cells/cm<sup>2</sup> and isolation in 2% FBS supplemented with FGF-2 at a seeding density of  $5 \times 10^4$  cells/cm<sup>2</sup>. Subsequent to this, MSCs were cryopreserved and shipped back to NUIG in Galway where all the cells underwent surface marker characterisation using BD FACS™ CAPS proteomics array analysis which assessed expression of 230 surface markers and their relative expression compared to the appropriate isotype control. Of the 230 markers assessed, 74 markers were positive in at least one of the three culture conditions (Figure 5). Of the 74 markers, 57 markers were maintained on MSCs during various culture conditions and thus were identified as the “MSC markers”.

**Experimental Methodology**

230 markers profiled using BD FACS Cap Array  
74 Positive Markers (>50%)

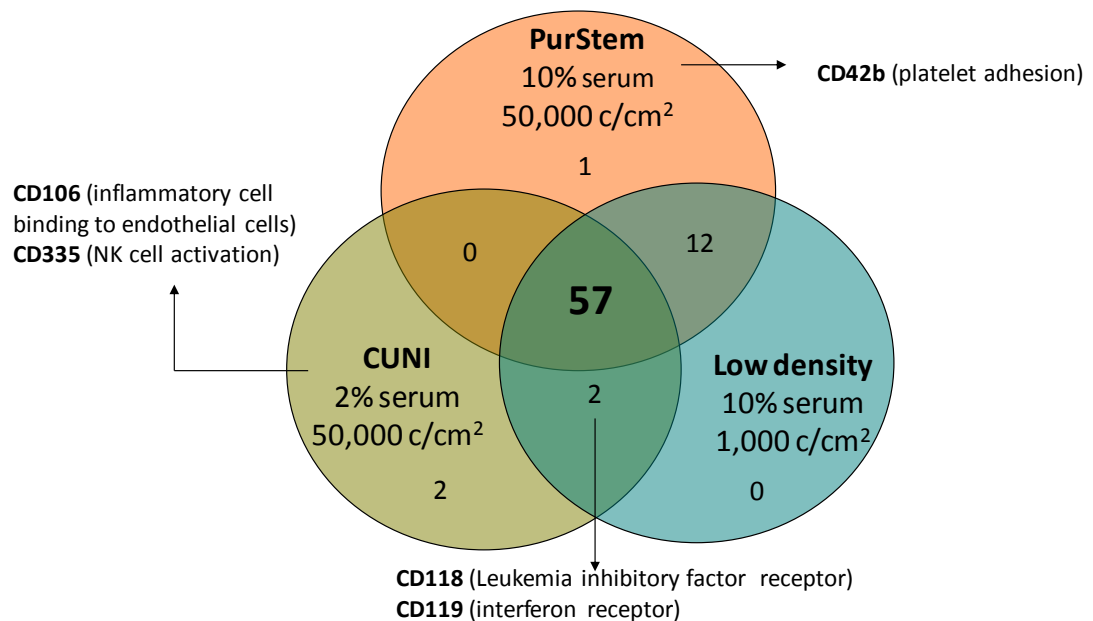


**Figure 5: Distribution of markers expressed on MSCs under previously described culture conditions.** Biological and technical replicates (n=3). (Frank Barry, unpublished data)

## Chapter One

The 57 markers identified to be unchanged on MSCs cultured in the various conditions were assumed to be “true” MSC markers and not merely expressed as a response to their culture environment. With that in mind, these markers were further investigated to assess their known biological role. These experiments were focused on determining growth factors and adhesion molecules that could be recognised by MSCs with the ultimate goal of then testing these factors for their ability to not only sustain MSC proliferation in a serum-free medium but also to facilitate the isolation of MSCs. These data were combined with the current literature at the time detailing the essential components of media to form eight variations of serum-free media (Barry et al., 2015). The eight formulations of medium were tested for their ability to isolate MSCs from bone marrow and maintain the cells in proliferation rates equivalent to conventionally used 10% FBS-containing medium. The various formulations all consisted of a basal medium supplemented with ascorbic acid, dexamethasone, human serum albumin, ITS and low-density lipoprotein. The addition of various growth factor combinations based on the proteomics data resulted in the various formulations being tested.

Of the eight serum-free media formulations, 6 resulted in early senescence of the cells as observed by a decrease in cumulative population doublings over time (results not shown). In contrast, 2 formulations maintained proliferation capacity of the cells at levels superior to that observed in FBS-cultured cells. Based on these data, two media were developed at the end of PurStem with the potential to compete against serum-containing medium. The only difference between both media formulation was the addition of EGF to medium 8 which offered no additional increase in proliferation of the cells and was excluded from future work. This work resulted in the generation of a serum-free medium with the potential to replace the dependence on FBS for MSC cultures. This lead to the hypothesis and aims outlined below.

## 1.6 Aims and Objectives

### Hypothesis:

Bone marrow-derived MSCs isolated and cultured in serum-free medium have a similar phenotype to the same cells isolated and cultured in standard 10% serum-containing medium and that this phenotype can be altered by the use of varying oxygen tension to prime cells prior to use in *in vivo* models of bone repair and regeneration.

### Aims:

This thesis plans to address the following specific aims:

- 1. To assess the effects of oxygen tension on growth kinetics and differentiation of bone-marrow derived MSCs, isolated and expanded using the novel serum/xeno-free medium (Chapter 3).**

The specific aim of this chapter was to determine the optimal culture conditions for the culture of bone marrow-derived MSCs to be used in *in vivo* models of bone regeneration. *In vitro* characterisation of bone marrow derived MSCs that were isolated and cultured in either serum-containing or serum-free medium was performed. Both groups were also cultured in either normoxia (21% O<sub>2</sub>) or hypoxia (2% O<sub>2</sub>).

- 2. To assess the *in vivo* osteogenic potential of the four cell groups listed above in an ectopic mouse model of bone formation (Chapter 4).**

The aim of this chapter was to determine the capacity of the four cell groups listed above to form bone *in vivo* after being loaded onto hydroxyapatite/tri-calcium phosphate (HA/TCP)-based scaffolds. Based on data from aim 1, the hypothesis was the pro-chondrogenic hypoxia cultured cells may produce superior bone to the pro-osteogenic

## Aims and Objectives

normoxia cultured cells by forming bone via endochondral ossification as opposed to forming bone via intramembranous ossification.

- 3. To assess the ability of four cell groups listed in aim 1 to repair an *in vivo* rat critical size defect model (Chapter 5).**

The aim of this chapter was to determine the bone regeneration potential of the four cell groups. This was determined by *in vivo*  $\mu$ CT analysis of bone formation, *in vivo* photoacoustic imaging of neovascularisation and histological evaluation of both. Similar to the previous chapter, cells were loaded onto a hydroxyapatite/tri-calcium phosphate (HA/TCP)-based scaffold and bone formation was assessed after 8 weeks.

- 4. To compare the serum-free medium directly with commercially available media for the isolation of bone marrow-derived MSCs (Chapter 6).**

Potentially competitive serum-free media were identified for their use in the isolation and *in vitro* maintenance of MSCs. *In vitro* characterisation of cells isolated and cultured in the media in either hypoxia or normoxia was carried out. This included tri-lineage differentiation, surface marker characterisation, proliferation, pro-angiogenic potential, immunosuppression and immunogenicity.

- 5. To determine the feasibility of the serum-free medium in a three dimensional (3D) culture system for the scalable production of MSCs (Chapter 7).**

The aim of this chapter was to determine if MSCs could be cultured and grown in a 3D bioreactor system on macrocarriers as a prototype, ultimately to be scaled up for large scale production of MSCs. This was

## Aims and Objectives

determined by comparing MSCs grown in standard 2D culture and in the 3D bioreactor system in both serum-containing and serum-free medium. *In vitro* characterisation was carried out on these cells including tri-lineage differentiation, surface marker characterisation and proliferation. The ability to perform tri-lineage differentiation assays directly on the macrocarriers was also evaluated.



# **Chapter 2**

## **Materials & Methods**

## 2.0 Materials & Methods

All reagents were purchased from Sigma-Aldrich unless otherwise stated.

### 2.1 Isolation of Serum-Free (SF)/ Serum-Containing (SC) MSCs from Human Bone Marrow

Bone marrow aspirates (30mLs) were obtained from healthy volunteers between the ages of 18 and 30 years old after informed consent and under ethical approval from Galway University Hospital and the National University of Ireland Galway Research Ethics Committees. Additionally bone marrow aspirates were purchased from Lonza (Walkersville, Maryland) when not available through Galway University Hospital. Bone marrow aspirates were transferred into a 50mL tube and the volume was recorded. A bone marrow sample was taken aseptically and diluted 1:10 in Dulbecco's phosphate buffered saline (D-PBS). This diluted sample was diluted 1:1 in 4% (v/v) acetic acid to lyse red blood cells (RBCs) for 1min before performing cell counts using a haemocytometer. Cells were plated at a seeding density of between  $23\text{-}29 \times 10^5$  mononuclear cells (MNCs)/cm<sup>2</sup> in 25mLs of serum-free (SF) medium plated on fibronectin pre-coated flasks or 10% serum-containing medium (SC) plated directly onto tissue culture plastic. SC medium consists of alpha Minimum Essential Medium Eagle ( $\alpha$ MEM) (Gibco) supplemented with 10% foetal bovine serum (FBS) (Hyclone, SV30160.03 (Lot RWA25887)) and 1% Penicillin/Streptomycin (P/S). SF medium is proprietary to REMEDI (Barry et al., 2015). Cells were then incubated at 37°C, 5% CO<sub>2</sub>, 90% humidity in either hypoxia (5% O<sub>2</sub>) or normoxia (21% O<sub>2</sub>). Cultures were washed on day 4 to remove non-adhered cells. Medium was removed and discarded. 10mLs of PBS was added to each flask and pipetted over the growth surface. PBS was discarded and the process was repeated. 20mLs of fresh SF or SC medium was added to each flask before returning to the relevant incubator. Media changes were performed every 2-3 days until cells reached 80-90% confluency.

Chapter	Donor Gender	Donor Age	Supplier
3 & 4	Male	24	Lonza
3 & 4	Female	22	Lonza
3 & 4	Female	24	UHG
3 & 6	Male	23	Lonza
5	Male	25	UHG
5	Female	23	UHG
5	Female	20	UHG
6	Female	23	UHG
6	Female	24	UHG
6	Male	22	UHG
7	Female	25	UHG
7	Male	24	UHG
7	Male	24	UHG

**Table 2.1: Bone marrow details of specific donors used in each study. UHG: University Hospital, Galway.**

### **2.1.1 Isolation of Serum-Free MSCs from Bone Marrow with Commercially**

#### **Available Serum-free Media**

Four commercially available serum-free media were tested for their ability to isolate MSCs from bone marrow. Media tested were DXF (Promocell, C-28019), Therapeak, MSCGM (Lonza, 190632), Mesencult (Stem Cell Technologies, 05429) and Xuri (GE Healthcare, 29064332). All media were prepared according to the manufacturer's protocols. Some protocols recommended the use of 2% FBS in addition to their SF medium for the initial isolation of MSCs from bone marrow. Other manufacturers made no claims about the ability to isolate MSCs from bone marrow and were typically used purely for propagation of the cells. To standardise methods, all media were tested for their ability to isolate MSCs from bone marrow

with and without the addition of 2% FBS. The isolation method as described in section 2.1 was carried out.

### **2.2 Coating of Tissue Culture Plastic with Fibronectin**

Cell culture plastics were coated with fibronectin at a concentration of 240pg/cm<sup>2</sup>. To coat a T-175 flask, 42µL of fibronectin was added to 7mL of D-PBS in a sterile 15mL tube. The working solution was mixed by pipetting and added to the flask, which was rocked back and forth to ensure the surface was covered in fibronectin solution. The flask was then incubated at 37°C for between 90mins to overnight. The solution was aspirated from the T-175 and discarded prior to use.

#### **2.2.1 Coating of Tissue Culture Plastic for Use with Commercial Serum-Free Media**

All commercially available SF media used recommended the use of an attachment factor for plating of cells in tissue culture plastic. Both Therapeak and DXF required fibronectin and methods used are described in section 2.2. Xuri and Mesencult attachment factors have not been publically disclosed but were used according to the manufacturer's protocols. Briefly, Xuri attachment solution (GE 29062457) was provided as a liquid and stored at 4°C until use. The solution was diluted 1:100 in D-PBS and plated at a volume of 5mL/cm<sup>2</sup>. Plates were incubated for 2hrs at 37°C in a cell culture incubator. The attachment factor was removed and the plate rinsed with D-PBS prior to use. For the Mesencult attachment substrate (Stem Cell Technologies 05424), powder was dissolved in tissue culture grade water to a final concentration of 1mg/mL and incubated for 30-60mins at 37°C to fully dissolve the lyophilizate. The solution was then stored at -20°C until use. For use, the solution was thawed and diluted 1:20 in PBS prior to the addition to tissue culture plastic at a concentration of 680pg/cm<sup>2</sup>. Plates were incubated overnight at 4°C, the solution was removed and plates were rinsed in D-PBS. Plates were allowed to dry for 15mins prior to use.

### **2.3 Colony Forming Unit-fibroblast (CFU-f) Assay**

CFU-f assays were performed at time of isolation of MSCs from bone marrow to assess initial MSC seeding numbers/mononuclear cells of bone marrow plated.

CFU-fs were defined as colonies of 50 cells or more in a discrete cluster. After a cell count was performed as above,  $3 \times 10^6$  MNCs were taken for determination of SC and SF CFU-fs. Cells were diluted in 9mLs of complete SF or SC medium and 3mLs were plated in triplicate in 6-well plates. This was done for cells going into hypoxia and normoxia. Media changes were performed as above. The plates were removed from incubators between days 10 to 14 depending on colony growth rates. Plates were washed twice with D-PBS and fixed in 95% ice cold methanol for 10mins. Samples were washed twice with D-PBS and then stained with crystal violet (2.3% crystal violet, 0.1% ammonium oxalate and 20% ethyl alcohol) for 15mins. After staining samples were washed twice in D-PBS and plates were left inverted overnight to air dry. CFU-f numbers were determined by counting colonies with  $\geq 50$  cells.

### **2.3.1 CFU-f assays for Commercial media**

For all commercial media, except Mesencult, CFU-f assays were performed using the same methods as described in section 2.3. For Mesencult CFU-f assays, the concentration of attachment factor defined in section 2.2.1 had to be increased to 66 $\mu$ g/mL and methods described in section 2.3 were used.

## **2.4 Sub-culturing of MSCs**

At 80-90% confluency, MSCs were subcultured. The sub-culturing process varied between SF and SC MSCs. For SC MSCs, medium was removed and cells were washed with D-PBS (without  $Mg^{++}$  and  $Ca^{++}$ ). The cells were then incubated with 0.25% trypsin/Ethylenediaminetetraacetic acid (EDTA) at 37°C for 5mins. Flasks were gently tapped at the side to mechanically dislodge any remaining cells. Equal volume of SC medium to trypsin was added to the flask to neutralise the enzyme. The cell suspension was then transferred to a sterile tube and centrifuged at 400g for 5mins at room temperature. For SF MSCs, medium was removed and washed as above in  $Mg^{++}$  and  $Ca^{++}$ -free D-PBS. The cells were then incubated in TrypLE™

## Chapter Two

Express 1X (Gibco 12604-021) disassociation solution for 5-10mins at room temperature. Cells were mechanically dislodged by tapping the flask and the cell suspension was transferred to a sterile tube. Neutralising of TrypLE solution with medium was not necessary. Flasks were then washed with an equal volume of D-PBS as for TrypLE to remove any remaining cells and transferred to the sterile tube. Cells were centrifuged at 400g for 5mins at RT. For both cell types, the supernatant was aspirated without disturbing the cell pellet. Cells were resuspended in 5-10mLs of SC or SF-media and cell counts were performed. MSCs were then either subcultured at  $3\text{-}5 \times 10^3/\text{cm}^2$  or cryopreserved at  $1\text{-}2 \times 10^6$  cells/mL in freezing medium (50g/L HSA containing 10% dimethyl sulfoxide (DMSO)).

### **2.4.1 Subculture of Mesencult-cultured MSCs.**

The subculture of MSCs cultured in Mesencult was performed using Mesencult-ACF enzymatic dissociation solution (MC-EDS) and Mesencult-ACF Enzyme inhibition solution (MC-EIS) from Stemcell technologies (05426). Both solutions were pre-warmed at RT. Medium was removed from the cultures and washed once with D-PBS. 6mL of MC-EDS was added to each T-175 and incubated at 37°C for 2-5minutes. Cells were observed to be detached via microscopy and 6mL of MC-EIS was added to neutralise MC-EDS. Cells were collected in a 50mL tube. 10mL of basal  $\alpha$ MEM was rinsed over the flask to collect any remaining cells and transferred to 50mL tube containing cells. Cells were centrifuged at 300g for 5mins. Supernatant was aspirated and cells were resuspended in 10mLs of mesencult medium.

### **2.5 Cumulative Population Doublings**

To calculate growth kinetics of MSCs from bone marrow, CFU-f numbers/MNC count from marrow were calculated at the point of isolation as described above. Subsequently, MSCs were seeded at a known cell number at initial plating and cell yields were calculated at time of subculture. Population doublings were then graphed versus culture time (days). To calculate population doubling (PD), the following equation was used;

$$PD = \frac{\text{Log}_{10}(\text{Cell Yield}) - \text{Log}_{10}(\text{Initial Cell Number})}{\text{Log}_{10}(2)}$$

Where;

Cell yield = Cell numbers obtained at time of subculture.

Initial cell number = calculated based on CFU-f numbers seeded for P0 and cells seeded for subsequent passages.

Cumulative population doublings were calculated by obtaining the sum of the current passage with all the subsequent passages.

## **2.6 Seeding, Maintaining & Subculturing MSCs in GE Xuri™ Adherent Cell Expansion System Macrocarriers**

MSCs which have previously been isolated in either SF or SC media were seeded into the Xuri™ 3D culture system to assess how the culture of these cells affected their phenotype. The 3D culture system consists of a 125mL spinner flask and a 50mL tube containing macrocarrier “waffles” for seeding of MSCs. To prepare waffles for seeding of cells, 30mLs of D-PBS was added to the 50mL tube. The waffle tube was mixed several times by inversion to remove air bubbles. Air bubbles were deemed to be removed when the waffles sunk to the bottom of the tube at rest. Both the waffles and D-PBS were transferred to the spinner unit by gently pouring them down the side of the spinner flask. The D-PBS was aspirated 50mL of either SC or SF media was added to the flask. To this,  $2 \times 10^6$  SF or SC MSCs were added to the spinner flask and the final volume of medium was adjusted to 100mLs. The spinner unit was sealed and cells were dispersed amongst the waffles by gently swirling the entire flask. The spinner flask was then placed on a magnetic spinner (Scientific Industries SI-3006) with a continuous spin/rest cycle. Spinner flasks were agitated at 60rpm for 1min and then rested for 45mins. Media changes were carried out every other day by aspirating the medium from the unit and refilling with fresh media. To observe cell growth, a disk was selected at random, transferred to a sterile dish and observed under a microscope. Disks were returned to the unit if not at confluency. For subculturing of cells, a modified version of that

used for tissue culture flasks was used. Media was removed and discarded. Waffles were washed twice in 25mLs of D-PBS and cells were disassociated by added 25mLs of TrypLE to the bioreactor and swirling the waffles. Disks were incubated with TrypLE for 10mins and disassociation was confirmed by removing a disk from the spinner flask and observing under a microscope. The cell suspension was pipetted out of spinner flask and transferred to a 50mL tube. A D-PBS wash of waffles was carried out to collect any remaining cells and transferred to the 50mL tube with cells. Cells were centrifuged as described above and a cell count performed as previously described.

### **2.7 Osteogenic Differentiation**

Osteogenic assays were carried out at the end of passage (P) 3 in 24-well flat-bottom plates for between 10-14 days. Cells were seeded at a density of  $2 \times 10^4$  cells/cm<sup>2</sup> or  $4 \times 10^4$  cells/well. Four test wells and four control wells were set up. Both SF and SC cells were seeded in 1mL of SC culture medium in each well and were incubated at 37°C, 5% CO<sub>2</sub>. After 48hrs cells were viewed to confirm adherence and confluency. Medium in test wells was replaced with osteogenic medium and medium in control wells was replaced with complete SC culture medium. Standard osteogenic medium consisted of low glucose DMEM (DMEM-LG) supplemented with 10nM Dexamethasone, 10mM β-glycerophosphate, 100μM Ascorbate-2-phosphate, 100 Units/mL Penicillin, 100μg/mL Streptomycin and 10% foetal bovine serum. Media in all wells was changed twice weekly.

Cells were harvested between days 10-14 and assessed for calcium deposition. Of the four test and control wells, 1 of each was stained with Alizarin Red and the remaining 3 were used for quantification of calcium levels. Data for control samples is not presented in this thesis as no spontaneous osteogenesis in any cell groups was observed for Alizarin red staining or calcium quantification.

#### **2.7.1 Alizarin Red S Staining**

2% Alizarin Red S solution was prepared by dissolving 2g Alizarin Red S in 100mL of distilled H<sub>2</sub>O (dH<sub>2</sub>O). The pH of solution was then adjusted to between 4.1-4.3 with

1% ammonium hydroxide. Wells were washed 2x with PBS. 95% Ice cold methanol was prepared in water and stored at -20°C. Cells were fixed in ice cold methanol for 10mins. Well were washed in dH<sub>2</sub>O. 2% Alizarin Red S solution was added to wells for 5mins in the dark. Alizarin Red S solution was removed and discarded. Wells were washed with dH<sub>2</sub>O until water ran clear. dH<sub>2</sub>O was then added and wells were visualised using an inverted light microscope.

### **2.7.2 Quantitative Calcium Assay**

Calcium deposition was quantified using the Stanbio Calcium Liquicolor Kit (Stanbio). The remaining 3 test and control wells were washed twice in PBS. After washing, 0.2mL of 0.5M HCL was added to each well. Cells were then scraped and transferred in the 0.5M HCL to 1.5mL eppendorf tubes. Samples were then shaken overnight at 4°C. Samples were then centrifuged at 400g for 5mins to pellet and cell debris. Standards were prepared in triplicate with 0.5M HCL according to the manufacturer's protocol ranging from 0.05µg to 1µg. Liquicolor working solution was prepared as 1:1 of binding reagent and working dye and added to wells. Absorbance was measured on a Perkin Elmer Victor 1420 plate reader at 550nm and calcium levels were quantified by comparing to the standard curve.

### **2.7.3 *In situ* osteogenesis on Xuri bioreactor waffles**

To perform osteogenic differentiation of MSCs directly on GE waffles, 5 waffles were harvested from the bioreactor at random and transferred by their attachment to serological pipette to a 6-well plate containing D-PBS. Cells were rinsed in D-PBS for 5mins before being transferred using a sterile forceps to a 96-well plate containing 250µL of osteogenic medium. One disk was added per well. Similarly, control wells were also set up but placed in standard SC MSC medium. Assays were performed for the same duration as standard osteogenic assays and subsequent analysis was also performed as outlined in section 2.7.1-2.

## **2.8 Adipogenic Differentiation**

Cells were plated at 40,000 cells/well, as described above, in a 24-well, flat-bottomed plate. There were four test wells and four control wells set up. Cells were

seeded in 1mL of SC culture medium in each well. Cells were incubated at 37°C, 5% CO<sub>2</sub> and after 48hrs cells were viewed to have adhered and appeared confluent. Media in the test wells was replaced with adipogenic induction medium and the medium in the control wells was replaced with standard culture medium. Standard adipogenic medium consisted of high glucose DMEM supplemented with 1µM Dexamethasone, 500µM 3-isobutyl-1-Methyl-xanthine (IBMX), 200µM Indomethacin, 10µg/mL Insulin, 100U/mL Penicillin, 100µg/mL Streptomycin and 10% FBS. Media in all wells was changed twice weekly. Cells were harvested on day 15. Data for control samples is not presented in this thesis as no spontaneous adipogenesis in any cell groups was observed for Oil red O staining quantification.

### **2.8.1 Oil Red O staining**

To examine their adipogenic differentiation, cells were washed twice with 1ml of D-PBS and then fixed with 1ml of 10% neutral buffered formalin for 15mins. After fixation, wells were rinsed with distilled water and 200 µL of working solution of Oil Red O was added. To prepare working solution of Oil Red O, 0.3mg of Oil Red O was dissolved in 99% isopropanol. This Oil Red O stock was mixed 3:2 with distilled water and filtered through Whatman No.1 filter paper. Oil Red O working solution was added to wells and incubated in the dark for 5mins. Stain was discarded and 2 ml of 60 % Isopropanol was added per well in order to remove excess staining. Then wells were washed twice with dH<sub>2</sub>O. A further 400µL of dH<sub>2</sub>O was added per well and stored at 4°C until imaging was performed. Extraction of the stained lipid was performed after imaging.

### **2.8.2 Extraction/Quantification of Oil Red O staining**

Oil red O was extracted by adding 350µL/well of 99% Isopropanol, left to stand for 5min and solution was transferred into tubes. Tubes were centrifuged 2min at 500g. 100µL of extracted stain were placed in triplicate in a 96-well plate. Absorbance was measured at 520 nm on a Perkin Elmer Victor 1420 plate reader.

### **2.8.3 *In situ* adipogenesis on Xuri bioreactor waffle**

To perform adipogenic differentiation of MSCs directly on GE waffles, 4 waffles were harvested from the bioreactor at random and transferred by their attachment to a serological pipette to a 6-well plate containing D-PBS. Cells were rinsed in D-PBS for 5mins before being transferred using a sterile forceps to a 96-well plate containing 250µL of adipogenic induction medium. One disk was added per well. Similarly, control wells were also set up but placed in standard SC MSC medium. Assays were performed for the same duration as standard adipogenic assays and subsequent analysis was also performed as outlined in section 2.8.1-2.

### **2.9 Chondrogenic Differentiation**

MSC pellets were set up to assess chondrogenic differentiation of MSCs. Cells were seeded in culture medium into 1.5mL screw-cap eppendorf tubes, four test tubes and four control tubes. Approximately 250,000 cells were pelleted at 100xg for 5min and resuspended in incomplete chondrogenic medium (ICM). TGF-β3 was added into all test tubes to give a final concentration of 10ng/mL. Standard ICM medium consisted of high glucose DMEM supplemented with ITS + premix (6.25µg/mL bovine Insulin; 6.25µg/mL Transferrin; 6.25µg/mL Selenous acid; 5.33µg/mL Linoleic acid; 1.25µg/mL Bovine Serum Albumin), 40µg/mL L-Proline, 50µg/mL Ascorbate-2-phosphate, 1mM Sodium Pyruvate, 100U/mL Penicillin, 100mg/mL Streptomycin and 100nM Dexamethasone. The MSCs were centrifuged again at 100g for 5mins and incubated at 37°C, 5% CO<sub>2</sub>, relative humidity with their caps loosened to allow for gas exchange. Medium was changed 3 times weekly. Cell pellets were maintained for 21 days before harvesting. For histology, 1 control and 1 test pellet were used. The remaining 3 of each were used for dimethylmethylene blue (DMMB) and Picogreen assays. Data for control samples is not presented in this thesis as no spontaneous chondrogenesis in any cell groups was observed for Safranin O staining or sGAG measurement.

#### **2.9.1 Dimethylmethylene Blue (DMMB) Analysis**

DMMB assay was carried out to quantify levels of sulphated GAG content per chondrogenic pellet. Pellets were washed twice in D-PBS before being digested in papain solution. To digest pellets, 1 mg of papain powder was weighed and

## Chapter Two

dissolved in 10mL of DMMB dilution buffer (50nM sodium phosphate, 2mM EDTA, 2mM-acetyl cysteine, pH 6.5). 250 $\mu$ L of papain solution was added to 9.75 ml of dilution buffer; 200 $\mu$ L of the diluted papain was added to the each tube and then left to digest overnight at 60°C. Samples were vortexed and chondroitin-6-sulfate (C-6-S) stock solution was prepared ranging from 0 $\mu$ g - 2 $\mu$ g to be used as standards. To 10mL solution buffer 4 mg of C-6-S was added and vortexed. Later, 400 $\mu$ L of stock was added to 1.6 ml of dilution buffer in order to get 80 $\mu$ L/mL C-6-S working stock to prepare standards. To the flat bottomed 96-well plate, 25 $\mu$ L of appropriate standard or sample was added in triplicate, then 75 $\mu$ L of dilution buffer along with 200 $\mu$ L of DMMB stock solution (16mg of DMMB dissolved in 5mL of 100% ethanol supplemented with 2.73g NaCl, 3.04g glycine and 0.69mL of concentrated HCL (11.6M) in distilled water adjusted to pH 3; the final solution was brought to 1L) was added to each well. Absorbance was read on a Perkin Elmer Victor 1420 plate reader at 595nm within 5mins.

### 2.9.2 PicoGreen Assay

DNA content was assessed using the Quant-iT PicoGreen dsDNA assay kit (Molecular Probes) to measure DNA content per chondrogenic pellet to control for variations in cell number. Reagents were prepared according to manufacturer's instructions. From 20x stock solution provided in the Quant-iT Kit, 1xTE solution was prepared (for each sample 1.2 ml of 1xTE and for all standards 6 ml of 1xTE needed). Solution was vortexed and further dilution of PicoGreen solution was performed (200-fold dilution of dimethyl sulfoxide stock in 1xTE). The diluted solution was mixed again and DNA stock was diluted; 20 $\mu$ L of it was added to 980 $\mu$ L 1xTE to get a DNA working stock with a concentration of 800ng/mL. Samples were then diluted 1:20 (20 $\mu$ L of sample and 380 $\mu$ L of 1xTE). To the flat bottomed 96-well black plate, 100 $\mu$ L of the appropriate standards and samples were added to be assayed in triplicate. 100 $\mu$ L of PicoGreen solution was added per well and incubated at room temperature for 3min in the dark. Reading absorbance was set at 538nm on a Perkin Elmer Victor 1420 fluorescent plate reader.

### 2.9.3 Safranin O Staining

After 21 days of chondrogenic differentiation, pellets were washed twice in PBS before being fixed in 10% neutral buffered formalin for 30mins. The pellets were stained with a drop of eosin to allow easier visualisation later. Pellets were then wrapped in Whatman filter paper and soaked in 10% formalin. Pellets in Whatman paper were then carefully placed in a histology cassette and transferred to the Leica ASP300S automatic tissue processor. During processing within the machine, pellets were dehydrated and soaked in paraffin wax in preparation of sectioning (cycles of 70%, 95%, 100% IMS, xylene and paraffin wax). Next, pellets were removed from cassettes and carefully transferred to plastic moulds and submerged in paraffin wax using the Leica EG1150H heated paraffin embedder. Embedded pellets were then cooled to allow wax to set using the Leica EG1150C cold plate. Using a Leica RM2235 microtome, pellets were cut to a thickness of 5µm and mounted on SuperFrost Plus microscopic slides. Slides were then incubated for 1hr at 60°C. Mounted sections were stored at room temperature prior to being stained.

Slides were then deparaffinised and rehydrated as follows; 100% xylene for 5mins x2, 100% IMS for 2mins x2, 95% IMS for 1min, 70% IMS for 1min. Slides were then rinsed in distilled water for 1min. Samples were then stained in 0.02% Fast Green FCF for 4mins to stain cell cytoplasm and then in 1% acetic acid for 3sec. Slides were then incubated in 0.1% Safranin-O for 6mins. The sections were then dehydrated using increasing alcohol concentrations (95% for 1min, 100% for 2mins x2) followed by clearing in xylene twice for 2mins. Slides were mounted in DPX and a coverslip applied. Slides were then left to dry overnight before imaging using Olympus CKX41 microscope.

### **2.9.4 *In situ* chondrogenesis on Xuri waffle and Safranin O staining**

To perform chondrogenic differentiation of MSCs directly on GE waffles, 4 waffles were harvested from the bioreactor at random and transferred by their attachment to a serological pipette to a 6-well plate containing D-PBS. Cells were rinsed in D-PBS for 5mins before being transferred using a sterile forceps to a 96-well plate containing 250µL of complete chondrogenic medium. One disk was added per well. Similarly control wells were also set up but placed in standard SC MSC medium.

Assays were performed for the same duration as standard adipogenic assays and subsequent analysis was also performed as outlined in section 2.9.1-3.

### **2.10 Safranin O staining of Xuri™ 'Waffles'**

For Safranin O staining, waffles were fixed in 10% neutral buffered formalin for 1hr and rinsed twice in D-PBS. These waffles were not histologically processed as described above as samples could not be cut using the microtome. Waffles were directly stained using Safranin O protocol (2.9.3) with the removal of xylene steps.

### **2.11 Surface Marker Expression Analysis**

Flow cytometry analysis of MSCs was carried out to assess their expression of various MSC markers while being negative for expression of markers of other cell types found in bone marrow, namely haematopoietic cell markers. To prepare cells for flow cytometry analysis, MSCs were disassociated from tissue culture plastic as described previously. Cells were centrifuged at 400g for 5mins before being resuspended in FACS buffer (2% FBS in D-PBS). Cells were resuspended and blocked at  $1 \times 10^6$  cells/mL in 2% mouse serum for 1h in FACS buffer at 4°C to prevent non-specific binding during antibody staining. Cells were then centrifuged and resuspended at  $1 \times 10^6$  cells/mL in FACS buffer and 100µL of cell suspension was transferred into 14 wells of a 96-well v-bottom plate. Various antibodies were added according to figure 2.1;

Antibody	Expressed by	Expression Required	Supplier	Catalogue No.	Volume/100 $\mu$ L FACS Buffer
CD105	MSCs	$\geq 95\%$	Invitrogen	MHCD10504	2 $\mu$ L
CD73	MSCs	$\geq 95\%$	BD	550257	4 $\mu$ L
CD90	MSCs	$\geq 95\%$	BD	555596	2 $\mu$ L
CD14	Monocytes	$\leq 5\%$	AbD	MCA1568	2 $\mu$ L
CD19	B cells	$\leq 5\%$	BD	555413	4 $\mu$ L
CD3	T cells	$\leq 5\%$	BD	552127	4 $\mu$ L
CD34	HSCs	$\leq 5\%$	BD	555822	4 $\mu$ L
CD45	Leukocytes	$\leq 5\%$	BD	555483	4 $\mu$ L
IgG1,2a	Controls	$\leq 5\%$	BD	554680	4 $\mu$ L
HLA-DR	B cells	$\leq 5\%$	Invitrogen	MHCDR04	2 $\mu$ L
IgG2b	Controls	$\leq 5\%$	Invitrogen	MG2B04	4 $\mu$ L
CD271	MSCs	Undefined	Miltenyi	120-002-227	2 $\mu$ L
CD146	MSCs	Undefined	BD	550315	2 $\mu$ L

**Table 2.11: Antibody details for MSC surface marker expression**

## 2.12 Immunogenicity/Immunosuppression Assays

To assess the immunosuppressive and immunogenic potential of MSCs, MSCs were harvested and co-cultured with human peripheral blood mononuclear cells (PBMCs) in lymphocyte proliferation medium. Lymphocyte proliferation medium consists of RPMI (Gibco) supplemented with 10% FBS, 1% Pen/strep, 2mM L-glutamine, 0.1mM non-essential amino acids, 1mM sodium pyruvate and 55 $\mu$ M  $\beta$ -mercaptoethanol. For assays, 100,000 PBMCs were co-cultured with various ratios of MSC: PBMC from 1:5 – 1:100.

### **2.12.1 Preparation of MSCs**

MSCs were trypsinised as described above and resuspended in MSC medium. Cells were then washed in PBS and resuspended with the required number of cells in a final volume of 50 $\mu$ L medium. MSCs were then seeded in triplicate into 96-well U-bottom plates.

### **2.12.2 Isolation and Preparation of Peripheral Blood Mononuclear Cells**

20-25mLs of blood was collected from healthy donors into EDTA-coated tubes and stored at room temperature until ready for processing. Blood from all tubes was pooled into a 50mL tube and volume was recorded. Blood was then diluted 1:1 in D-PBS. To 15mL tubes, 2.5mL of Ficoll-paque was added carefully without creating bubbles. To each of these tubes, approximately 8mL of blood was gently added by allowing the blood to run down the side of the tube slowly to not disturb the underlying ficoll-paque. Samples were then centrifuged at 700g for 25mins without the brakes on. The lymphocyte/mononuclear cell layer was gently removed from the tubes and pooled in a 50mL tube. Sample was washed twice with 20mL of PBS and centrifuged at 300g for 5mins. Cells were then resuspended in 0.1% BSA solution. Cell count was performed and the required number of cells was transferred to a 15mL tube for carboxyfluorescein succinimidyl ester (CFSE) staining. A sample of cells was also taken to be used as a control without CFSE staining for establishing flow cytometry gating. Cells for CFSE staining were centrifuged and resuspended in 0.1% bovine serum albumin (BSA) solution in D-PBS. 10 $\mu$ M of CFSE was added to cell suspensions. Cells are then incubated in the dark at 37°C for 6mins. The staining process was stopped by adding 5mL of ice cold T-cell medium (RPMI 1640, 10% FBS, 1% Pen/Strep, 2mM L-glutamine, 0.1mM Non-essential amino acids, 1mM sodium pyruvate, 55 $\mu$ M  $\beta$ -mercaptoethanol) and centrifuged at 300g for 5mins. A wash step was carried out 3 times and cells resuspended at 4x10<sup>6</sup> cells/mL in T-cell medium. 50 $\mu$ L of stained T-cells were then added to each well of the U-bottomed plate containing MSCs.

### **2.12.3 Preparation of T-cell stimulant**

Immunosuppression and immunogenicity assays were set up in a similar manner except for the inclusion of T-cell proliferation stimulant. Immunogenicity assays were not exposed to a T-cell proliferation stimulant whereas in immunosuppression assays the cultures were exposed to CD3 (BD 555336) and CD8 (BD 555725) antibodies at 0.05µg and 10µg/mL, respectively. The desired volume of antibodies was prepared in 50µL with T-cell medium per well to be tested bringing the final volume of well to 150µL with the addition of 50µL of lymphocytes and 50µL of MSCs. Similarly for immunogenicity assays, 50µL of T-cell medium was added to each well without antibodies to a final volume of 150µL. As a positive proliferation control, CFSE-stained lymphocytes alone with antibody stimulation were used. As a negative control, CFSE-stained lymphocytes alone without antibody stimulation were used. CFSE-unstained lymphocytes with and without antibody stimulation were also used as gating controls. The plate was incubated for 4 days for the immunosuppression assay or 5 days for the immunogenicity assay at 37°C, 5% CO<sub>2</sub> relative humidity in a cell culture incubator.

### **2.12.4 CD4 Staining and Flow Cytometry Preparation**

At 4 or 5 days, depending on the assay, the plate was removed from the incubator and centrifuged at 300g for 5mins. The supernatant was removed and collected in a fresh 96-well bottom plate to be stored at -80°C for ELISA analysis if desired. Cells were resuspended in 200µL of FACS buffer and transferred to a 96-well V-bottom plate. Cells were centrifuged as above and resuspended in 200µL FACS buffer. This wash step was repeated twice more. Cells were subsequently incubated with CD4-PE-Cy7 at 4°C for 30-45mins in the dark. Samples were washed as described above and resuspended in 200µL of FACS buffer. Samples were transferred to FACS tubes and analysed on a BD FACS Canto.

## **2.13 *In vitro* Assessment of Angiogenesis by Matrigel assay**

To assess the ability of MSCs to induce neovascularisation *in vitro*, MSC conditioned media was co-cultured with human umbilical vein epithelial cord (HUVEC) cells on Matrigel. The formation of tubules was observed and tubule number was counted.

As MSCs were cultured in various media, controlling the effect of the basal media itself was accounted for. To achieve this, MSCs were seeded in a T175 flask in 25mLs of medium and fed every other day as described above. When cells reached 50% confluency, a full medium change was performed and replaced with 20mLs of fresh medium. Cells were left for 3 days and medium was collected and centrifuged at 400g for 5mins to pellet any cell debris. Collected medium was stored in 1mL aliquots and stored at -80°C until use. At the same time, basal medium was also placed in a flask for 3 days and collected as a medium control. This was done for all the various media used throughout the study. To perform the assay, 120µL of Matrigel was coated onto wells of a 48-well plate, being careful to prevent bubble formation. To these,  $2.5 \times 10^4$  HUVEC cells in 250µL of HUVEC medium and 250µL of test medium was added to the wells. Cells were incubated at 37°C, 5% CO<sub>2</sub>, 95% relative humidity for 18hrs. Plates were imaged using the GE Cytell system which imaged 5 random fields/well. Wells were seeded in technical triplicate with 3 biological replicates. Tubule numbers were counted and normalised to the basal medium of the respective cells and expressed as a fold change.

### **2.14 Preparation of Cell Implants for Ectopic Analysis of Bone Forming Ability of MSCs in Mice**

To assess the bone-forming ability of MSCs, cells were loaded onto hydroxyapatite: tricalcium phosphate (HA:TCP) constructs in fibrin gel and implanted subcutaneously into the backs of immunodeficient 6-8 week old female CD1 nude mice (CD1-Foxn1<sup>nu</sup>, Charles River Laboratories). Clinically approved HA: TCP granules; macro and microporous biphasic calcium phosphate (MBCP+) were sourced from Biomatlante (Nantes, France) (Miramond et al., 2014). The ratio of HA:TCP was 20:80 and particle sizes ranged from 0.5mm to 1mm. Particles were aliquoted as 50mg fractions in 1.8mL cryovials (Nunc). Following enumeration,  $2 \times 10^6$  cells were resuspended in 400µL culture medium and added to the cryovials containing MBCP+ granules. Cells were incubated with the granules for 90mins at 37°C, with gentle rotation at 15min intervals to mix cells and granules together. The supernatant was aspirated and cell counts were performed to assess loading

efficiency. To encapsulate the cells with the granules, a two component fibrin sealant 'Tyseel Lyo' (Baxter, 0000051) was used. Tyseel Lyo components were thawed in a 37°C water bath for 5mins before being transferred aseptically to a cell culture hood. The Tyseel components were transferred from the dual syringe as supplied to 2 cryovials. To the cell-BMCP+ granule mix, 25µL of component A (Fibrinogen: 72-100mg/mL, Aprotinin: 3000KIU/mL) were pipetted and mixed with granules and cells gently. Following this, 25µL of component B (Thrombin: 500IU, Calcium chloride: 40µmol/mL) were slowly added to the granules while slowly rotating the pipette tip in constantly expanding circles to form a 3D sphere of granules and cells as the components begin to crosslink. The samples were left for 1hr prior to surgery to allow crosslinking to complete. Cell constructs were allowed to set for an additional 1hr prior to implantation at RT.

### **2.14.1 Assessment of Viability and Loading Efficiency of MSCs in MBCP/Tyseel**

#### **Constructs**

To determine the viability of MSCs loaded onto Tyseel/MBCP+ constructs, cell loaded constructs were prepared and allowed to set for 1hr as outlined in section 2.14. Subsequently, these constructs were placed in 1mL of either SF or SC medium for 48hrs. Medium was removed and cells were placed in 1mL of fresh medium containing 10% celltitre blue (CTB) (Promega G8080) for 4hrs. CTB solution was removed and centrifuged at 400xg for 5mins to remove any debris. 100µL of solution was added to 96-well plate in triplicate and absorbance was read at 560nm and 600nm, subtracting the 600nm reading from 560nm reading on a Perkin Elmer plate reader. Metabolic activity was compared to cell-free constructs and an equal number of MSCs not loaded into constructs but allowed to form a 3D pellet in equal volumes of medium.

### **2.14.2 Preparation of Cell Implants for Orthotopic Analysis of Bone Forming**

#### **Ability of MSCs in Rats**

For preparation of cell implants for the orthotopic rat study, the process as described above was used. However, a cylindrical shape was formed to fit into the bone defect as described below. After addition of both components of Tyseel Lyo, constructs were shaped with a pipette as described above. The internal tubing from

## Chapter Two

a BD FACS Canto cell sorter with internal diameter of approximately 3mm was cut into 5mm long sections and a longitudinal cut was made on one side (Figure 2.2). The tubing was held open with a forceps at a fixed position. Constructs were transferred to the tubing and forceps removed to allow the tubing to close around the construct to create the cylindrical shape. Implants were left to set in tubing until ready for implantation into the animal for 1-3hr at RT.

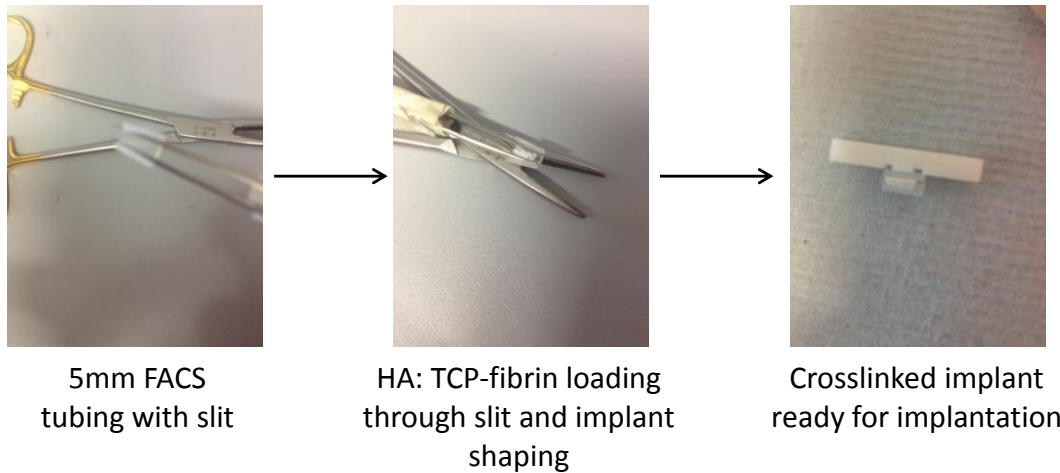


**Figure 2.14.2: Preparation of MSC-MBCP<sup>+</sup> constructs for In vivo implantation into rat femur**

### 2.14.3 Subcutaneous implantation of constructs

Subcutaneous assays were performed on immunodeficient 6-8 week old female CD1 nude mice (CD1-Foxn1<sup>nu</sup>, Charles River Laboratories). Mice were anesthetized by intraperitoneal injection of xylazine (0.005mL/g) per 20g mouse and ketamine (0.01 mL/g). A 1cm incision was created on the dorsal surface of each mouse at each location for implantation, 5 in total. A subcutaneous cavity was created using blunt dissection and a construct was placed in each cavity and cavity was sutured closed. Animals were recovered and monitored for 8 weeks at which point euthanasia via CO<sub>2</sub> inhalation was carried out and cervical dislocation to confirm. Implants were retrieved and fixed as described below.

### **2.15 Fixation and Decalcification of Cell Implants from Mouse Ectopic Bone Formation Assay**

*In vivo* bone samples underwent fixation in 10% formalin and were decalcified prior to sectioning and staining with Mallory's trichrome. To fix the samples, implants were placed in 15mL tubes containing 5mL of 10% neutral buffered formalin for 2 days before being gently washed with PBS. Samples were decalcified in Surgipath Decalcifier II solution for approximately two weeks. Samples were submerged in 5 times their own volume in decalcifier solution as per supplier protocols and gently rocked at 4°C, changing decalcifier solution every other day. Samples were deemed to be decalcified after 2 consecutive days of negative results for calcium analysis. To carry out this, 5% stock solutions of ammonium oxalate and ammonium hydroxide were prepared in distilled water. To determine if decalcification was completed, 500µL of decalcification solution from the samples was taken and transferred to a fresh 15mL tube. 1mL of a 1:1 working solution of 5% ammonium hydroxide and 5% ammonium oxalate was added to the solution. Samples were left overnight at room temperature and residual calcium was identified as a white precipitate in the solution.

### **2.16 Fixation and Decalcification and Histological Preparation of Cell Implants from Rat Femur CSD Model**

At the 8-week endpoint of the study, animals were culled by CO<sub>2</sub> inhalation and cervical dislocation. The entire right femur was excised, being careful not to damage defect region during necropsy. Excised samples were fixed in 100% ethanol prior to decalcification. To decalcify samples, 10% EDTA (pH7.0) w/v was used for 14 days. The defect region was cut away from the implant and screws using a scalpel blade and prepared for tissue processing as described in section 2.16.

### **2.17 Histological Preparation of Transplants**

Transplants were wax embedded and subsequently sectioned at a thickness of 5µm using the Leica RM2235 microtome, mounted on SuperFrost Plus slides (Gerhard-Menzel) and then incubated in a 60°C for at least 1-2hrs. During sectioning of

implants, regions of calcified tissue persisted which inhibited sectioning. To overcome this, mounted sections were placed in decalcifier II solution for 2-3mins and placed on ice block for 1min before sectioning resumed. Mounted sections were then stored at room temperature prior to staining.

### **2.18 Mallory's Trichrome Stain & Scoring**

The sections were deparaffinised in xylene (2 x 2mins) and rehydrated in ethanol (100%, 100%, 95%, 70%, 2mins sequentially) followed by rinsing the samples in water for 2mins. Slides were then placed in pre-heated Bouin's solution (Sigma-Aldrich) at 60°C for 1hr and washed in tap water until the majority of the yellow colour was gone. Slides were then dried in the microwave for 2mins on high. Subsequently, slides were placed in Acid Fuchsin solution (0.125% w/v acid fuchsin, 0.5% acetic acid v/v in water) for 1.5mins before being placed in Aniline Blue-Orange G stain solution (1% phototungstic acid w/v, 2% Orange G w/v, Aniline blue 0.5% w/v in water) for 30mins. Samples were rinsed in tap water and dehydrated through graded ethanol for 2mins each (95%, 95%, 100%, 100%). Slides were then placed in two fresh xylene steps for 2mins before being mounted using distyrene plasticizer/xylene (DPX). Slides were scored for presence of bone, cartilage and bone marrow from 0-4 with 0 indicating respective tissue in 0-20% of implant up to 4 indicating tissue in 80-100% of tissue. Scoring was performed blinded by 3 persons scoring 3 slides from each implant 100µm apart. Three biological MSC donors were implanted into 3 animals (technical replicates). All were scored indicating 81 slides were scored per group.

### **2.19 Preparation of Immunosuppression cocktail of FK506 and SEW2871**

An immunosuppression cocktail of FK506 (tacrolimus) and SEW2871 was prepared sterilely to be administered to animals. 100mg of FK506 (Cayman Chemical 10007965) was reconstituted by adding 1.5mL of molecular grade ethanol to transfer the powder to a 50mL tube. 300µL of Tween 80 was added to the solution and mixed well by vortexing. 13.2mL of D-PBS was added to the solution making

15mLs of a 6.67mg/mL solution. 50mg of SEW2871 (Cayman chemical 10006440) was prepared sterilely by transferring the powder to a sterile 50mL tube in 1.5mL of molecular grade ethanol. 300 $\mu$ L of Tween 80 was added and mixed well by vortexing. The solution was diluted in 10.7mL D-PBS, bringing the final volume to 15mL of a 3.33mg/mL solution. Both drugs were combined and mixed thoroughly giving a final solution of FK506 of 3.33mg/mL and 1.67mg/mL of SEW2871. Working aliquots were prepared and stored at -80°C until use. Drugs were administered to animals to give a final concentration of 1mg/kg/day of FK506 and 0.5mg/kg/day of SEW2871 daily.

### **2.20 Generation of Rat Critical Size Defect (CSD) Model**

A rat femoral bone defect model was used to assess the ability of MSCs to form bone *in vivo*. Male Fischer rats (F344/NCRHSD) (Harlan Laboratories) between 12-16 weeks old were used for the study. To generate the defect, animals were anaesthetized using 5% isoflurane and oxygen and then maintained at 2.5% isoflurane during the surgery (Figure 2.3). Animals received Caprofen (10mg/kg) and Baytril (5mg/kg) from day of surgery to 3-days post-surgery as analgesic and antibiotic. Animals were singly housed in individually ventilated cages for 1 week post-surgery prior to being re-housed 2-3 rats/cage. Prior to the surgery, animals were shaved from their right leg up to the base of the rib cage and back to the spine. An incision was made with a scalpel along the length of the femur. The right femur was exposed by blunt dissection and the periosteum was carefully scraped away to expose the underlying bone. A weight bearing polyetheretherketone (PEEK) plate was held in place on the femur using two bone clamps. Four K-wire screws (0.9mm diameter) were then drilled through the PEEK plate and femur approximately 3mm either side of the defect region. Bone clamps were removed and exposed screws were cut to be flush with the PEEK plate using bone cutters to prevent irritation to the animal. A Gigli saw was used to cut bone to create a 5mm defect. The study contained 6 groups; empty defect (ED), a vehicle control which was implanted with the empty MBCP+ scaffold without cells (ES), and four cell groups; serum-cultured cells cultured in normoxia (SC), cultured in hypoxia (SCH),

## Chapter Two

serum-free cultured cells cultured in normoxia (SF) and hypoxia (SFH). For the ED group, the defect was left empty as described below. For all other groups, the scaffold was carefully fitted into the defect region and positioned using a curved forceps placed behind the scaffold for support and a forceps to position the scaffold. The scaffold was then held in place by sutures tied at either side of the defect region in between the two screws as to avoid any movement of the sutures which could interfere with the scaffold. The surrounding muscle was then closed using interrupted stitches and subcutaneous tissue was sutured to reduce strain on skin sutures as recovered animals return to walking immediately. The skin was then sutured using continuous internal sutures to prevent the animal opening the wound site during grooming. Animals were allowed to recover by removal of isoflurane and were left on oxygen until full recovery was observed. The entire surgery was performed on heating pads to counter the effect of isoflurane on the animal's ability to regulate body temperature. Pain relief and antibiotics were given to the animal prior to surgery and for 3 days post operatively. As this was a xenogenic model of bone repair transplanting human MSCs to rats, animals required immunosuppression daily for first 3 weeks post-operatively. An immunosuppression cocktail was prepared as described previously and was administered daily to the animals subcutaneously.

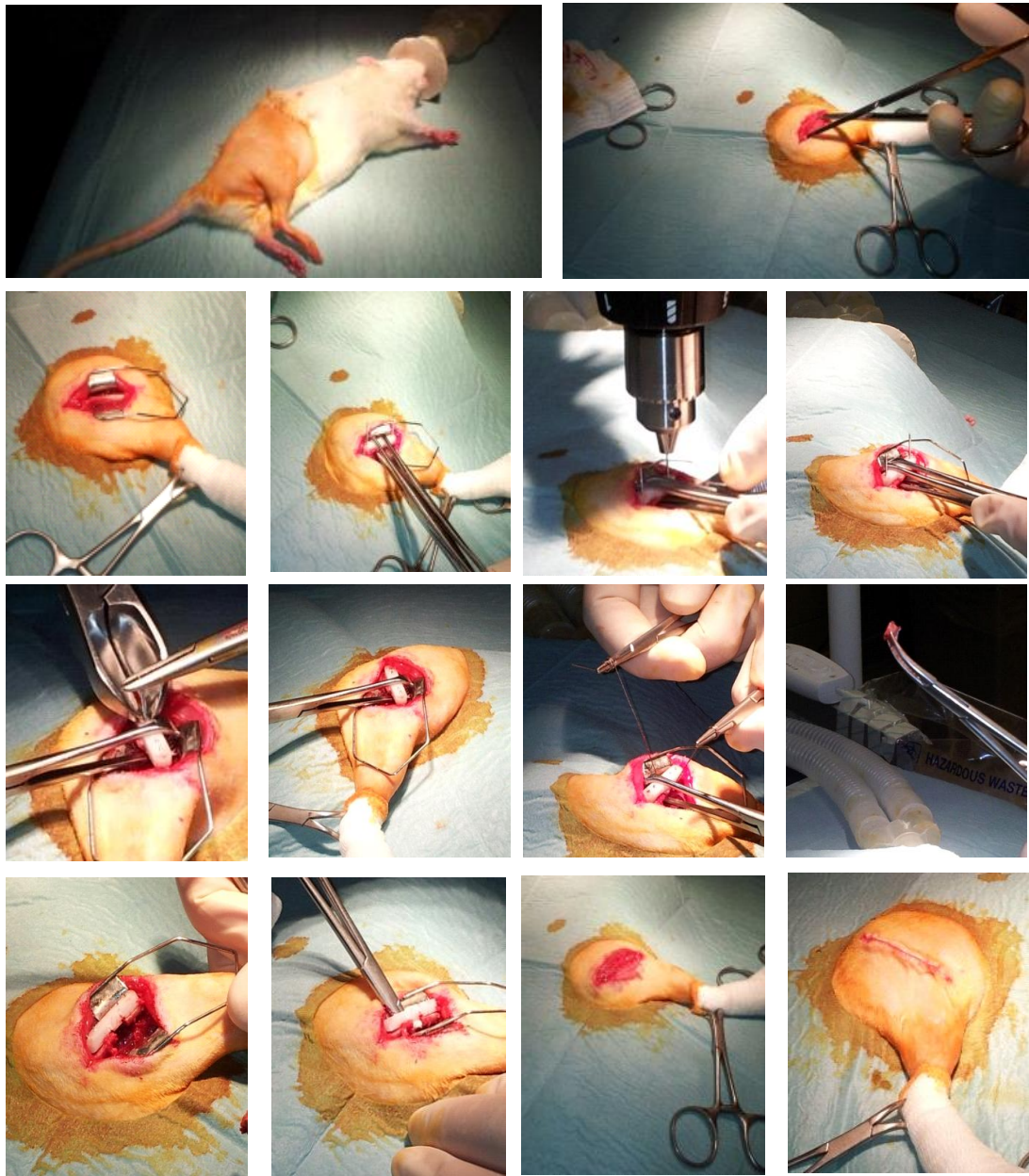


**Figure 2.3: Surgical procedure for generation of rat femoral critical size defect model**

## **2.21 Micro-Computed Tomography ( $\mu$ CT) Imaging of Bone Formation**

### **2.21.1 $\mu$ CT of Mouse Constructs**

Bone formation in subcutaneous implants was assessed at end of the 8-week study. Samples were harvested and fixed as described above.  $\mu$ CT analysis was performed using a Scanco medical ex-vivo CT 100 (Scancon Medical, Bassersdorf, Switzerland). Nine constructs were analysed for the experimental groups loaded with MSCs. Four constructs were analysed for the control groups. For calculating bone volume per tissue volume (BV/TV) to be possible, it was necessary to gate out the HA/TCP particles (MBCP+) used in this model which have a density similar to bone. To achieve this, only tissue in a density region of 40-80 native file units which corresponds to a range of -86.0 – 32.6 mg hydroxyapatite/cm<sup>3</sup> assessed. This region identifies new bone but excludes denser objects including the MBCP+ particles and the metallic screws. 3D scans were generated to visualise mineral deposition within the defect region.

### **2.21.2 $\mu$ CT Rat Femur CSD**

Bone formation was assessed at 4 and 8 weeks by  $\mu$ CT using a Scanco Medical 40 $\mu$ CT system (Scanco Medical, Bassersdorf, Switzerland), evaluating with a 70kVp x-ray source at 110 $\mu$ A. Six constructs were analysed per experimental group. Scans were performed at medium resolution with a voxel size of 19 $\mu$ m. Typically 211 slices were taken over 6.5mins. The defect region was selected as the region between the inner screws, excluding the screws themselves, to reduce variation in samples.

## **2.22 Photoacoustic Imaging of Blood Vessel Infiltration of Rat Femur CSD**

Photoacoustic (PA) and ultrasound (US) images were acquired after 4 and 8 weeks of surgery (Figure 2.4). The rat was anesthetized using 5% isoflurane gas and the anaesthesia was maintained with 2% isoflurane thereafter. Before every imaging session, the rats was shaved and positioned on a flat support. The skin was acoustically coupled to the transducer probe head through ultrasound gel and successive *in vivo* PA and US images were acquired. 3D data sets were collected by

linearly translating the transducer (with integrated optical fibres) with a stepper motor over a region of interest, while capturing each 2D image of the 3D stack. Multi-wavelength PA images were acquired at 690 to 970 nm wavelengths. An experimental set up used for PA/US imaging in this study is shown in Figure 2.4. An integrated PA/US imaging system (Vevo LAZR, Fujifilm VisualSonics) was operated with a 21 MHz (centre frequency) linear-array transducer probe. The transducer probe consisted of 256 elements, divided in 4 quadrants each with 64 elements. The 21 MHz transducer probe provided an axial and lateral resolutions of 75 $\mu$ m and 158 $\mu$ m, respectively.

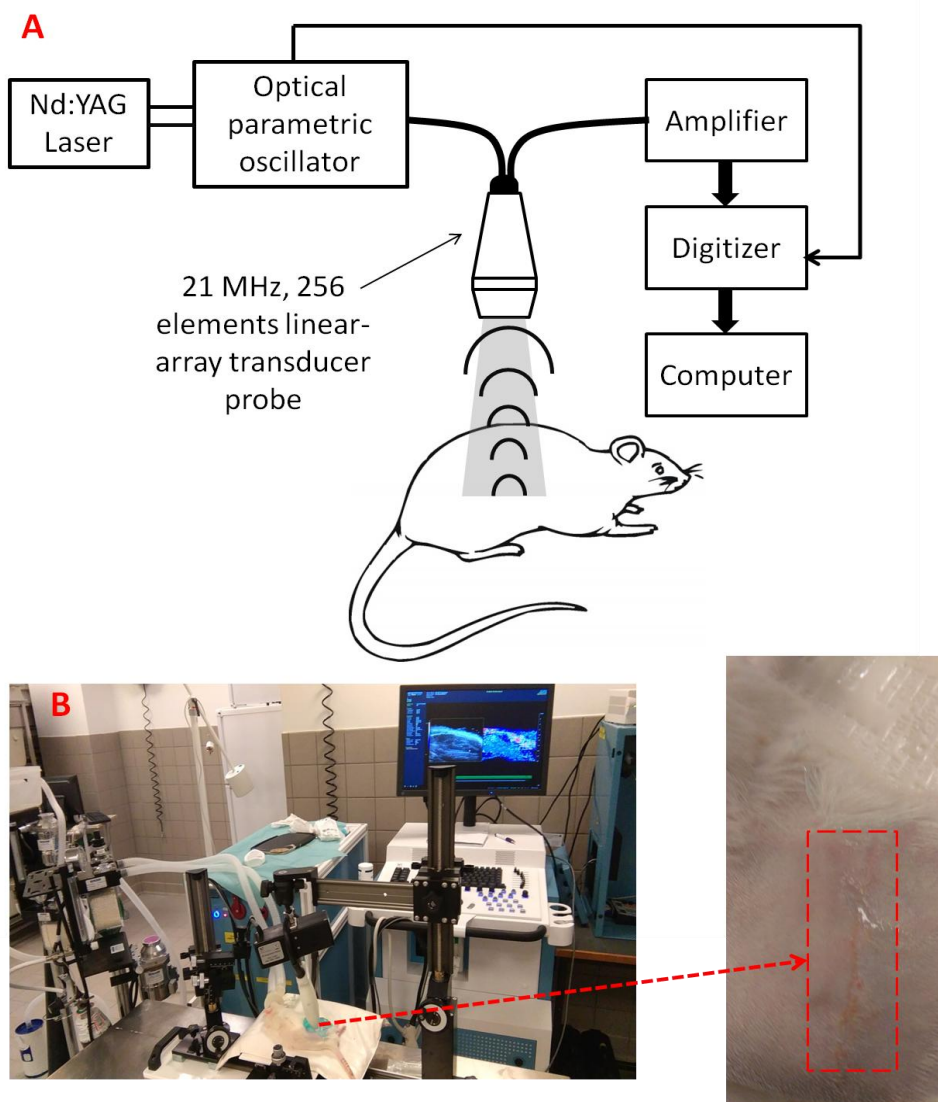


**Figure 2.22** *Experimental setup for PA imaging of rat defect. (A) Schematic of the combined PA and US imaging system using a 21 MHz frequency linear-array transducer probe. (B) Experimental set up used for the assessment of reparative ability of MSCs in a rat critical size bone repair defect model.*

### 2.23 Blood Vessel Staining using Ulex Europaeus Agglutinin (UEA-1)

UEA-1 was used to stain blood vessels as it binds to the sugar L-fucose found on endothelial cells. Lectin binding buffer (10x solution) was prepared by dissolving 23.83g of 4-(2-hydroxyethyl)-1-piperazineethanesulfonic acid (HEPES), 87.66g of sodium chloride (NaCl), 12.5mg of magnesium chloride ( $MgCl_2$ ) and 11.1mg of calcium chloride ( $CaCl_2$ ) to 800mL of distilled deionised water ( $ddH_2O$ ). The pH of

the solution was then adjusted to 7.5 with sodium hydroxide (NaOH). The final volume was brought to 1L and stored at RT until use. For staining, slides were deparaffinised in 2 changes of xylene (15mins each) and rehydrated through graded alcohols for 2mins each (100%, 100%, 95%, 70%, 50%). Slides were then incubated in lectin buffer for 2mins prior to being incubated in lectin buffer containing FBS for 30mins. Slides were then washed in two changes of lectin buffer for 2mins each and incubated for 1hr in lectin stain in the dark. Lectin stain was prepared by diluting UEA-1 1:500 in lectin buffer containing 5% FBS. Slides were then washed through 3 changes of lectin buffer for 5mins each. Samples were mounted with 4'6-diamidino-2-phenylindole (DAPI) and coverslip added. Slides were viewed using the TRITC filter on a Leica upright brightfield microscope. As a negative staining control, 100mM of L-fucose was incubated with the lectin solution for 1hr in the dark at RT prior to being added to control slide.

### **2.24 Movat's Pentachrome staining**

The sections were deparaffinised in xylene (2 x 5mins) and rehydrated in ethanol (100%, 100%, 95%, 70%, 1min sequentially) followed by rinsing the samples in deionised water for 1min. Subsequently the slides were placed in the Verhoeff's elastic stain for 15 minutes and rinsed with deionised water for 2 minutes directly after. The slides were then placed in 2% ferric chloride for 1 minute, rinsed with distilled water for 2 minutes and placed in 5% sodium thiosulfate solution for 1 minute. Immediately after, the slides were rinsed with running distilled water for 2 minutes before being placed in 3% acetic acid for 3 minutes. Following this step the slides were inserted into the 1% Alcian blue solution for 15 minutes, removed and rinsed under warm, running water for 2 minutes and then placed in crocein scarlet-acid fuchsin for 2 minutes. The slides were dipped in 1% acetic acid 5 times and placed in 5% phosphotungstic acid for 2 minutes. The sections were then checked under the microscope to check there is differentiation in the connective tissues. When satisfied with the appearance the slides were dipped in 1% acetic acid a further 5 times followed by 2 x 1mins in fresh 100 % EtOH. The slides were added to alcoholic saffron solution for 15 mins and washed again for 2 x 1min in 100% EtOH.

In the fume hood the slides were placed in 100% xylene solution for 2 x 1 minutes before mounting with DPX.

### **2.25 statistical analysis**

Data was assessed for normal distribution using D'Agostino-Pearson omnibus normality test. Due to low number of biological replicates (n=3) typically, normality could not be determined. Specific statistics is listed in figure legend for each data set. Typically data was analysed as parametric using either one-way or two-way ANOVA with Bonferroni post-test.

Statistical significance was considered at  $p < 0.05$ . Statistical analysis was carried out using GraphPad® Prism Version 5 (GraphPad Software, CA, USA) and Microsoft® Excel 2010 (Microsoft Corporation, Washington, USA).

# **Chapter 3**

**The effect of oxygen tension on *in vitro*  
phenotype of bone marrow-derived  
MSCs, isolated and expanded using a  
novel serum/xeno-free medium**

### 3.1 Introduction

The majority of early work on developing *in vitro* culture conditions of cells has focused primarily on nutrients, pH and growth factors. This has resulted in a wide variety of media formulations and supplements with varying degrees of success for culture of stem cells. More recently, oxygen tension has also been recognized as an essential component of culture conditions for cells (Fehrer et al., 2007, Meyer et al., 2010, Sheehy et al., 2012). Historically, with oxygen tension for cell culture receiving little attention, atmospheric or ambient oxygen levels were primarily used (Shooter and Gey, 1952). To a large extent this continues to be the standard oxygen tension for the expansion of the majority of mammalian cells including MSCs. In contrast, the majority of stem cells *in vivo* exist in far lower oxygen tensions. Lower oxygen tension in tissues, such as bone marrow (1-5%), known to harbour stem cells raised the question as to whether or not these lower oxygen tensions were essential for the maintenance of stem cells. Stem cells exist in a specific niche which conventionally refers to an anatomical location. This definition has been expanded to incorporate physical, chemical and hormonal cues which regulate stem cell biology (Mohyeldin et al., 2010). Oxygen tension measured in atmospheric air is 21% or 160mm Hg. As this air is inhaled, the partial pressure oxygen (pO<sub>2</sub>) decreases and by the time it reaches organs and tissues has reduced to 2-9% pO<sub>2</sub> or 14-65 mm Hg. This oxygen level is a dramatic reduction on the oxygen tension which classically has been identified as normoxic (21%). Ironically, 2-9% pO<sub>2</sub>, the cells' normoxia, has been reported as 'hypoxic' in much of the literature. With that in mind a number of studies have been carried out which report that altering of oxygen tension during culture of MSCs does alter the phenotype of these cells. Numerous studies have reported an effect of oxygen tension on growth, tri-lineage differentiation potential and production of cytokines. However, these studies have generated conflicting data regarding the effect of hypoxia on MSCs. Although some of this can be attributed to experimental conditions, there are still discrepancies. This also has implications for the therapeutic potential of MSCs. For example, bone fracture sites and cartilage are hypoxic by nature and also have limited vascularisation (Lu et al., 2008). MSCs, grown at 21% pO<sub>2</sub>, transplanted into this

environment may undergo a stress response which could alter their survival and therapeutic efficacy.

One area where there appears to be consensus is the effect of low oxygen levels or hypoxia on MSC proliferation (Kakudo et al., 2015, Iida et al., 2010, Grayson et al., 2007b, Fotia et al., 2015). In one study that assessed the long term effect of *in vitro* culture of MSCs in hypoxia, the cells were cultured for seven passages in either hypoxia or normoxia and a 30-fold increase in cell yield was observed in the former. This increase in proliferation of cells in hypoxia appeared to be due to cells in normoxia, or 21% oxygen, undergoing oxidative stress thus limiting their proliferation (Estrada et al., 2012). In this same study, cells cultured at normoxia underwent increased telomere shortening and thus a reduced lifespan. This effect was mirrored in a similar study comparing hypoxia (5%) with normoxia-cultured MSCs, which showed that hypoxia-cultured cells were genetically more stable in an undifferentiated state and again underwent a significant increase in proliferation. In a contrasting study, culture of cells in 1% O<sub>2</sub> underwent reduced proliferation compared to cells in 21% O<sub>2</sub> (Holzwarth et al., 2010a). Based on literature regarding oxygen tension in bone marrow and culture, the range of hypoxia which seems to demonstrate a pro-proliferative effect is between 2-7% with oxygen tension below this having an inhibitory effect. Moreover, no studies have been reported looking at O<sub>2</sub> levels between 7-21% to assess when the switch from hypoxia to normoxia occurs or rather whether increasing oxygen tension has a gradient effect on MSCs (Liu et al., 2015, Tsai et al., 2012, Holzwarth et al., 2010a, Kakudo et al., 2015, Iida et al., 2010, Grayson et al., 2007b, Fotia et al., 2015).

In addition to the effect of hypoxia on proliferation of MSCs, a number of studies have reported an effect of hypoxia on tri-lineage differentiation potential of the cells (Sheehy et al., 2012)]. With respect to osteogenic differentiation, the majority of data seems to indicate an inhibitory effect of hypoxia on osteogenesis of bone marrow-derived MSCs (Fehrer et al., 2007, Holzwarth et al., 2010a, Lee and Kemp, 2006). A similar effect has also been reported with adipose-derived MSCs (Malladi et al., 2006). In these studies, when compared to the same cells in normoxia, a reduction in a number of markers of osteogenesis was reported, including reduced

alkaline phosphatase production and mineralisation ability in combination with a reduction in osteogenic genes such as Runt-related transcription factor 2 (Runx2) and Osteocalcin (Fehrer et al., 2007, Holzwarth et al., 2010a, Lee and Kemp, 2006) (Malladi et al., 2006). A mechanism for the down regulation of Runx2 has been associated with the HIF-TWIST (Hypoxia inducible factor-Twist related protein) pathway (Yang et al., 2011). In contrast to these studies, osteogenesis has been shown to be enhanced in hypoxia (2% O<sub>2</sub>) with increased Runx2 expression (Valorani et al., 2012). This data was also replicated in a second study using a hypoxia mimicking agent desferrioxamine, an iron chelator that enhances HIF-1 $\alpha$  accumulation (Wagegg et al., 2012). Some of this conflicting data can be explained by timing of the use of hypoxia. Some studies maintain the cells in hypoxia entirely for both proliferation and differentiation whereas other studies culture the cells in either hypoxia or normoxia for proliferation and then switch the oxygen tension for differentiation. This effect has been observed in adipose-derived MSCs when pre-cultured in hypoxia and differentiated in normoxia (Valorani et al., 2012). In these studies hypoxia is reported to increase osteogenesis. However, it is likely that hypoxia priming of cells during proliferation before differentiation may have been the inducer of the increased osteogenesis in this study (Valorani et al., 2012). This may highlight an anomaly in reporting on the effect of hypoxia in the literature.

Hypoxia also appears to have an effect on MSC adipogenic differentiation. However, the same issues remain in reporting on how hypoxia was used during these experiments. In studies directly comparing MSCs cultured and differentiated in either hypoxia (2-5%) or normoxia (18-21%), the overall data reports an inhibition in adipogenesis of cells cultured in hypoxia (Zhou et al., 2005). Similar to osteogenesis, the mechanism through which this effect is mediated appears to be through the HIF-1 $\alpha$  pathway, but through the interplay of HIF-1 $\alpha$  and DEC1/Stra13, a member of the drosophila hairy/Enhancer of split transcription repressor family, which inhibits peroxisome proliferator-activated receptor gamma (PPAR $\gamma$ 2), a transcriptional enhancer of adipogenesis (Yun et al., 2002). In mouse embryonic fibroblasts deficient in HIF-1 $\alpha$ , hypoxia-mediated inhibition of adipogenesis was not observed (Yun et al., 2002). Hypoxia-induced inhibition of MSC adipogenic

differentiation may not be surprising, particularly in adipose-derived MSCs; these cells in their natural physiological niche, adipose tissue, are exposed to an oxygen level of less than 3% and in this niche, MSCs reside in an undifferentiated state (Valorani et al., 2012, Chung et al., 2009). Similar to studies of osteogenesis, defining hypoxia is necessary for consistency in the literature. Hypoxia of between 2-5% (Yun et al., 2002) appears to inhibit adipogenesis. Conversely, where O<sub>2</sub> levels below 2% are used, an increase in adipogenesis of hypoxia cultured cells may be seen (Fink et al., 2004). This effect was also observed in extreme hypoxia (0.2% O<sub>2</sub>), where bone marrow MSCs underwent increased adipogenesis and expression of adipocyte-specific genes such as lipoprotein lipase (LPL), complement factor D (CFD), and hypoxia-inducible gene-2 (HIG2). A lack of standardisation in experimental design between studies has again resulted in conflicting data regarding the effect of hypoxia on adipogenesis.

In addition to the general consensus that hypoxia increases MSC proliferation, there is also general agreement in the literature that hypoxia increases chondrogenesis (Khan et al., 2007b). In a study comparing cells cultured in normoxia (21% O<sub>2</sub>) and hypoxia (3% O<sub>2</sub>) and then differentiated in both conditions, the oxygen levels during culture appeared to have a greater effect on chondrogenesis than the oxygen levels during chondrogenic differentiation (Adesida et al., 2012). In this instance, hypoxia-cultured cells underwent increased chondrogenesis compared to normoxia-cultured cells after 21 day pellet culture as assessed by sGAG levels and Safranin O staining. This was independent of oxygen levels during chondrogenesis. Furthermore these data were complimented by increased mRNA levels of chondrogenesis-associated genes *Aggrecan*, *Collagen II* and *Sox9* (Adesida et al., 2012). This increased chondrogenic potential of MSCs isolated in hypoxia may be due to the early selection of a chondroprogenitor subpopulation of MSCs. Adipose-derived MSCs isolated in hypoxia had reduced matrix metalloproteinase synthesis and reduced osteogenic potential (Xu et al., 2007). In this study, re-oxygenation of MSCs by culturing them in 21% O<sub>2</sub> didn't recover the osteogenic phenotype indicating that isolation and culture of cells in hypoxia may select a different subpopulation of MSCs, in this case a

chondroprogenitor with increased chondrogenic potential is maintained. This study is contradicted in a second study where the transcriptional profile of MSCs preconditioned in either hypoxia or normoxia prior to chondrogenesis was analysed using a microarray. Here hypoxic pre-conditioning had no effect on subsequent chondrogenesis assays performed in normoxia. Similar to previous studies the transition to normoxia resulted in increased proliferation and also a reduction in apoptosis which may be due to a reduction in oxidative stress experienced by the cells (Pilgaard et al., 2009, Estrada et al., 2012).

With these data in mind, it is reasonable to assume isolation of MSCs in varying oxygen levels may select for different subpopulations of MSCs with altered phenotypes. This may have far reaching implications for the field of cell therapies as identifying the optimal culture conditions for the therapeutic target may be key to the therapeutic efficacy of MSCs. Unanswered questions in the field include the optimal oxygen tension level as numerous studies vary the oxygen levels defined as hypoxia.

### **3.2 Methods**

To determine the effect of hypoxia on MSCs isolated in either hypoxia (2% O<sub>2</sub>) or normoxia (21% O<sub>2</sub>), human bone marrow was obtained from healthy donors as outlined in section 2.1 and MSCs were isolated in either serum-containing or serum-free media. These cells were incubated in hypoxia (2% O<sub>2</sub>) or normoxia (21% O<sub>2</sub>) for three passages (section 2.4) at which time the cell tri-lineage differentiation potential (sections 2.7-2.9), pro-angiogenic (section 2.13) and immunosuppressive effect (section 2.12) was assessed. Cells were also assessed for their surface marker phenotype (section 2.11) using the ISCT panel with the addition of CD271 and CD146 (Sacchetti et al., 2007b, Jones et al., 2002). The immunogenicity of the cells was also determined (section 2.12). CFU-f capability (section 2.3) and growth throughout culture was also determined (Section 2.5). A schematic outline of the experimental design is given in figure 3.2.1. No deviations from these protocols were carried out in this chapter unless otherwise stated.

## Chapter Three



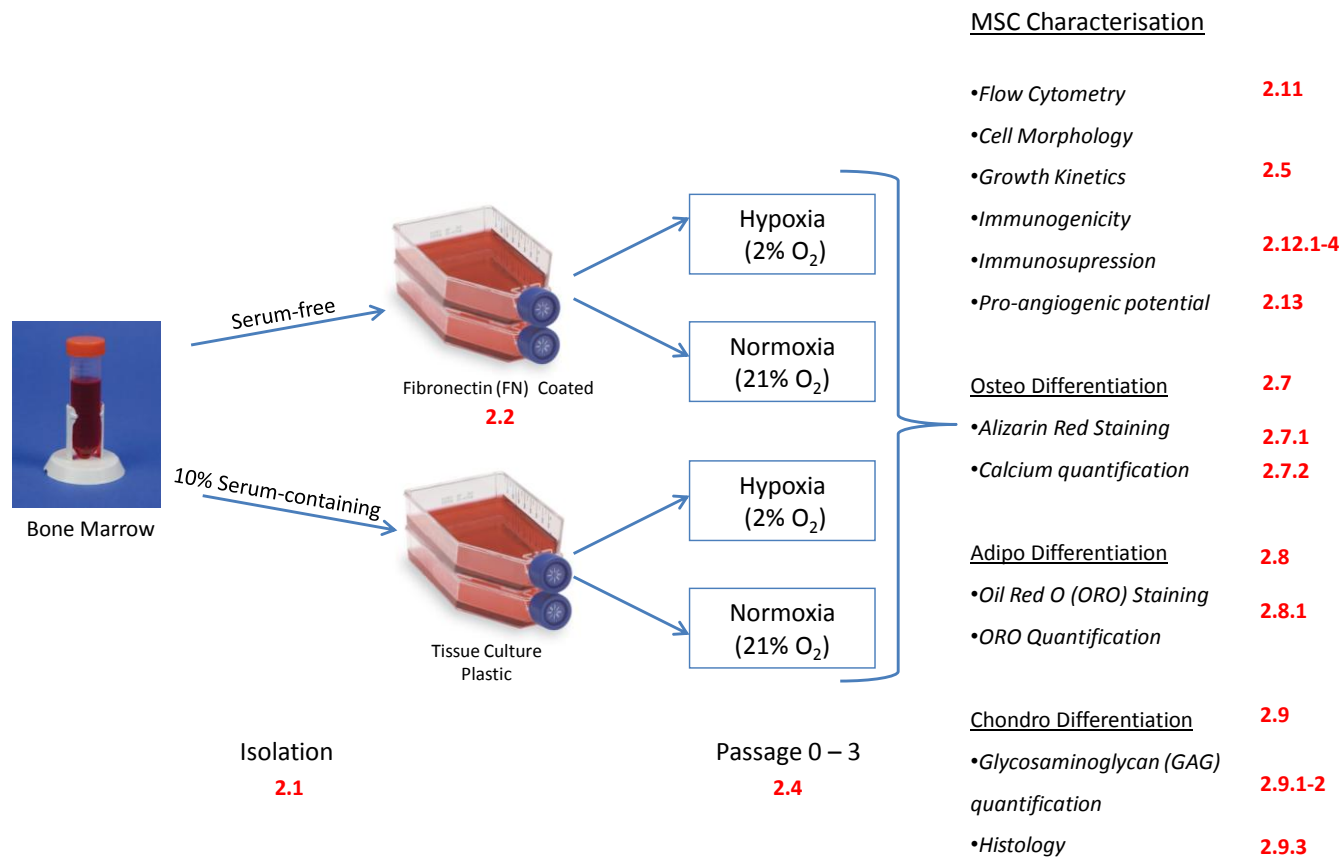
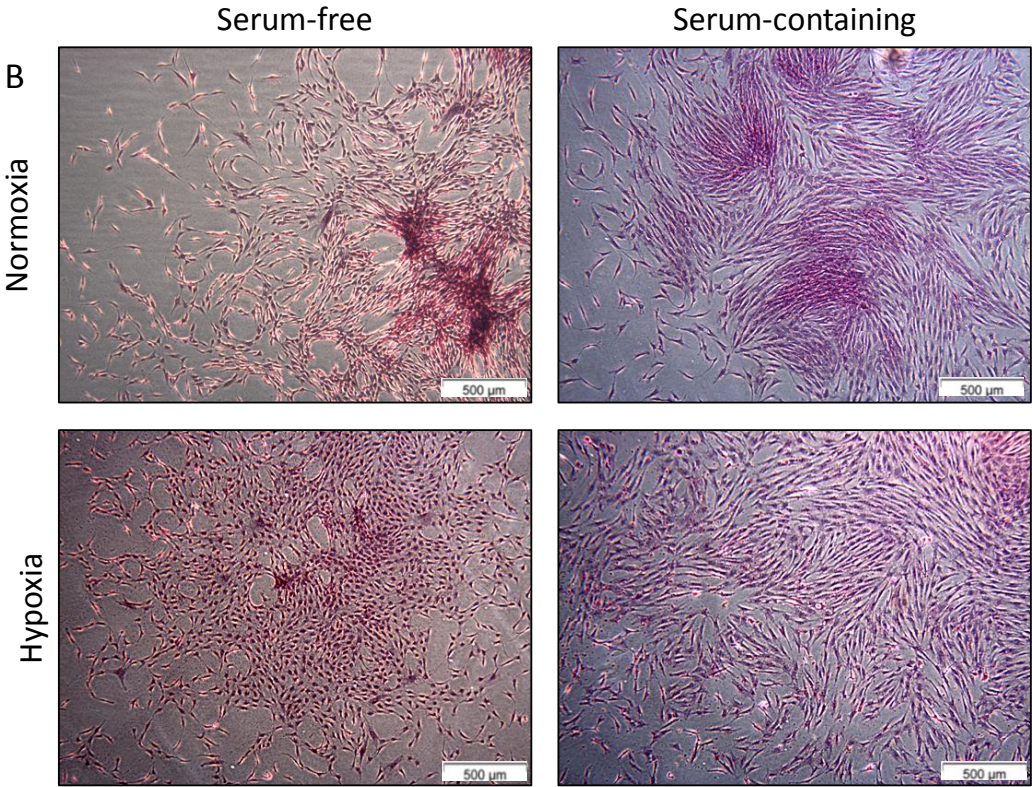
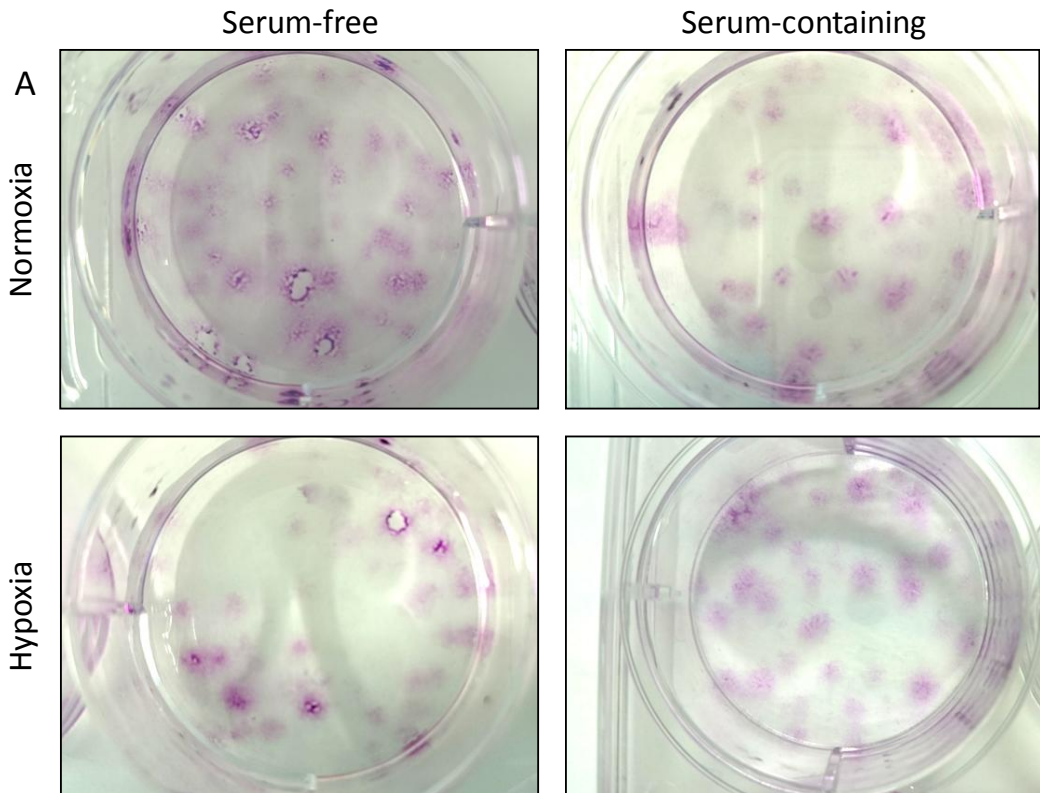


**Figure 3.2.1: Schematic representation of the approach taken for the in vitro characterisation of bone marrow-derived mesenchymal stem cells isolated in serum-containing (SC) or serum-free (SF) culture medium. Specific methods (as described in chapter 2) are indicated by associated number in red.**

### **3.3 Results**

#### **3.3.1 Serum-free medium isolates CFU-fs with distinct size and shape similar to serum-containing isolated CFU-fs**

The serum-free (SF) medium was assessed for its ability to isolate CFU-fs from bone marrow in both hypoxia and normoxia. Bone marrow aspirates were obtained from healthy donors and whole marrow was plated directly onto tissue culture plastic. Both SF and SC media were assessed for their ability to isolate CFU-fs from human bone marrow in hypoxia and normoxia (Figure 3.3.1a). CFU-fs were stained with crystal violet and imaged (Figure 3.3.1b). Quantification of crystal violet stained colonies indicated no statistical difference in CFU-f numbers in either hypoxia or normoxia in SF and SC groups was observed due to variation between donors. (Figure 3.3.1c).



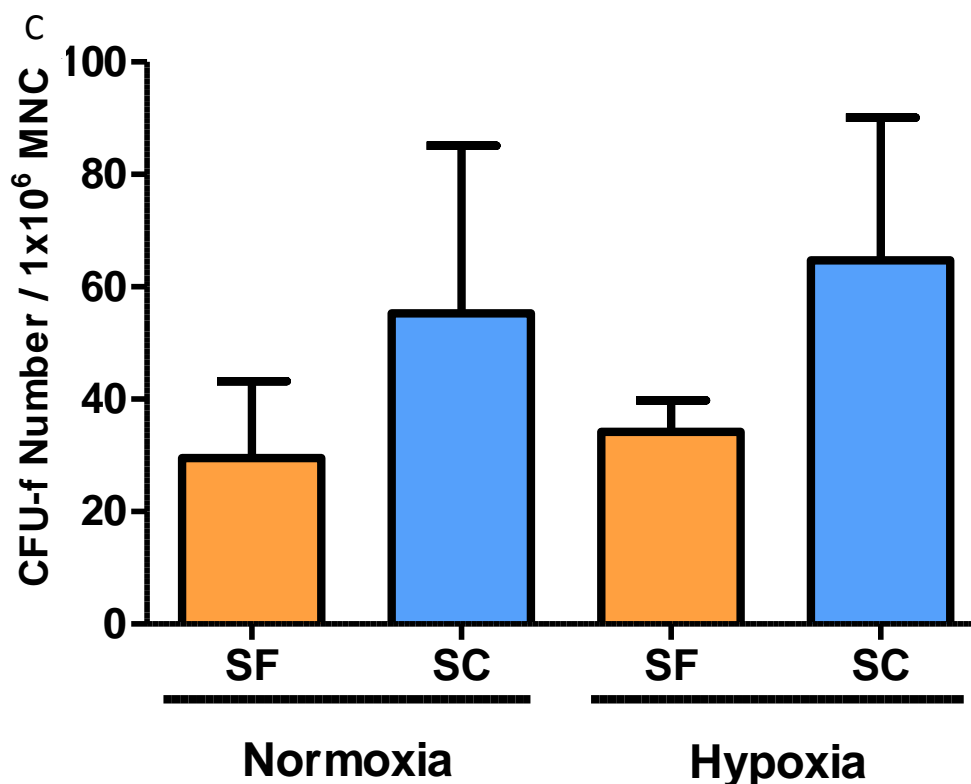
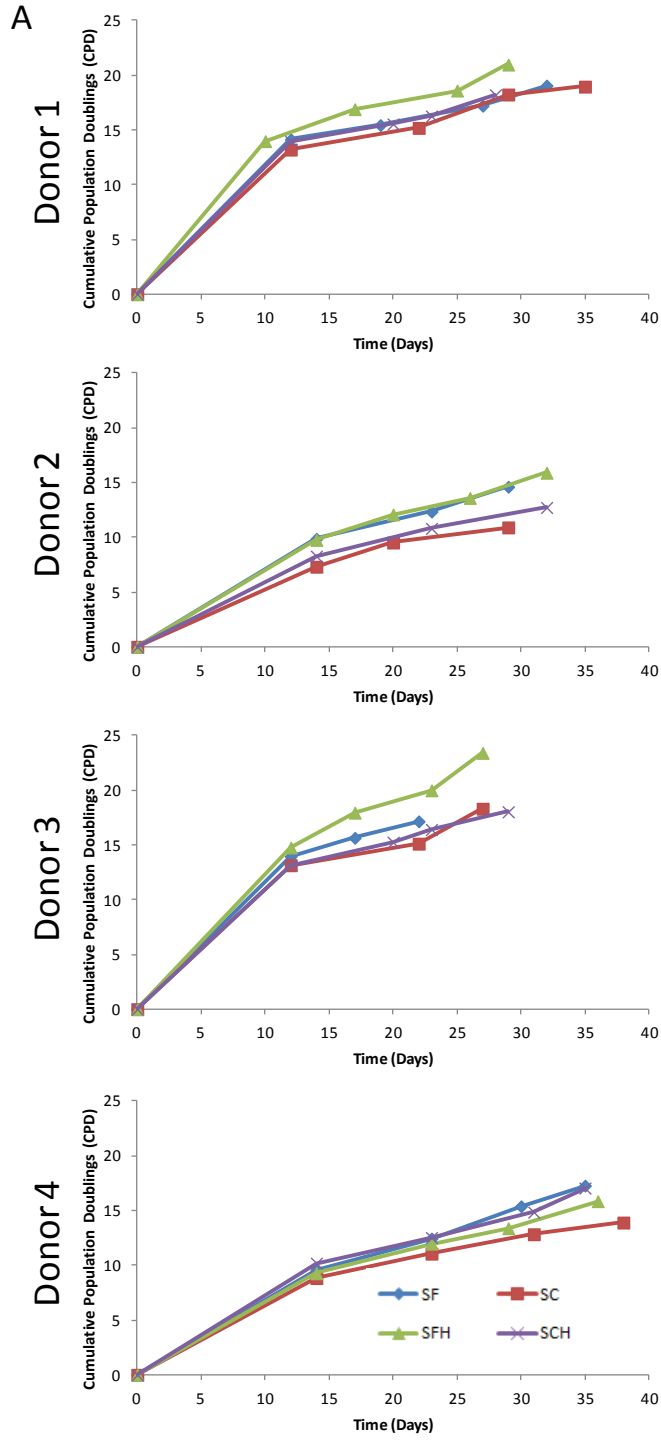


**Figure 3.3.1: CFU-fs isolated using serum-free medium are equivalent to serum-containing medium.** (A) Representative images of CFU-fs in 6-well plates stained 10 days post-isolation from bone marrow. (B) Representative images of typical colonies observed at 4x magnification (Scale bar: 500 $\mu$ m). Quantitative analysis of CFU-f number normalised to  $1 \times 10^6$  MNCs seeded. No statistical difference was observed in CFU-f number. Data is presented as the mean  $\pm$  SD,  $n=3$  biological replicates. Statistical analysis performed using two-way ANOVA with Bonferroni post-test.

### 3.3.2 Growth kinetics of SF and SC cells isolated and cultured in hypoxia and normoxia

Growth kinetics of each culture were assessed by calculating population doublings of cells versus days in culture based on cell yields at the end of each passage. Growth curves indicate similar growth profiles of MSCs in all conditions. Predicted cell yields for four MSC donors are presented in figure 3.3.2b. These are based on growth kinetics of MSCs in the appropriate group, assuming the entire marrow was isolated and cultured in that condition. Data indicates SF MSCs in hypoxia may proliferate faster in hypoxia but this difference was not statistically significant due to inter-group and inter-donor variation.

# Chapter Three



B

Donor	1	2	3	4	
Serum	1.3E+10	9.1E+09	2.4E+08	3.5E+08	Normoxia
Serum-free	1.5E+10	1.5E+10	6.2E+09	1.1E+09	
Serum	7.9E+09	7.5E+09	1.5E+09	1.4E+09	Hypoxia
Serum-free	5.6E+10	3.9E+11	2.2E+09	9.8E+08	

Predicted Yields (30mL marrow) @ P3

**Figure 3.3.2: Growth kinetics of serum-free (SF) and serum-containing (SC) isolated cells in normoxia (21% O<sub>2</sub>) compared to hypoxia (2% O<sub>2</sub>).** (A) Representative growth kinetics of 4 biological replicates of SF and SC MSCs cultured in normoxia and hypoxia. SF; serum-free normoxia, SC; serum-containing normoxia, SFH; serum-free hypoxia, SCH; serum-containing hypoxia. (B) Predicted cell yields of 4 MSC donors based on calculated growth curves for those donors assuming the entire marrow was cultured in the relevant group. No statistical difference observed in predicted cell yields using one-way ANOVA with Bonferroni post-test. Inter-donor variability.

### 3.3.3 Serum-free isolated cells have morphology distinct from serum-containing isolated cells

MSC morphology was observed using microscopy. SF MSCs appear to be smaller in size in both hypoxia and normoxia compared to SC MSCs. The morphology of each cell group was unaffected by culture in either hypoxia or normoxia. MSC images were taken at passage 3. Both cells maintained the typical fibroblastic cell morphology but were distinct from each other. Cell size was assessed using the Sceptor hand-held automated cell counter 2.0 (Millipore). Increase in cell size is observed in SC cultured MSCs. Data presented on cell size was carried out on normoxia-cultured MSCs. Data not available for hypoxia-cultured MSCs.

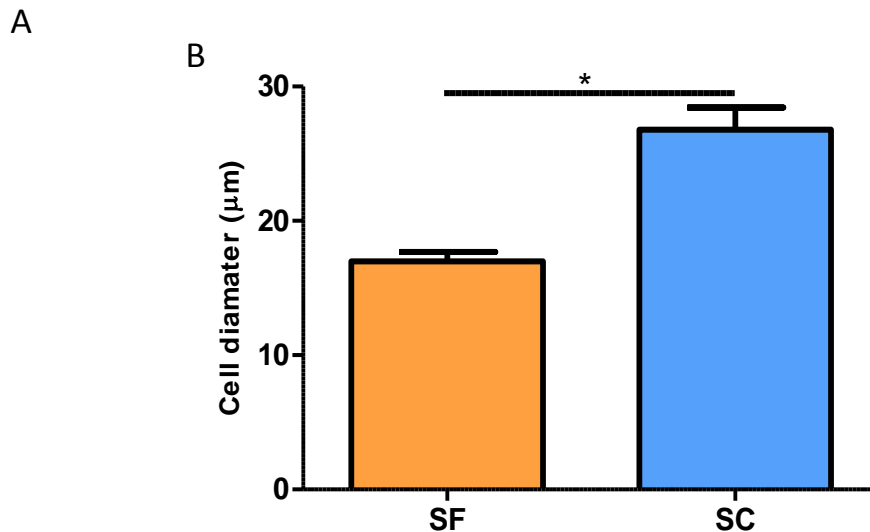


**Figure 3.3.3 Morphology and size of MSCs was altered by culture of MSCs in SF and SC medium.** (A) Images presented are 4x magnification images and are representative of 4 MSC donors. Scale bar: 500µm. (B) Cell diameter of SF and SC MSCs cultured in normoxia. Increase observed in cell diameter of SC MSCs compared to SF-cultured MSCs. Statistical analysis was performed using an unpaired T-test with Welch's correction; \* $p \leq 0.05$ .

### 3.3.4 Normoxia cultured cells have increased osteogenic potential compared to hypoxia cultured cells

To determine the optimal culture conditions for MSCs to undergo osteogenic differentiation, SF and SC isolated and cultured cells in either hypoxia or normoxia were differentiated in osteogenic medium to assess the optimal culture conditions for osteogenesis. Cells were cultured in osteogenic medium for between 14-17 days and calcium deposition was assessed visually by alizarin red staining and quantitatively using the 'Stanbio Calcium Liquicolour Kit'. Results from alizarin red staining indicate increased calcium deposition in SC and SF cells cultured and differentiated in normoxia in comparison to hypoxia cultured/differentiated cells (Figure 3.3.4a). These findings were further verified by quantitative measurement of calcium levels. Quantification of calcium levels indicated that normoxia-cultured MSCs had increased calcium production which was reduced by culture of these cells in hypoxia (Figure 3.3.4b). No statistical difference was observed between SF and SC cells within either hypoxia or normoxia groups. Negative control MSCs i.e. MSCs

cultured in standard SC MSCs for the duration of the differentiation assay demonstrated no spontaneous osteogenesis (data not shown).

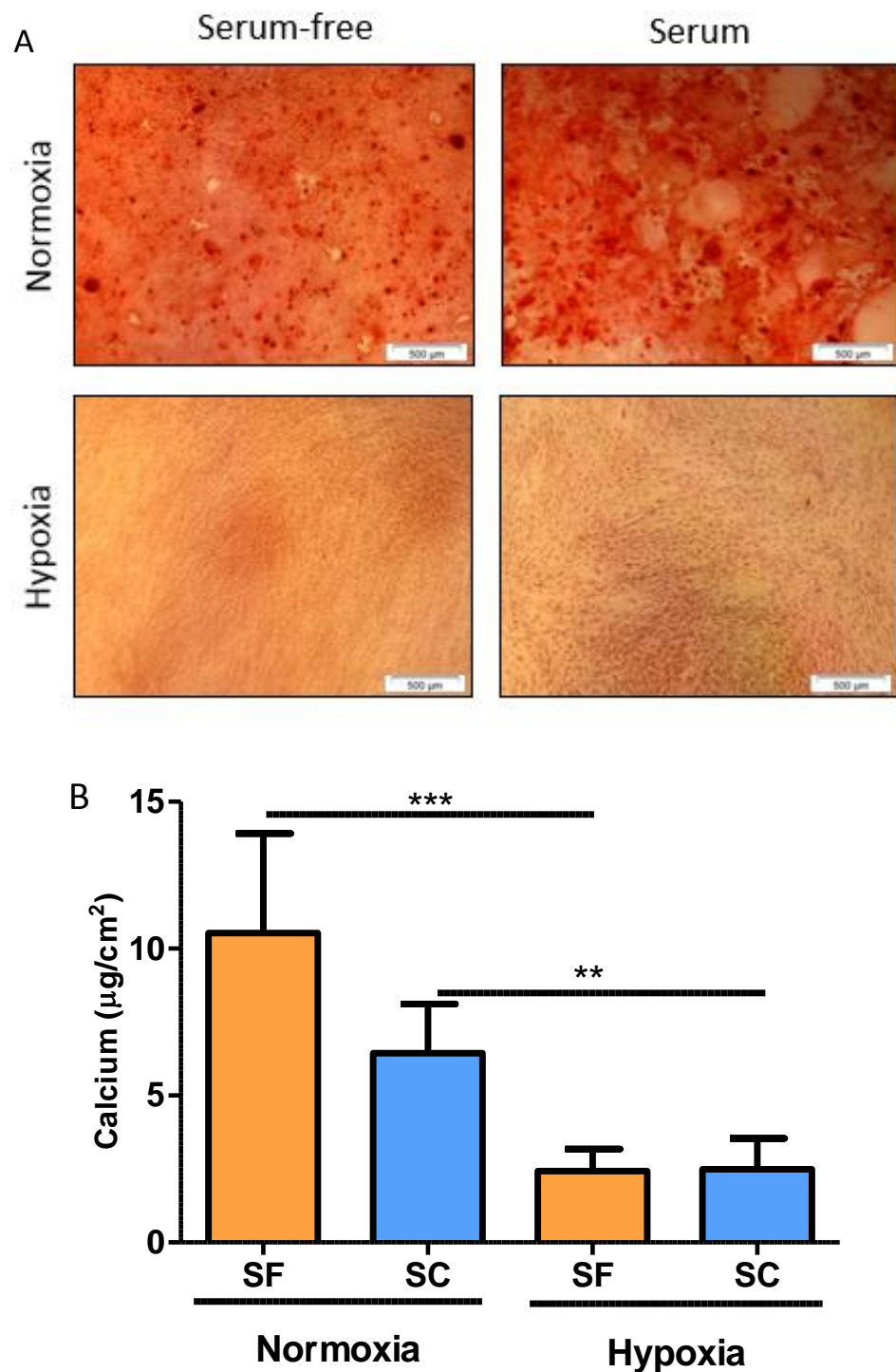


**Figure 3.3.4: Osteogenic potential of cells was enhanced in normoxia cultured cells and was maintained in all conditions. (A) Representative alizarin red staining of SF and SC cells in normoxia or hypoxia cultured MSCs indicate osteogenic potential of MSCs is maintained in various culture conditions and is increased in**

*normoxia compared to hypoxia. (B) Osteogenic differentiation potential was further assessed by quantification of calcium deposition displayed as calcium levels represented as  $\mu\text{g}/\text{cm}^2$ . These results further validated the results observed by the alizarin red staining. Results are presented as the mean  $\pm$  standard deviation (SD) of 3 biological replicates,  $**p\leq 0.01$ ,  $***p\leq 0.001$  as determined using two-way ANOVA and Bonferroni's multiple comparisons post-test.*

### **3.3.5 Adipogenic potential of MSCs is reduced by hypoxia and is unaffected by use of SF or SC media**

To determine the optimal culture conditions for MSCs to undergo adipogenic differentiation, SF and SC isolated and cultured cells in either hypoxia or normoxia were differentiated in adipogenic medium to assess the optimal culture conditions for adipogenesis. Cells were induced with adipogenic induction medium and fed for approximately 15 days in altering cycles of adipogenic induction medium and adipogenic maintenance medium. Oil red O staining of lipid vacuoles demonstrated a significant depletion of the adipogenic potential of MSCs in hypoxia in comparison to normoxia (Figure 3.3.5a). Quantification of Oil red O staining was performed by extraction of Oil red O staining in 99% isopropanol and measurement of the extracted stain (Figure 3.3.5b). SF and SC cells in normoxia displayed equivalent lipid accumulation indicated by Oil red O staining and quantification. This lipid accumulation was reduced in both cell groups when cultured in hypoxia (Figure 3.3.5a & b). Negative control MSCs i.e. MSCs cultured in standard SC MSCs for the duration of the differentiation assay demonstrated no spontaneous adipogenesis (data not shown).

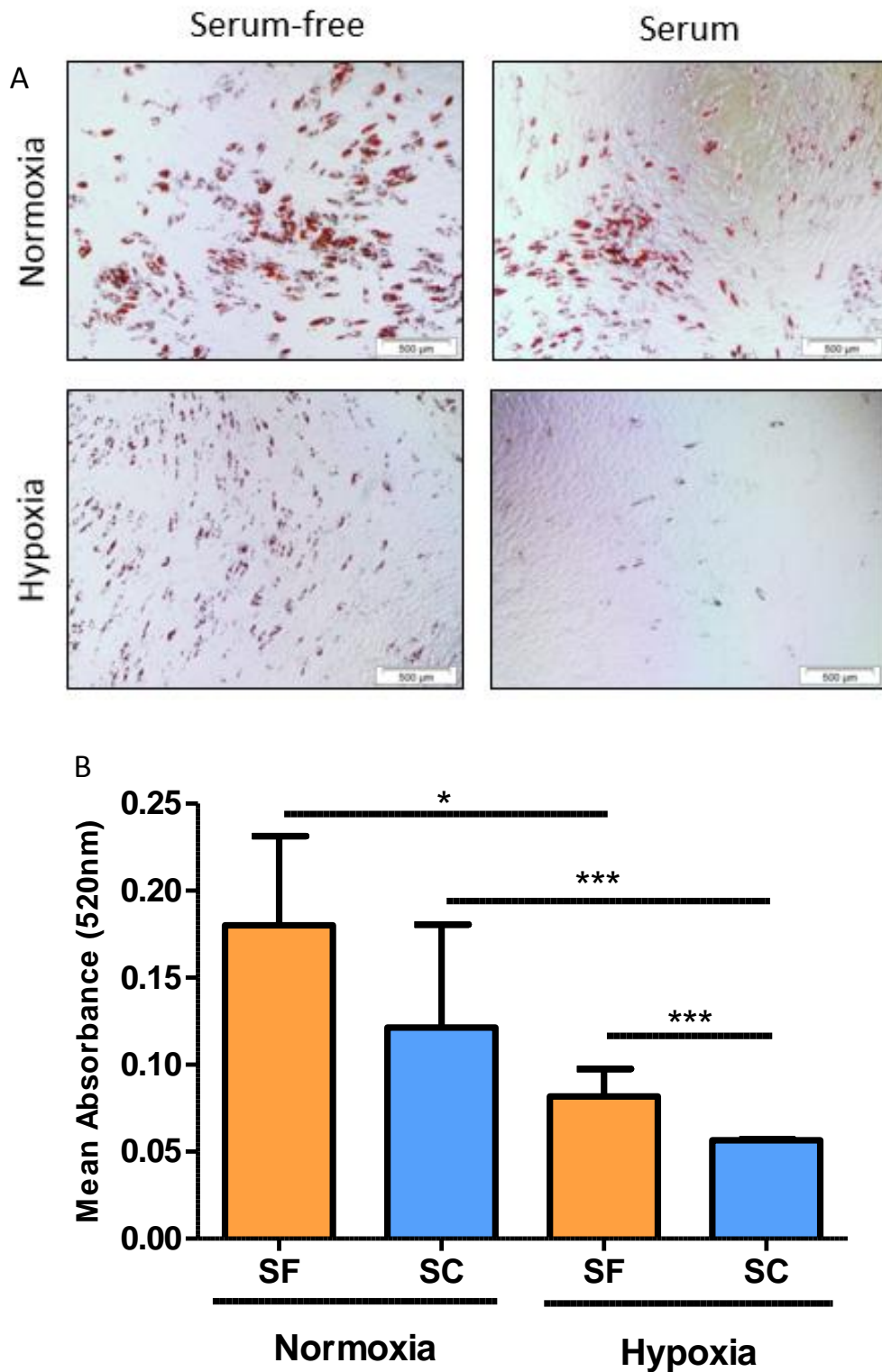


**Figure 3.3.5: Adipogenic potential of cells was enhanced in normoxia cultured cells and was maintained in all conditions. (A) Representative Oil red O staining of SF and SC cells in normoxia or hypoxia cultured MSCs indicates adipogenic potential of MSCs is maintained in various culture conditions and is increased in normoxia compared to hypoxia. (B) Adipogenic differentiation potential was further assessed by quantification of Oil red O. These results further validated the results observed by**

*the Oil red O staining. Results are presented as the mean  $\pm$  standard deviation (SD) of 3 biological replicates, \* $p \leq 0.05$ , \*\*\* $p \leq 0.001$  as determined using two-way ANOVA and Bonferroni's multiple comparisons post-test.*

### **3.3.6 Chondrogenic potential of SF cultured cells is increased in hypoxia**

To determine the optimal culture conditions for MSCs to undergo chondrogenic differentiation, SF and SC isolated and cultured cells in either hypoxia or normoxia were differentiated in chondrogenic medium supplemented with TGF- $\beta$ 3 to assess the optimal culture conditions for chondrogenesis. Cells were cultured in chondrogenic medium for 21 days. Chondrogenesis was assessed histologically by Safranin O staining (Figure 3.3.6a) and by measurement of sulfated-glycosaminoglycan (sGAG) using the DMMB assay (Figure 3.3.6b). Sulfated-GAG levels were normalised to DNA content using the picogreen assay (Figure 3.3.6b). SF cultured cells displayed increased chondrogenesis assessed by GAG: DNA levels in hypoxia compared to SF cells in normoxia. No differences were observed between SF and SC cells cultured in normoxia or hypoxia. Safranin O staining of GAG indicated an increase in chondrogenesis of SF and SC cells in hypoxia compared to normoxia. This pro-chondrogenic effect of hypoxia was observed by the slight but not significant increase in chondrogenesis of SC cells cultured in hypoxia compared to normoxia and the significant increase in GAG levels of SF cells in hypoxia compared to normoxia. Differences in Safranin O staining of sGAG and quantitative sGAG levels can be accounted for due to the random selection of histological slides for Safranin O staining and the non-uniform presence of sGAG in chondro pellets. Quantitative sGAG levels measure the total sGAG levels normalised to DNA content. Negative control MSCs i.e. MSCs cultured in ICM for the duration of the differentiation assay demonstrated no spontaneous chondrogenesis (data not shown).

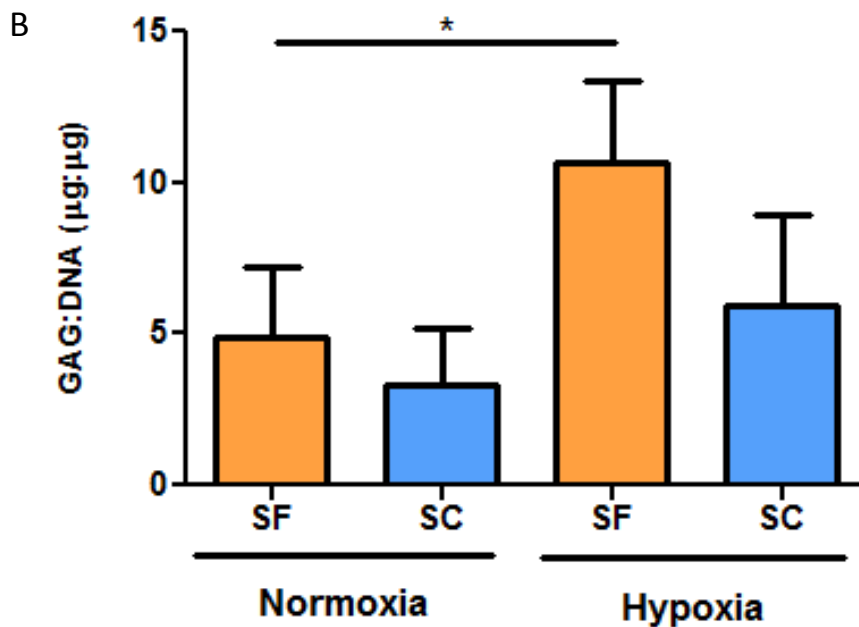
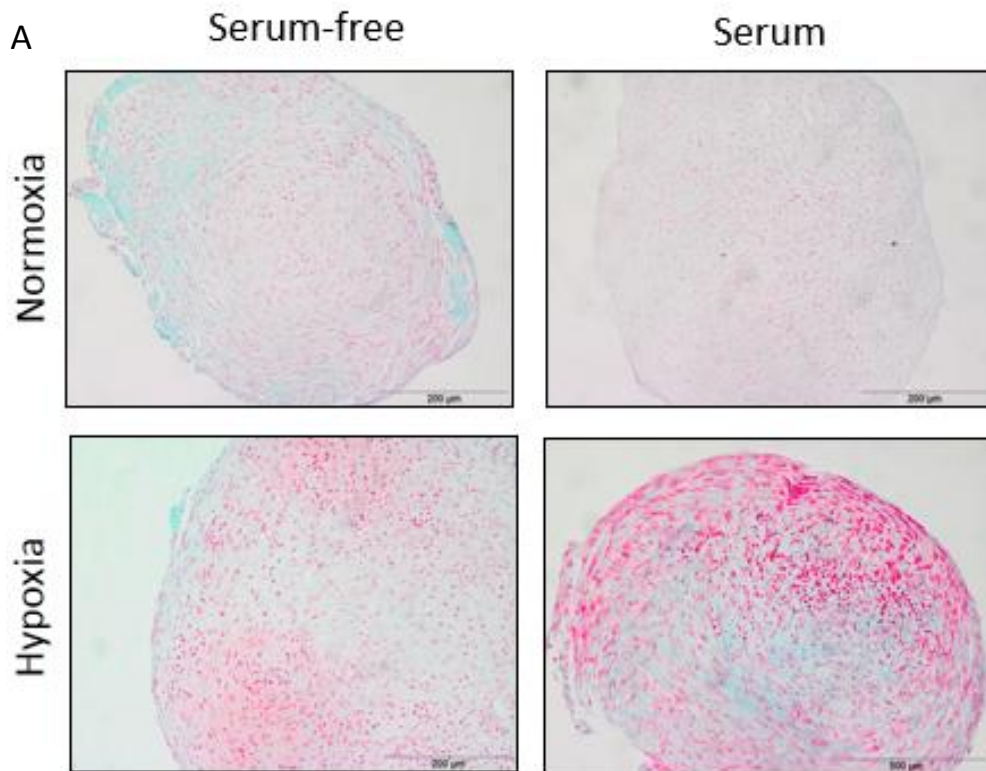


**Figure 3.3.6: Chondrogenic potential of SF cells was enhanced in hypoxia cultured cells and was maintained in all conditions.** (A) Representative Safranin O staining of SF and SC cells in normoxia or hypoxia cultured MSCs indicates chondrogenic potential of MSCs is maintained in various culture conditions and is increased in hypoxia compared to normoxia. (B) Chondrogenic differentiation potential was further assessed by quantification of sGAG levels normalised to DNA content. These

*results further validated the results observed by the Safranin O staining. Results are presented as the mean  $\pm$  standard deviation (SD) of 3 biological replicates, \* $p \leq 0.05$ , as determined using two-way ANOVA and Bonferroni's multiple comparisons post-test.*

### **3.3.7 Flow cytometry evaluation of bone marrow-derived MSCs**

As part of the criteria for defining a bone marrow-derived MSC according to the ISCT (Dominici et al., 2006a), surface marker expression of MSC markers CD105, CD73 and CD90 must be observed at levels  $\geq 95\%$  and haematopoietic markers as outlined in table 2.1 must be expressed on less than 2% of the cells. To robustly assess marker expression on cells by flow cytometry, an appropriate gating strategy must be used. Issues that can generate false positive/negative data include high levels of cell debris, cell clumping and insufficient antigen blocking steps. To overcome these issues, the gating strategy outline below was used for all flow cytometry experiments assessing surface marker expression. All antibodies used were phycoerythrin (PE) conjugated IgG1 antibodies with the exception of HLA-DR which was a PE-conjugated IgG2b as defined in table 2.1. Cell staining protocols used are outlined in 2.11. The gating strategy first separates MSCs from cell debris and proteins which may be in staining buffer by plotting cell size (forward scatter area, FSC-A) versus cell granularity (side scatter area, SSC-A). Following separation of MSCs from debris, cell doublets or clumps need to be excluded. Cell doublets are an issue where two or more cells are stuck together and those cells have different expression profiles. Depending on which cell is read by the flow cytometer, this may report both a false positive or negative expression of both cells for a specific marker as it is not possible to distinguish the two cells from each other. Doublets are excluded by plotting the cell size or area (FSC-A) versus the cell diameter (Forward scatter height, FSC-H). Where, clumping occurs cells will fall outside the defined region in figure 3.3.7 'Single Cell gate'. Dead cells are also excluded from analysis as false binding of antibodies can bind to the compromised cell membrane. Finally expression of all antibodies was assessed in relation to expression of the isotype control at a matched concentration to the antibody to distinguish non-

specific binding from true antigen recognition. In all experiments,  $1 \times 10^4$  live, single cells were assessed sample.

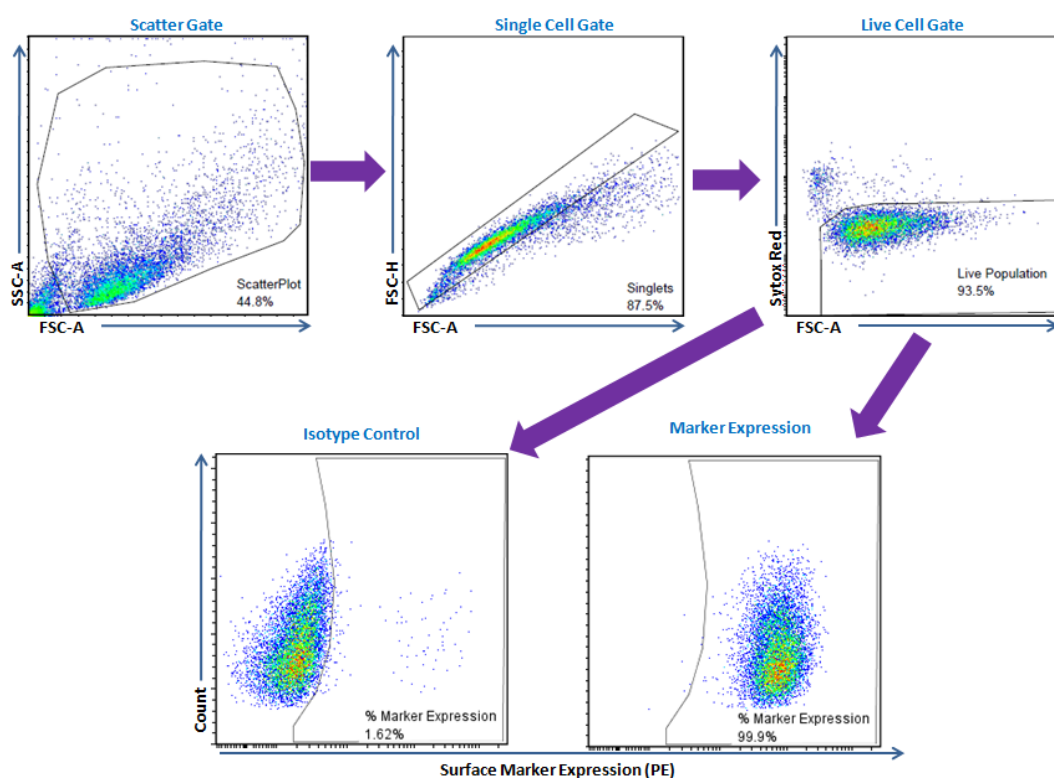


**Figure 3.3.7: Gating strategy for flow cytometry analysis of surface marker expression of bone marrow-derived MSCs.** MSCs were first identified based on cell size and granularity by plotting forward scatter area (FSC-A) versus side scatter area (SSC-A) to exclude debris. Subsequently, double cells and cell clumps were excluded by plotting forward scatter height (FSC-H) versus forward scatter area (FSC-A). Sytox red viability stain was used to exclude non-viable cells. MSCs were then assessed for specific marker expression in comparison to the appropriate isotype control. All antibodies tested were IgG1 antibodies with the exception of HLA-DR which is an IgG2 antibody and was plotted versus its appropriate control. Staining protocols are outlined in section 2.11.

### 3.3.8 Increased expression of CD271 and CD146 on serum-free MSCs

To assess whether the MSCs isolated and cultured in SF medium satisfied the ISCT criteria for definition as MSCs, SF and SC MSCs isolated and cultured in normoxia and hypoxia were assessed for expression of the markers reported in figures 3.3.8a&b. SF MSCs maintained  $\geq 95\%$  expression of MSC markers CD105, CD73 and

## Chapter Three

CD90 in both hypoxia and normoxia. Equivalent expression profiles were observed for the SC MSCs in both conditions. In addition to the ISCT panel, expression of CD271 and CD146 was also assessed. CD271 was a marker previously reported to select the entire CFU-f population of stromal cells from bone marrow (Jones et al., 2002). This marker is typically lost during culture of MSCs in the presence of FBS and is not observed in cells beyond the end of P0 (Boxall and Jones, 2012). SF isolated and expanded MSCs maintained expression of CD271 in both normoxia (figure 3.3.8a) and hypoxia (3.3.8b). Expression of CD271 is highly variable between MSC donors in normoxia and more stably expressed in hypoxia. Expression of CD271 was not observed in SC MSCs in either hypoxia or normoxia. Furthermore, CD146 has also previously been reported to enrich for a population of MSCs from bone marrow (Sacchetti et al., 2007b). Expression of CD146 was maintained in SC isolated and expanded cells in both hypoxia and normoxia. This expression was mirrored in the SF cells but with a higher number of cells maintaining this expression.

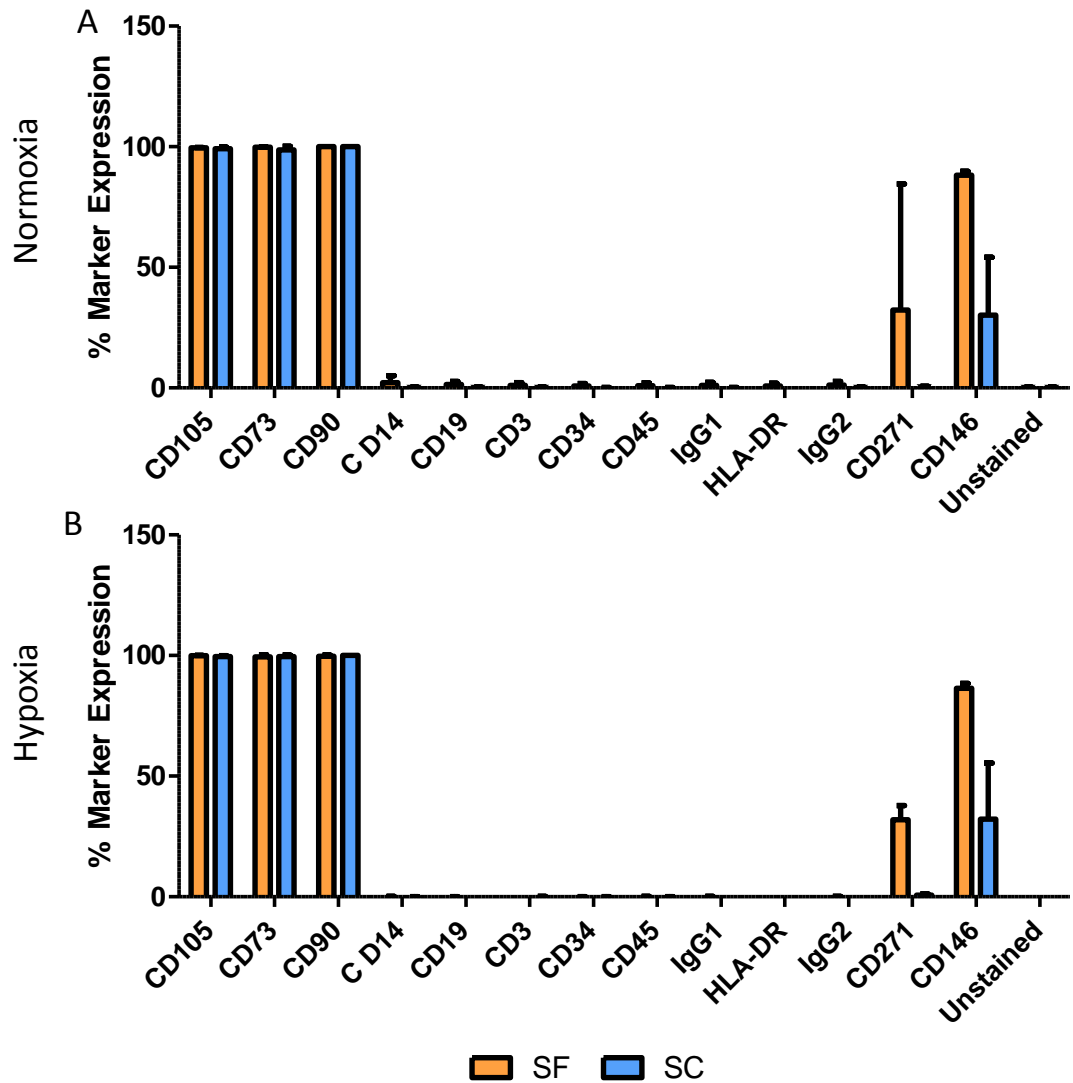


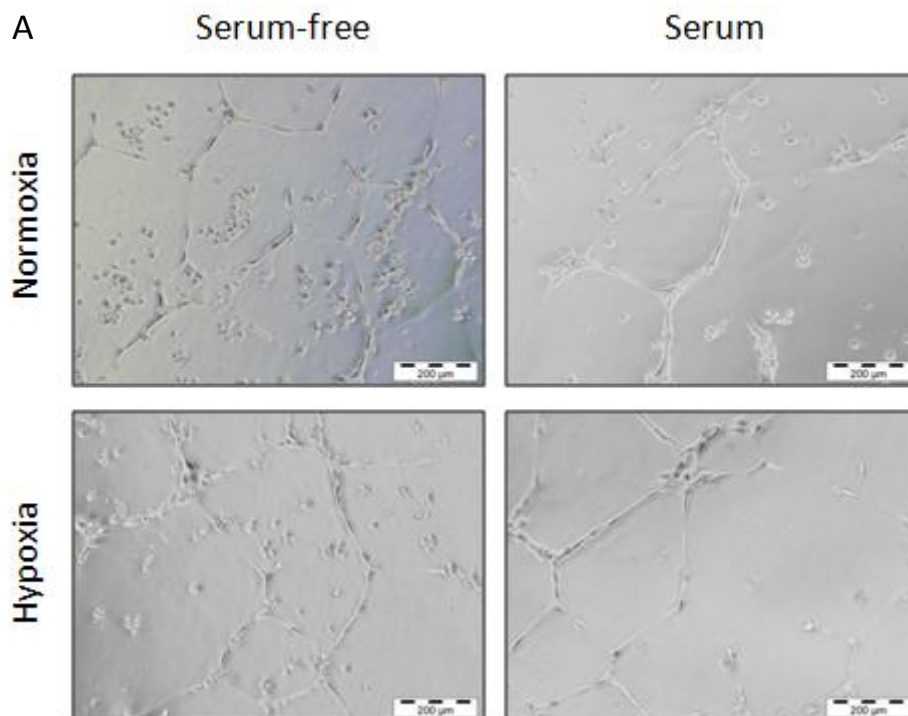
**Figure 3.3.8: Surface marker characterisation of bone marrow-derived MSCs.** (A) Quantitative marker expression of SF (orange) and SC (blue) MSCs cultured in normoxia. (B) Quantitative marker expression of SF (orange) and SC (blue) MSCs cultured in hypoxia. Results are presented as the mean  $\pm$  standard deviation (SD) of 3 biological replicates of MSCs at the end of P3.

### 3.3.9 Serum-free MSCs display increased pro-angiogenic potential

MSCs have previously been reported to secrete pro-angiogenic factors (Singer and Caplan, 2011) that can contribute to their therapeutic efficacy. The pro-angiogenic effect of MSCs was assessed by co-culturing of human umbilical cord vein epithelial cells (HUVECs) with conditioned medium from MSCs in SF and SC medium in either hypoxia or normoxia. Details of the experimental setup are outlined in section 2.13.

## Chapter Three

Briefly, to standardise collection of medium, equivalent numbers of MSCs were seeded in T-175 flasks and allowed to reach 50% confluency at which point a full medium change was carried out. Subsequently, after 3 days of conditioning of the medium with the cells, the medium was harvested. Conditioned media was harvested and centrifuged at 400xg for 5mins to remove any cells present. Conditioned media was then stored at -80°C until use. To discriminate between the effect of the medium itself and the cells, unconditioned medium (not exposed to cells) was prepared in T-175 flasks in conjunction with conditioned medium. Media samples were co-cultured with HUVEC cells for 18hrs and tubule numbers per well were determined. Tubules were defined as any fully formed tube joining two or more bridging points. All groups resulted in the formation of tubules. Oxygen level had no intra-group effect in either SC or SF media groups. SF media groups demonstrated a greater fold increase in tubule formation compared to the media control compared to SC media groups. This effect was independent of oxygen levels.



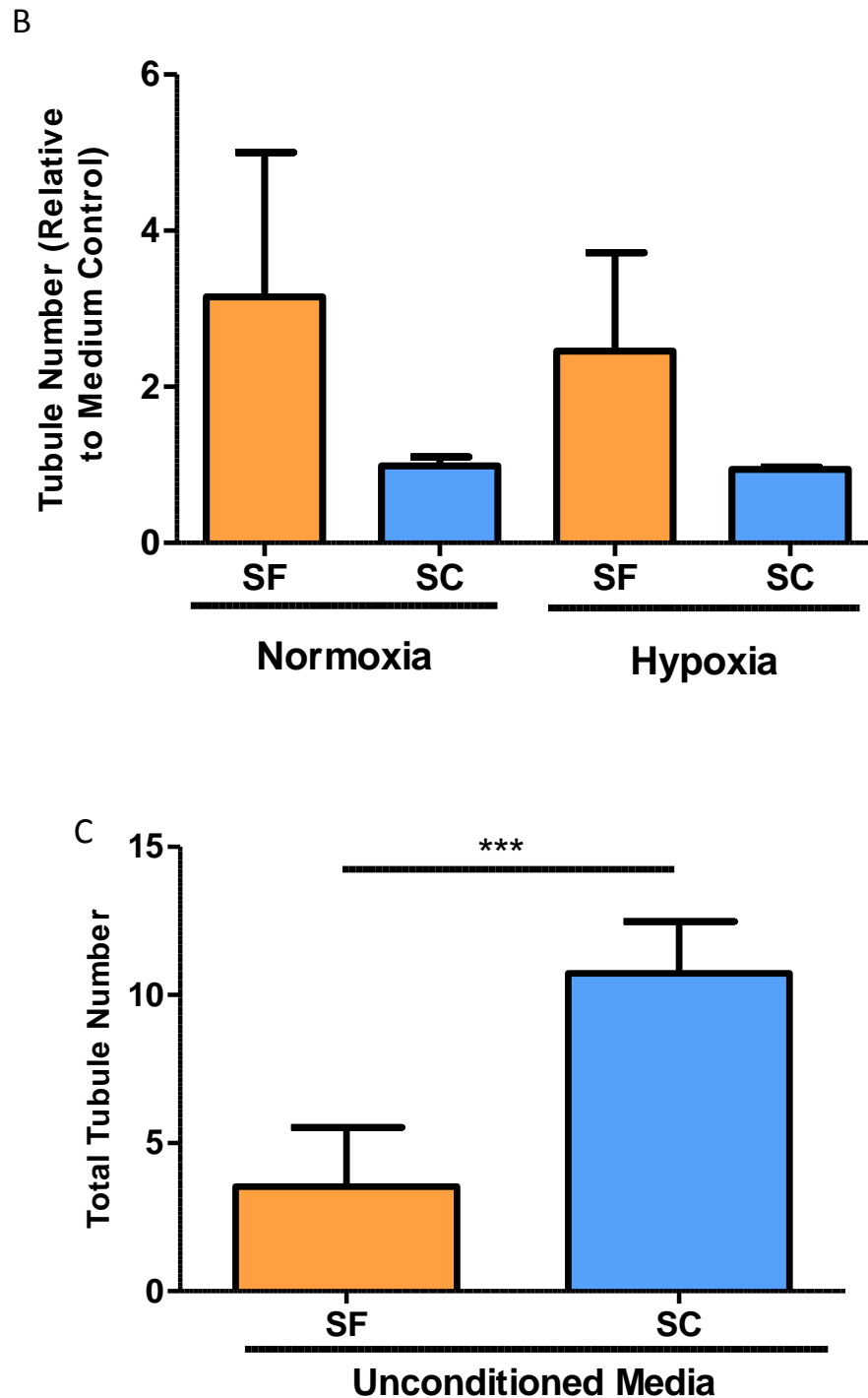


**Figure 3.3.9: Angiogenic potential of human umbilical vein epithelial cells (HUVEC) cells cultured in the presence of MSC conditioned medium.** (A) Representative images of HUVEC-derived tubules 18hrs post culture in the presence of MSC conditioned media on Matrigel. Scale bar: 200 $\mu$ m. (B) Quantitative analysis of tubule number formed after co-culture of SF and SC MSC conditioned medium from either hypoxia or normoxia. Three biological replicates were assessed with three technical replicates. Five random fields were selected in each well and tubules identified as a complete connection of tubule between at least two bridging points. Tubule number is represented as a fold change of unconditioned basal media

*appropriate to each cell group. (C) Quantitative analysis of total tubule number generated by HUVEC cells exposed to either SF or SC medium unconditioned by cells. Results are presented as the mean  $\pm$  standard deviation (SD) of 3 biological replicates, \* $p \leq 0.001$  using two-way ANOVA and Bonferroni's multiple comparisons post-test.*

### **3.3.10 Flow cytometry gating strategies to assess the immunosuppressive & immunogenic potential of MSCs**

To determine the effect of MSCs on T-lymphocyte proliferation, PBMCs were isolated from healthy volunteers as described in 2.12. After stimulation of T-lymphocytes, cells were stained with CD4 and assessed for proliferation by flow cytometry. The gating strategy outlined below outlines the process for determining T-lymphocyte proliferation. Initially, lymphocytes are distinguished from other mononuclear cells based on cell size and granularity. Following this, doublets and cell clumps are excluded. Subsequently, a CD4+ and CD4- T-lymphocyte population is identified. These populations are then assessed for proliferation assessed by CFSE expression.

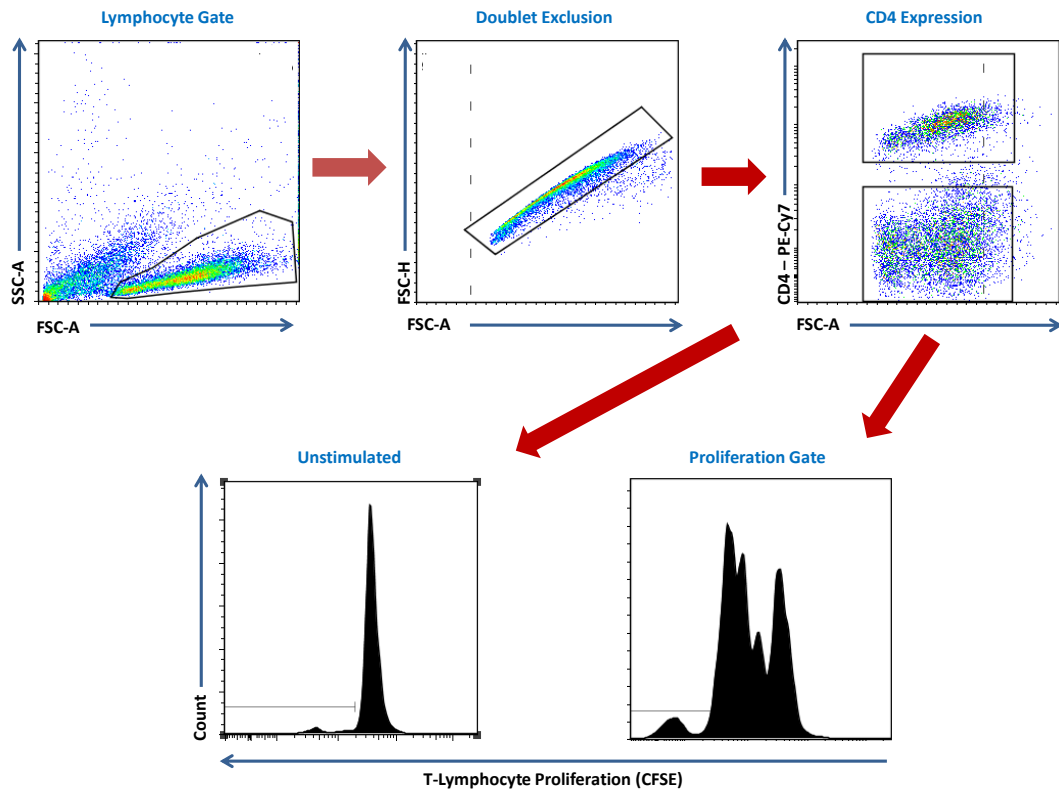


**Figure 3.3.10: Gating strategy for flow cytometry analysis of T-lymphocyte expression.** Lymphocytes were first identified based on cell size and granularity by plotting forward scatter area (FSC-A) versus side scatter area (SSC-A) to exclude debris. Subsequently, double cells and cell clumps were excluded by plotting forward scatter height (FSC-H) versus forward scatter area (FSC-A). CD4 expression was then used to distinguish CD4+ and CD4- (CD8+) T-lymphocytes.

### **3.3.11 Immunosuppressive effect of MSCs is unaffected by use of serum-free medium**

To demonstrate the immunosuppressive nature of MSCs cultured in SF and SC medium in hypoxia and normoxia, peripheral blood mononuclear cells (PBMCs) were isolated from healthy volunteers as outlined in sections 2.12.1-4. PBMCs were labelled with CFSE and co-cultured with various ratios of MSCs to PBMCs as reported in figure 3.3.11 for 4 days. T-lymphocytes were distinguished from other PBMCs including monocytes based on the scatter plot as described in figure 3.3.10. Additionally, cells were stained with CD4 to identify the CD4<sup>+</sup> and CD4<sup>-</sup> fraction of T-lymphocytes. T-cells were activated to proliferate by the addition of CD3 and CD28 antibodies. Proliferation of cells was measured by flow cytometric analysis of CFSE expression. CFSE expression is sequentially halved in daughter cells following cell division. For this reason, it can be used to measure the number of divisions undertaken by a cell. Immunosuppression of stimulated T-cells by MSCs resulted in a reduction of proliferation (Figure 3.3.11). Figures 3.3.11a-b report the immunosuppressive effect of CD4<sup>+</sup> and CD4<sup>-</sup> T-lymphocytes respectively at 1:5, 1:20 and 1:50 ratios of MSC: T-lymphocyte with MSCs cultured in normoxia. Both cell types suppressed the stimulated lymphocyte group (black) with no difference observed between SF and SC groups at any ratio. Figures 3.3.11c-d report the immunosuppressive effect of CD4<sup>+</sup> and CD4<sup>-</sup> T-lymphocytes respectively at 1:5, 1:20 and 1:50 ratios of MSC: T-lymphocyte with MSCs cultured in hypoxia. Functionality of the assay is defined by stimulated T-lymphocytes undergoing proliferation in  $\geq 50\%$  of the population compared to the unstimulated T-lymphocytes. Assessment of the immunosuppressive effect of hypoxia cultured T-lymphocytes was not possible in low oxygen levels due to insufficient proliferation of T-lymphocytes. Results are presented as the mean  $\pm$  standard deviation (SD) of 3 biological replicates. No statistical difference was observed in normoxia using two-way ANOVA and Bonferroni's multiple comparisons post-test. Statistical difference was observed in CD4<sup>-</sup> T-lymphocytes at 1:20 and 1:50 ratio of MSC: T-lymphocyte in hypoxia. \*\*  $p \leq 0.01$ .

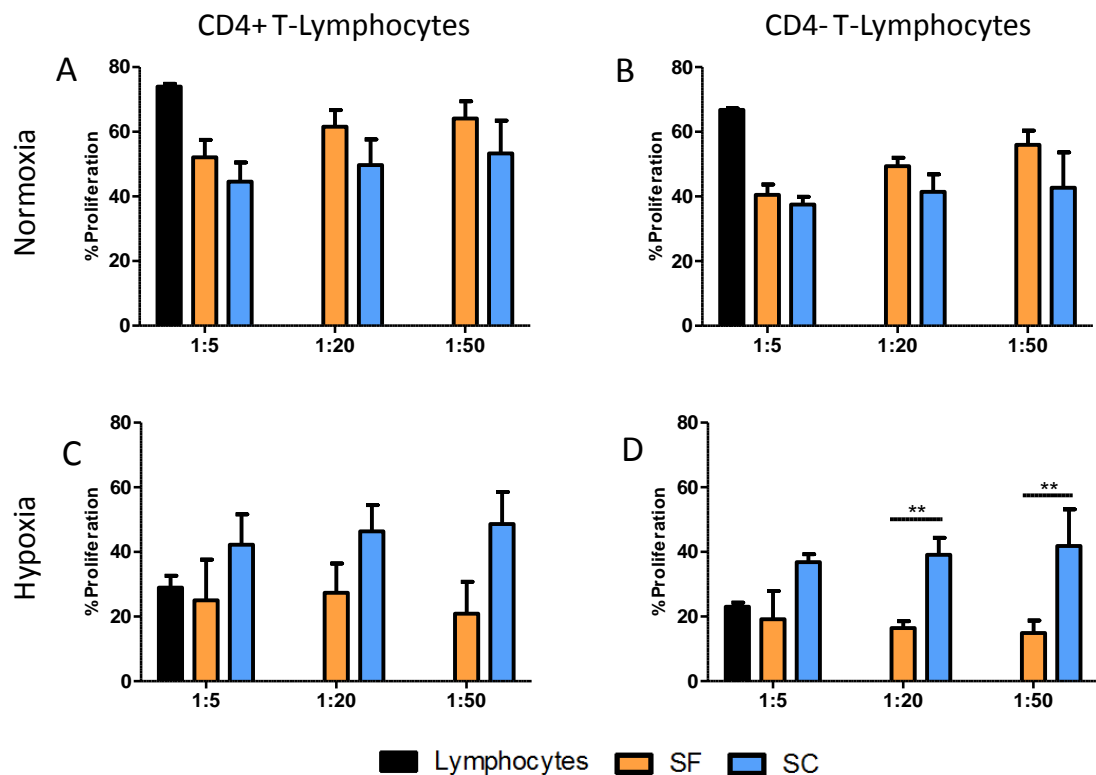


**Figure 3.3.11: Immunosuppressive effect of MSCs on CD28/CD3 antibody stimulated peripheral blood T-lymphocytes.** Percentage proliferation of CD3/CD28 stimulated T-lymphocytes compared to unstimulated T-lymphocytes. (Black) Non-immunosuppressed T-lymphocytes, (Red) Co-culture of SF-cultured MSCs with stimulated T-lymphocytes, (Blue) Co-culture of SC-cultured MSCs with stimulated T-lymphocytes. (A) Effect of normoxia cultured MSCs on CD4+ T-lymphocytes at various ratios of MSCs: T-lymphocytes. (B) Effect of normoxia cultured MSCs on CD4- T-lymphocytes at various ratios of MSCs: T-lymphocytes. (C) Effect of hypoxia cultured MSCs on CD4+ T-lymphocytes at various ratios of MSCs: T-lymphocytes. (D) Effect of hypoxia cultured MSCs on CD4- T-lymphocytes at various ratios of MSCs: T-lymphocytes. Results are presented as the mean  $\pm$  standard deviation (SD) of 3 biological replicates with 3 technical replicates,  $**p < 0.01$ , as determined using two-way ANOVA and Bonferroni's multiple comparisons post-test.

### 3.3.12 Immunogenicity of MSCs cultured in SF and SC media

To demonstrate the immunogenic nature of MSCs cultured in SF and SC medium in hypoxia and normoxia, PBMCs were isolated from healthy volunteers as outlined in sections 2.12.1-4 in an identical experimental setup as described above in section 3.3.11. PBMCs were labelled with CFSE and co-cultured with various ratios of MSCs

## Chapter Three

to PBMCs as reported in figure 3.3.12 for 5 days. T-lymphocytes were distinguished from other PBMCs including monocytes based on scatter plot as described in figure 3.3.10. Additionally, cells were stained with CD4 to identify the CD4<sup>+</sup> and CD4<sup>-</sup> fraction of T-lymphocytes. Stimulated T-lymphocytes (black) were activated to proliferate by the addition of CD3 and CD28. T-lymphocytes in MSC groups (Orange and blue) were not stimulated to proliferate by CD3 and CD28. MSCs were co-cultured with T-lymphocytes to assess ability to activate proliferation and thus an immune response. Proliferation of cells was measured by flow cytometric analysis of CFSE expression (Figure 3.3.12). Figures 3.3.12a-b report the immunogenic effect of CD4<sup>+</sup> and CD4<sup>-</sup> T-lymphocytes respectively at 1:5, 1:20 and 1:50 ratios of MSCs: T-lymphocytes with MSCs cultured in normoxia. No difference was observed in the CD4<sup>-</sup> group (Figure 3.3.12b) at any ratio. At the 1:5 ratio in the CD4<sup>+</sup> group (Figure 3.3.12a) a statistically significant increase in T-lymphocyte activation was reported with no difference at other ratios. Figures 3.3.12c-d report the immunogenic effect of CD4<sup>+</sup> and CD4<sup>-</sup> T-lymphocytes respectively at 1:5, 1:20 and 1:50 ratios of MSCs: T-lymphocytes with MSCs cultured in hypoxia. Mirroring the immunosuppressive assay (Figure 3.3.11), the assessment of immunogenic effect of hypoxia cultured T-lymphocytes is not possible in low oxygen levels due to insufficient proliferation of T-lymphocytes. Results are presented as the mean  $\pm$  standard deviation (SD) of 3 biological replicates. Statistical analysis was performed using two-way ANOVA and Bonferroni's multiple comparisons post-test. Statistical difference was observed in CD4<sup>+</sup> T-lymphocytes at 1:5 in normoxia. \* $p \leq 0.01$ .

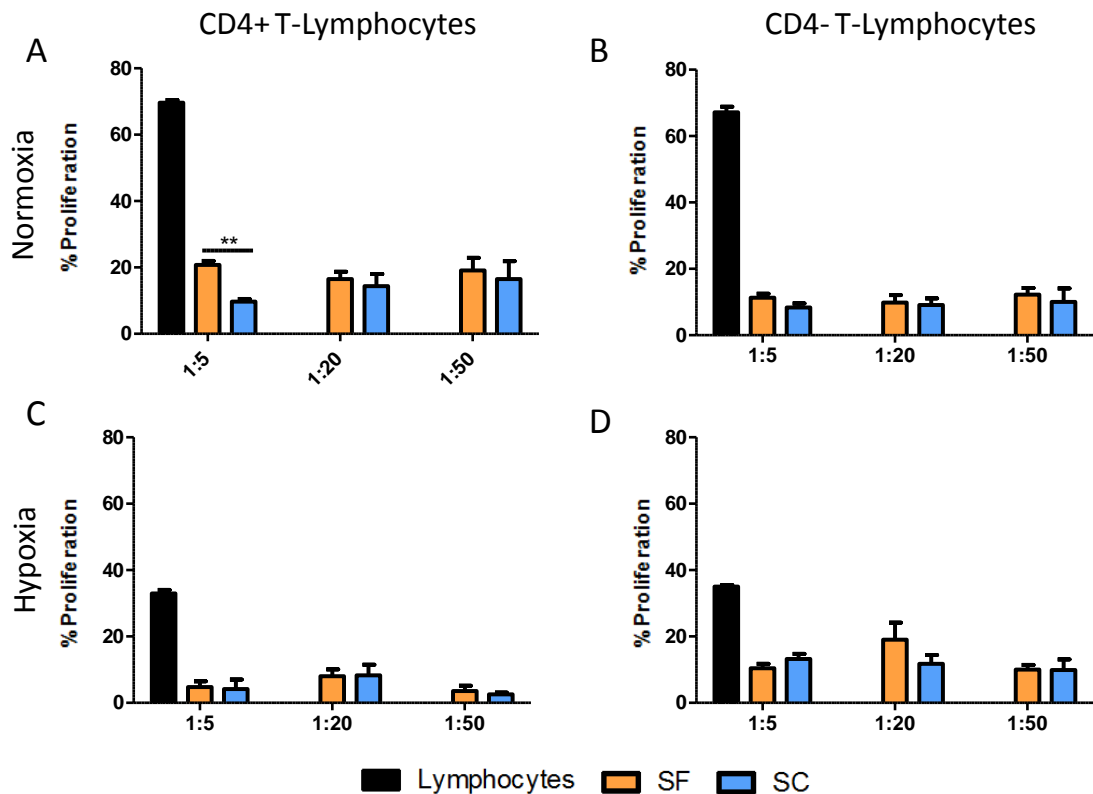


**Figure 3.3.12: Immunogenic potential of MSCs on unstimulated peripheral blood T-lymphocytes.** Percentage proliferation of CD3/CD28 stimulated T-lymphocytes compared to unstimulated T-lymphocytes. (Black) Stimulated T-lymphocytes alone, (Red) Co-culture of SF-cultured MSCs with unstimulated T-lymphocytes, (Blue) Co-culture of SC-cultured MSCs with unstimulated T-lymphocytes. (A) Effect of normoxia cultured MSCs on CD4+ T-lymphocytes at various ratios of MSC: T-lymphocytes. (B) Effect of normoxia cultured MSCs on CD4- T-lymphocytes at various ratios of MSCs: T-lymphocytes. (C) Effect of hypoxia cultured MSCs on CD4+ T-lymphocytes at various ratios of MSCs: T-lymphocytes. (D) Effect of hypoxia cultured MSCs on CD4- T-lymphocytes at various ratios of MSCs: T-lymphocytes. Results are presented as the mean  $\pm$  standard deviation (SD) of 3 biological replicates with 3 technical replicates, \*\* $p \leq 0.01$ , as determined using two-way ANOVA and Bonferroni's multiple comparisons post-test.

### 3.4 Discussion

The aim of this chapter was to assess the effect of isolating MSCs in either hypoxia or normoxia in standard serum-containing or serum-free medium and to determine how this affected the MSC phenotype. This was done by isolating MSCs from the bone marrow of healthy volunteers directly into the serum-free medium defined in section 2.1 or standard 10% serum-containing medium. These cells were culture expanded until the end of passage 3 at which point they were assessed for their tri-lineage differentiation capacity, surface marker phenotype and immunosuppressive/immunogenicity characteristics. Additionally conditioned medium was collected from these cells during culture to assess the pro-angiogenic potential of these cells.

After isolation of cells from bone marrow, MSCs were assessed for their ability to form CFU-f as this was how the MSCs were originally identified by Freidenstein et al (Friedenstein et al., 1976). CFU-fs were stained with crystal violet and colony numbers counted. No statistical difference in colony number was observed between SF or SC groups or due to culture of cells in either hypoxia or normoxia. This was in contrast to literature which typically indicates an increase in colony number for MSCs isolated in 2% hypoxia (Grayson et al., 2006, Grayson et al., 2007b, Rochefort et al., 2006). The reasons for this inconsistency with current data are unclear especially since subsequently the behaviour of cells in hypoxia broadly falls in line with the literature. It is worth noting, these cells were maintained in a hypoxic incubator and feed and passaged in atmospheric normoxia. The use of a hypoxic chamber was not used to maintain these cells entirely in hypoxia. In addition, due to the nature of the harvest process, it is reasonable to assume MSCs isolated from bone marrow were those cells primarily in the perivascular niche with limited MSCs likely to be derived from endosteal niche. This would also increase the oxygen tension these cells are exposed to *in vivo*. In terms of differences between the SF and SC cells, there was a trend for higher numbers of colonies in SC medium but not to a significant degree. Additionally, cells in SF colonies appear to be smaller in size and more diffuse compared to SC colonies. This may be due to the presence of fibronectin used for the culture of SF MSCs although this is unlikely as

SF cells cultured in the absence of fibronectin have similar cell morphology (data not shown). Instead this may merely be a consequence of using a serum-free medium for the culture of cells as MSCs isolated in commercially available serum-free medium adopt a similar reduced cell size compared to serum-containing cells (Chapter 6).

In line with current literature, hypoxia improved the growth kinetics of MSCs compared to the same cells isolated and cultured in normoxia (Grayson et al., 2007a, Hung et al., 2012b). This was particularly evident in SF cultured cells which demonstrated an early increase in proliferation rates compared to their normoxia counterparts. Hypoxia has been repeatedly shown to increase MSC proliferation in culture exposed to serum (dos Santos et al., 2010, Holzwarth et al., 2010b, Hung et al., 2012a, Nekanti et al., 2010), a result mirrored here in MSC cultured in this novel SF medium. This increased proliferation of MSCs in hypoxia is vitally important for translation of MSC therapies as the use of hypoxia can result in faster production of cell products and ultimately delivery of cellular therapies to the clinic. In addition to increases in proliferation, hypoxia has been reported to maintain the undifferentiated state of the MSC via the Notch pathway although the exact mechanism for this process is not known (Gustafsson et al., 2005). It has been reported in the literature that Notch is associated with HIF-1 $\alpha$  blocks neuronal and myogenic differentiation. During this process HIF-1 $\alpha$  is recruited to a Notch promoter resulting in elevated expression of Notch (Gustafsson et al., 2005). In addition to this, increased expression of the stemness associated gene Oct-4 and associated protein were observed when umbilical cord-derived MSCs were maintained in hypoxia. Although no change in other stemness genes SOX2 and NANOG were observed which may suggest maintenance of stemness of MSCs in hypoxia (Tsang et al., 2013). This maintenance of stemness genes was also observed in a second study which demonstrated increased expression of NANOG and SOX2 in adipose-derived MSCs in hypoxia (Fotia et al., 2015).

Tri-lineage differentiation is a hallmark of MSCs and is required by the ISCT as part of the classification of a cell as an MSC (Krampera et al., 2013, Dominici et al., 2006a). To determine the effect of the use of the SF medium on MSC

differentiation, tri-lineage assays were carried out at the oxygen level that the cells were maintained in during culture. Osteogenesis was determined by Alizarin red staining of mineralisation and by quantification of calcium levels after 14 days of induction of the cells in osteogenic medium as outlined in section 2.7. No difference was observed between the SF and SC cells within either the hypoxia or normoxia groups indicating the SF medium maintains a similar osteogenic potential to conventional SC-cultured MSCs. A statistical increase in osteogenesis was observed in cells cultured in normoxia compared to those in hypoxia. A proposed mechanism for this was highlighted above; the down regulation of the master regulator of osteogenesis Runx2 by the HIF-TWIST pathway (Yang et al., 2011). TWIST is a downstream target of the Hif-1 $\alpha$  pathway and acts as a transcriptional repressor of runx2 resulting in the inhibition of osteogenesis. Here, this resulted in both a drop in calcium levels and alizarin red staining. Hypoxia has also been proposed reduce osteogenesis of MSCs by Notch signalling. Here Notch1 binds to Runx2 preventing its transcriptional activity and thus inhibiting osteogenesis (Xu et al., 2013). Conversely, the hypoxia mimicking drug desferrioxamine has been reported to increase osteogenesis via the Wnt canonical or  $\beta$ -catenin pathway (Qu et al., 2008), an effect not observed in this study.

A similar effect was observed in adipogenic assays. Adipogenesis was measured by Oil red O visualisation of fat formation and also quantified. No difference was observed between SF and SC groups in either hypoxia or normoxia. However, like osteogenesis, adipogenesis was observed to be reduced in hypoxia. This effect of hypoxia on adipogenesis is widely reported in the literature (Yun et al., 2002, Kim et al., 2005, Lin et al., 2006) and similarly to osteogenesis appears to be via HIF inhibition of differentiation control genes, in this case inhibition of PPAR $\gamma$ 2 (Yun et al., 2002). The inhibitory effect observed in this study was reflected by a reduction in Oil red O staining indicating reduced fat deposition.

Unlike, osteogenesis and adipogenesis, hypoxia has been reported to increase the chondrogenic potential of MSCs, an effect mirrored in this study (Kanichai et al., 2008, Khan et al., 2007b, Schipani, 2005). SF MSCs underwent a statistical increase in chondrogenesis as measured by sGAG levels compared to the same cells in

normoxia. Although there was a trend, no statistical increase in chondrogenic potential of SC MSCs was observed in hypoxia. A direct link between hypoxia and chondrogenesis is less defined than reported in osteogenesis and adipogenesis. However, it seems as though the HIF pathway is involved with an increase in HIF-1 $\alpha$  correlating with an increase in levels of chondrogenic transcription factors Sox5, Sox6 and Sox9 as well as increases in aggrecan and ColIII and ColX. Similarly an upregulation of HIF-2 $\alpha$  results in increased synthesis and assembly of matrix during chondrogenesis (Khan et al., 2007b).

In addition to assessing the tri-lineage differentiation potential of MSCs, the ISCT require assessment of a panel of markers that identify the cells and exclude potential contaminating cells from cultures, typically cells of haematopoietic origin found in bone marrow (Dominici et al., 2006a). MSCs were assessed for the full ISCT panel and no differences were observed between SF and SC cells in either hypoxia or normoxia indicating that the MSC phenotype was not affected by the use of the SF medium or the use of hypoxia during culture. In addition to the ISCT panel, MSCs were assessed for expression of CD271 and CD146. As discussed in chapter 1, the use of CD271 during isolation of MSCs from culture identifies the entire CFU-f forming cells (Jones et al., 2002). It is however lost during culture of MSCs in the presence of serum. In this study, we reported the maintenance of a subpopulation of cells that maintain CD271 expression. In normoxia, this expression was highly variable and was observed between 20-90% depending on the donor. Its maintenance was more stable in hypoxia, being maintained at approximately 30%. The presence of CD271 may indicate that the cells cultured in SF medium are more closely related to their *in vivo* progenitors. Similarly, it may be that CD271 expression is downregulated by a component of FBS or conversely upregulated by a component of the serum-free medium. One experiment, which may indicate the role of FBS on CD271 expression would be the switching of cells from SF and SC medium to the alternative and assessing the effect of this on CD271 expression. There has been one report which links CD271 expression with an increased immunosuppressive effect of MSCs (Kuci et al., 2010). Understanding this effect of FBS on CD271 may contribute to the *in vivo* function of CD271 for MSCs which is

currently predominantly used to identify the anatomical location of MSCs in bone marrow when assessed in conjunction with CD146 as described in chapter 1 (Tormin et al., 2011b). Combining both CD146 and CD271 expression resulted in the identification of the two distinct MSC niches, the endosteal niche and the perivascular niche with CD271<sup>+</sup> CD146<sup>+</sup> cells residing in the perivascular niche and CD271<sup>+</sup> CD146<sup>-</sup> residing in the endosteal niche (Tormin et al., 2011a). The presence of MSCs at a bone lining niche and their osteogenic potential suggests a role for these cells in maintaining bone homeostasis. Like CD271, CD146-positive MSCs have been reported to be more immunosuppressive than CD146-negative MSCs (Wu et al., 2016). This was also assessed in a collagen-induced model of arthritis in mice where CD146<sup>+</sup> MSCs displayed greater cartilage protection via suppression of Th17 cell activation compared to CD146<sup>-</sup> MSCs. In this study, CD146 expression was maintained at higher levels in SF cells compared to SC cells in both hypoxia and normoxia. However, further experiments would be required to correlate this higher expression in SF MSCs with an increase in a therapeutic function of the cells.

The production of paracrine factors by MSCs has widely been reported to contribute to their therapeutic potential as discussed previously (Singer and Caplan, 2011). To assess the production of pro-angiogenic factors by MSCs, medium conditioned MSCs in culture was collected. HUVEC cells were co-cultured with the conditioned medium from MSCs and the induction of tubule formation by HUVECs was assessed. Although no statistical difference was observed, SF MSCs appeared to be more pro-angiogenic in both hypoxia and normoxia compared to SC MSCs. To distinguish the effect of the MSC versus the medium used, unconditioned medium was also assessed. Interestingly, unconditioned SC medium was far more pro-angiogenic than SF unconditioned medium. Data presented in fig 3.3.9b is represented as a fold change of the appropriate unconditioned medium versus the cell-treated groups. Based on this data, SC MSCs don't appear to contribute an additional pro-angiogenic factor above those present in the FBS. Conversely, SF MSCs appear to produce pro-angiogenic factors above those observed in the SF medium itself. This is the first functional set of data that would indicate a difference in phenotype between SF and SC MSCs. Further analysis would be required to

identify specific factors produced by the SF MSCs that contribute to this increased pro-angiogenic phenotype.

MSCs have been reported to be immunosuppressive via the production of soluble factors outlined in detail in chapter 1. To determine the immunosuppressive effect of MSCs on T-lymphocytes, peripheral blood mononuclear cells from healthy donors were co-cultured with MSCs after exposure to CD3 and CD28 to stimulate proliferation. MSCs were then assessed at various ratios to suppressive T-lymphocytes. Assays were performed in hypoxia and normoxia, however due to the inability of T-lymphocytes to proliferate in hypoxia, only normoxia cultured cells could be assessed. Both SC and SF cells in normoxia demonstrated an immunosuppressive effect on CD4<sup>+</sup> and CD4<sup>-</sup> T-lymphocytes with no difference between groups. CD4 identifies T-helper cells whereas CD4<sup>-</sup> T-cells would typically be considered CD8<sup>+</sup> cytotoxic T-cells. These data indicate that the use of SF medium for the culture of MSCs maintained the immunosuppressive effect of MSCs at comparable levels to that seen with SC-cultured MSCs. Further assays would need to be performed to assess the extent of this immunosuppressive effect. Is it specific to T-lymphocytes or are these MSCs also capable of suppressing macrophage activation for example. In a similar assay, the immunogenic potential of SF MSCs was assessed. This involved the co-culture of MSCs with unstimulated T-lymphocytes to determine if the presence of MSCs results in the activation of the T-lymphocytes to proliferate. No difference was observed in CD4<sup>-</sup> T-lymphocytes but an increase in proliferation of CD4<sup>+</sup> T-lymphocytes was observed at the highest ratio of SF MSCs to T-lymphocytes which may indicate an immunogenic response. Something to consider however is the lack of physiological relevance of the ratio of MSCs: T-lymphocytes used. Further analysis of surface expression and secreted factors of MSCs may be required to elucidate the mechanism of this response.

In this chapter, a detailed *in vitro* comparison of SF and SC MSCs was performed in cells isolated and cultured in both hypoxia and normoxia. The data outlined above broadly suggests the suitability of the SF medium as an alternative to the use of FBS. This is a particularly attractive prospect considering the issues associated with FBS including high costs, lack of definition of the product and limited supply. The

## Chapter Three

use of a chemically defined medium would result in a more seamless upscaling for the production of MSC for therapies. From a regulatory point of view, a degree of uncertainty from the manufacturing process would be removed. This would also lead to more predictable and ultimately reduced costing of MSC therapies for clinical use. From a research point of view, MSC heterogeneity reported widely in the literature may be reduced by the use of a standardised medium formulation. In summary, the serum-free medium described here offers real potential to be used as an alternative to the cumbersome and costly use of FBS.



# **Chapter 4**

**Assessment of *In vivo* Osteogenic  
Potential of Hypoxia/Normoxia Primed  
Bone Marrow MSCs in an Ectopic Model  
of Bone Formation**

### 4.1 Introduction

A reported six million bone fractures or other conditions are reported each year in the United States (Scolaro et al., 2014). 10% of these will require some form of bone graft procedure due to the presence of non-healing defects, tumour resection or age-related bone disease (Lane et al., 1999, Bucholz, 2002). Although orthopaedic conditions are rarely fatal, they represent a leading cause of morbidity in the developed world combined with the associated socioeconomic burden. This trend will continue to rise in aging populations that continue to gain weight (Evans et al., 2008). To date a number of strategies for bone repair have been explored with some commercially available treatments showing varying levels of success (Wang et al., 2001, Govender et al., 2002). None of these treatment options fully recapitulate normal bone repair and can have significant limitations such as implant loosening where biologically inert biomaterials are used that are incapable of interacting with the surrounding tissue (Branemark et al., 2001).

Bone plays an important role in both providing mechanical support and acting as a reservoir for haematopoietic and stromal stem cells (Sacchetti et al., 2007b). Bone is in a constant state of remodelling and is unique to other tissues in that it is capable of undergoing scarless repair of fractures (Schmidt-Bleek et al., 2014). This constant remodelling is controlled by two cell types; osteoblasts derived from MSCs which lay down new bone and osteoclasts which are derived from haematopoietic stem cells and resorb bone by release of proteases. Bone is comprised of two tissue types; compact cortical bone and spongy trabecular bone. Normal bone development occurs via two processes; intramembranous ossification and endochondral ossification (Cohen, 2000). Intramembranous ossification is the process where mesenchymal stem cells differentiate into an osteoblastic phenotype. This mainly occurs during embryonic development of flat bones. Endochondral ossification occurs during embryogenesis, limb growth and fracture healing where a cartilage template is formed prior to being calcified and ultimately remodelled into mature bone.

Intramembranous ossification can also occur during fracture healing in the presence of mechanical stability although with most fractures there is always some

degree of mechanical instability. Although the process of bone repair is greatly understood, there are still a number of clinically significant conditions which either don't have a treatment plan or for which the current treatment option is not viable in the long term.

Osteoporosis is recognised as a global epidemic, with management and treatment-related costs estimated at tens of billions globally (Burge et al., 2007, Kanis and Johnell, 2005). Currently over 200 million sufferers are reported globally, with prevalence of the disease set to increase further (Kanis, 2007). While treatment of osteoporosis normally involves pharmacological intervention, sobering data suggests the cost associated with drug treatment modalities reportedly accounts for as little as 5% of the overall disease related costs in some instances (Hausler et al., 2007). While this figure still accounts for investments of several billion annually, what is perhaps more surprising is that the majority of the economic burden related to osteoporosis refers to management and treatment of osteoporotic-related fractures (Desai et al., 2003). Current clinical treatments, demonstrating different levels of efficacy on both treatment of the diseases and fracture fixation, less than satisfactory clinical predictability of pharmacological intervention and a still excessively high morbidity post-fracture have led to sustained research into alternative treatments (Vestergaard et al., 2007). There is also the issue of large bone defects, non-union fractures and tumour resections where it is not possible for unaided endogenous bone regeneration to occur. Various different methods of addressing these issues have been attempted including the introduction of biomaterials to assist in restoring the mechanical properties of bone while repair is underway. These materials can also induce bone regeneration (Barradas et al., 2011). To further enhance bone repair and regeneration using materials, research has explored delivering cells capable of undergoing or inducing bone repair and/or the growth factors used in natural bone development and regeneration.

Growth factors play a vital role in bone repair whether it is via direct interaction with osteoblasts as local regulators of cell function and growth, the induction of angiogenesis or by inducing cell migration and differentiation of endothelial and osteoprogenitor cells (Hing, 2004). As a consequence of this, growth factors have

been of significant interest in the development of new therapeutic applications for bone repair. A number of growth factors have been investigated based on their involvement in normal bone development and repair; including bone morphogenic proteins (BMPs), platelet-derived growth factor (PDGF), fibroblast growth factors (FGF), insulin-like growth factor (IGF) and transforming growth factor- $\beta$  (TGF- $\beta$ ) (Ai-Aqi et al., 2008). The TGF- $\beta$  superfamily of secreted molecules, including BMPs have also been identified as key factors in the induction of bone formation (Wu et al., 2007). TGF- $\beta$ /BMP signalling is involved in a wide array of cellular processes both during prenatal development and postnatally during bone formation. TGF- $\beta$ /BMPs act via two pathways during bone formation which merge at the Runx2 gene directing MSCs towards differentiation (Wu et al., 2007). The first pathway is the canonical SMAD-dependent pathway whereby isoforms of TGF $\beta$  and their receptors: TGF $\beta$ RI (ALK5) and TGF $\beta$ RII (TGF $\beta$ R2) are essential for both intramembranous and endochondral ossification (Chen et al., 2012b). The non-canonical TGF $\beta$  pathway which is not dependent on SMAD is also essential for osteoblast differentiation (Chen et al., 2012b). The non-canonical pathways are activated by direct ligand-bound receptor activation to modulate downstream cellular processes (Zhang, 2009). *In vitro* analysis of murine osteoprogenitors deficient in TGF $\beta$ RI indicated TGF $\beta$  is involved in proliferation, differentiation and osteoblast lineage commitment via selective MAPKs and SMADs 2/3 (Matsunobu et al., 2009). The phenotype of animals with this defect displayed skeletal abnormalities including the presence of short and wide long bones and reduced bone collars and trabecular bone. Moreover, TGF $\beta$ RI-deficient mice possessed growth plates with unusually thin perichondral cell layers which the authors suggest may be caused by the short bones and ectopic cartilaginous protrusions observed (Matsunobu et al., 2009). This indicates the essential role of TGF $\beta$  signalling in perichondrium formation/differentiation and growth plate integrity during development (Matsunobu et al., 2009).

BMPs have shown significant promise in the treatment of bone defects. They are vital in the modulation of mesenchymal differentiation essential for endochondral ossification to occur. Overexpression of BMP-6 and BMP-2 results in increased

osteogenic differentiation *in vitro* and *in vivo*, with BMP-6 having the greatest effect (Mizrahi et al., 2013). BMP-2 is involved in initiating osteoblast differentiation and regulating bone mineral density (Bragdon et al., 2012). Knockout studies indicate a role of BMP -2 and -4 in normal bone development and maintenance; knockouts result in reduced osteogenesis and increased bone fracture (Chen et al., 2012b). BMP-7 or osteogenic protein-1 (OP-1) have been used clinically for the treatment of long bone and scaphoid fractures and non-unions. Similarly, there is supportive evidence for the use of BMP-7 as a therapy for spinal fusion and as a replacement of autograft where patients receive bone grafts from non-loading bearing areas of their own body (White et al., 2007). However, BMP-7 knockdown does not result in an observable negative effect in bone development or maintenance (Tsuji et al., 2010). Conversely, BMP-3 can negatively regulate bone marrow stromal cells (Kokabu et al., 2012) with targeted deletion of BMP-3 resulting in increased trabecular bone loss and transgenic overexpression of BMP-3 leading to spontaneous fracture (Kokabu et al., 2012). Of all the BMPs, BMP-2 and BMP-7 are the most commonly investigated. Recombinant BMP-7 and BMP-2 have been tested in the Osigraft and InductOs clinical trials, respectively (Calori et al., 2008, Meisel et al., 2008). When compared to autologous bone grafts, these cytokines have been shown to induce equivalent bone repair for tibial non-unions (Zimmermann and Moghaddam, 2011). However there are issues with costs and toxicity as much higher doses are required than would typically be seen in the body as these proteins degrade rapidly. Furthermore, BMP-3, -4, and 8 have also been shown to be expressed during fracture healing (Cho et al., 2002) and BMP-6 and 9 have been shown to be potent inducers of MSC osteoblastic differentiation (Cheng et al., 2003). From this it is clear that BMPs are key players involved in bone repair. Again, the dose of these recombinant growth factors required to accelerate healing is much higher than the levels seen during normal bone repair. This is most likely due to unsuitable delivery methods combined with rapid *in vivo* degradation of these growth factors. This makes the use of direct delivery of growth factors too cost prohibitive for large scale clinical use. For this reason, MSCs have been explored for their therapeutic potential in bone repair. This is despite the lack of identification of a mechanism of action i.e., whether MSCs contribute to bone

regeneration via osteochondral differentiation or the production of paracrine factors that result in activation of endogenous cells to regenerate bone. However, autologous bone grafting is still the gold standard for bone repair. This is due to the apparent lack of efficacy of MSCs in clinical trials (Si et al., 2011). This may be due to detrimental effects of *in vitro* expansion of MSCs as reported in numerous studies with the loss of differentiation potential over time. Similarly this may also require further optimisation of culture conditions depending on the targeted therapeutic effect of the MSCs.

The effect of oxygen tension of bone marrow MSCs isolated and cultured in either hypoxia or normoxia was determined in chapter 3. Results from this study indicate equivalent growth kinetics of SC and SF cells in normoxia and superior growth kinetics of SF in hypoxia when compared to SC cells. Both cells types maintained equivalent surface marker phenotype in relation to the ISCT panel. Differences were observed in expression of CD271 and CD146. Increased expression of CD271 was observed in SF cells compared to SC cells which did not maintain CD271 in culture. This expression was highly variable in normoxia and more stable in hypoxia. Similarly with CD146, higher, more stable expression of this marker was observed in SF cells independent of oxygen levels. Differences were observed in the differentiation potential of cells cultured in hypoxia versus normoxia. In osteogenic, adipogenic and chondrogenic assays, no differences were observed between SC and SF groups within hypoxia and normoxia groups. Where differences were observed was between hypoxia and normoxia. In osteogenic assays, normoxia cultured cells displayed increased osteogenesis in both SF and SC groups compared to their hypoxia counterparts. Similarly with adipogenesis, normoxia increased the adipogenic potential of both SF and SC cells. Conversely for chondrogenic assays, hypoxia displayed a trend towards increasing chondrogenesis in SC cells compared to normoxia and a significant increase in chondrogenesis of SF cells in hypoxia compared to normoxia. These results showed that the SF cells are primed differently towards osteogenic and chondrogenic lineages when cultured in normoxia and hypoxia respectively. This raised the question of which cell type is optimal for *in vivo* bone repair, the normoxic pro-osteogenic cell which may repair

bone by direct bone formation via intramembranous ossification or the hypoxic pro-chondrogenic cell which may repair bone indirectly via endochondral ossification? In addition, the increased pro-angiogenic potential of the SF cells further reinforced the hypothesis that they may possess increased bone healing ability.

A commonly used method for the *in vivo* assessment of chondrogenic and osteogenic potential of MSCs is the loading of MSCs onto an osteoconductive scaffold and loading of the construct into immunodeficient mice (Krebsbach et al., 1997). The system is attractive due to its ease of use and the ability to retrieve implants. However, with this model there are a number of considerations to be taken into account as outlined by Krebsbach et al (Krebsbach et al., 1997). These include the *in vitro* expansion conditions of the cells used, cell seeding density and the transplantation vehicle. In this study, reproducible bone formation was observed when using hydroxyapatite/tri-calcium phosphate vehicles regardless of form. Bone was formed with HA/TCP scaffolds in the form of powder, 3D blocks or HA/TCP-collagen strips (Krebsbach et al., 1997). Since these initial studies, the system has used routinely to assess the *in vivo* osteochondral potential of MSCs from various sources (Mirabella et al., 2011, Muraglia et al., 1998, Martin et al., 1997, Tortelli et al., 2010, Jaquiéry et al., 2005, Braccini et al., 2005, Elabd et al., 2007). Simultaneously, the use of the clinically approved HA/TCP granules, 'macro and microporous biphasic calcium phosphate (MBCP+™, Biomatlante) has widely been reported for facilitating *in vivo de novo* bone formation in numerous animal models including mouse, rabbit and sheep (Le Guehennec et al., 2005, Malard et al., 2005, Le Nihouannen et al., 2005, Gauthier et al., 2001, Arinze et al., 2005).

This chapter focuses on determining the osteogenic potential of bone marrow-derived MSCs isolated and expanded in hypoxia (2% O<sub>2</sub>) or normoxia (21% O<sub>2</sub>) as described in chapter 3. In this study, 2x10<sup>6</sup> MSCs were loaded onto HA: TCP (20:80) granules encapsulated in a fibrin sealant and assessed for their viability on the scaffolds and their ability to form bone *in vivo* after 8 weeks as detailed in section 4.2 below.

## 4.2 Methods

To assess the *in vivo* bone forming ability of SF and SC derived MSCs isolated and cultured in hypoxia and normoxia (section 2.1),  $2 \times 10^6$  MSCs were loaded onto HA:TCP granules and encapsulated in fibrin as described in section 2.14. Constructs were implanted subcutaneously into the backs of CD1 nude mice for 8 weeks as described in section 2.14.3. Constructs were also prepared to assess viability of MSCs using CTB assay as described in section 2.14.1. Following retrieval, MSCs were assessed for their osteochondral potential by  $\mu$ CT analysis as described in section 2.21 and decalcified and histology for presence of bone and cartilage tissue as outlined in sections 2.21 and 2.15 respectively. Experimental methodology is schematically represented in figure 4.2.1. As a positive control, equivalent numbers of Sarcoma osteogenic (Saos-2) cells were implanted. These cells were tested *in vitro* prior to implantation for their osteogenic potential (data not shown)



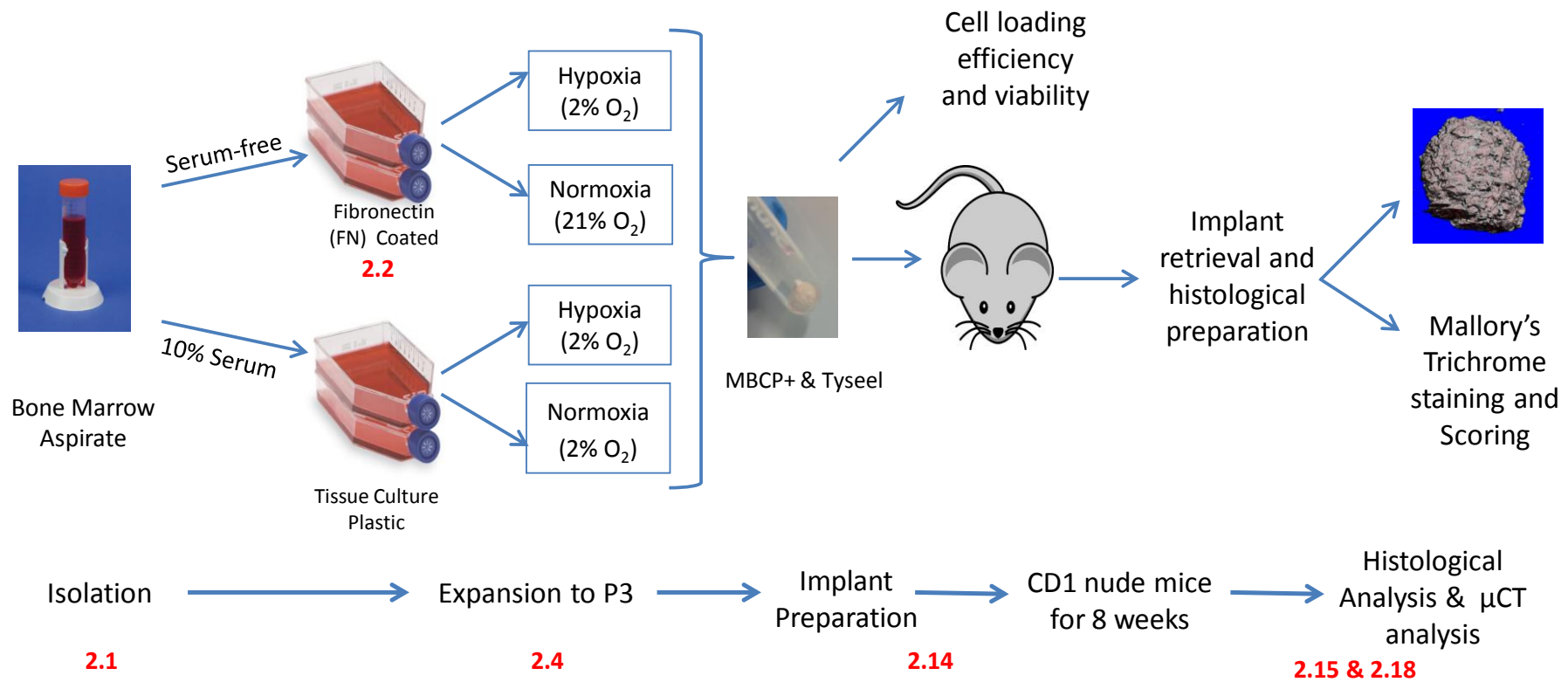


**Figure 4.2.1: Schematic representation of experimental design to assess the effect of hypoxic/normoxic priming on bone marrow-derived MSCs isolated in serum-containing and serum-free media.**

## 4.3 Results

### 4.3.1 Cells were retained in MBCP<sup>+</sup> following encapsulation and remained metabolically active

To evaluate the loading efficiency of MSCs post encapsulation,  $2 \times 10^6$  cells were loaded into scaffolds as described in section 2.14 and cells retained in media after loading assessed by cell counting using a haemocytometer. Figure 4.3.1a shows the total number of cells loaded onto scaffolds per cell group. Total cell numbers loaded varied from  $1.8\text{--}2.0 \times 10^6$  cells per scaffold. Figure 4.3.1b reports the loading efficiency of cells per group as determined as a percentage by calculating the total number of cells added and the number of cells retained on scaffolds after loading. Loading efficiency for all groups is >95%.

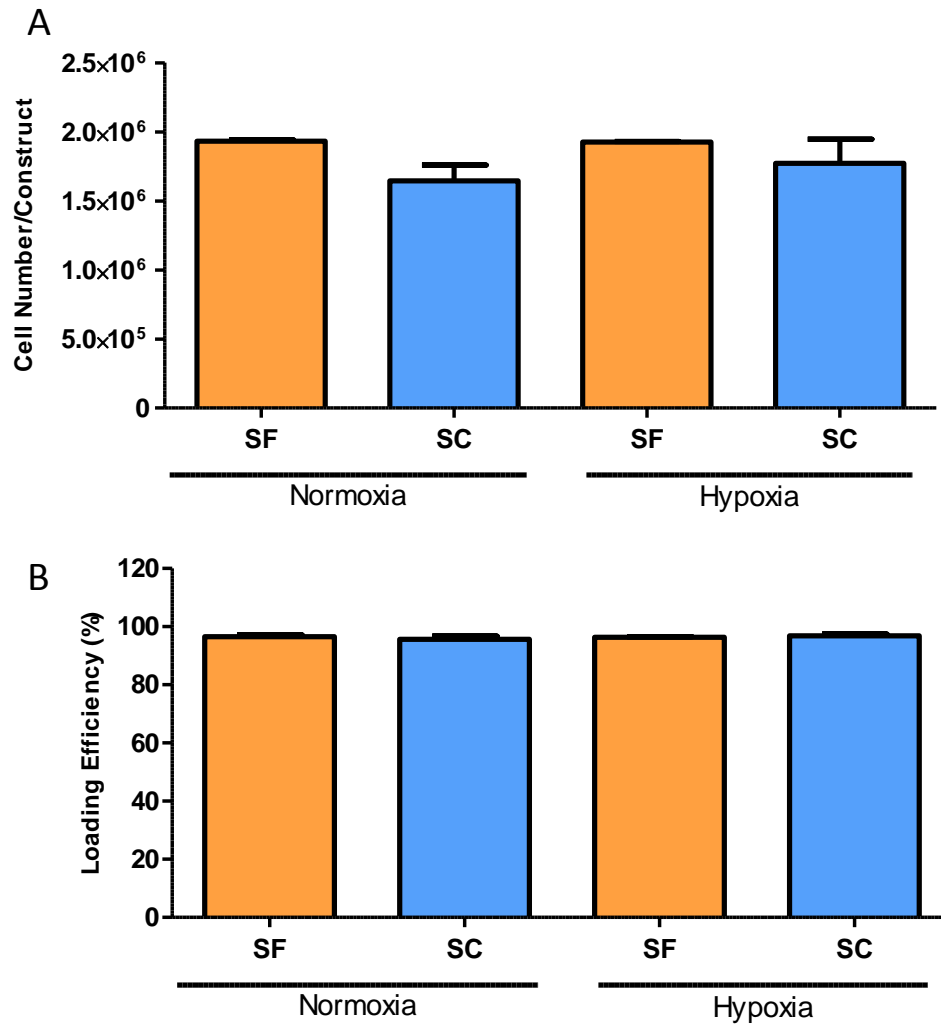


**Figure 4.3.1: Efficient loading of MSCs onto MBCP+/Tyseel scaffolds prior to implantation.** Cell counts were used to assess the loading efficiency of cells onto constructs. (A) Total cell number loaded onto constructs per group  $\pm$  standard deviation demonstrating equivalent numbers of cells loaded per construct per cell groups. (B) Loading efficiency of cells per construct indicating no difference in retention of different cells groups by constructs. These data collectively indicate effective and reproducible loading of MSCs onto constructs. Data (mean  $\pm$  SD) is representative of 3 biological replicates with 3 technical replicates.

#### 4.3.2 MSCs retained metabolic activity following encapsulation

To evaluate MSC metabolic activity 24hrs post encapsulation, constructs composed of MBCP+ alone, MBCP+ with Tyseel were compared to cells alone for metabolic activity by CellTitre blue. Figure 4.3.2 shows % viability of MSCs loaded on constructs as determined by their metabolic activity compared to cells alone.

Reduction in metabolism was determined based on absorbance levels based on 550nm and 600nm readings normalised to medium alone. Cells loaded on either MBCP+ alone or on MBCP+ encapsulated in Tyseel showed equivalent metabolism levels compared to cells alone indicating MSCs on constructs remain metabolically active 24hrs post encapsulation.

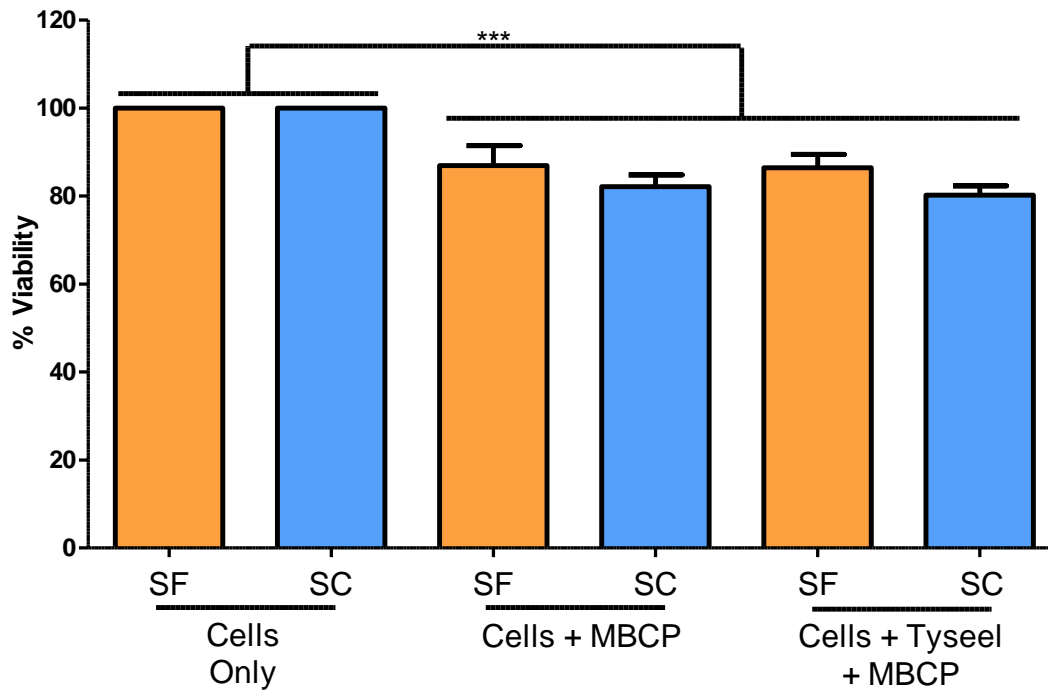
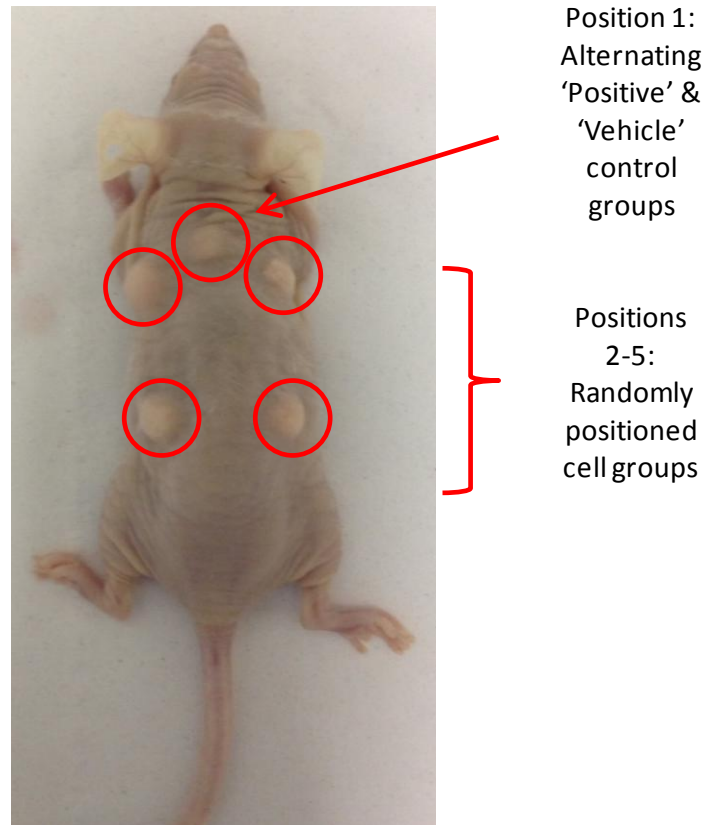


**Figure 4.3.2: Cells remain metabolically viable following encapsulation.** CellTitre Blue dye was used to indicate the metabolic activity of cells following encapsulation. Results demonstrate a limited reduction in metabolism of cells following encapsulation. No difference was observed between SF and SC groups or between cells loaded on MBCP+ alone or loaded on MBCP+ followed by encapsulation with Tyseel. This data indicated maintained metabolic viability of MSCs following encapsulation. Data (mean  $\pm$  SD) is representative of 3 biological replicates with 3 technical replicates. \*\*\* $p < 0.001$  as determined using two-way ANOVA and Bonferroni's multiple comparisons post-test.

### 4.3.3 Implanted constructs were successfully retrieved at 8 weeks

Eight weeks post-implantation, mice were sacrificed and assessed for the presence

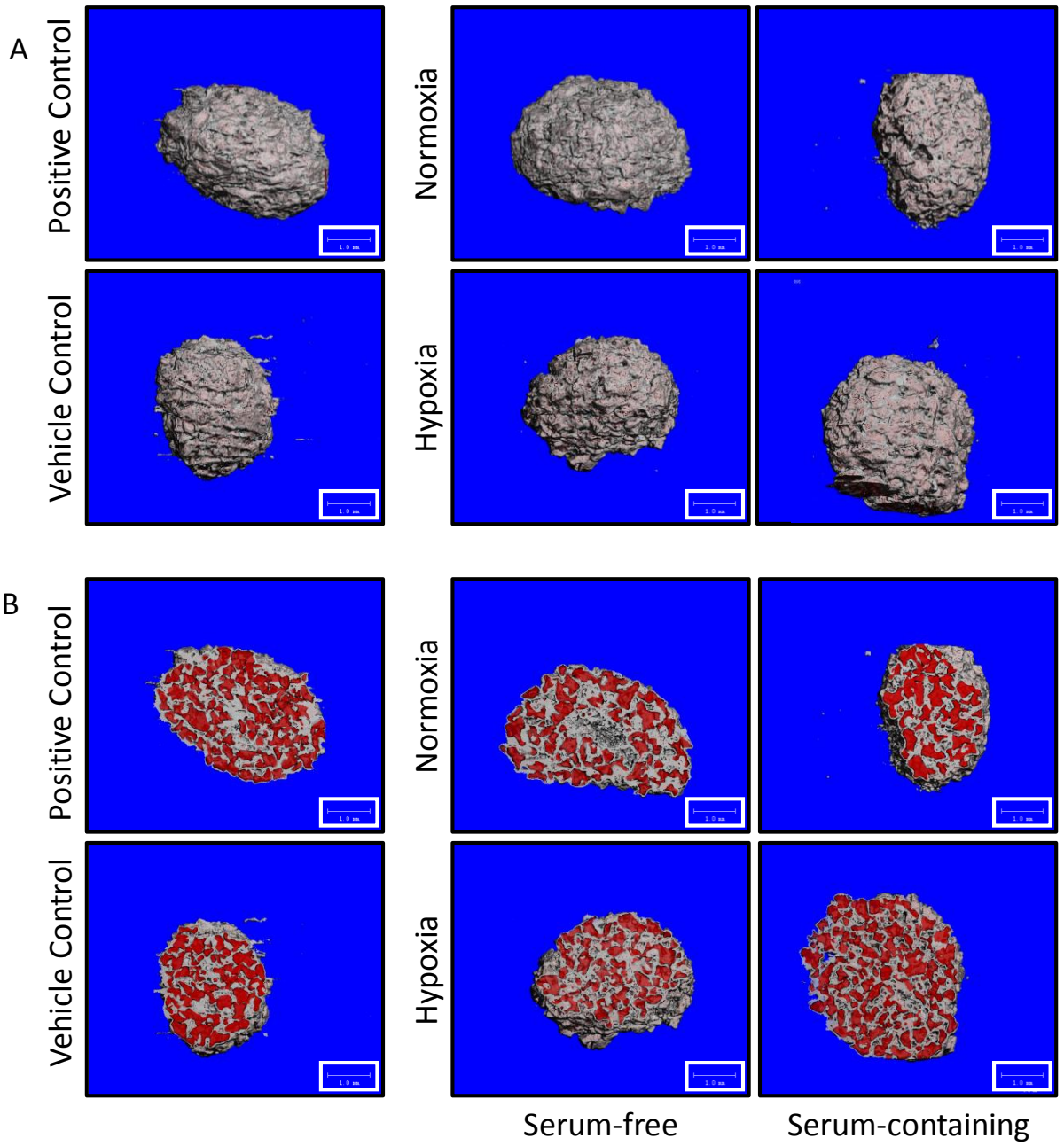
of implanted constructs. All five implants were clearly visible and of similar size in all recipients as reported in figure 4.3.3. Position 1 indicates the position where either the positive control (Saos-2 cells) or vehicle control (cell-free scaffold) were positioned in the animal. Saos-2 cells are a human osteosarcoma cell line derived from a 11yr old female with a reported high osteogenic potential (Czekanska et al., 2012). Positions 2-5 indicate the locations of the test groups (SF and SC from either hypoxia or normoxia). Cells in these groups were randomly assigned a position prior to surgery.



**Figure 4.3.3:** *Implanted constructs were clearly visible 8 weeks following implantation. Results reveal the clear presence of all five implanted constructs following 8 week transplantation as visualised by photography. Constructs were comparable in size and shape. Representative image of 9 recipient animals at 8 weeks post-transplantation.*

#### **4.3.4 Micro-computed ( $\mu$ CT) tomography of retrieved constructs 8-weeks post implantation**

To determine the bone mineral density of the implants post-transplantation, constructs were assessed for presence of bone mineral by use of *ex vivo*  $\mu$ CT analysis using the Scanco  $\mu$ CT 100 evaluating with a 70kVp x-ray source at 110 $\mu$ A. Analysis was performed on 3 biological replicates with 3 technical replicates for each group. Bone volume was calculated as a percentage of total tissue volume excluding the presence of the MBCP+ granules which have a similar density to bone. 3D images of implants were generated (figure 4.3.4a) and cross-sections of implants indicating new bone (white) and MBCP+ granules (red) in figure 4.3.4b. Bone formation was observed in all 6 groups (Figure 4.3.4b). All implants were of comparable size. Bone volume/ tissue volume was also quantified (Figure 4.3.4c). Positive and vehicle controls demonstrated equivalent *de novo* bone formation. No difference was observed between cell groups with no statistical significance being observed between cell groups and controls. The presence of bone in the vehicle control indicates this material is unsuitable to be used as a negative control due to its osteoinductive effect on endogenous cells. Bone was determined by measurement of the density of the individual materials and range of densities were excluded which contain the MBCP+ granules. This process may also exclude mature bone which has a density similar to that of MBCP+.



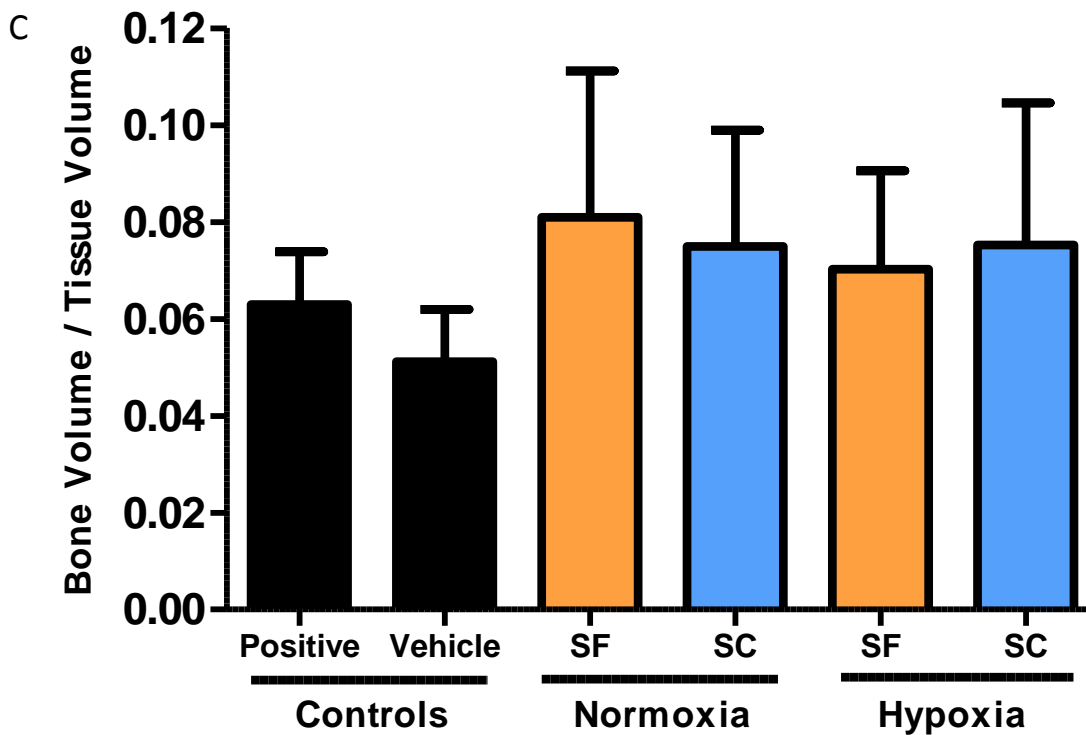
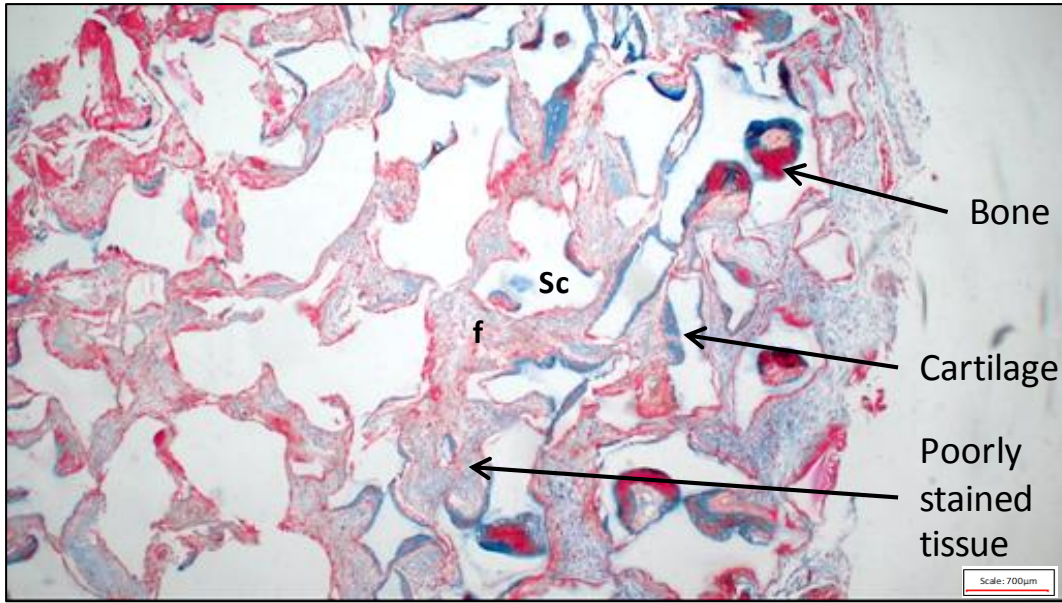


**Figure 4.3.4** *Micro-computed tomography ( $\mu$ CT) analysis of bone formation in implants 8 weeks following transplantation. (A) Representative 3D images of scaffolds 8 weeks post implantation indicating similar implant size between groups. (B) Cross-sectional image of implants distinguishing new bone formation (white) and MBCP+ granules (red). Bone is present in all groups. (C) Quantitative analysis of bone volume calculated as a percentage of tissue volume indicating comparable levels of bone formation occurring in all cell groups. Bone is also present in vehicle control groups. Data (mean  $\pm$  SD) representative of 3 biological replicated with 3 technical replicates.*

#### **4.3.5 Representative images of Mallory's modified Trichrome stain defining various observed tissues.**

Histological analysis of the implanted constructs was carried out after  $\mu$ CT analysis to determine the presence of various tissues histologically as described in sections 2.15 and 2.17-2.18. Briefly, sections were fixed in 100% ethanol and decalcified using Surgipath decalcifer II. Samples were subsequently paraffin embedded and histological samples were taken from 3 locations within the implant at 100 $\mu$ m intervals. Figure 4.3.5a&b show representative images identifying the various tissues observed in the constructs. MBCP+ scaffolds (Sc) appear as empty white or pink areas due to the decalcification process. Fibrous tissue (f) is present as poorly stained low density tissue. Bone is present as dark red tissue often surrounding the MBCP+ granules. Cartilage is observed as blue stained tissue often also present near MBCP+ granules. Bone marrow is present in figure 4.3.5b as areas of fat with or without the presence of blood vessels (red). Fibrous encapsulation of the implants is observed in figure 4.3.5b as red stained striated tissue surrounding the implant.

A



B

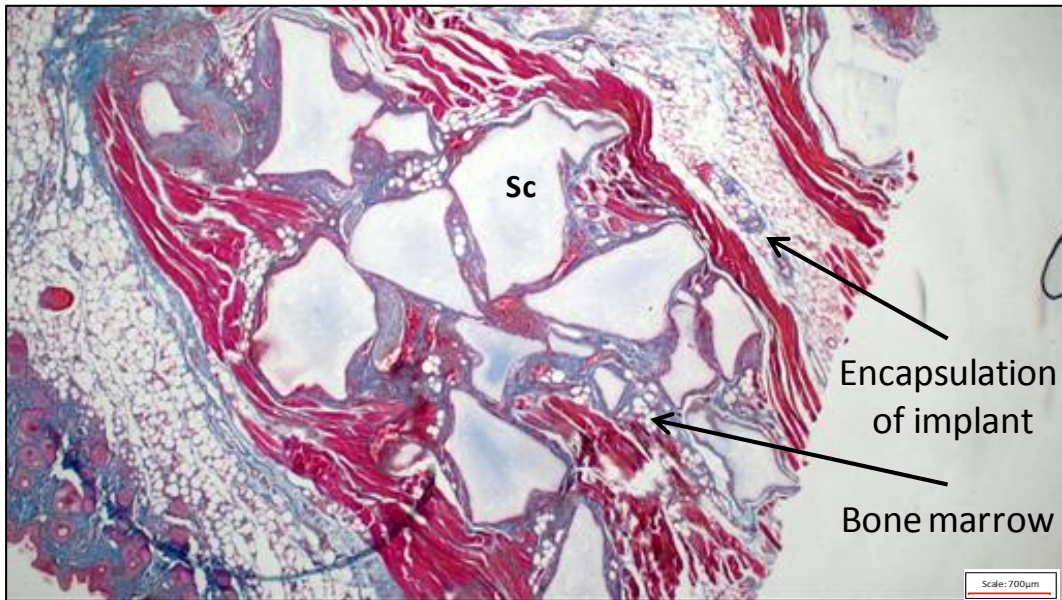


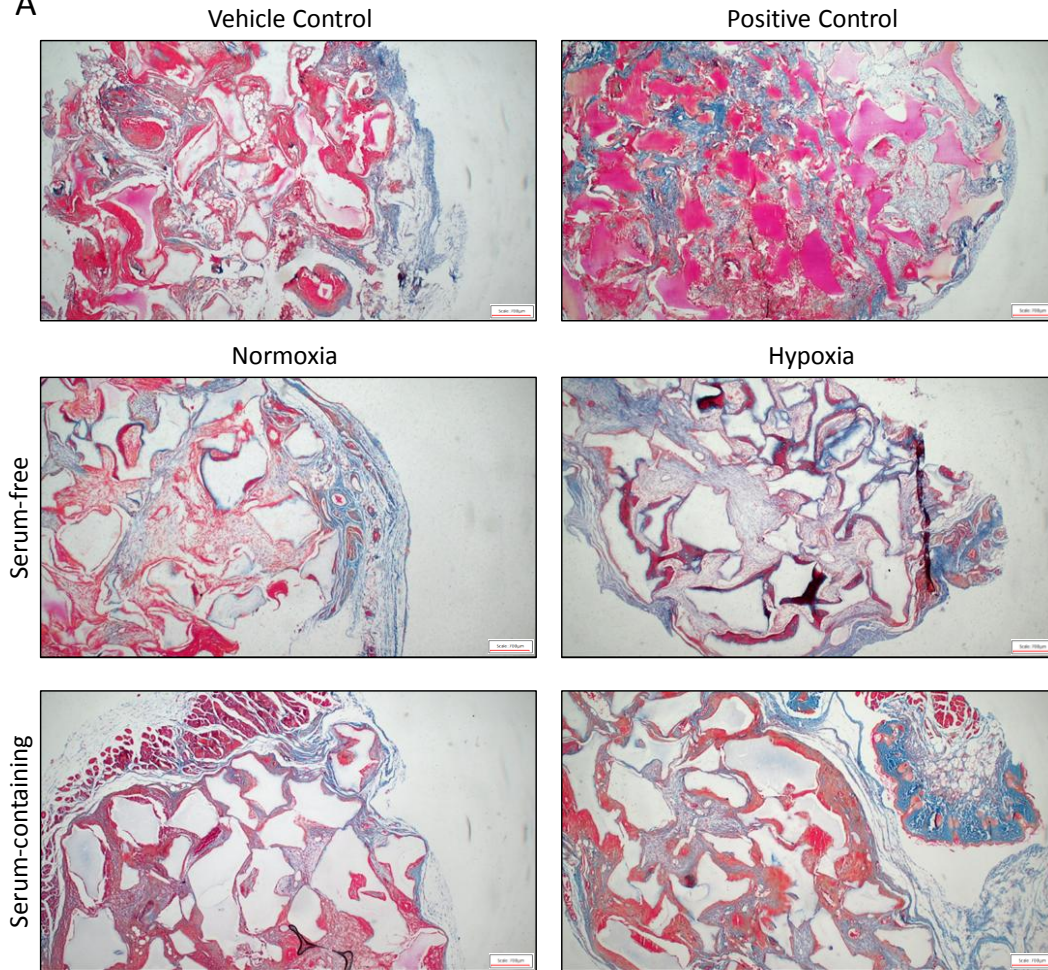
**Figure 4.3.5: Representative images of Mallory's Trichrome stain after implantation of MSCs ectopically.** (A) Representative tissue indicating the presence of bone (red), cartilage (blue) and fibrous tissue (poorly stained tissue). MBCP scaffolds (Sc) observed as white or poorly stained solid shapes throughout the tissue. (B) Presence of bone marrow formation and implant encapsulation. Bone marrow is observed throughout the tissue as presence of fat tissue with or without the presence of blood vessels depending on the stage of bone marrow development. Encapsulation of implant by fibrous tissue is also observed as a striated tissue surrounding implant. Scale bar: 700µm.

#### **4.3.6 Bone and cartilage tissue observed in all implanted groups.**

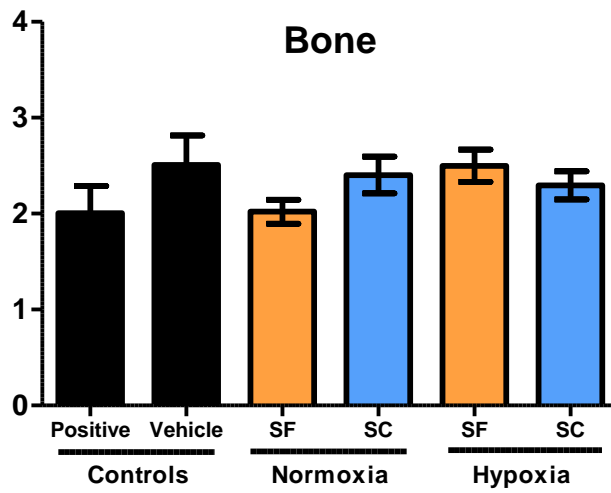
To determine if SF and SC cells cultured in either hypoxia or normoxia contribute to the formation of osteochondral tissue in subcutaneous implantation, MBCP+ constructs loaded with cells were explanted, decalcified and histologically assessed by modified mallory's trichrome stain. (A) Bone and cartilage were evident in all cells groups and the vehicle control group, which was not pre-loaded with cells. MBCP+ particle remnants were visible as clear or pink spaces in all samples. Fibrous tissue was also observed in all samples. No difference in the level of bone or cartilage in cell groups was observed in comparison to the vehicle control group. The positive control group which received Saos-2 cells appears to have formed a denser tissue overall which resulted in less decalcification of MBCP granules as observed by the pink colour. Additionally, the positive control group tissue seems more disordered compared to other cell groups which formed bone and cartilage predominantly at the interface between the cells and the MBCP granules. Overall, all cells groups contributed to the formation of bone and cartilage. Similarly bone marrow was identified in all groups as evidence by the presence of fat tissue with or without blood vessels. (B) Semi-quantitative analysis of bone cartilage and bone marrow present in implanted groups. Positive and vehicle control groups demonstrated no difference in levels of bone, cartilage or bone marrow. No difference was observed within cell groups or between cell groups and control groups.

# Chapter Four

A



B



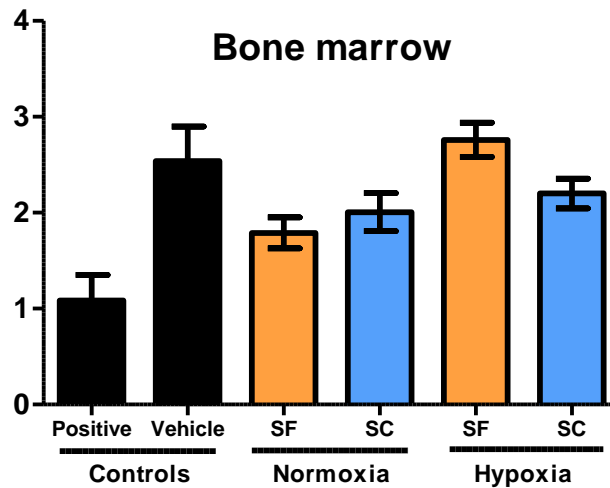
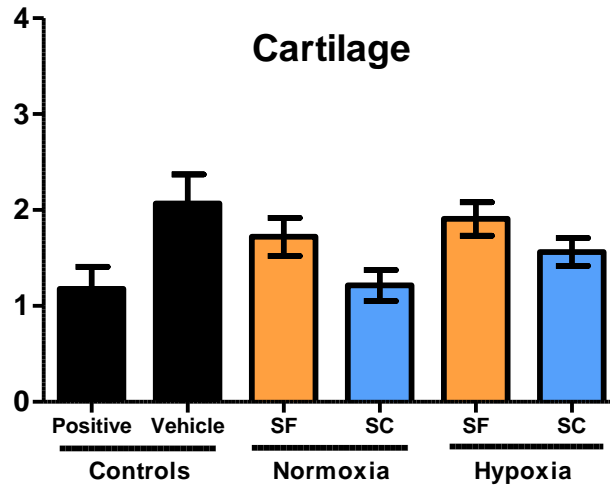


**Figure 4.3.6 Histological analysis of bone, cartilage and bone marrow present in implanted constructs.** (A) Representative images of modified Mallory's trichrome stain of implanted groups. Bone, cartilage and bone marrow were evident in all groups. Scale bar: 700 $\mu$ m. (B) Histological scoring of tissue presence in implants. Slides scored from 0-4 with each interval indicating a 20% increase from 0 (0-20%), 1(20-40%), 2(40-60%), 3(60-80%) and 4 (80-100%) indicating the presence of the relevant tissue in the sample. Data is representative of the mean  $\pm$  SEM of 3 biological replicates with 3 technical replicates assessed at 3 locations within the construct.

#### 4.4 Discussion

From chapter 3, the *in vitro* osteogenic and chondrogenic potential of serum-free and serum-containing cells was demonstrated. It was also observed that depending on whether these cells were cultured in either hypoxia or normoxia, the level of differentiation observed by the cells was affected. Particularly, hypoxia resulted in a more pro-chondrogenic phenotype whereas normoxia-cultured cells were pro-osteogenic. In this chapter, the *in vivo* osteochondral potential of SF and SC cells cultured in hypoxia and normoxia was assessed. Specifically, this was assessed by loading  $2 \times 10^6$  MSCs onto 80:20 HA/TCP granules and encapsulating them in a fibrin sealant. Initially loading efficiency and viability of cells loaded onto the scaffolds was determined. Finally the ability of the cells to differentiate and contribute to the formation of an osteochondral tissue was determined. The hypothesis being investigated in this chapter was whether cells with a pro-osteogenic phenotype contribute to bone formation directly via intramembranous ossification or indirectly via formation of a cartilage template as seen in endochondral ossification. A caveat of this hypothesis is that the osteogenic medium used does not reflect a biologically relevant process and thus may not be indicative of the *in vivo* osteogenic potential of MSCs. The *in vivo* assay described in this chapter is a semi-quantitative assay for the assessment of bone formation. This combined with  $\mu$ CT analysis has resulted in the addition of quantitative data to reinforce any observed effect seen from histological scoring. In this assay, MSCs are loaded onto an osteoconductive scaffold and subcutaneous implantation of this scaffold into the backs of immunodeficient mice is performed. This model has been used routinely by a number of groups to evaluate the osteochondral potential of MSCs from various sources on a variety of scaffold types (Krebsbach et al., 1997, Mirabella et al., 2011, Muraglia et al., 1998, Martin et al., 1997, Tortelli et al., 2010, Jaquiéry et al., 2005, Braccini et al., 2005, Elabd et al., 2007, Le Guehennec et al., 2005, Malard et al., 2005, Le Nihouannen et al., 2005, Gauthier et al., 2001, Arinzeh et al., 2005).

In this study, MSCs were loaded onto MBCP+ granules and encapsulated by use of Tyseel fibrin sealant. Following this, cell loading efficiency and metabolic activity 24hrs post-encapsulation were determined. Results indicated that cell loading onto

the scaffold was highly effective with over 95% of cells being successfully loaded resulting in limited variability between cell numbers for constructs generated for the study. This result was typical of similar studies published in the literature which also demonstrated highly efficient loading of cells onto HA/TCP scaffolds (Kuznetsov et al., 1997, Kuznetsov et al., 2000, Janicki et al., 2011).

Following encapsulation of MSCs into constructs, metabolic activity was assessed by use of CellTitre blue (CTB). CTB uses resazurin to measure the metabolic activity of cells as an indicator of cell viability. Viable cells reduce resazurin into resorufin which results in a blue shift to pink in the light absorbance properties of CTB (Squatrito et al., 1995, Voytik-Harbin et al., 1998). Results here demonstrated that MSCs encapsulated with MBCP+ maintained metabolic activity equivalent to that of cells alone indicating that MSCs remain metabolically active on MBCP+ scaffold prior to implantation.

Implanted scaffolds remained visible in the animal throughout the study with no adverse effect to the mice being identified. Following implant retrieval, samples were fixed using ethanol and  $\mu$ CT analysis of mineralisation was carried out. This analysis excluded the HA/TCP granules which have a similar density to that of bone.  $\mu$ CT analysis indicated the presence of mineralised tissue in all groups including the vehicle control which was not loaded with cells. This would indicate that recruitment of endogenous cells to the implants occurred. Similarly, there was no statistical increase in the level of mineralisation that occurred in the MSC groups or Saos-2 group above the vehicle control indicating that the transplanted cells had little to no effect on the formation of endochondral tissue in the cell-loaded constructs.

Following  $\mu$ CT analysis, the samples were decalcified and histological analysis of bone was performed using modified mallory's trichrome stain to identify specific tissues. Microscopic analysis reported the presence of bone, cartilage and bone marrow in all treatment groups with an abundance of fibrous tissue also observed. The presence of new bone and cartilage was predominantly observed at the interface between the MBCP+ granules and surrounding tissue. Areas composed

entirely of cartilage or bone were observed. There were also regions of combined bone and cartilage tissue indicating that bone formation in implants could be occurring via both endochondral and intramembranous formation. Similar to  $\mu$ CT data, little improvement in the levels or quality of osteochondral tissue formed in cell-treated groups was observed above that seen in the vehicle control indicating that the dominant source of cells contributing to new bone formation was in fact the endogenous cells which had been recruited to the implants by some undetermined means. Further analysis including the use of *in situ* hybridisation looking at the Alu sequence may be beneficial to determine definitively whether the new tissue formed was in fact due to the transplanted human cells or via the recruitment of endogenous cells to the implants or in fact via the synergistic cooperation of both cell types. The latter seems unlikely as if this were the case an increase in endochondral tissue formation above the vehicle control would have been observed.

The lack of bone formation by the transplanted cells is somewhat surprising as numerous studies listed previously have clearly documented the ability of MSCs to form bone *in vivo* in very similar models. Data assessing cell retention and viability of cells at the time of implant indicated sufficient loading and cell metabolic activity to indicate good health at the time of transplantation. This was observed with cell loading above 95% and cell metabolism at comparable levels to MSCs plated on tissue culture plastic. However, there have been numerous previous studies which have altered pre-implantation protocols with various effects on the *in vivo* potential of MSCs which may offer some understanding into the issue of limited osteogenic differentiation observed here. Prior to implantation MSCs were maintained in either the serum-free medium or standard 10% serum-containing medium, an approach which has been reported to work previously (Dennis et al., 1998). However, other studies have reported success by priming the MSCs to differentiate by the addition of factors to the medium. A number of studies have reported successful *in vitro* osteogenesis of MSCs following *in vitro* priming of the cells in medium containing dexamethasone, ascorbic acid-2-phosphate and  $\beta$ -glycerol (Hicok et al., 2004, Agata et al., 2010), factors typically found in osteogenic media.

Similarly, other groups have also seen success with just the addition of dexamethasone and ascorbic acid-2-phosphate (Kuznetsov et al., 2000, Mankani et al., 2001, Mankani et al., 2008). Also being explored in the literature is the pre-chondrogenic priming of MSC for bone repair (van der Stok et al., 2014a, Farrell et al., 2009). In these studies, the pre-chondrogenic priming of cells prior to *in vivo* implantation resulted in bone via endochondral ossification with improved quality compared to osteogenically-primed MSCs. In addition, the bone formed had improved vascularisation resulting in formation of better bone overall (Farrell et al., 2009).

A second reason which may account for the lack of osteogenesis is the extent of culture the cells underwent prior to implantation. The cells used in this study were implanted at passage 3. Numerous studies have reported a loss of multipotency and specifically tri-lineage differentiation potential of MSCs during *in vitro* expansion (Bonab et al., 2006, Baxter et al., 2004). The majority of studies use cells at passages 1-3 as was performed in this study but typically these studies have also included an *in vitro* priming step, although not always (Dennis et al., 1998, Hicok et al., 2004, Kuznetsov et al., 2000, Mankani et al., 2008, Janicki et al., 2011). A more definitive answer came from a study where MSCs at each passage from passage 1-5 were implanted following priming of cells in osteogenic medium. This study reported a loss of osteogenic potential with passage number (Agata et al., 2010) indicating that the age of cells may be pivotal for these assays. A similar effect was observed comparing MSCs implanted at passages 1, 3 and 5 (Janicki et al., 2011). In this study, none of the implants delivered at P5 resulted in bone formation versus 75% of implants at P3 and 100% of implants at P1. Based on these data, *in vitro* expansion is clearly important for the *in vivo* osteogenic potential of MSCs but priming of cells prior to implantation may overcome these issues.

The purpose of this study was to assess the *in vivo* potential of MSCs to form bone in a subcutaneous model of bone formation. In this study, metabolically active cells were successfully loaded onto osteoconductive scaffolds and implanted into CD1 nude mice for 8 weeks. Implants were successfully retrieved and assessed for bone repair. However, limited bone formation was observed in the cell-treated groups

above that observed in the vehicle control indicating that the tissue formed was presumably predominantly formed by endogenous cells recruited to the implants. Further development of this assay is required to optimise its use for assessing MSC for *in vivo* bone formation ability. This optimisation may include using MSCs at an earlier passage or by the *in vitro* priming of MSCs prior to implantation.

Whilst this assay did not perform effectively as a mechanism of bone repair, what was apparent was the recruitment of endogenous cells to the implant site. This raises the question of what mechanism is involved in the recruitment of MSCs to sites of injury or new tissue repair.

MSCs exist within a number of anatomical locations and have been shown to be capable of homing to injured tissues. This has been seen in a number of injury models including migration of MSCs to bone fractures (Granero-Molto et al., 2009, Lee et al., 2009, Kumagai et al., 2008), lung injury (Ortiz et al., 2003), brain injury (Ji et al., 2004) and to sites of wound healing (Fu et al., 2009). Mobilization of MSCs to other injury sites has also been reported (Fong et al., 2011). During the normal fracture process, circulating progenitor cells are recruited to the site of injury as part of their therapeutic mechanism of action (Kumagai et al., 2008). The mechanism of this homing process of MSCs is the subject of a huge research effort in the hopes of identifying a means to improve tissue repair by endogenous cells. The current consensus suggests injured tissue produces factors and ligands which can be used by MSCs to migrate, adhere and infiltrate damaged tissue (Abbott et al., 2004, Wang et al., 2008, Schenk et al., 2007), a process similar to that seen by leukocytes migrating to sites of inflammation. This idea was validated in a recent paper which described the migration of MSCs in an *in vitro* model (Teo et al., 2012). MSC migration is dependent on their ability to adhere to and migrate through TNF- $\alpha$  activated endothelium, a process dependent on both the G-protein coupled receptor and VCAM-1 pathways. The process occurs in 5 steps (Figure 4.4). Firstly, rounded MSCs adhere to epithelium in an integrin-dependent manner. Next, a transmigratory cup is formed where VCAM-1 enriched microvilli projections extend around the MSC and form a cup shape. Step three involves formation of a gap or pore by a process described as blebbing where MSCs apply a force on the

epithelium which is associated with the formation of gaps or pores. This stage is not observed in leukocyte migration which migrates through intact gap junction, a process known as diapedesis. Following this, MSCs penetrate and spread through the subendothelium layer and transmigration is complete (Teo et al., 2012).

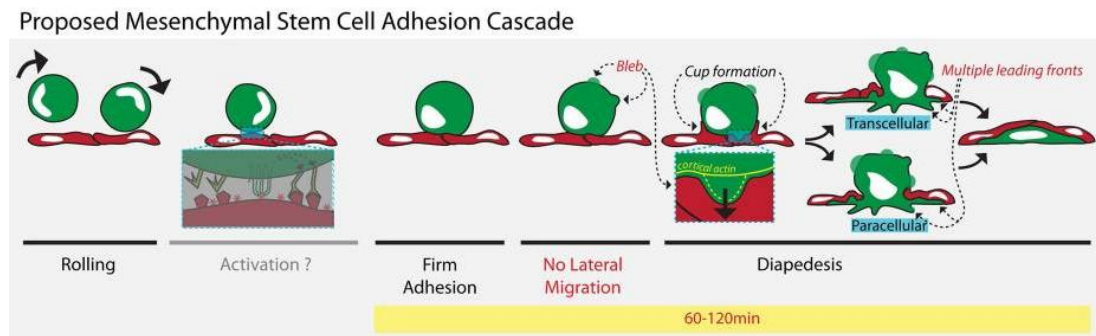


**Figure 4.4: Proposed Mechanism of MSC migration to injured tissue in comparison to leukocyte migration to inflammation.** (Published with permission from (Teo et al., 2012), see appendix II).

Initiation of this migration is induced by chemokines and cytokines at the injury site. A number of studies have been published looking at the chemotactic effect of particular cytokines on migration of MSCs. CXCR4, the receptor for stromal-derived factor-1 (SDF-1) which is encoded by the C-X-C motif chemokine 12 (CXCL12) gene, has been associated with migration of murine and human MSCs from various sources including bone marrow, adipose tissue and umbilical cord (Park et al., 2011, Yu et al., 2012, Liu et al., 2011, Jones et al., 2012, Bobis-Wozowicz et al., 2011). Within the studies, overexpression of CXCR4 enhanced the migratory ability of MSCs (Cheng et al., 2008). The migration of MSCs to sites of fracture healing is exclusively CXCR4-dependent with migrated MSCs contributing to fracture repair via production of BMP-2 upon engraftment (Granero-Molto et al., 2009). Additionally, during healing of live bone grafts, increased expression of SDF-1 messenger RNA is observed in the periosteum with the addition of anti-SDF-1 antibody (TF14016) inhibiting bone formation (Kitaori et al., 2009b). This study also reported the ability of CXCR4-expressing MSCs which have homed to the site of

bone injury to contribute to bone repair via endochondral ossification (Kitaori et al., 2009b). In addition to CXCR4, a number of additional factors have been identified which can both enhance or reduce MSC migration. In a study carried out by Ozaki *et al* (Ozaki et al., 2007), a number of growth factors which can also contribute to MSC migration were also identified. In this study, 26 growth factors were assessed for migration of human and rabbit MSCs. The growth factors that consistently enhanced MSC migration were PDGF –BB & -AB, EGF, TGF- $\alpha$ , FGF-2, IGF-1) and hepatocyte growth factor (HGF), with PDGF-BB having the greatest effect on migration. Interestingly, combinations of these growth factors which shared the same receptor did not result in an enhanced effect on migration of MSCs while other combinations of these migratory factors such as FGF-2 and PDGF-BB actually inhibited migration. This indicates a highly complex, regulated process of MSC migration.

As this migration occurred in the vehicle control in this study, presumably the mechanism of MSC recruitment was due to the infiltration of another cell type initially which produced the factors outlined above which resulted in the activation and mobilisation of the endogenous MSCs to the site implants and resulted in the bone and cartilage tissue formation observed. The presence of blood vessels in the newly formed tissue would support this theory.

# Chapter 5

*In vivo* imaging and assessment of  
bone repair in a rat femoral  
critical size defect (CSD) model

## 5.1 Introduction

Bone regeneration is typically a highly efficient process facilitating the scarless regeneration of most bone defects (Young et al., 2009). Larger defects or defects where the natural regeneration response is impaired such as in osteoporosis or non-union fractures require intervention (Harwood and Ferguson, 2015). Non-union or delayed union fractures represent a serious problem for orthopaedic healthcare with incidence rates been reported at between 5 and 20% (Giannoudis et al., 2007). This provides an ever growing problem as the proportion of older people who typically are diagnosed with non-union fractures (Parker et al., 2007) is increasing. Furthermore, as the survival rate of older people after these falls has increased, these patients are exposed to the risk of falling again, leading to what can only be described as an orthopaedic epidemic in older people. Furthermore, the burden on healthcare is enormous with an annual cost in the US of nearly \$10 billion for non-union fractures of the femoral neck alone (Raaymakers, 2006) which comprise only 5-10% of all fractures (Markey, 1987). A number of therapeutics have emerged which have greatly improved bone regeneration capability. These include autologous bone grafting of the patients own bone, allograft transplantation, osteoconductive scaffolds which can be used on their own or in combination with cell and gene therapies or growth factors (Dimitriou et al., 2011). However, despite the advancement of these treatment modalities, there have been reported drawbacks including issues with cost and efficacy, particularly in cases of large bone defects in which regeneration can be difficult to achieve (Amini et al., 2012). Similarly, there are co-morbidities associated with the use of autologous bone grafting such as pain and morbidity at donor site as well as a lack of availability of tissue (Harwood and Ferguson, 2015). This has driven the field of tissue engineering to explore alternatives such as cell-based therapies.

Cell-based therapies offer huge potential for treatment of bone defects as large numbers of osteoprogenitors such as MSCs can be delivered to the defect site. Normal bone healing occurs in a well-orchestrated series of events where cells, cytokines, osteoconductive matrix and adequate blood supply performing together

in a mechanically stable environment leading to bone repair. This concept is known as the “diamond concept” and indicates that limitation of any of these components can disrupt tissue repair (Giannoudis et al., 2007). Significant work has been focussed on determining the efficacy of growth factors such as BMPs and parathyroid hormone (see chapter 4) or osteoconductive scaffolds such as HA:TCP-based materials separately and in combination with these growth factors (Schopper et al., 2008). The use of growth factors, although reported to be efficacious can be cost prohibitive (Dahabreh et al., 2007). MSCs have previously been reported to produce a number of growth factors and cytokines involved in angiogenesis, anti-apoptosis and immunomodulation (Singer and Caplan, 2011). This makes MSCs particularly attractive as the cells may produce multiple factors that stimulate bone repair by recruitment of endogenous osteoprogenitors as well as directly differentiate to osteochondral cells themselves which may directly contribute to bone healing. Although the exact mechanism by which MSCs contribute to bone repair is unclear, the potential of MSCs to heal bone is apparent. Optimising the culture conditions of these MSCs prior to implantation may improve the efficacy rates of these cells in clinical studies of bone repair which as of yet has not been convincing (Steinert et al., 2012). Some studies have assessed the potential of chondrogenically-primed MSCs in ectopic and orthotopic models of bone repair indicating a potential role for *in vitro* priming of MSCs towards an osteochondral fate prior to implantation (Farrell et al., 2011, van der Stok et al., 2014b). The aim of this chapter was to determine if SF-isolated and cultured MSCs could contribute to the healing of a critical size bone defect model at comparable levels to conventionally cultured MSCs. Additionally, the aim was to determine if the use of hypoxic or normoxic culture for isolation and expansion of MSCs resulted in selection of a population of MSCs that would repair bone via alternate means e.g., intramembranous versus endochondral bone formation as a reported effect on the *in vitro* differentiation potential of MSCs was shown in chapter 3 and *in vivo* potential in chapter 4 using a ectopic model of bone repair. However, ectopic implantation of MSCs does not accurately represent the complex physical and biochemical cues MSCs would be subject to in an orthotopic clinical setting, thus

the MSCs were assessed in a rat femoral defect model representative of an atrophic non-union (van der Stok et al., 2014b).

### 5.2 Methods

To assess the *in vivo* bone forming ability of SF and SC MSCs,  $1 \times 10^6$  MSCs were loaded onto MBCP+ and implanted into a rat unilateral critical size femoral defect for 8 weeks (Section 2.14.1). A critical size defect, 5mm in length, was created in the right femur with a Gigli saw (Section 2.20). Internal fixation with a polyetheretherketone (PEEK) plate and titanium screws was performed. *In vivo* imaging of bone formation using  $\mu$ CT (Section 2.21) and neovascularisation with photoacoustic imaging (2.22) was assessed at 4 and 8 weeks. Rats were immunosuppressed for the first 3 weeks of the study with FK506 and SEW2871 (Section 2.19) to prevent rejection of human MSCs. Animals were individually housed in individually ventilated cages (IVC) for the first week post-surgery to prevent interference at the surgical site and together in IVCs for the remainder of the study to reduce the risk of infection as animals are immunocompromised. At 8 weeks post-surgery, animals were euthanized using CO<sub>2</sub> inhalation and cervical dislocation. Rat femurs were harvested and fixed in 100% ethanol. Samples were decalcified using EDTA for 14 days and sectioned using a microtome. Staining of bone was performed using Movat's Pentachrome stain and blood vessels by staining for lectin UEA-1 (Section 2.23). A total of 6 rats were assessed per group for  $\mu$ CT and photoacoustic imaging.

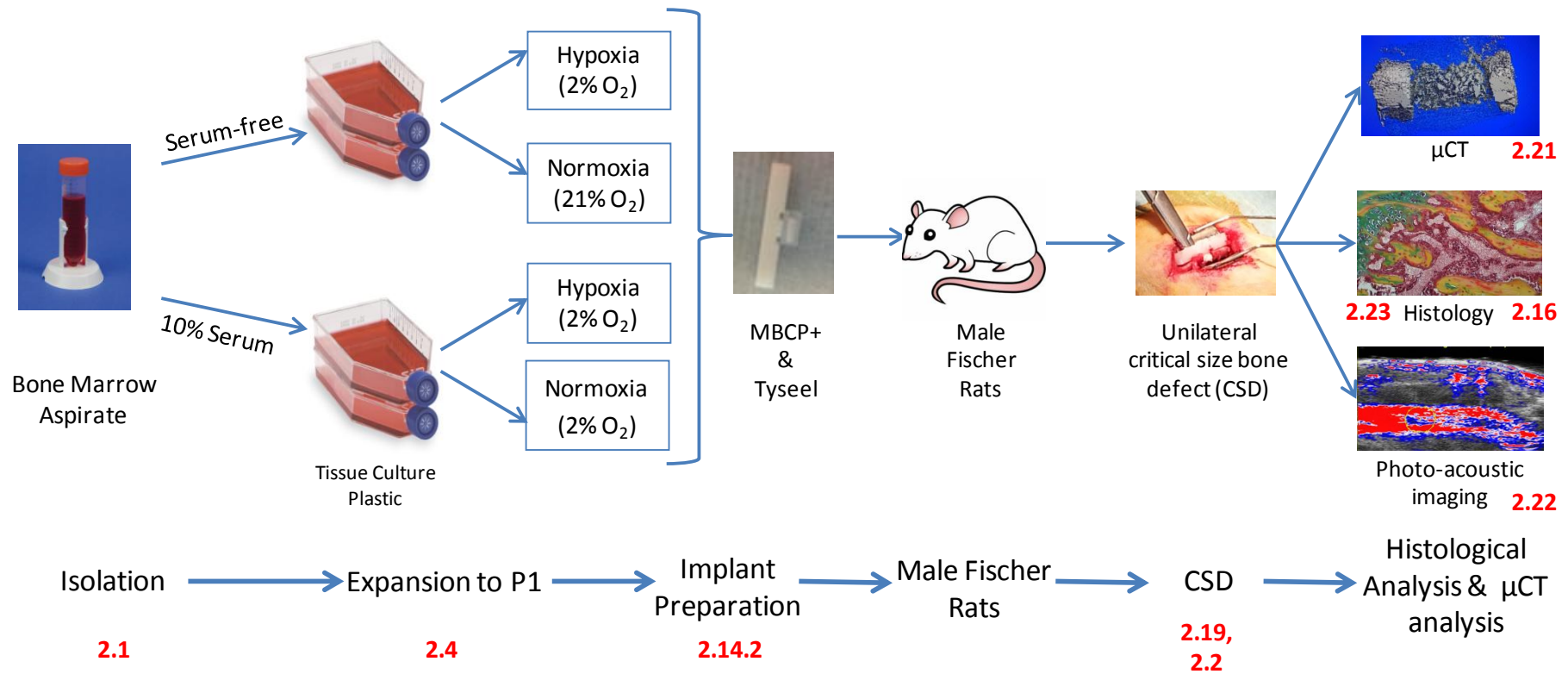
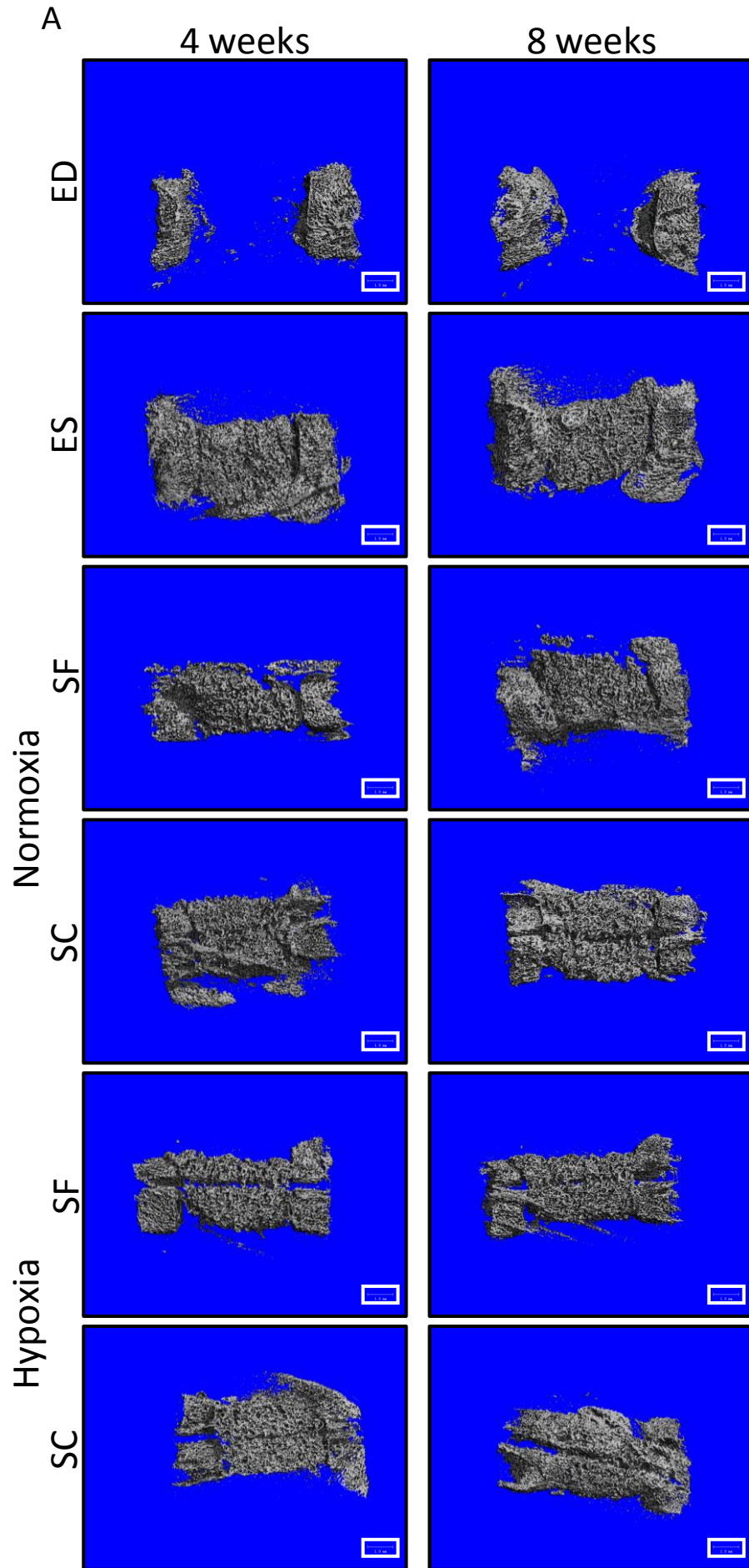


**Figure 5.2.1 Schematic representation of the experimental design used to assess the in vivo ability of SF and SC MSCs to repair bone in a rat femoral critical size bone defect model.**

## 5.3 Results

### 5.3.1 In vivo quantification of bone formation using $\mu$ CT

*In vivo* assessment of bone formation was assessed at 4 and 8 weeks post-implantation using the *in vivo*  $\mu$ CT analysis using Scanco  $\mu$ CT 40. Analysis was performed on 3 biological replicates (MSC donors) with 2 technical replicates (rat femurs) for each group. Bone volume was calculated as a percentage of total tissue volume excluding the presence of the MBCP+ granules which have a similar density to bone. 3D images of implants were generated (figure 5.3.1a) of implant regions at 4 and 8 weeks indicating the absence of bone repair in ED group. Lack of integration of implant is observed in SF-normoxia and ES group as evident by clear distinction between implant and surrounding bone tissue. Integration of implants is evident in SC groups (both hypoxia and normoxia) at 4 and 8 weeks. Partial integration of SF-hypoxia group implant was evident at 8 weeks. Quantification of new bone formation was carried out and is represented in figure 5.3.1b. To accurately assess new bone formation, the density range which detects MBCP+ granules was gated out and remaining tissue was assessed for bone formation. These may result in the underestimation of total bone formation as mature bone may also be excluded by this type of analysis. All cell-treated groups, except for the SF-hypoxia group, improved bone formation in comparison to the ES group at 4 weeks. All cell groups improved bone formation compared to ES group at 8 weeks. This data indicates that all cell groups improved bone formation in model compared to the vehicle group. The SC group consistently produced higher levels of bone in comparison to the SF group in both hypoxia and normoxia at both time points. No differences were observed between SC-normoxia or hypoxia groups at 4 weeks. However, at 8 weeks significantly increased levels of bone formation were observed in SC-normoxia group. Overall these data indicate that MSCs cultured in normoxia in SC medium contribute to greater levels of bone repair in this model. However it is worth indicating that levels of 'mature' bone are not represented in this data as the density of this tissue would be too similar to MBCP+ granules to distinguish the two.



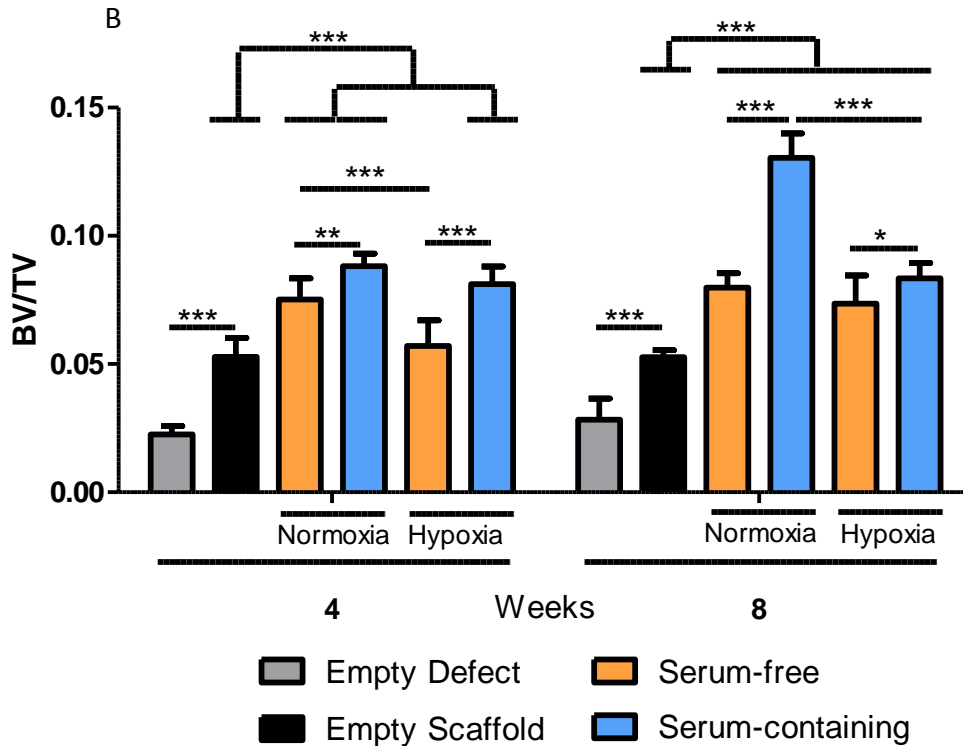


**Figure 5.3.1 Serum-containing MSCs cultured in normoxia are superior at in vivo bone formation.** Empty defect, ED; empty scaffold, ES; serum-free, SF; serum-containing, SC. (A) Representative 3D images of defect region at 4 and 8 weeks post implantation. Scale bar: 1mm. (B) Quantification of bone volume calculated as a percentage of tissue volume. All cell-treated groups results in increased bone formation compared to ES group by 8 weeks. Increased levels of bone formation observed in SC-normoxia group over time. Results are presented as the mean  $\pm$  standard deviation (SD) of 3 biological replicates with 2 technical replicates, \* $p \leq 0.05$ , \*\* $p \leq 0.01$ , \*\*\* $p \leq 0.001$  as determined using two-way ANOVA and Bonferroni's multiple comparisons post-test.

### 5.3.1 Histological staining control using Movat's Pentachrome stain of goat knee

Prior to beginning this study, the decision was determined to switch from the use of Mallory's modified trichrome stain to Movat's Pentachrome stain as a clearer distinction between bone, cartilage and bone marrow is evident by yellow, green and purple colours, respectively. As a staining control for this tissue, a healthy goat knee which had previously been decalcified using EDTA, in a similar method to the decalcification of samples described below, was used. Here the cartilage surface can clearly be seen by rich by green colour with a clear switch from green to yellow colour as tissue changes from cartilage to subchondral bone. Bone marrow is observed throughout bone as the purple colour.

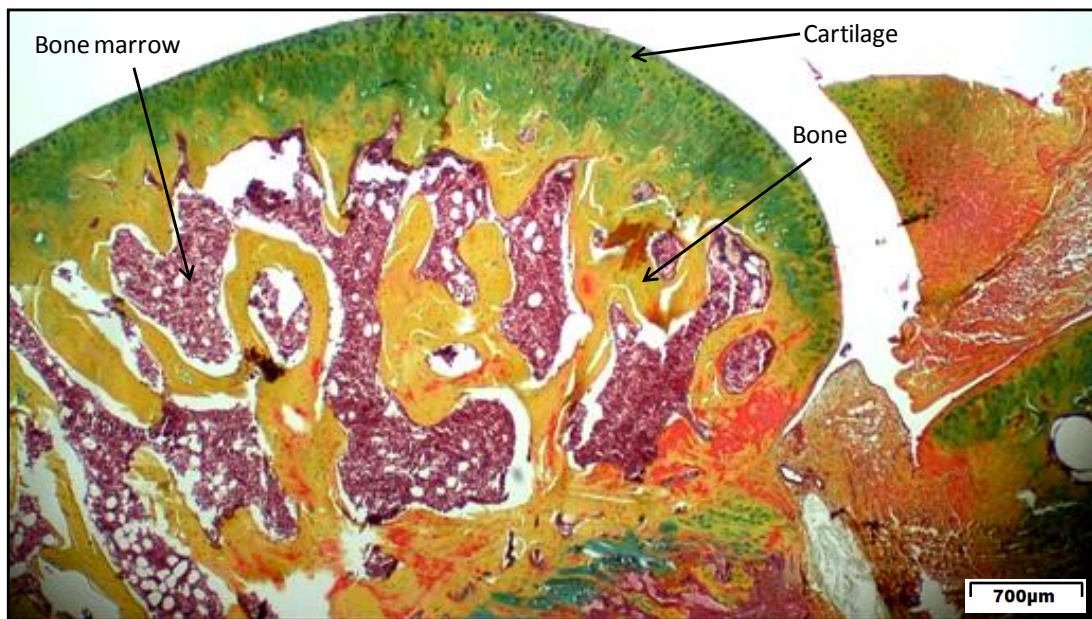


**Figure 5.3.2** Representative staining control for Movat's Pentachrome using healthy goat knee. Bone is indicated by yellow, cartilage by green and bone marrow by purple.

### 5.3.3 Histological analysis of bone repair superior regeneration of defect by SC

#### MSCs

Movat's Pentachrome stain was used to assess bone repair of the CSD. Due to the large size of the defect region 9 images at 4x magnification were taken and merged together (Figure 5.3.3a). Enlarged versions of the images, highlighting specific regions of interest, are represented in Figures 5.3.3b-g. No repair of bone in the empty defect region was observed as seen by the lack of tissue present indicating that this CSD model is incapable of regeneration and represents a critical-sized defect. The formation of a cartilaginous tissue on one side of the bone defect (figure 5.3.3b, red box) indicated an attempt to repair the tissue via formation of endochondral bone formation. This attempted repair was only apparent on one side of defect region (figure 5.3.3b, green box). Similarly low levels of regeneration were observed in the empty scaffold group, the vehicle control. However, there was an increase in osteogenic repair in this region as evident by the surrounding of MBCP+ granules across the upper side of defect by bone indicated by yellow staining (figure 5.3.3c, red box). Additionally formation of bone is also evident surrounding some MBCP+ granules within the defect region indicating the addition of MBCP+ granules improves the ability of the defect region to self-repair (figure 5.3.3c, green box). However, levels of self repair are insufficient to fully repair the defect region. The SF MSCs cultured in normoxia did not improve bone repair. Low levels of new bone formation were observed in a small region of defect (figure 5.3.3d, red box). Overall, the SF implant failed to integrate into the surrounding tissue (figure 5.3.3d, green box). An increase in osteogenic potential was observed in the group treated with SF MSCs cultured in hypoxia as indicated by the formation of bone surrounding the outside of the implant region and traversing the length of the defect region (figure 5.3.3e, red box). Additionally this tissue integrated into the surrounding tissue indicating a superior bone repair than SF MSCs cultured in normoxia. High levels of bone regeneration were observed in the group treated with SC MSCs cultured in normoxia (figure 5.3.3f). The presence of *de nova* bone and cartilage indicates repair of the defect via endochondral bone formation (figure 5.3.3f, red box). The presence of bone, and more commonly cartilage, was observed throughout the tissue with full integration of the cell implant with

surrounding tissue (Figure 5.3.3f, green box). A reduction in the bone healing ability of SC MSCs cultured in hypoxia is observed compared to their normoxic counterparts (figure 5.3.3g). Almost complete bridging of defect region is observed on one side of the defect region (figure5.3.3g, red box) and full integration of cell implant is observed at both sides of the defect. The presence of cartilage tissue is also observed within the defect region (figure 5.3.3g, green box) with bone present throughout the defect region around MBCP+ granules. This data indicates that the SC MSCs seem to be superior to SF MSCs at repairing bone and the culture of SC MSCs in normoxia improves their bone forming ability. No cartilage tissue was observed in the SF groups indicating that bone repair by these cells is primarily via direct osteogenic differentiation or intramembranous bone formation. Conversely, the presence of bone and cartilage tissue in SC groups indicates that these cells repair bone via endochondral bone formation or a combination of endochondral and intramembranous bone formation.

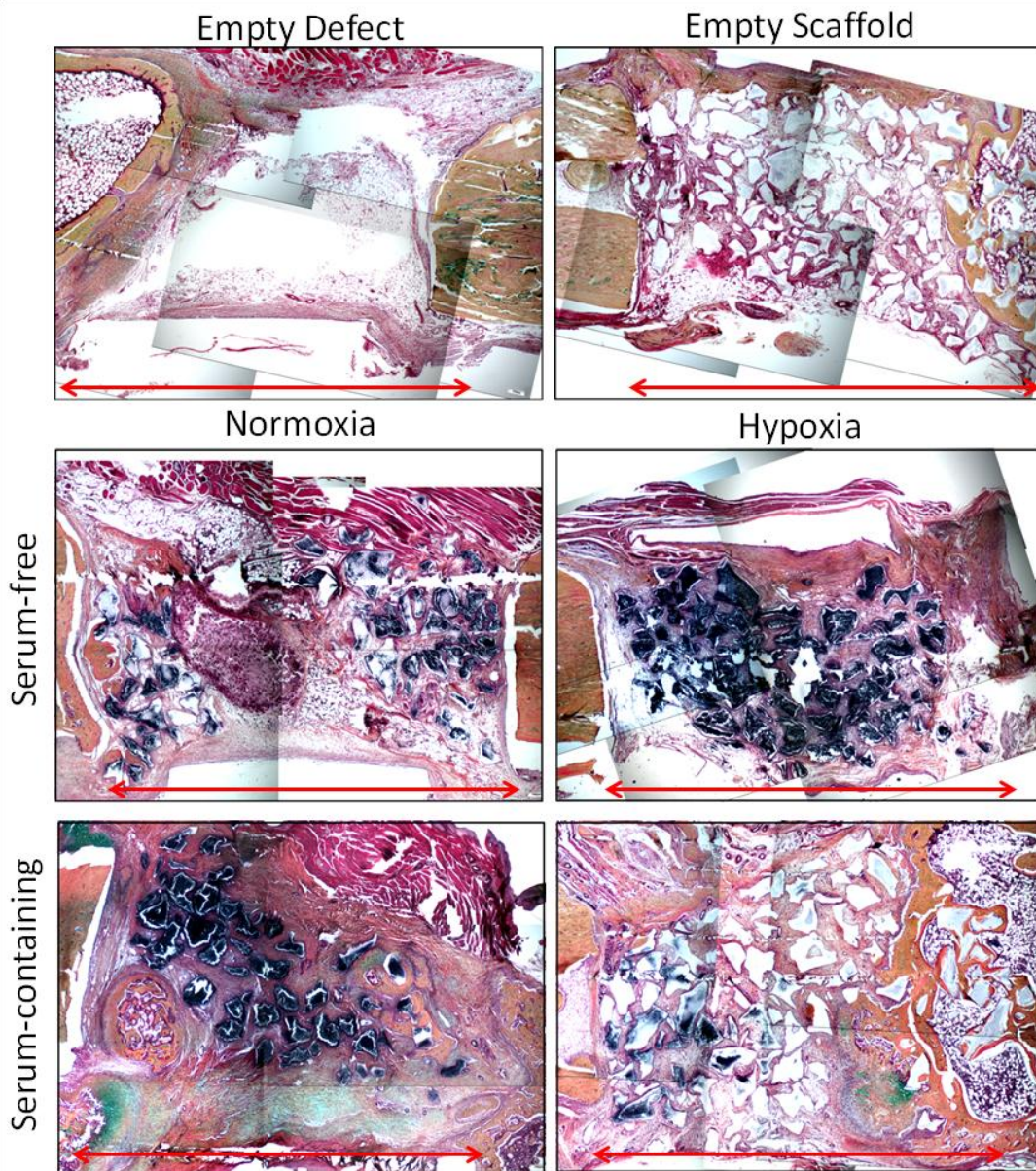


**Figure 5.3.2a: Representative histological analysis of bone, cartilage and bone marrow present in implanted constructs.** Representative images of Movat's Pentachrome stained images of implanted groups. Bone (Yellow), cartilage (Green) and bone marrow (purple). Implanted MPCP+ (Dark blue or absent of colour). Scale bar 700 $\mu$ m. Width of defect region indicated by red arrows

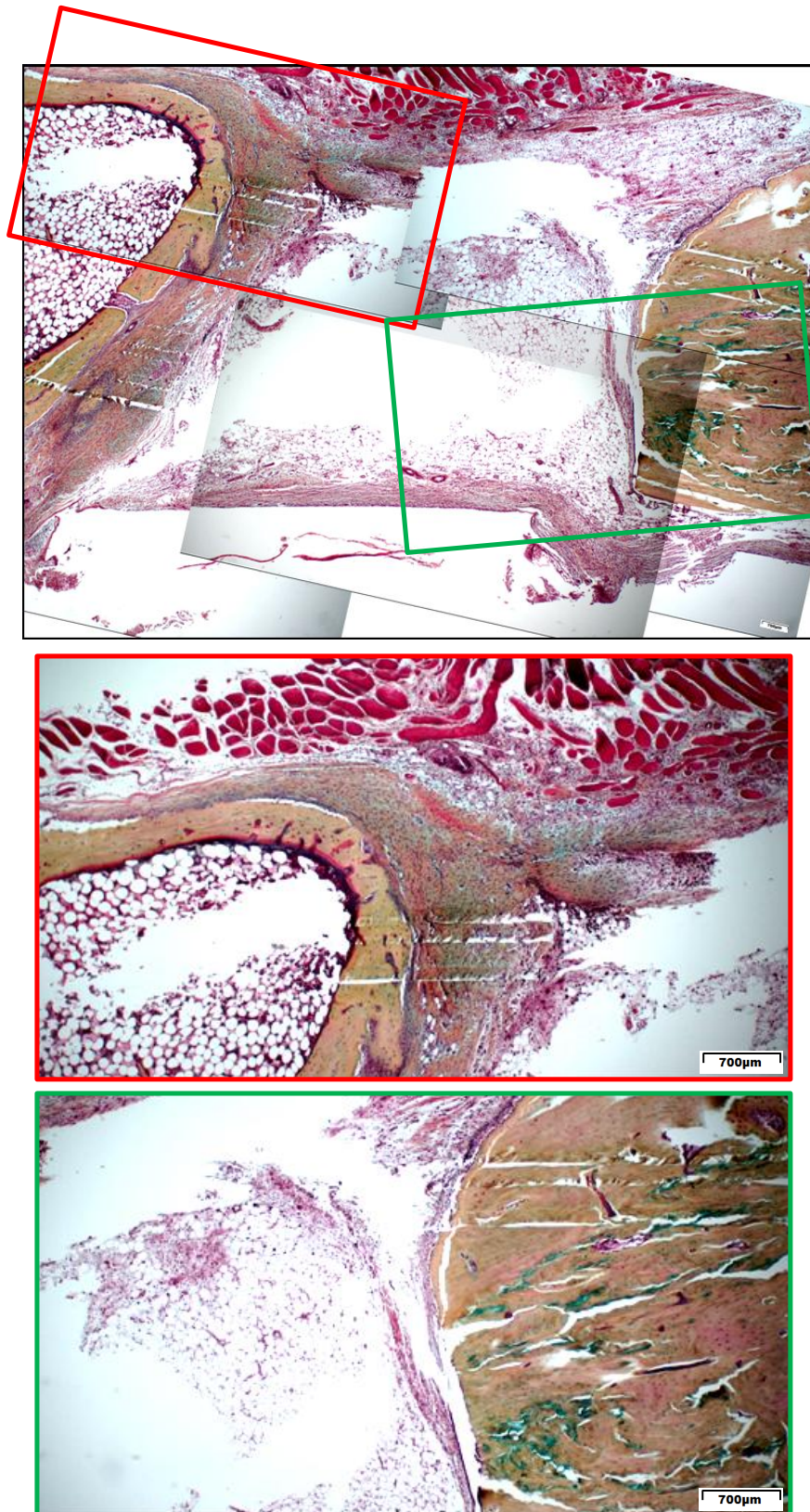


**Figure 5.3.3b: Representative “Empty defect” group staining.** Areas indicated by the yellow and green rectangles are magnified in the middle and bottom images, respectively.

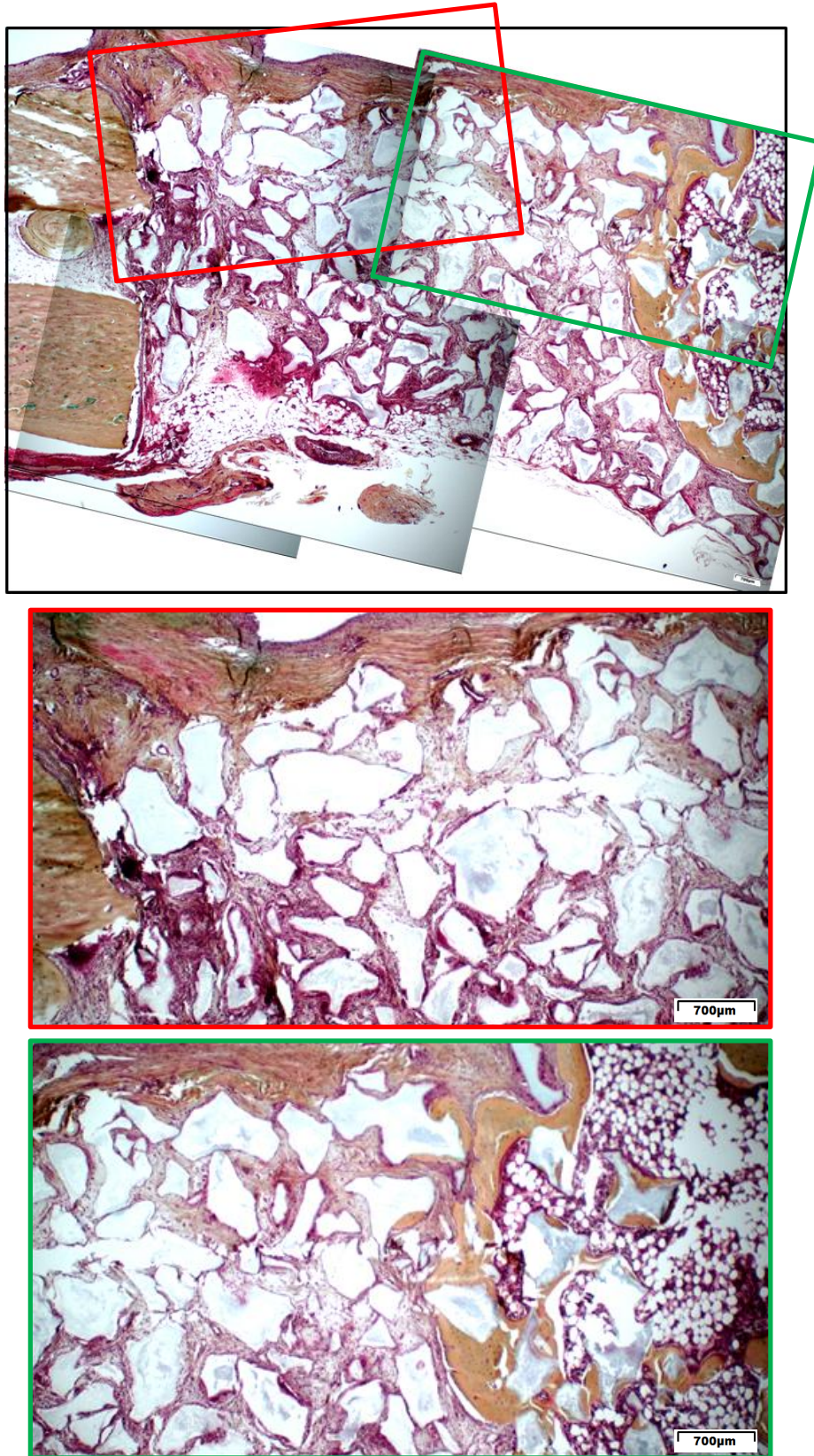


**Figure 5.3.3c: Representative “Empty scaffold” group staining.** Areas indicated by the yellow and green rectangles are magnified in the middle and bottom images, respectively.

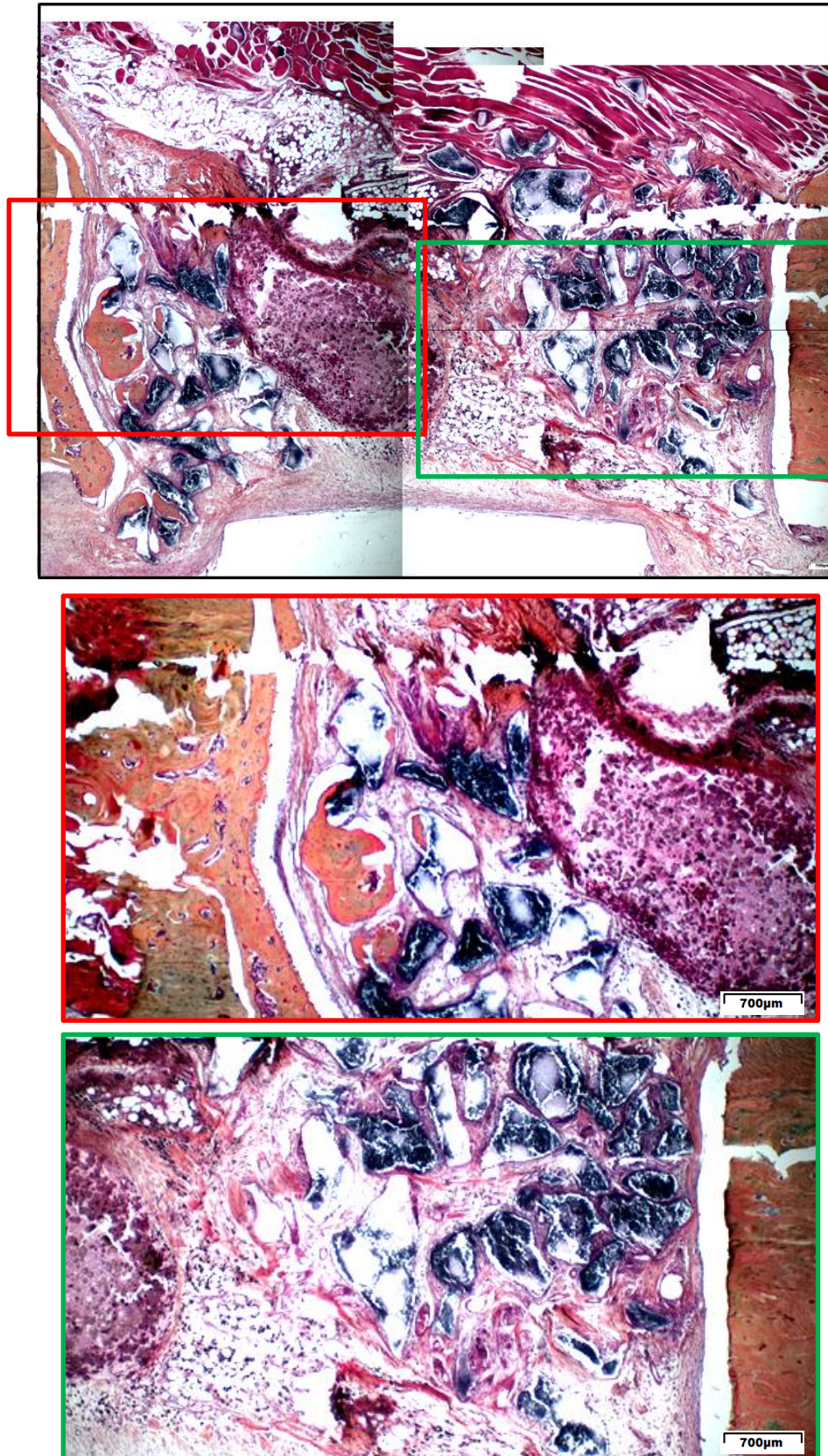


**Figure 5.3.3d:** Representative “Serum-free normoxia” group staining. Areas indicated by the yellow and green rectangles are magnified in the middle and bottom images, respectively.

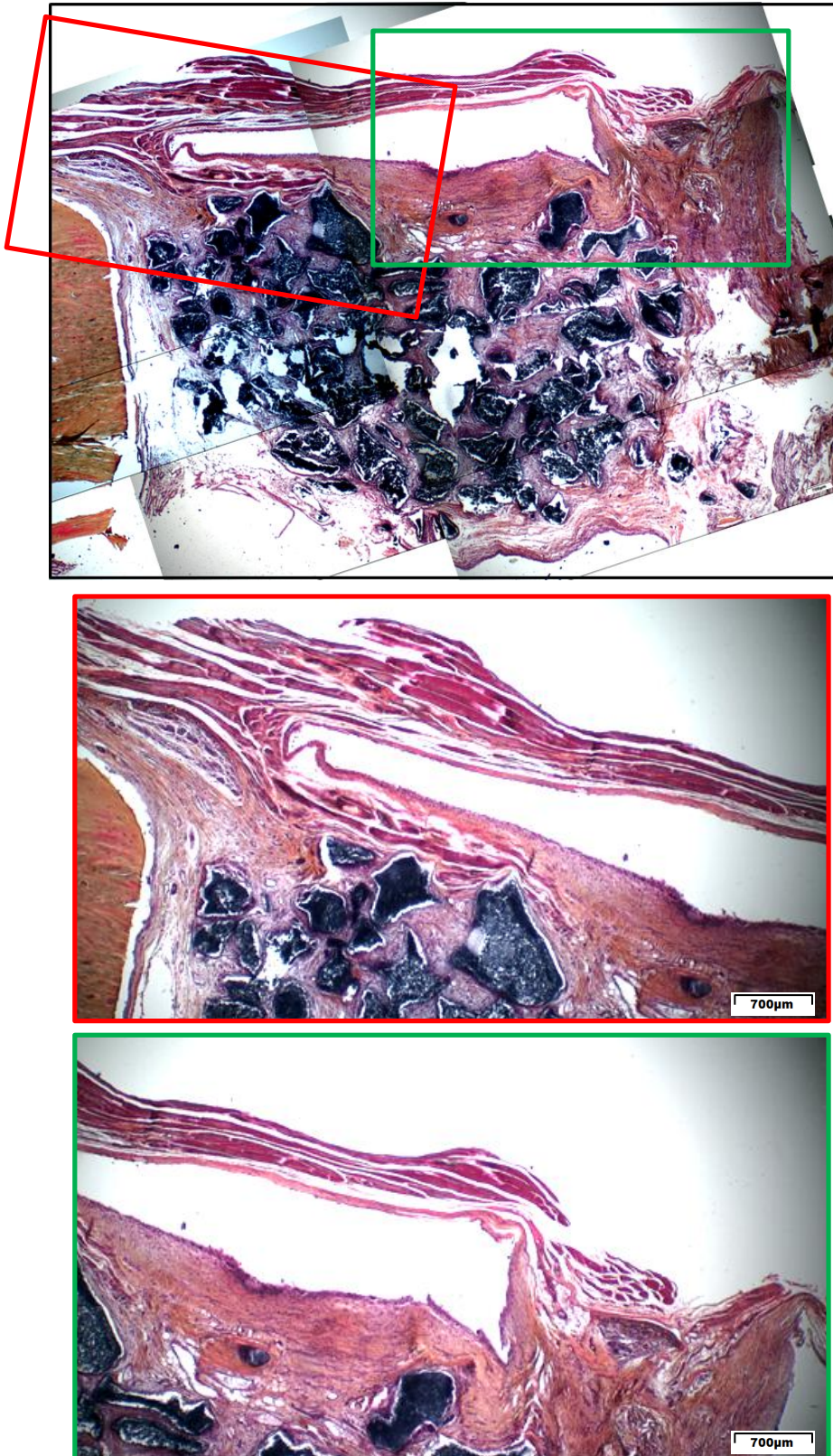


**Figure 5.3.3e: Representative “Serum-free hypoxia” group staining.** Areas indicated by the yellow and green rectangles are magnified in the middle and bottom images, respectively.

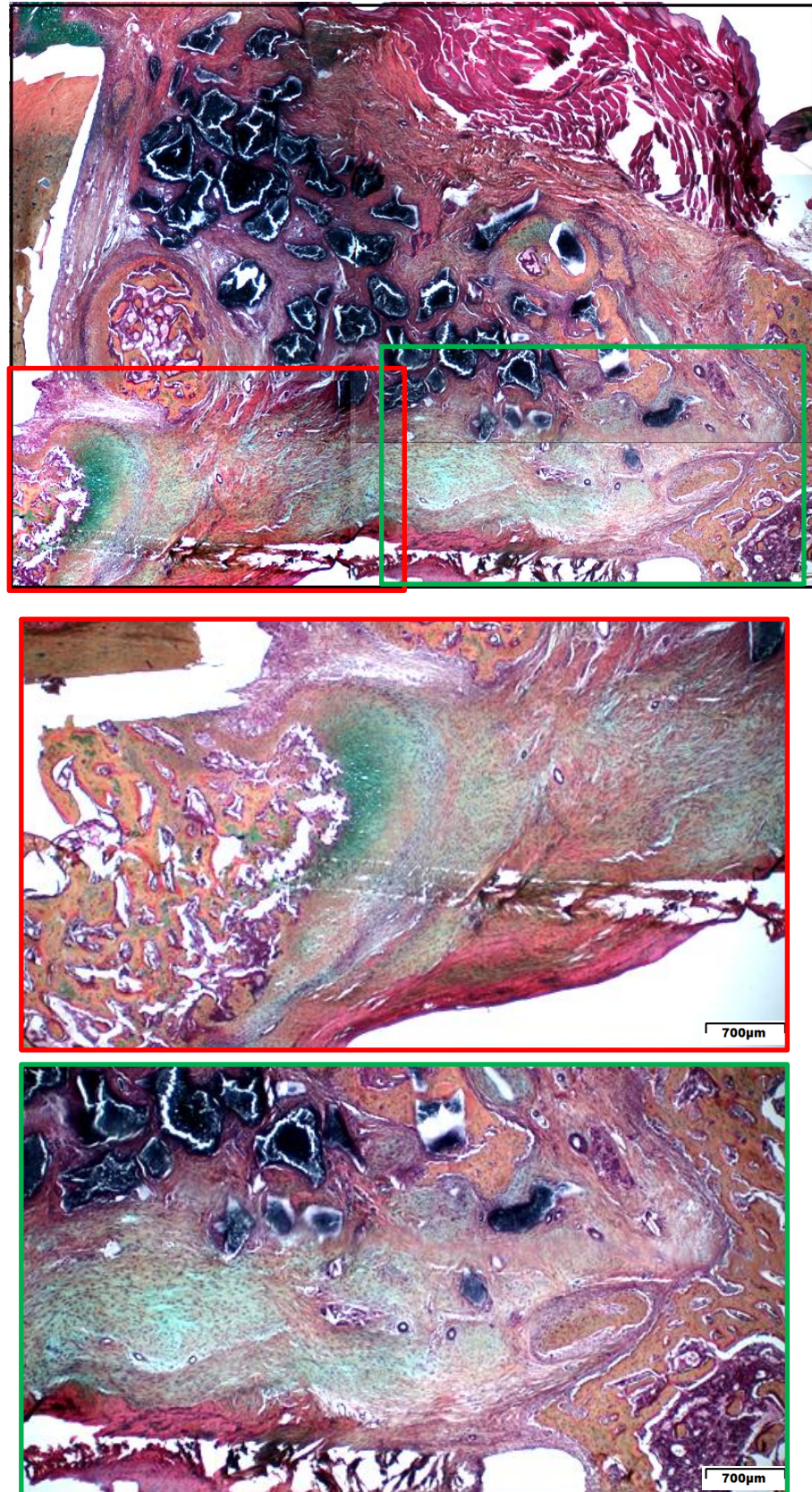


**Figure 5.3.3f:** Representative “Serum-containing normoxia” group staining. Areas indicated by the yellow and green rectangles are magnified in the middle and bottom mages, respectively.

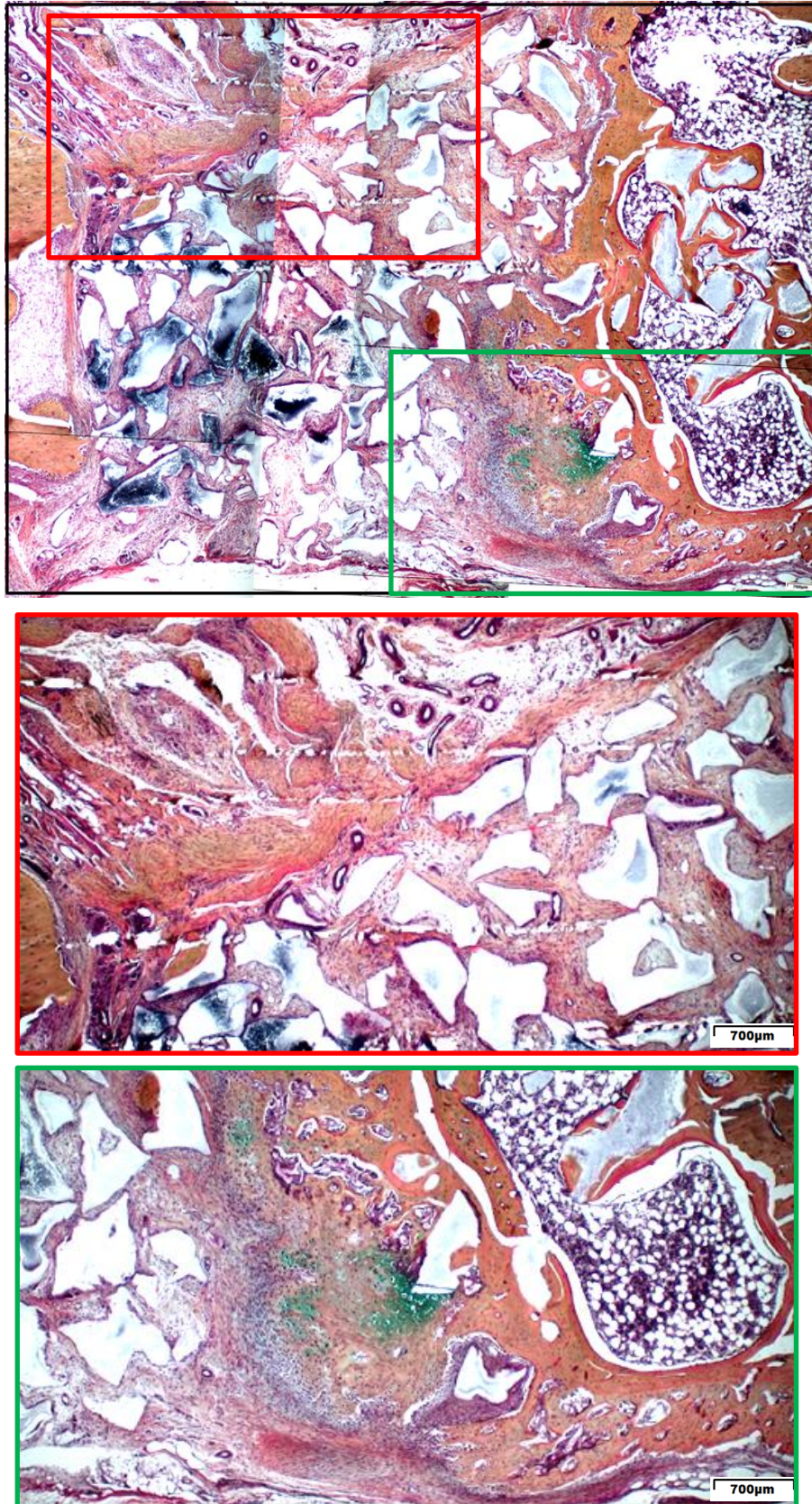
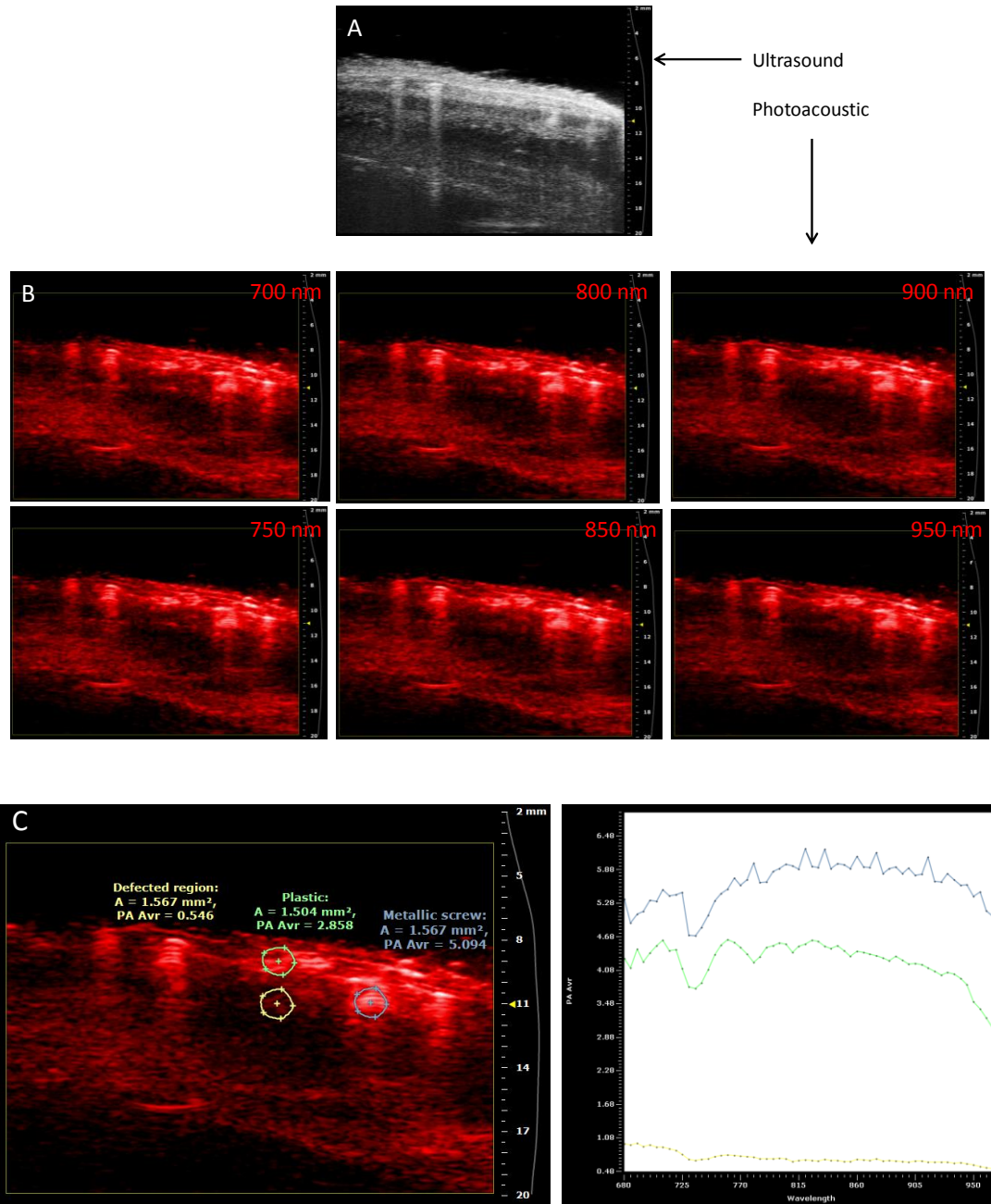


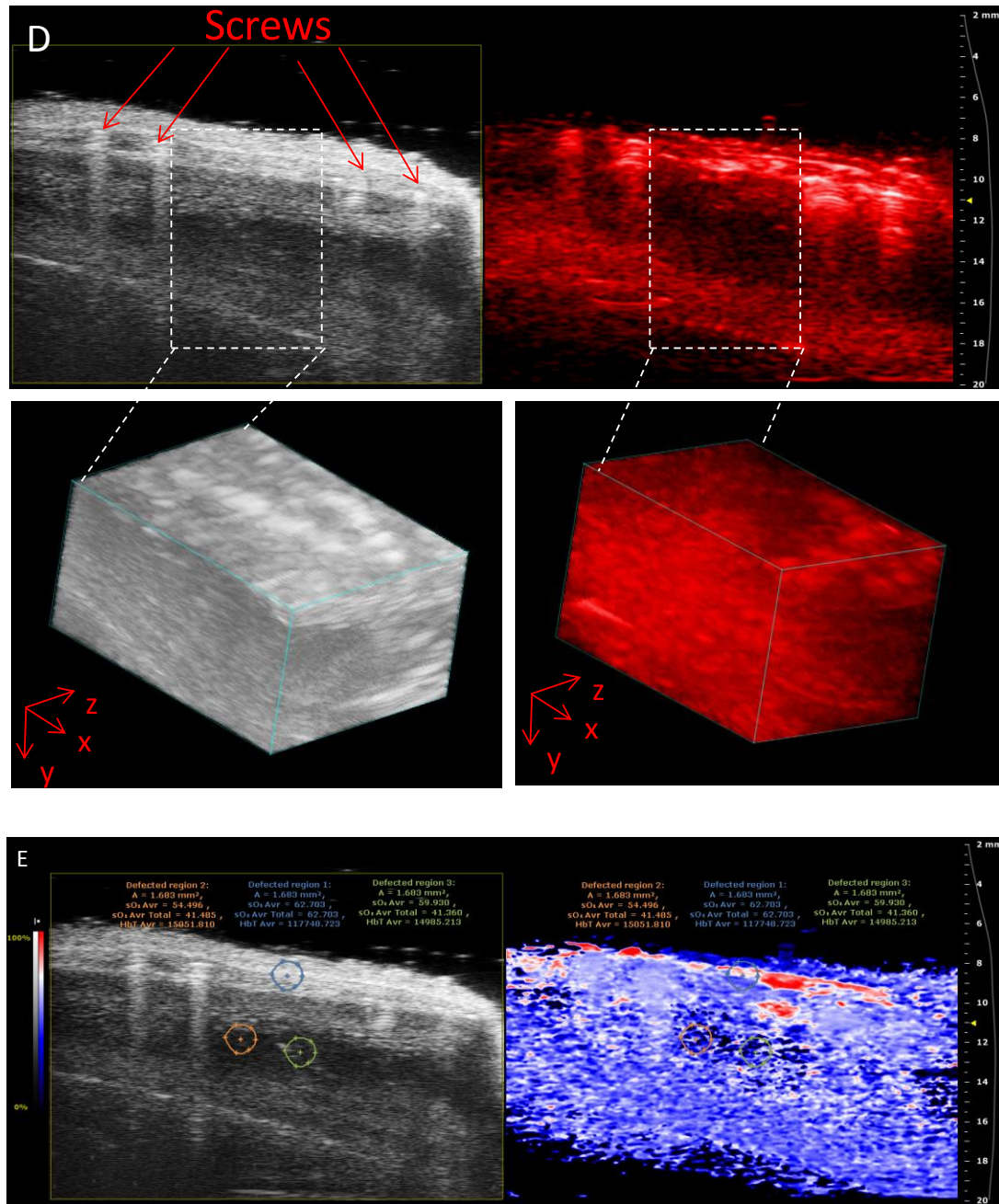
**Figure 5.3.3g:** Representative “Serum-containing hypoxia” group staining. Areas indicated by the yellow and green rectangles are magnified in the middle and bottom images, respectively.

#### **5.3.4 Optimisation of *in vivo* visualisation of angiogenesis by photoacoustic imaging (PA)**

An integrated photoacoustic and ultrasound (US) imaging system was used to visualise neovascularisation of defect regions using a linear-array transducer probe. The probe was operated at 21MHz providing an axial and lateral resolution of 75 $\mu$ m and 158 $\mu$ m respectively. Optimisation of the system was first established to determine the suitability of PA imaging of the rat femur. Figure 5.3.4a is a 2D ultrasound image of the defect region with screws visible as two sets of two vertical lines indicating the position of the titanium screws. The PEEK plate is undetectable by PA or US imaging. Figure 5.3.4b represents PA imaging of the same region at 6 different wavelengths to determine the optimal wavelength for identification of neovascularisation. No major difference was observed between wavelength frequencies and 800nm was chosen for future scans. To determine if the titanium screws or PEEK plate interfered with the reading of defect zone, PA readings of each region was measured individually and readings were compared (figure 5.3.4c). The various regions were clearly distinguishable from each other indicating the suitability of PA analysis for assessment of neovascularisation in this model. To standardise the region being measured, the region between the two sets of two screws was selected and a 3D rendering of this region (figure 5.3.4d) was generated and used for assessment of oxygen and haemoglobin saturation (figure 5.3.4e).

# Chapter Five

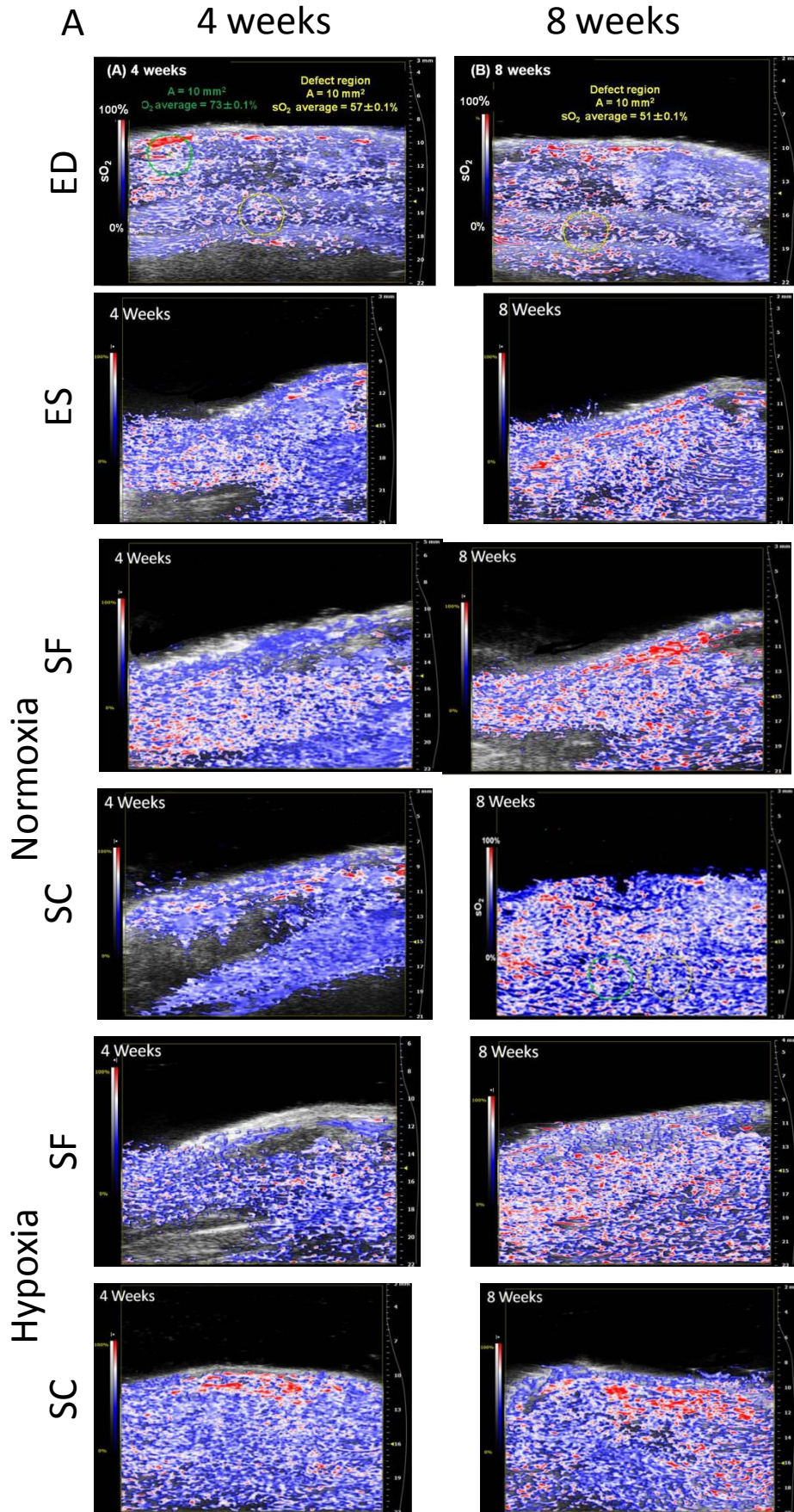


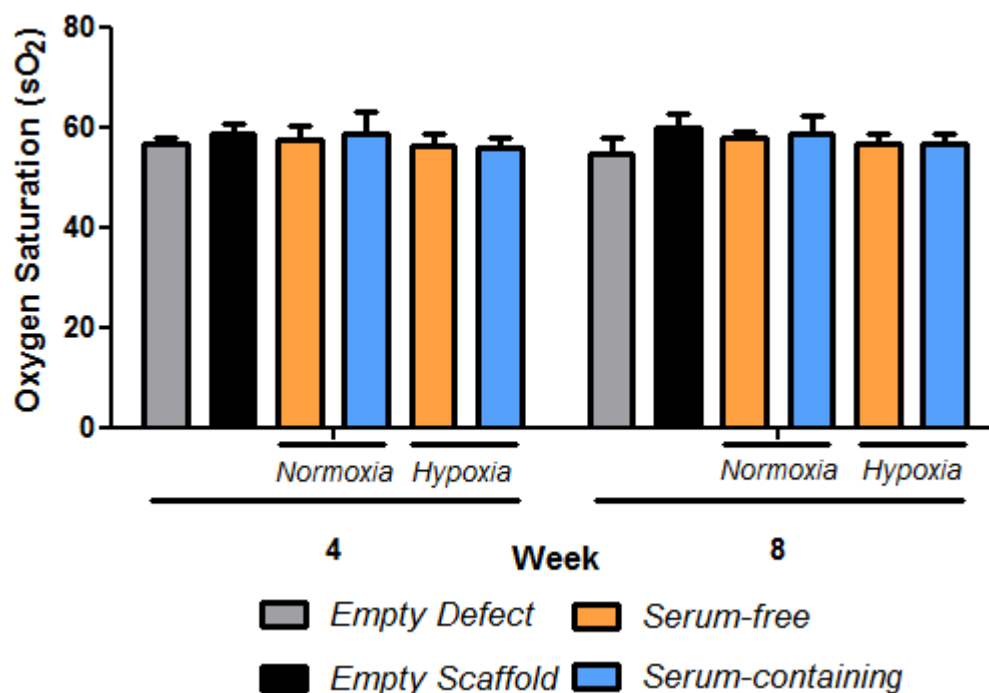


**Figure 5.3.4: Optimisation of PA imaging of neovascularisation.** (A) Representative 2D ultrasound image of the CSD region of rat femur containing 4 titanium screws. (B) PA readings of the region identified in (A) at multiple wavelengths to determine the optimal wavelength for visualisation of the region. (C) Measurement of specific materials within the defect region to determine basal PA reading. PEEK plate (green), Titanium screws (blue) and defect region (yellow). (D) Standardisation of CSD region between titanium screws to be analysed. Representative image of the CSD region indicating sO<sub>2</sub> levels as a colour change from blue to white to red indicating an increase in sO<sub>2</sub> levels.

### **5.3.5 Oxygen saturation levels of CSD does not change over time**

The oxygen saturation (sO<sub>2</sub>) levels of the defect region were measured at 4 and 8 weeks post-surgery to determine if sO<sub>2</sub> levels change over time during bone repair. Six animals were measured per group. Representative images of sO<sub>2</sub> levels of a single slice of defect region are presented in figure 5.3.5a. No changes in sO<sub>2</sub> levels in the CSD region were observed between time points for any of the groups. Quantification of sO<sub>2</sub> levels of a 10mm<sup>2</sup> area within the defect region are presented in figure 5.3.5b. This data correlates with figure 5.3.5a indicating no difference between the groups at each time point and indicates no changes in sO<sub>2</sub> levels over time. These data indicates that either sO<sub>2</sub> levels of CSD don't change over time or that changes are not detectable by PA imaging.

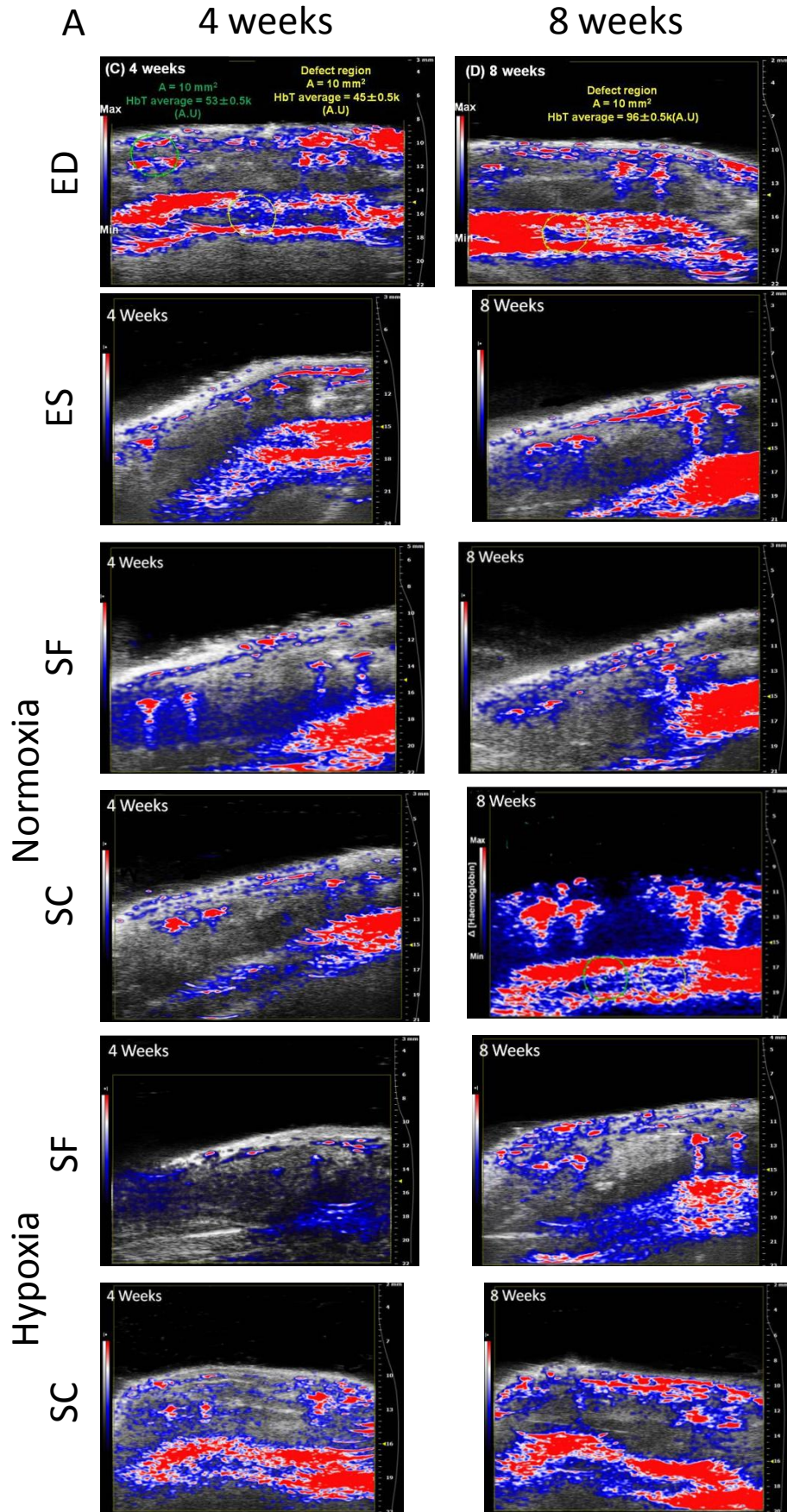




**Figure 5.3.5 Assessment of sO<sub>2</sub> levels of CSD over time.** (A) Representative 2D slices of sO<sub>2</sub> levels at 4 and 8 weeks post-surgery indicating no difference in sO<sub>2</sub> levels. Empty defect, ED; empty scaffold, ES; serum-free, SF; serum-containing, SC. (B) Quantification of sO<sub>2</sub> levels measured at weeks 4 and 8 post surgery indicating no change in sO<sub>2</sub> levels.

### 5.3.6 Haemoglobin saturation levels of CSD do not statistically change over time

The haemoglobin (Hbt) saturation levels of the defect region were measured at 4 and 8 weeks post-surgery to determine if Hbt levels change over time during bone repair and could be used as an indicator of bone regeneration. Six animals were measured per group. Representative images of Hbt levels of a single slice of the defect region are presented in figure 5.3.6a. HbT levels appear to increase in the ED and SC normoxia group over time. Quantification of HbT levels of a 10mm<sup>2</sup> area within the defect region are presented in figure 5.3.6b. A high level of variance in the hypoxia groups at 4 weeks was noted. No difference was observed between groups over time indicating HbT levels did not change during the course of this study.



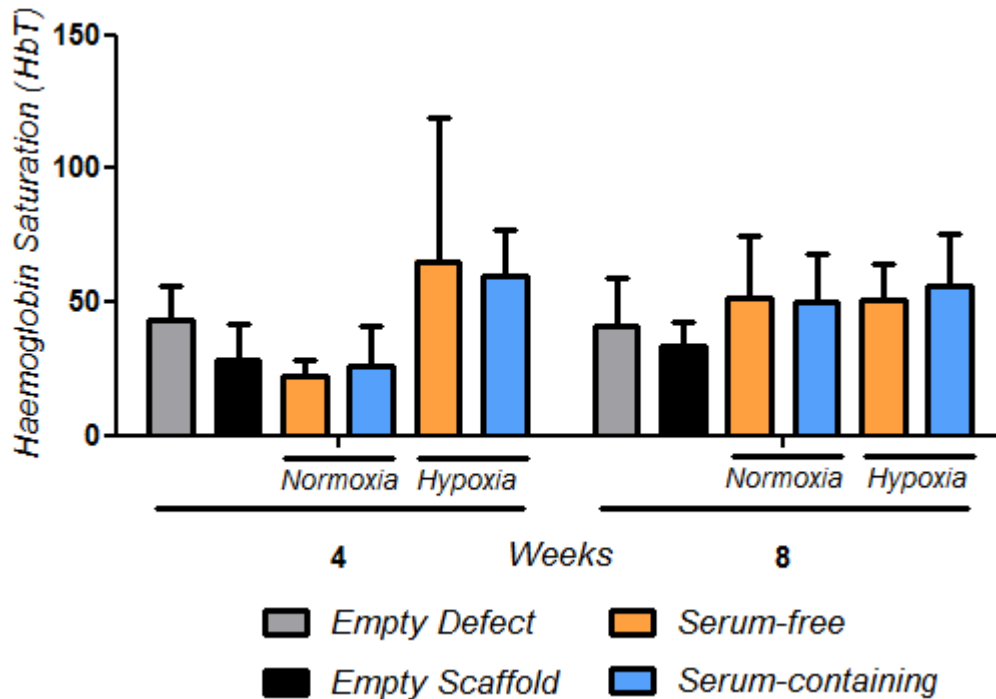


**Figure 5.3.6 Assessment of HbT levels of the CSD region over time.** (A) Representative 2D slices of HbT levels at 4 and 8 weeks post-surgery indicating no difference in HbT levels. Empty defect, ED; empty scaffold, ES; serum-free, SF; serum-containing, SC. (B) Quantification of HbT levels measured at weeks 4 and 8 post surgery indicating no change in HbT levels.

### 5.3.7 Histological analysis of neovascularisation indicate low levels of vascularisation in all groups

To determine if the delivery of MSCs improved neovascularisation of the defect region, histology slides prepared from the study (as described in section 2.17) were stained for UEA-1 which identified L-fucose found on endothelial cells to indicate the presence of blood vessels. Samples were counterstained with Hoechst 33342 nuclear stain to identify cells. Low levels of blood vessels were identified in the groups that received SF or SC cells previously cultured in normoxia. No blood vessels were observed in control groups or hypoxia groups indicating normoxia cultured MSCs may induce superior neovascularisation compared to hypoxia cultured MSCs.

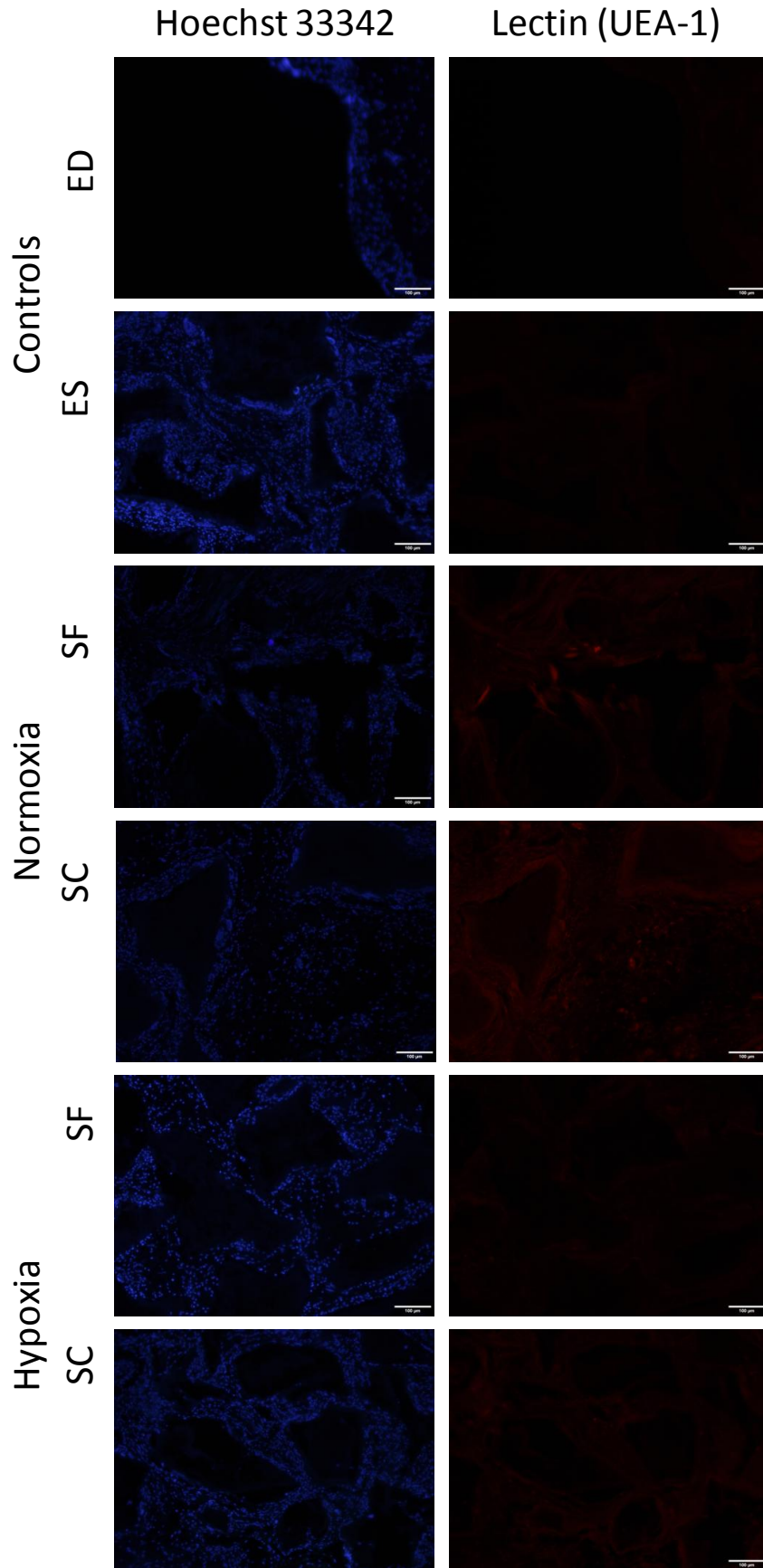


**Figure 5.3.7: Lectin staining detects the presence of blood vessels in groups that received normoxia-cultured MSCs.** Histological sections stained with Hoechst 33342 to identify cell nuclei and UEA-1 to identify endothelial cells. Empty defect, ED; empty scaffold, ES; serum-free, SF; serum-containing, SC. Presence of positive UEA-1 staining in groups that received normoxia-cultured MSCs indicating the presence of blood vessels. Scale bar: 100 $\mu$ m.

## 5.4 Discussion

The aim of this chapter was to assess the ability of SF MSCs to repair an orthotopic bone healing model. MSCs previously isolated from healthy human bone marrow were cultured until the end of P1 prior to implantation into a CSD defect created in a rat femur. This model has previously been shown to demonstrate the *in vivo* bone repair efficacy of MSCs at 8 weeks (Peterson et al., 2005, Hollinger and Kleinschmidt, 1990, Oest et al., 2007, Kadiyala et al., 1997). In these studies the defect is typically 5-6mm in length and the studies ran for 8 weeks. Bridging and repair of the defect was observed. This model was utilised to determine the efficacy of SF MSCs. Assessment of bone repair was assessed *in vivo* by  $\mu$ CT analysis and *ex vivo* via histological analysis. Additionally, the revascularisation of defect region was assessed *in vivo* by photoacoustic analysis and *ex vivo* by histological staining. *In vivo* quantitative data of bone formation from  $\mu$ CT analysis indicates increased levels of bone formation in groups that received SC MSCs cultured in normoxia compared to other groups. These data are verified by histological analysis of bone formation. Movat's Pentachrome stain indicated that no bone repair occurred in the empty defect model and minimal bone formation occurred in the empty scaffold group which validates the model as a CSD model, incapable of self-repair. Noticeable differences were observed in the four MSC treated groups. SF MSCs cultured in normoxia generated the least amount of bone repair in this model. Very little bone was observed and the implant failed to integrate into the surrounding bone (figure 5.3.3d). An improvement in the bone forming ability of these MSCs was observed in the groups that received SF MSCs cultured in hypoxia (figure 5.3.3e). Bridging of the defect region was observed externally to the implant region. Little to no bone was observed in this group within the defect region itself suggesting that the bone formed in this group occurred via recruitment of

endogenous MSCs and not by the implanted MSCs themselves. Future work to explore the contribution of human versus endogenous MSCs could be performed via Alu sequence staining to identify human MSCs. This would need to be further assessed. The results would indicate that where the SF MSCs contribute to bone repair, this occurs via production of paracrine factors which stimulates local progenitors to carry out repair. Conversely, groups that received the SC MSCs cultured in normoxia, formed abundant levels of cartilage and bone tissue within the defect region (figure 5.3.3f). This would indicate that these cells underwent direct differentiation in order to repair bone. The high levels of cartilage tissue also indicate that the SC MSCs repair bone via endochondral ossification or a combination of endochondral ossification and intramembranous ossification. Integration of the implant into the surrounding bone tissue also indicates these cells are better at bone repair in this model. Groups which received the SC MSCs cultured in hypoxia had a reduction in the repair of the bone defect region. Also a significant reduction in the level of cartilage tissue was observed. This may suggest that the culture of these SC MSCs in either hypoxia or normoxia alter the mechanism by which they repair bone. In the SC-hypoxia groups, bone tissue is present surrounding the MBCP+ implants with a much lower level of cartilage staining. This would suggest that the primary means of bone repair in these tissues is via intramembranous bone repair. Overall these data indicate that the SC MSCs are superior to the SF MSCs at repairing bone and that SC MSCs cultured in normoxia provide the best bone repair due to the formation of a cartilage template indicating endochondral bone which would be considered of superior quality to bone repaired via intramembranous bone formation (Yang et al., 2013a, Janicki et al., 2010). The lack of bone repair in the SF cultured group in normoxia is concerning. The lack of cartilage tissue in these tissues may not be surprising when you look at the *in vitro* chondrogenic potential of these MSCs which is quite low. The SF MSCs presented in this study may represent a different population of SF MSCs than those reported in chapters 3 and 4. SF MSCs isolated here were isolated without the use of fibronectin as previous studies (data not shown) had determined fibronectin was no longer essential for the isolation of SF MSCs from bone marrow. A reduction in the chondrogenic potential of SF MSCs isolated without the presence

of fibronectin is observed in chapter 6. This preliminary data may suggest a role for fibronectin in the selection of a more chondrogenically-primed MSCs or rather prevents the loss of this subpopulation of MSCs. Although, the authors are unaware of the effect of fibronectin at the time of isolation on MSC phenotype, studies indicate the inhibition of fibronectin on chondrogenesis when present at time of differentiation assay *in vitro* (Connelly et al., 2011, Connelly et al., 2007) indicating further investigation is required to identify the lack of chondrogenic potential of the SF MSCs. Further investigation into this could result in the development of a superior SF formulation for the production of MSCs.

Also important in bone repair is vascularisation. The SF MSCs have previously been shown to be pro-angiogenic and thus the hypothesis that they may be capable of contributing to superior bone repair was considered. Neovascularisation of the defect region was assessed *in vivo* by PA imaging at 4 and 8 weeks. Using this system  $sO_2$  levels and haemoglobin levels were measured to determine if either were suitable indicators of revascularisation of the defect region were. Prior to this study, optimisation of the PA imaging of the defect region had to be optimised. It was unclear what impact the titanium screws or PEEK plate would have on assessing vascularisation. Ultrasound imaging was used to identify the defect region which was clearly visible by the presence of the titanium screws. The screws provided a fortuitous opportunity to insure reproducibility in assessment as they would provide markers to identify the defect region. PA scans of the screws, the PEEK plate and defect region were all performed indicating clear distinction between these regions would insure no errors in assessment of neoangiogenesis (figure 5.3.4). Oxygen saturation was assessed at 4 and 8 weeks with no changes observed between any of the groups within or between time-points indicating that  $sO_2$  levels may not be a suitable indicator of revascularisation. Similarly, haemoglobin levels were assessed. Higher levels of variation were observed when measuring HbT levels. However, no difference was observed between control groups and cell-treated groups indicating that HbT levels were also not suitable for assessment of neoangiogenesis of rat CSD model. It may also be true that the time-points selected were not suitable to observe changes in either  $sO_2$  levels of

haemoglobin levels as typically a decrease in these factors occurs in the initial 72hrs post-fracture before returning to almost normal levels (Chen et al., 2015, Fugere et al., 1994, Kajja et al., 2010). For future studies, *in vivo* assessment of revascularisation may be better performed by  $\mu$ CT visualisation of blood vessels (Kajja et al., 2010). Subsequent to the *in vivo* assessment of revascularisation, the presence of blood vessels was assessed histologically using lectin staining to identify endothelial cells. Low levels of blood vessels were detected overall with blood vessels being most prominent in groups that received SF or SC MSCs, previously cultured in normoxia. As these data is qualitative and the visualisation of blood vessels may be difficult to identify depending on their orientation, it would be incorrect to use this outcome to indicate whether the normoxia or hypoxia cultured MSCs were more pro-angiogenic. Current literature would indicate that hypoxic preconditioning of MSCs improves their *in vivo* pro-angiogenic potential (Hu et al., 2008, Rasmussen et al., 2011), an effect that was not observed in this study.

Overall these data indicate that the mechanism by which SF and SC MSCs repair bone may be distinct from each other and warrants further investigation. Similarly, oxygen tension during culture may also compound the differences in these phenotypes and further work is needed to attempt to correlate an *in vitro* function of MSCs to their *in vivo* repair capability to help predict success rates of transplanted tissues for clinical use.



# **Chapter 6**

**Evaluation of a novel xeno and serum-free medium with commercially available serum-free media**

## 6.1 Introduction

The therapeutic potential of MSCs is currently being explored in a number of clinical trials in areas such as osteoarthritis, graft-versus-host disease, Crohn's disease and diabetes-associated complications such as critical limb ischemia and transplant survival (Bartholomew et al., 2002, García-Olmo et al., 2005, Emadedin et al., 2012, Bura et al., 2014, Le Blanc et al.). Although there is still controversy as to the exact mechanism of action, the clinical use of the cells may be due to their tri-lineage differentiation potential, the ability to be expanded *ex vivo*, the production of paracrine factors in response to the host environment and low levels of immunogenicity (Singer and Caplan, 2011, Nauta and Fibbe, 2007). Predominantly, MSCs used in clinical trials require *in vitro* culture expansion due to the relatively low number of MSCs in source tissues and the high numbers of MSCs required for therapeutic doses. There is a requirement for various growth factors for the *in vitro* proliferation of MSCs as for many other cells. This led to the use of FBS, as a rich source of growth factors, initially and MSC expansion is still performed routinely in the presence of this supplement, even for clinical production. Not only does FBS have a high abundance of growth factors, it also acts as a source of attachment factors and cytokines which facilitate the *in vitro* expansion of MSCs (Honn et al., 1975). A major disadvantage is the chemically undefined nature of FBS and issues such as volatility in FBS pricing, lot-to-lot variability in performance and dramatic changes in availability may ultimately lead to insufficient FBS stocks for sustainable supply of clinical product to the cell therapy industry (Brindley et al., 2012).

The use of humanised sera products arose due to concerns associated with the use of FBS for clinical production, primarily disease transmission due to potential contamination with prions and viruses. Moreover, there are also concerns of immune reactions to xenogeneic serum antigens (Agata et al., 2009). Human autologous serum (HAS), pooled allogeneic human sera and human platelet lysate have been used successfully for MSC isolation and expansion (Stute et al., 2004, Schallmoser et al., 2007). However, the use of human products also raises concerns with respect to disease transmission (Iudicone et al., 2014).

These concerns as well as supply issues have resulted in the cell therapy industry moving towards chemically defined and animal component-free media as more desirable for clinical MSC manufacturing from a safety point of view. The use of alternatives such as a serum-free medium has a number of practical advantages over FBS. As serum-free media would be chemically defined and reproducible, they can be mass produced which would reduce manufacturing costs.

For these reasons research, predominantly led by commercial entities, has resulted in the generation of a number of commercial serum-free media for various cell types. However, due to the commercial necessity to protect intellectual property, there is little published literature focussed on the development of serum-free media or identification of the media components. To date, there are a handful of media formulations that report the ability to expand MSCs from multiple sources with some also being able to isolate MSCs from the tissue source (Table 6.1.1). Despite availability of these alternatives, FBS is still considered the gold standard for MSC production. This less than ideal uptake of the use of serum-free medium as an alternative to FBS may be due to fears that the medium may affect the phenotype of MSCs. Moreover, MSC products entering clinical trials currently are the results of years of *in vitro* and pre-clinical efficacy and safety studies using FBS for isolation and growth. As MSCs have been previously shown to be highly responsive to their environment such as changes in oxygen tension, a reasonable concern over the use of a serum-free medium may be the effect it could have on MSCs leading to molecular, phenotypic and functional changes that might impact their clinical performance (Crapnell et al., 2013). As mentioned above research on serum-free media is predominantly performed in commercial entities and there is little data in the literature assessing the media or performing comparative experiments with FBS and other alternatives such as human-based products such as human serum, both autologous and allogeneic, and human platelet lysate.

Identifying a truly animal component-free medium can also be challenging as confusing terminologies are often be used by manufacturers. Many media are classified as serum-free which only indicates the absence of serum in the product, not the total absence of animal-derived products. Truly, animal component-free

## Chapter Six

media are classified as xeno-free but similarly may not be chemically defined and may contain humanised products. The ideal medium formulation to reduce variation between cell batches would ideally be both xeno-free and fully chemically defined. This would allow for large-scale production of batches, an option not available to alternatives such as human platelet-derived products. To date, the majority of the literature available compares these media to the use of FBS. However, there is little to no data comparing the commercially available media with competitor formulations making identifying the optimal formulation difficult.

Chapter Six

Company	Serum-free Medium	MSC Source	Xeno-free	Chemically defined	Requires Attachment factor	Can isolate from tissue	GMP-grade available	References
Promocell	DXF	BM, UC, AT	Yes	Yes	Yes (fibronectin)	Undetermined	No	(Lakhkar et al., 2015)
Lonza	Therapeak™ MSCGM-CD™	BM	Yes	Yes	Yes (fibronectin)	Undetermined	No	(Ishikawa et al., 2009, Sawada et al., 2010, Rajaraman et al., 2013, Jung et al., 2012, Gottipamula et al., 2016)
Stemcell Technologies	Mesencult-XF	BM, AT	Yes	Yes	Yes (Undisclosed)	Yes	No	(Al-Saqi et al., 2015, Cunha et al., 2015, Yang et al., 2012b, Pal et al., 2009, Miwa et al., 2012)
Irvine Scientific	Prime-XV™	BM, AT, UC	Yes	Undisclosed	Yes (Undisclosed)	Undetermined	Yes	(Heathman et al., 2016, Heathman et al., 2015)
Thermo Fisher	StemPro SFX-XF	BM, AT	Yes	Undisclosed	Yes (CellStart™)	Yes (Requires 2.5% FBS)	Yes	(Wuchter et al., 2016, Simoes et al., 2013, Lindroos et al., 2009, Yang et al., 2012a)
GE Healthcare	Xuri	BM, UC, AT	Yes	Undisclosed	Yes (Undisclosed)	Yes	No	Not cited

**Table 6.1.1: Various commercially available serum-free, xeno-free media.** BM, bone-marrow; UC, umbilical cord; AT, adipose tissue.

## 6.2 Methods

To compare the efficacy of the developed SF medium with commercially available media, two commercial media were assessed for their ability to isolate MSCs from bone marrow in both hypoxia and normoxia. Initially four commercial media were tested (Therapeak, DXF, Mesencult and Xuri) but two were excluded (Therapeak and DXF) from future work after failing to isolate CFU-fs. Prime-XV was not commercially available at the time of the study and StemPro SFX-XF required the use of FBS for initial isolation and thus was also excluded. Cells isolated in the various media were incubated in hypoxia (2% O<sub>2</sub>) or normoxia (21% O<sub>2</sub>) for three passages (section 2.4) at which time the cell tri-lineage differentiation potential (sections 2.7-2.9), and pro-angiogenic (section 2.13) and immunosuppressive effects (section 2.12) were assessed. Cells were also characterised with respect to their surface marker phenotype (section 2.11) using the ISCT panel with the addition of CD271 and CD146. The immunogenicity of the cells was further determined (section 2.12). CFU-f capability in primary culture (section 2.3) and growth throughout culture was also measured (Section 2.5). A schematic outline of the experimental design is outlined in figure 6.2.1. For this study, individual commercial media required substrate coating with undisclosed attachment factors as outlined in section 2.2.1. Furthermore, disassociation of cells from tissue culture plastic utilised a media-specific protocol as outlined in section 2.4. The REMEDI serum-free (SF) medium outlined in this study did not require the use of attachment factor; previous studies indicated the use of an attachment factor, namely fibronectin, was not required (data not shown).

## Chapter Six

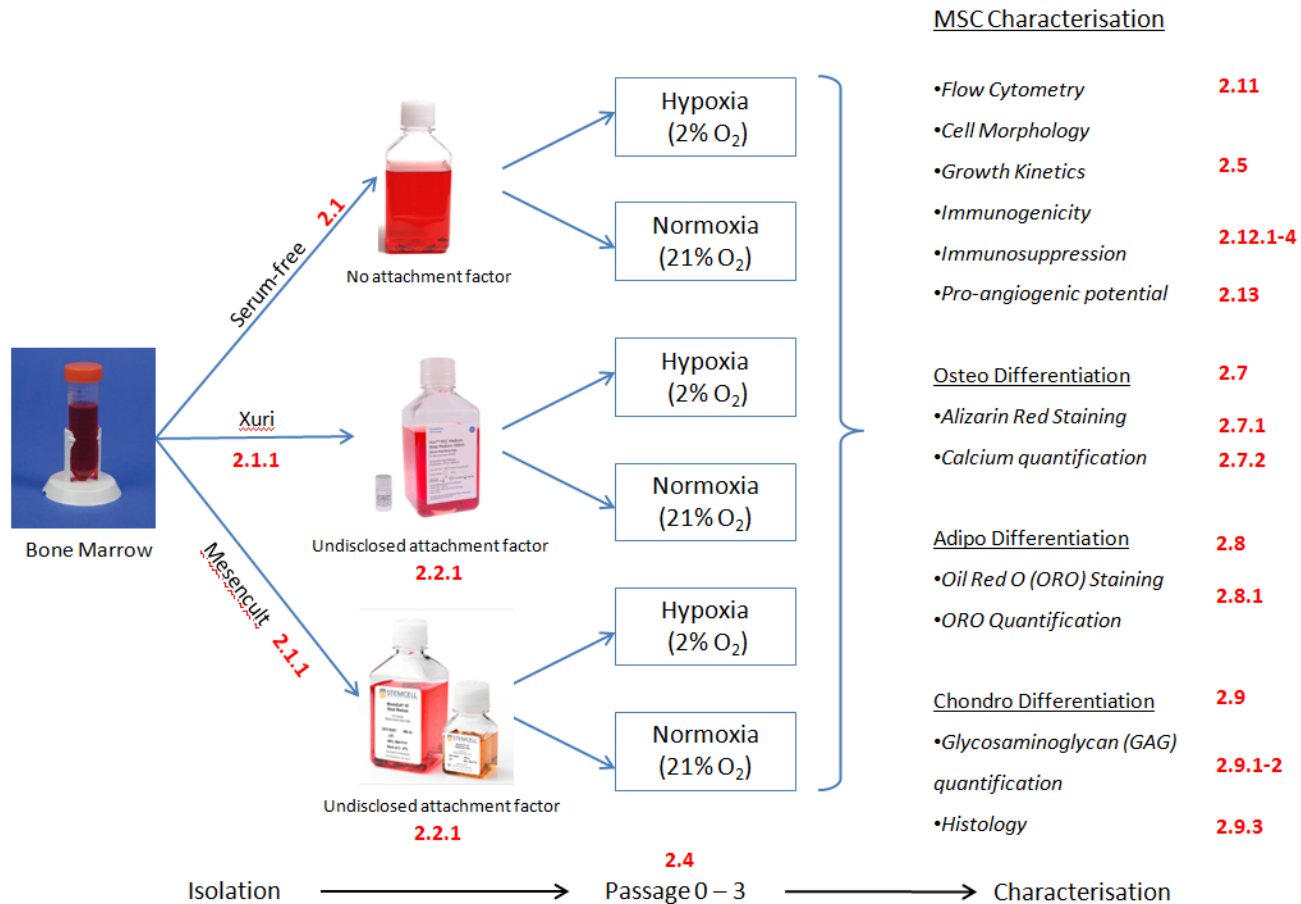
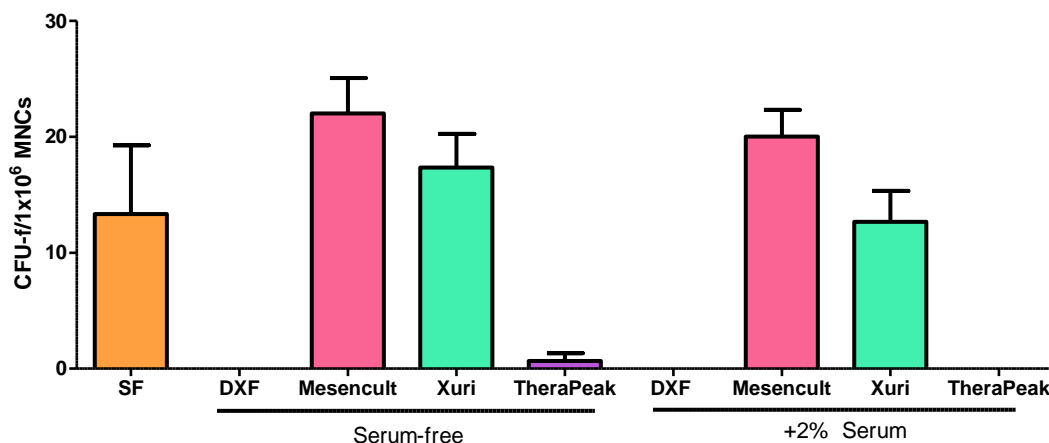


**Figure 6.2.1: Schematic representation of the approach taken for the in vitro characterisation of bone marrow-derived mesenchymal stem cells isolated in serum-free (SF), Xuri and Mesencult (MC) culture media. Specific methods (as described in chapter 2) are indicated by the associated number in red.**

## 6.3 Results

### 6.3.1 Assessment of various commercial serum-free media for ability to isolate MSCs from bone marrow with and without the support of 2% serum

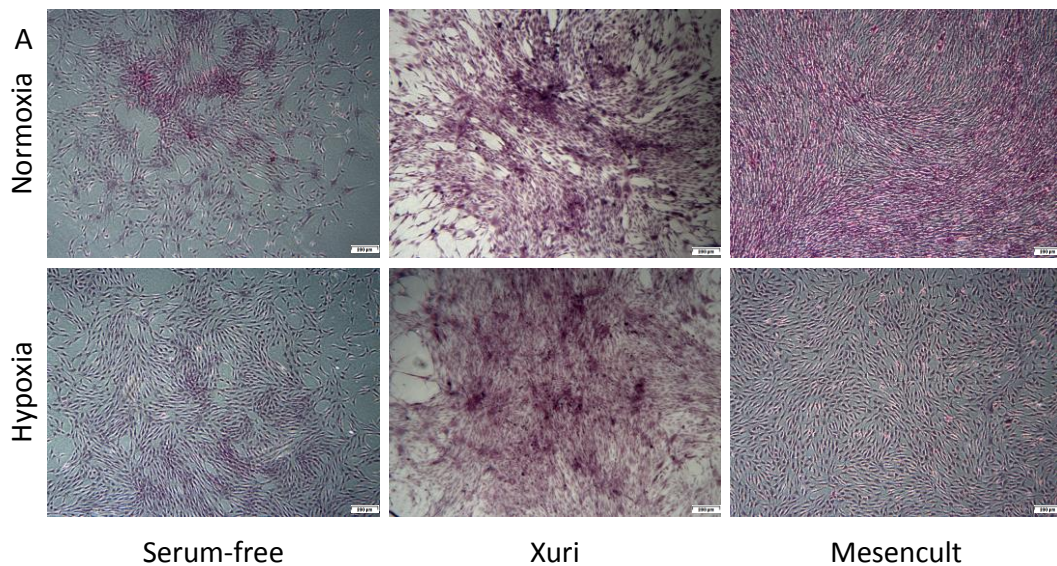
Four commercial media were tested for their ability to isolate CFU-fs from bone marrow. At the time of this study, none of the commercial media reported the ability to isolate MSCs from bone marrow and were merely reported as MSC proliferation media. Some commercial serum-free media reported the addition of 2% serum to the media for the isolation of CFU-fs to facilitate isolation. Here, four commercial media were assessed for their ability to isolate CFU-fs from bone marrow with/without the addition of 2% FBS v/v to the medium. These were compared to the REMEDI SF medium. Mesencult and Xuri isolated CFU-fs at comparable levels to SF medium. The addition of 2% serum did not improve the ability to isolate CFU-fs. DXF failed to isolate any CFU-fs in the presence/absence of 2% serum. Some CFU-fs were identified in Therapeak medium cultures in the absence of serum but failed to proliferate. Based on these data, Mesencult and Xuri were assessed in future experiments in comparison to SF media. Therapeak and DXF were excluded from all future work.



**Figure 6.3.1: Mesencult and Xuri media are capable of isolating CFU-fs from bone marrow.** Quantitative analysis of CFU-f per 1x10<sup>6</sup> MNCs isolated in the relevant media with and without the addition of 2% serum. Data is representative of 1 biological replicate with 3 technical replicates per group.

### 6.3.2 Serum-free and commercial media isolate equivalent CFU-fs in hypoxia and normoxia

The SF medium was assessed for its ability to isolate CFU-fs from bone marrow in both hypoxia and normoxia in comparison to commercially available mesencult (MC) and Xuri media. Bone marrow aspirates were obtained from healthy donors and whole marrow was plated directly onto tissue culture plastic. Both SF and commercial media were assessed for their ability to isolate CFU-fs from human bone marrow in hypoxia and normoxia. CFU-fs were stained with crystal violet and imaged (Figure 6.3.2a). Differences in colony size and shape were observed. SF CFU-fs were smaller in size and cells within CFU-f were less densely packed compared to Xuri and MC. Xuri CFU-fs consisted of larger cells very densely packed. Quantification of crystal violet stained colonies indicated no statistical difference between media in normoxia with respect to CFU-f numbers (Figure 6.3.2b). An increase in CFU-f number was observed in SF media when MSCs were isolated in hypoxia compared to both Xuri and Mesencult media in either hypoxia or normoxia in SF and SC groups (Figure 6.3.2b).



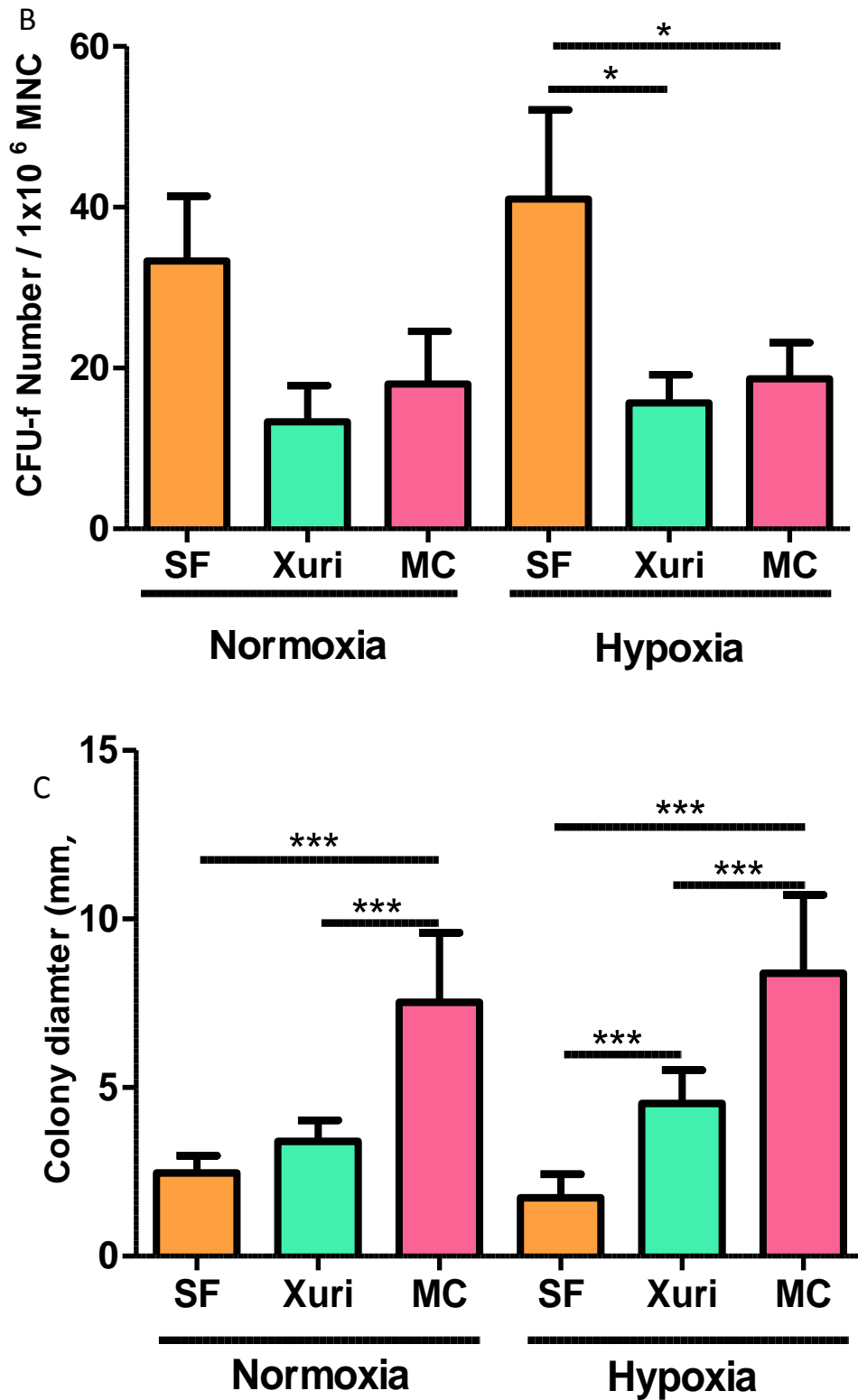
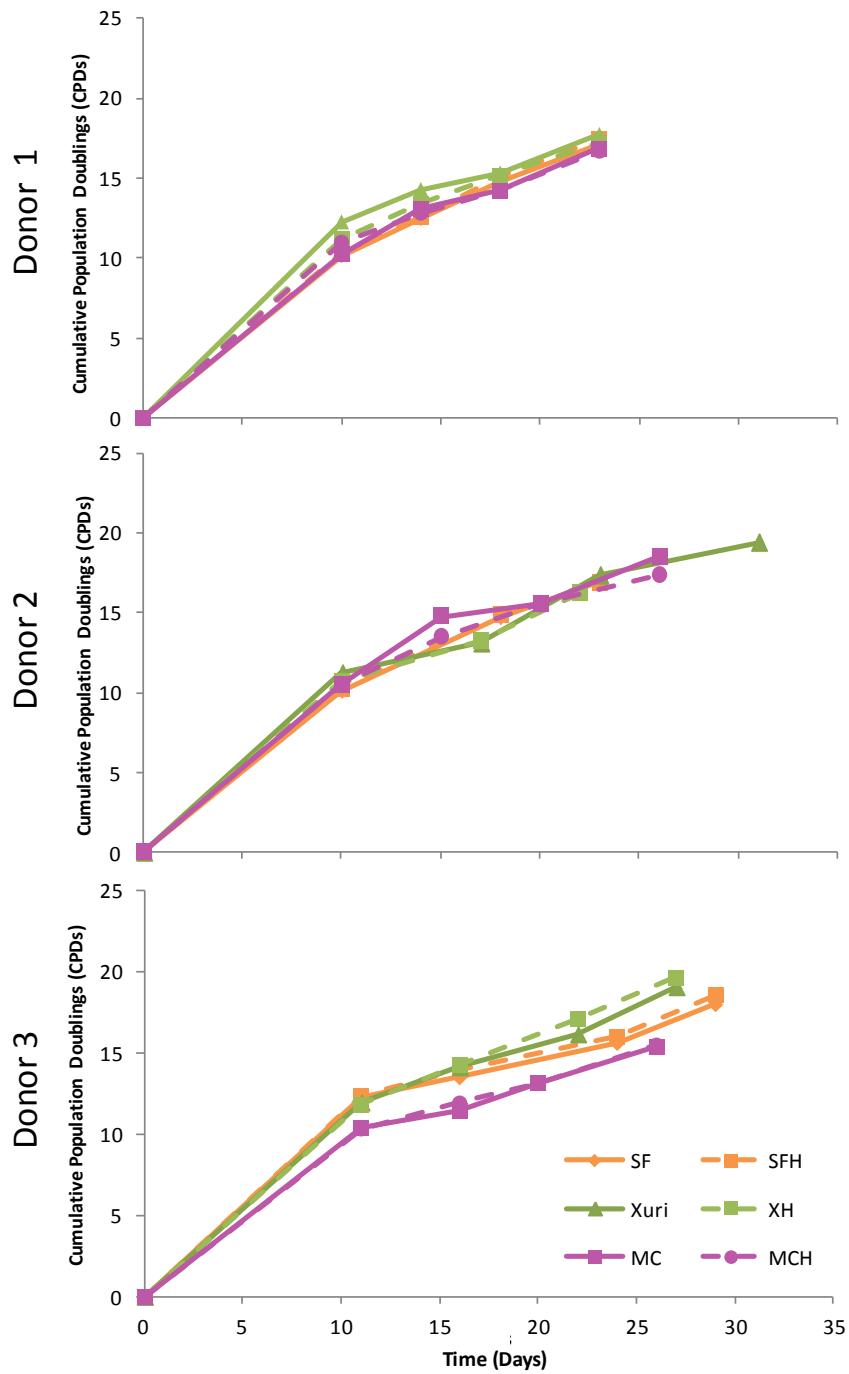


**Figure 6.3.2: CFU-f size and number are affected by the culture medium.** (A) Representative images of CFU-fs in 6-well plates stained 10 days post-isolation from bone marrow. Typical colonies are shown at 4x magnification (Scale bar: 500 $\mu$ m). (B) Quantitative analysis of CFU-f number normalised to 1x10<sup>6</sup> MNCs seeded. Increases in SF CFU-f numbers isolated in hypoxia compared to Xuri and Mesencult.

*(C) Average CFU-f colony size (mm) of MSCs isolated in various conditions. Data analysed using two-way ANOVA with Bonferroni post-test, \* $p \leq 0.05$ , \*\*\* $p \leq 0.001$ . Data is presented as the mean  $\pm$  SD,  $n=3$  biological replicates.*

### **6.3.3 Growth kinetics MSCs in SF and commercial media cells isolated and cultured in hypoxia and normoxia**

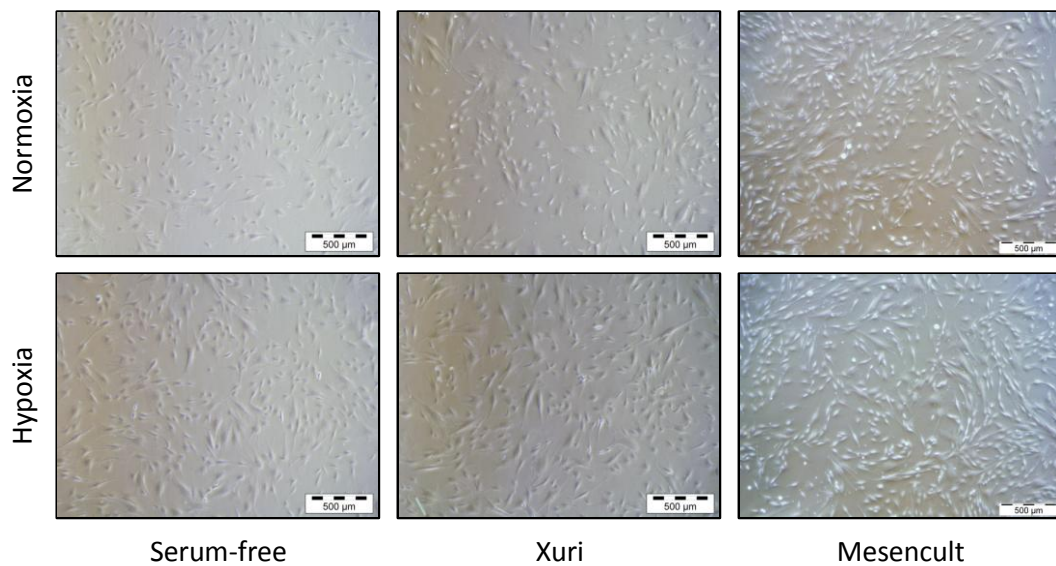
Growth kinetics of each culture were assessed by calculating population doublings of cells versus days in culture based on cell yields at the end of each passage. Equivalent growth of all media groups in both hypoxia and normoxia was seen. Data represented in figure 6.3.3 indicate equivalent population doublings per media groups from P0-P3.



**Figure 6.3.3: Growth kinetics of serum-free (SF), Xuri (X) and Mesencult (MC) isolated cells in normoxia (21% O<sub>2</sub>) compared to hypoxia (2% O<sub>2</sub>).** Representative growth kinetics of 3 MSC donors isolated in normoxia (SF, X, MC) or hypoxia (SFH, XH, MCH) represented as cumulative population doublings versus time (days). Each graph represents a biological donor isolated with the various media. No difference was observed between media within each donor group.

### 6.3.4 Morphology of MSCs is unaffected by use of commercial media in either hypoxia or normoxia

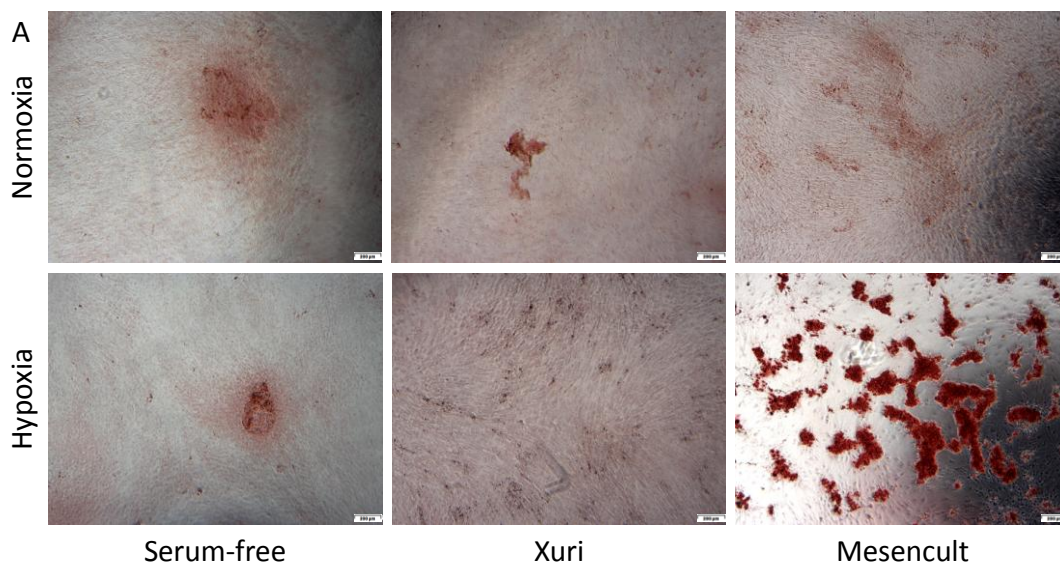
MSC morphology was observed using microscopy. A similar morphology was observed in media groups and appears to be unaffected by oxygen tension. This is in contrast to the noticeable differences observed in these groups at the time of isolation as evident in their CFU-fs (figure 6.3.3 above). Images presented here were taken during passage 3. The similar morphology observed here may represent that typical of MSCs when not exposed to FBS.

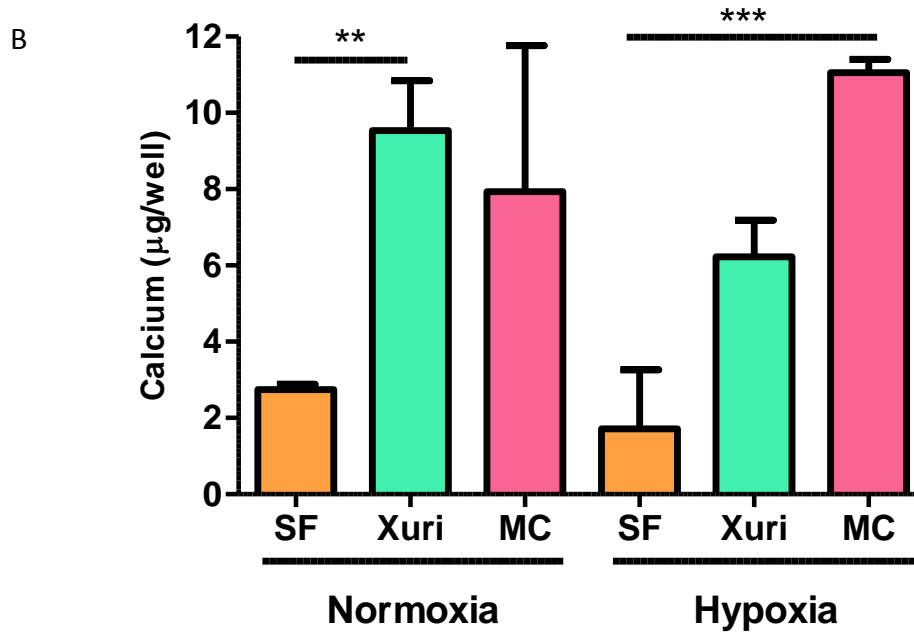


**Figure 6.3.4: Morphology of MSCs was altered by culture of MSCs in SF, Xuri and MC medium irrespective of oxygen levels. Images presented are 4x magnification images and are representative of 3 MSC donors. Scale bar: 500µm.**

### 6.3.5 Commercial media isolated MSCs have superior osteogenic potential compared to SF cultured MSCs

To assess the ability of the commercial media cultured MSCs to undergo osteogenic differentiation, SF, Xuri and Mesencult MSCs isolated and cultured in either hypoxia or normoxia were differentiated in osteogenic medium. Cells were cultured in osteogenic medium for 14 days and calcium deposition was assessed visually by alizarin red staining and quantitatively using the Stanbio Calcium Liquicolour Kit. Results from alizarin red staining indicated low levels of matrix deposition in all groups except for mesencult hypoxia which has high levels of calcified matrix (Figure 6.3.5a). These findings were further verified by quantitative measurement of calcium levels. Quantification of calcium levels indicated MSCs cultured in Xuri medium produced increased levels of calcium compared to SF MSCs in normoxia (Figure 6.3.5b). A similar trend was observed with Mesencult (MC) medium but results were not statistically significant due to inter-donor variability in the MC group. Hypoxia resulted in a reduction of calcium deposition by MSCs cultured in Xuri medium. No difference was observed in SF and MC medium between hypoxia and normoxia. MC MSCs indicated increased calcium deposition compared to SF MSCs in hypoxia.

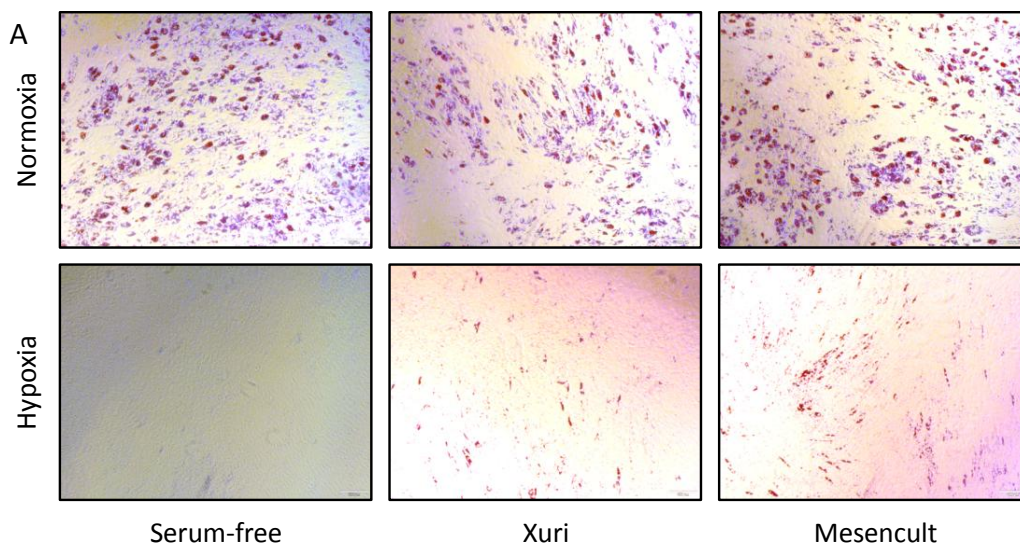




**Figure 6.3.5: Commercial media isolated MSCs demonstrate increased osteogenic potential in hypoxia and normoxia.** (A) Representative alizarin red staining of SF, Xuri and MC cells in normoxia and hypoxia cultured MSCs indicate low levels of osteogenesis in all groups except Mesencult-hypoxia. (B) Osteogenic differentiation potential was further assessed by quantification of calcium deposition displayed as calcium levels represented as  $\mu\text{g}/\text{well}$ . These results indicate increased levels of calcium deposition in Xuri and MC media compared to SF in both hypoxia and normoxia. Results are presented as the mean  $\pm$  standard deviation (SD) of 3 biological replicates,  $**p \leq 0.01$ ,  $***p \leq 0.001$  as determined using two-way ANOVA and Bonferroni's multiple comparisons post-test.

### 6.3.6 Adipogenic potential of MSCs is increased in cells cultured in commercial media and inhibited by hypoxia

To determine the optimal culture conditions for MSCs to undergo adipogenic differentiation, SF, Xuri and MC isolated and cultured cells in either hypoxia or normoxia were differentiated in adipogenic medium to assess the optimal culture conditions for adipogenesis. Cells were induced with adipogenic induction medium and fed for approximately 15 days in altering cycles of adipogenic induction medium and adipogenic maintenance medium. Oil red O staining of lipid vacuoles demonstrated a significant depletion of the adipogenic potential of MSCs in hypoxia in comparison to normoxia. No difference in Oil red O staining was observed between media groups in normoxia. Absence of Oil red O staining was observed in SF group in hypoxia. Minimal staining was visible in Xuri and MC groups (Figure 6.3.6a). Quantification of Oil red O staining was performed by extraction of Oil red O staining in 99% isopropanol and measurement of the extracted stain (Figure 6.3.6b). Xuri MSCs displayed increased adipogenesis compared to MC and SF MSCs in normoxia. Similarly MC MSCs displayed increased adipogenesis compared to SF MSCs. All groups showed a significant reduction in adipogenesis in hypoxia compared to normoxia.



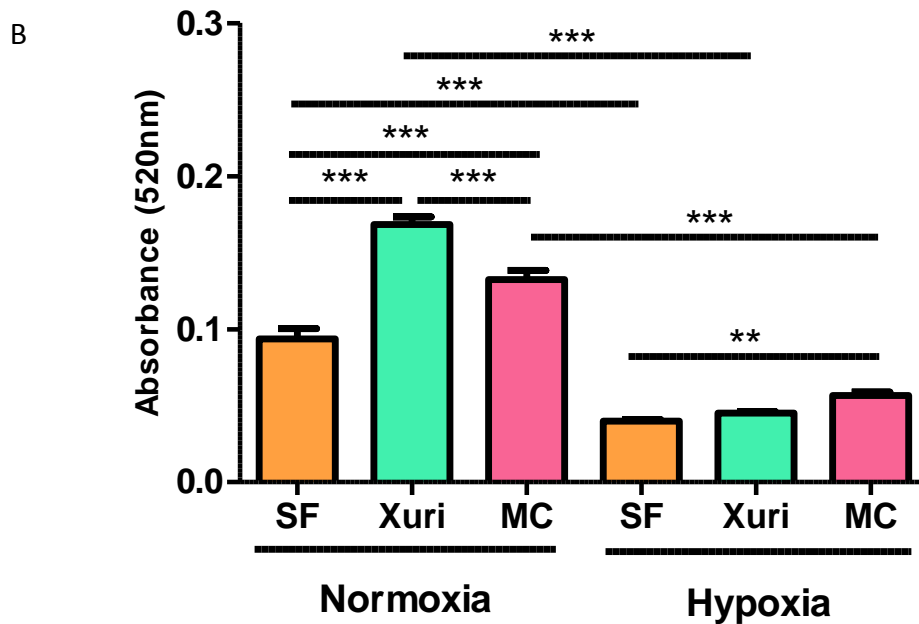


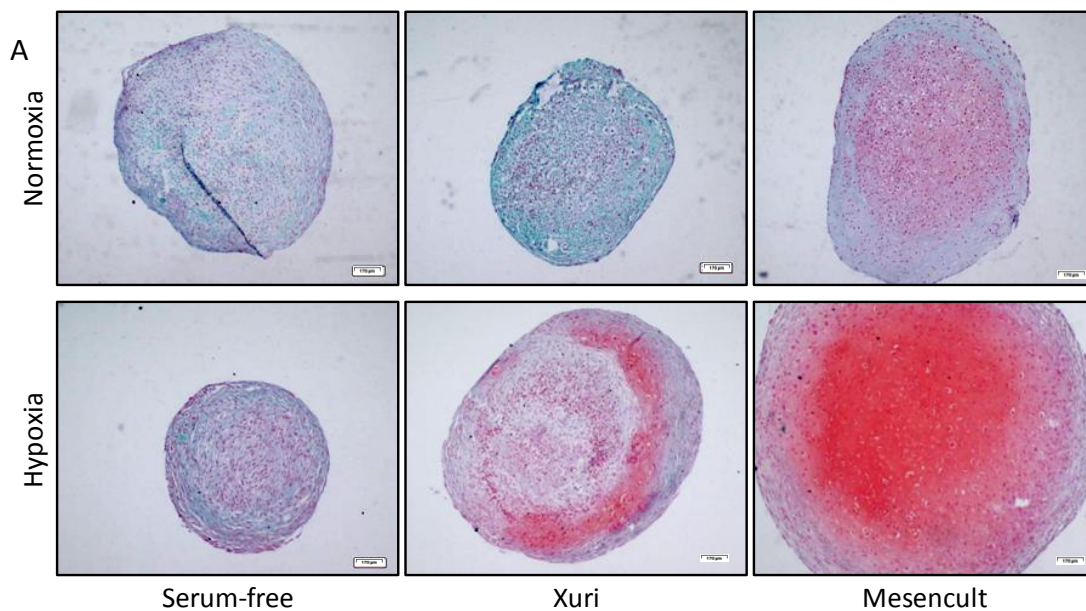
**Figure 6.3.6: Adipogenic potential of cells was enhanced in normoxia cultured cells and was maintained in all conditions.** (A) Representative Oil red O staining of SF, MC and Xuri cells in normoxia or hypoxia indicates adipogenic potential of MSCs is maintained in various culture conditions and is increased in normoxia compared to hypoxia. (B) Adipogenic differentiation potential was further assessed by quantification of Oil red O. Xuri MSCs displayed a statistical increase in adipogenesis compared to MC and SF groups. MC also displayed significantly increased adipogenesis compared to the SF group. All media groups displayed significant reduction in adipogenesis in hypoxia. Results are presented as the mean  $\pm$  standard deviation (SD) of 3 biological replicates, \*\* $p \leq 0.01$ , \*\*\* $p \leq 0.001$  as determined using two-way ANOVA and Bonferroni's multiple comparisons post-test.

### 6.3.7 Chondrogenic potential of SF cultured cells is increased in hypoxia

To determine the chondrogenic potential of MSCs isolated in SF, MC and Xuri in either hypoxia or normoxia, cells were differentiated in chondrogenic medium supplemented with TGF- $\beta$ 3 to assess the optimal culture conditions for chondrogenesis. Cells were cultured in chondrogenic medium for 21 days. Chondrogenesis was assessed histologically by Safranin O staining (Figure 6.3.7a) and by measurement of sGAG using the DMMB assay (Figure 6.3.7b). Safranin O staining indicated high levels of sGAG in MC group in normoxia. Levels of sGAG were reduced in Xuri group and further reduced in SF group. A similar trend was observed in hypoxia with significantly less sGAG levels in all groups in hypoxia

## Chapter Six

compared to the same groups in normoxia. Quantitative sGAG levels were normalised to DNA content using the picogreen assay (Figure 6.3.7b). No statistical difference was observed in media groups in normoxia as determined by GAG: DNA ratio. MC cultured cells displayed increased chondrogenesis assessed by GAG: DNA levels in hypoxia compared to SF cells in normoxia. No difference was observed between media groups in normoxia. Total GAG and DNA levels were also assessed during chondrogenesis (Figure 6.3.7c&d). Highest levels of variability between donors were observed in MC group with respect to GAG levels. Higher levels of proliferation were observed in all media groups in normoxia (Figure 6.3.7d).



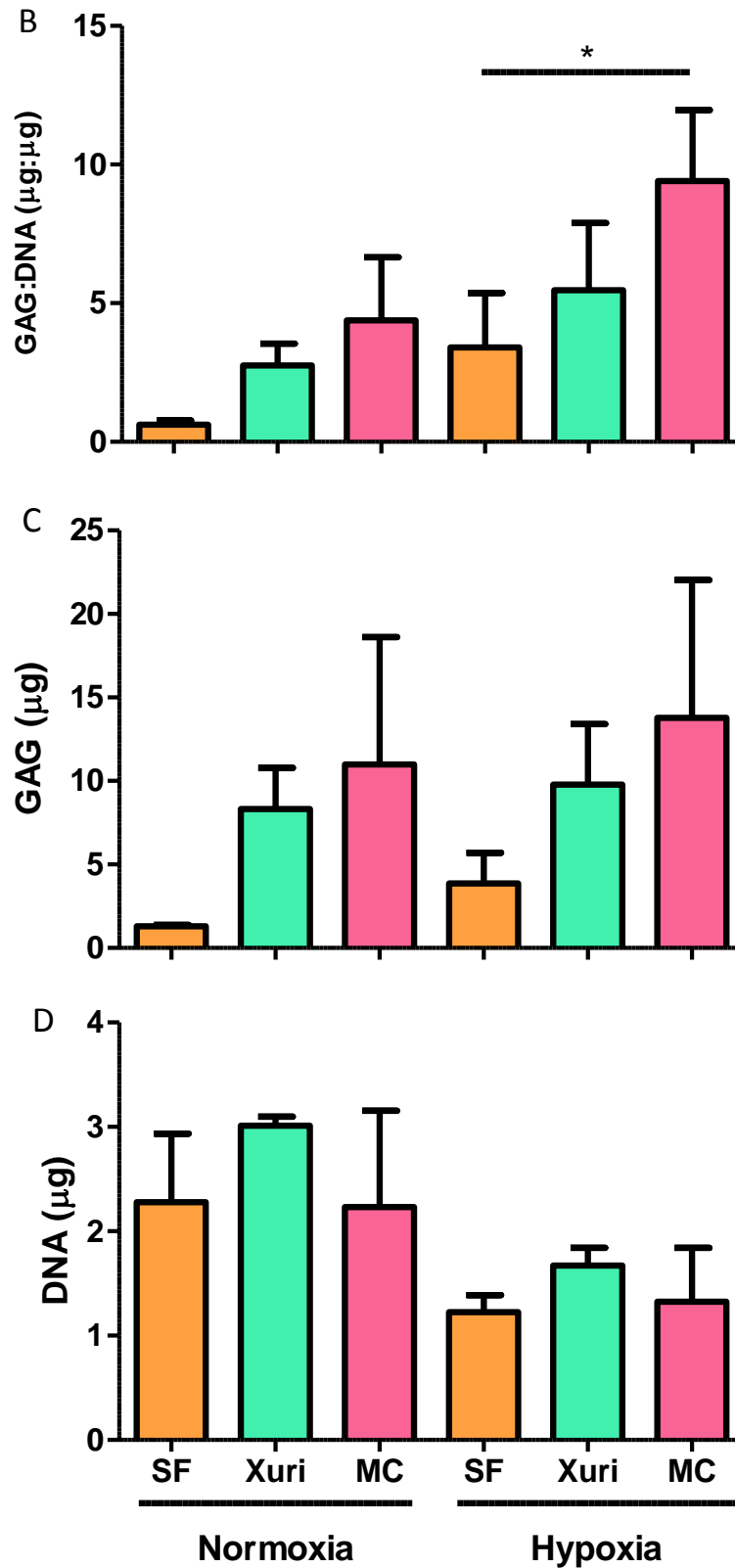


**Figure 6.3.7: Chondrogenic potential of SF cells was enhanced in hypoxia cultured cells and was maintained in all conditions.** (A) Representative Safranin O staining of SF, MC and Xuri cells in normoxia or hypoxia cultured MSCs indicates chondrogenic potential of MSCs is maintained in various culture conditions and is

*increased in hypoxia compared to normoxia. (B) Chondrogenic differentiation potential was further assessed by quantification of sGAG levels normalised to DNA content. These results further validated the results observed by the Safranin O staining. MC cultured cells underwent significantly higher chondrogenic differentiation compared to SF MSCs in hypoxia. No other statistical differences were observed between groups. Results are presented as the mean  $\pm$  standard deviation (SD) of 3 biological replicates,  $*p \leq 0.05$ , as determined using two-way ANOVA and Bonferroni's multiple comparisons post-test.*

### **6.3.8 Assessment of MSCs Surface marker expression**

To assess whether the MSCs isolated and cultured in SF, Xuri or MC media satisfied the ISCT criteria for definition as MSCs, the cells were isolated in all media in either normoxia or hypoxia and were assessed for expression of the markers as reported in figures 6.3.8a&b. All groups maintained  $\geq 95\%$  expression of MSC markers CD105, CD73 and CD90 in both hypoxia and normoxia. Increased HLA-DR expression was observed in the MC group at levels ranging from 14-26% in both hypoxia and normoxia indicating a technical fail of these cells to satisfy the ISCT definition of an MSC based on surface marker expression. In addition to the ISCT panel, expression of CD271 and CD146 was also assessed. CD271 was a marker previously reported to select the entire CFU-f population of stromal cells from bone marrow (Jones et al., 2002). This marker is typically lost during culture of MSCs in presence of FBS and is not observed in cells beyond the end of P0. All media groups maintained a low level of expression of this marker. Expression was most prominently observed in Xuri medium in both hypoxia and normoxia (figure 6.3.8a&b). Furthermore, CD146 has also previously been reported (Sacchetti et al., 2007a) to enrich for a population of MSCs from bone marrow. Expression of CD146 is maintained in all media groups in both hypoxia and normoxia. A reduction in CD146 expression was observed in MC group in hypoxia in comparison to normoxia. This may indicate the selection of a slightly different MSC subpopulation from bone marrow as CD146 identifies a MSCs typically located in a perivascular niche as compared to CD271 positive cells which reside in a bone lining niche (Tormin et al., 2011a).

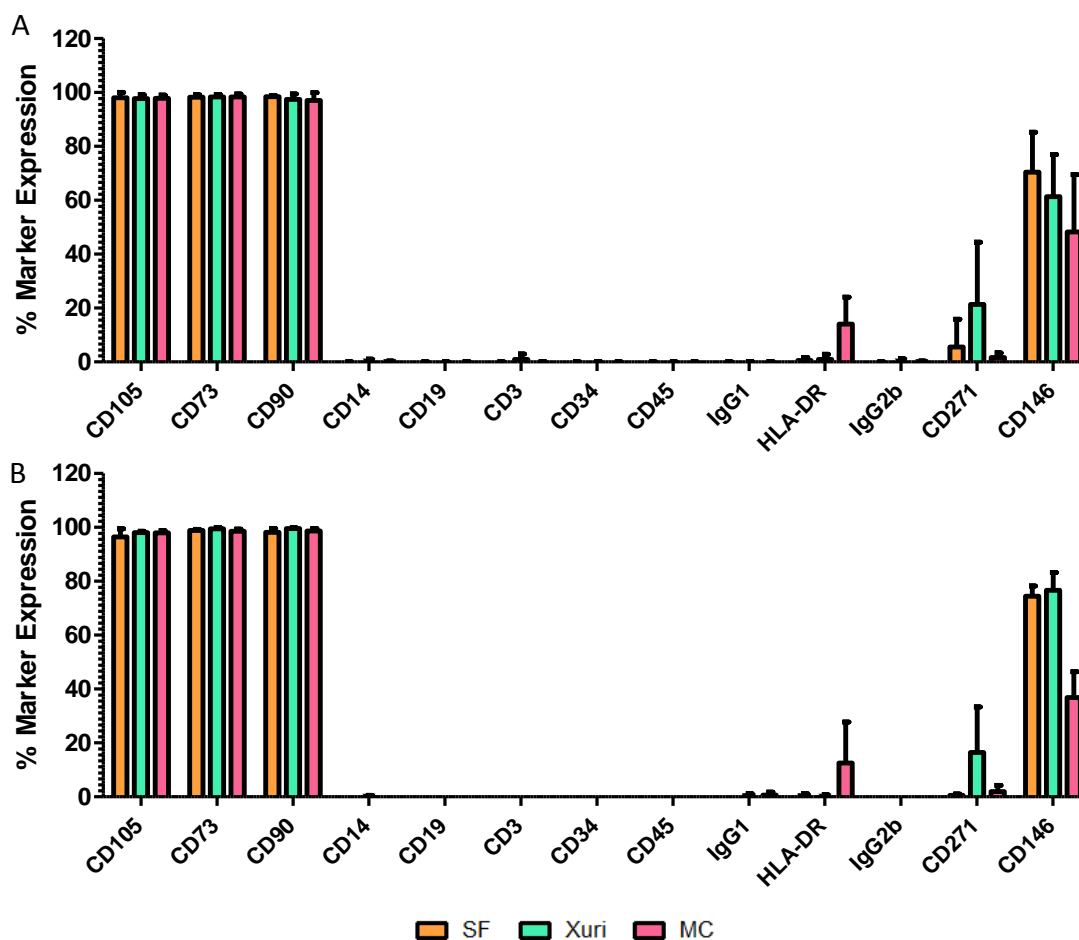
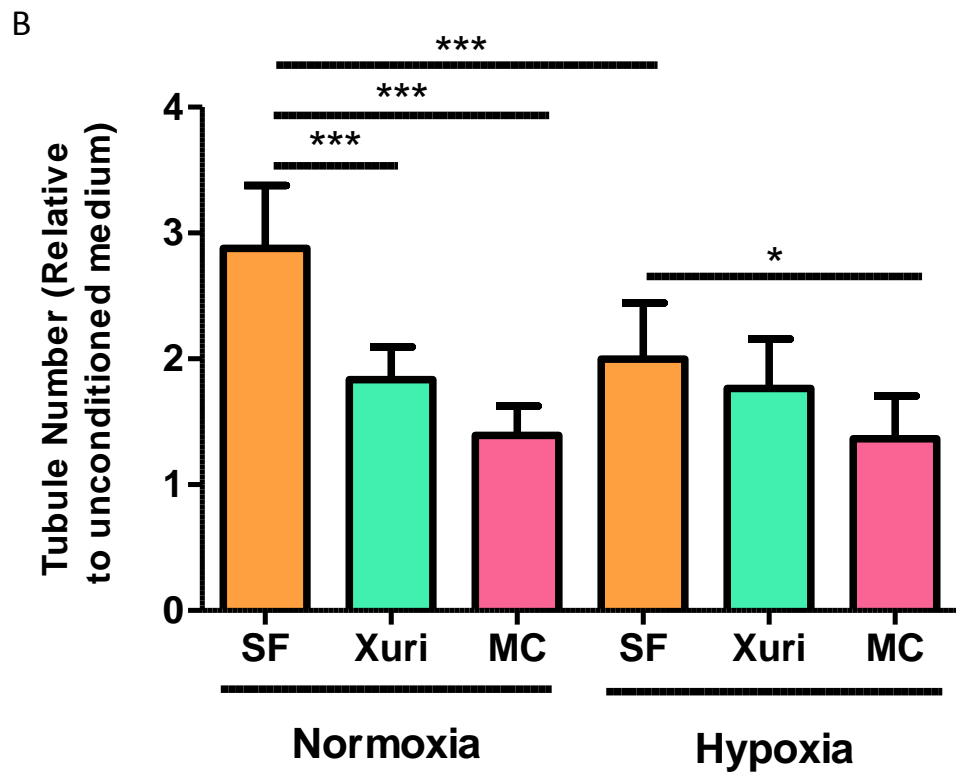
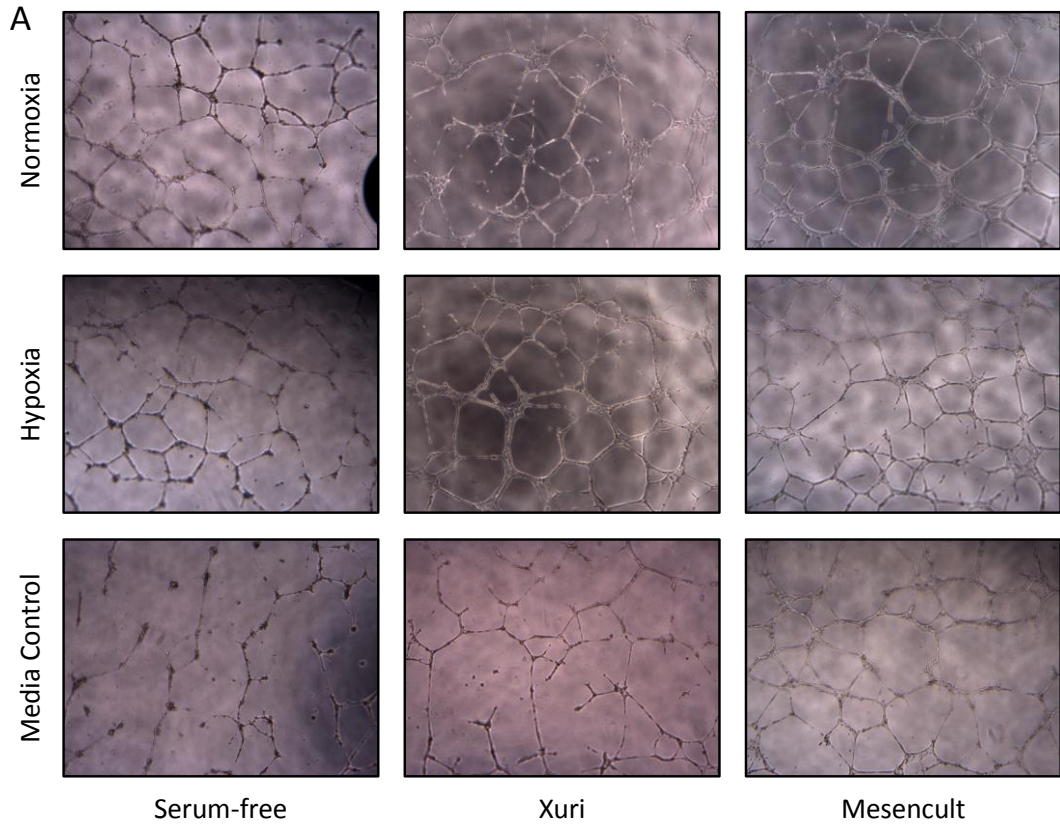


**Figure 6.3.8: Surface marker characterisation of bone marrow derived MSCs isolated in SF and commercially available media.** (A) Quantitative marker expression of SF (orange), Xuri (green) and MC (pink) isolated MSCs cultured in normoxia. (B) Quantitative marker expression of SF (orange), Xuri (green) and MC (pink) isolated MSCs cultured in hypoxia. Results are presented as the mean  $\pm$  standard deviation (SD) of 3 biological replicates.

### 6.3.9 Serum-free MSCs display increased pro-angiogenic potential

MSCs have previously been reported to secrete pro-angiogenic factors that can contribute to their therapeutic efficacy. The pro-angiogenic effect of MSCs was assessed by co-culturing of human umbilical cord vein epithelial cells (HUVECs) with conditioned medium from MSCs in SF, Xuri and MC media in either hypoxia or normoxia. Details of experimental setup are outlined in section 2.13. Briefly, to standardise collection of medium, equivalent numbers of MSCs were seeded in T-175 flasks and allowed to reach 50% confluency at which point a full medium

change was carried out. Subsequently, after 3 days of conditioning of the medium with the cells, the medium was harvested. The harvested conditioned medium was centrifuged at 400xg for 5mins to remove any cells present. Conditioned medium was then stored at -80°C until use. To discriminate between the effect of the medium itself and the cells, unconditioned medium (not exposed to cells) was prepared in T-175 flasks in conjunction with conditioned medium in a 37°C cell culture incubator. Media samples were co-cultured with HUVEC cells for 18hrs on matrigel and tubule numbers per well were determined. Tubules were defined as any fully formed tube joining two or more bridging points. All groups resulted in the formation of tubules (Figure 6.3.9a). SF conditioned medium resulted in a significant increase in tubule number compared to MC conditioned medium in hypoxia and was significantly increased compared to both Xuri and MC in normoxia (Figure 6.3.9b). Assessment of total tubule number of media control groups indicated that Mesencult unconditioned medium resulted in the formation of significantly more tubules compared to both Xuri and SF indicating the presence of more pro-angiogenic growth factors in MC medium compared to other groups (figure 6.3.9c).



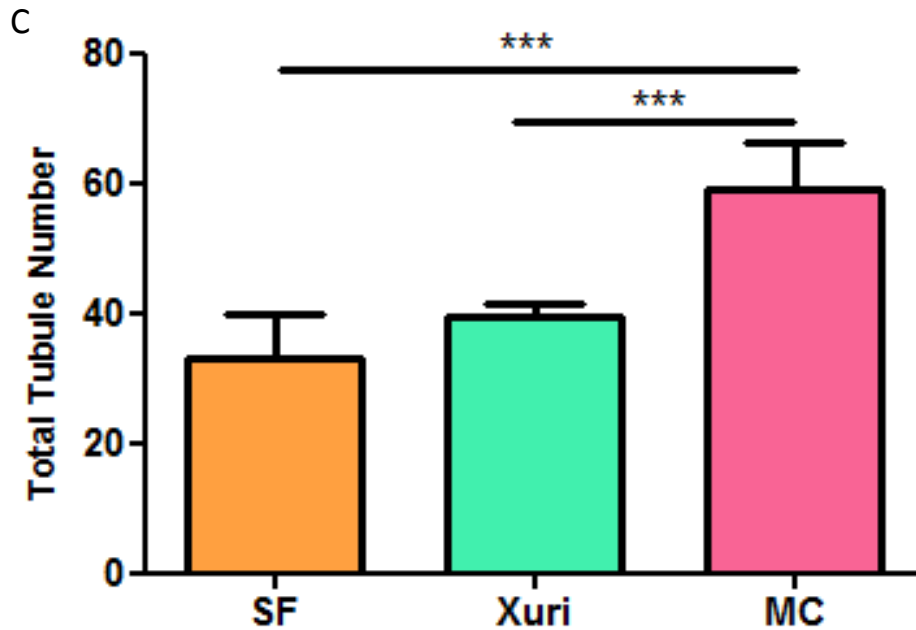


**Figure 6.3.9: Angiogenic potential of human umbilical vein epithelial cells (HUVEC) cells cultured in the presence of MSC conditioned medium.** (A) Representative images of HUVEC-derived tubules 18hrs post culture in the presence of MSC conditioned and unconditioned medium on Matrigel. (B) Quantitative analysis of tubule number formed after co-culture of SF, Xuri and MC MSC conditioned medium from either hypoxia or normoxia. Three biological replicates were assessed with three technical replicates. Five random fields were selected in each well (technical replicate) and tubules identified as a complete connection of tubule between at least two bridging points. Tubule number is represented as a fold change over the unconditioned basal media appropriate to each cell group. (C) Quantitative analysis of total tubule number generated by HUVEC cells exposed to SF, Xuri or MC medium unconditioned by cells. Unconditioned medium was generated at 37°C concurrently with that of conditioned medium. Results are presented as the mean  $\pm$  standard deviation (SD) of 3 biological replicates, \*\*\* $p \leq 0.001$  using two-way ANOVA and Bonferroni's multiple comparisons post-test.

### 6.3.10 Immunosuppressive effect of MSCs is unaffected by use of commercial media

To assess the immunosuppressive nature of MSCs cultured in SF, Xuri and MC media in hypoxia and normoxia, peripheral blood mononuclear cells (PBMCs) were isolated from healthy volunteers as outlined in sections 2.12.1-4. PBMCs were labelled with CFSE and co-cultured with various ratios of MSCs to PBMCs as

reported in figure 3.3.11 for 4 days. Experimental design and gating strategy was identical to that reported in figure 3.3.10. Assessment of immunosuppressive effects of hypoxia cultured T-lymphocytes is not possible in low oxygen levels due to insufficient proliferation of T-lymphocytes as reported previously. All cell groups resulted in immunosuppression of stimulated T-lymphocytes (Black). No statistical difference was observed between media groups on CD4<sup>+</sup> populations. Results are presented as the mean  $\pm$  standard deviation (SD) of 3 biological replicates. No statistical difference was observed in normoxia using one-way ANOVA and Bonferroni's multiple comparisons post-test (figure 6.3.10).

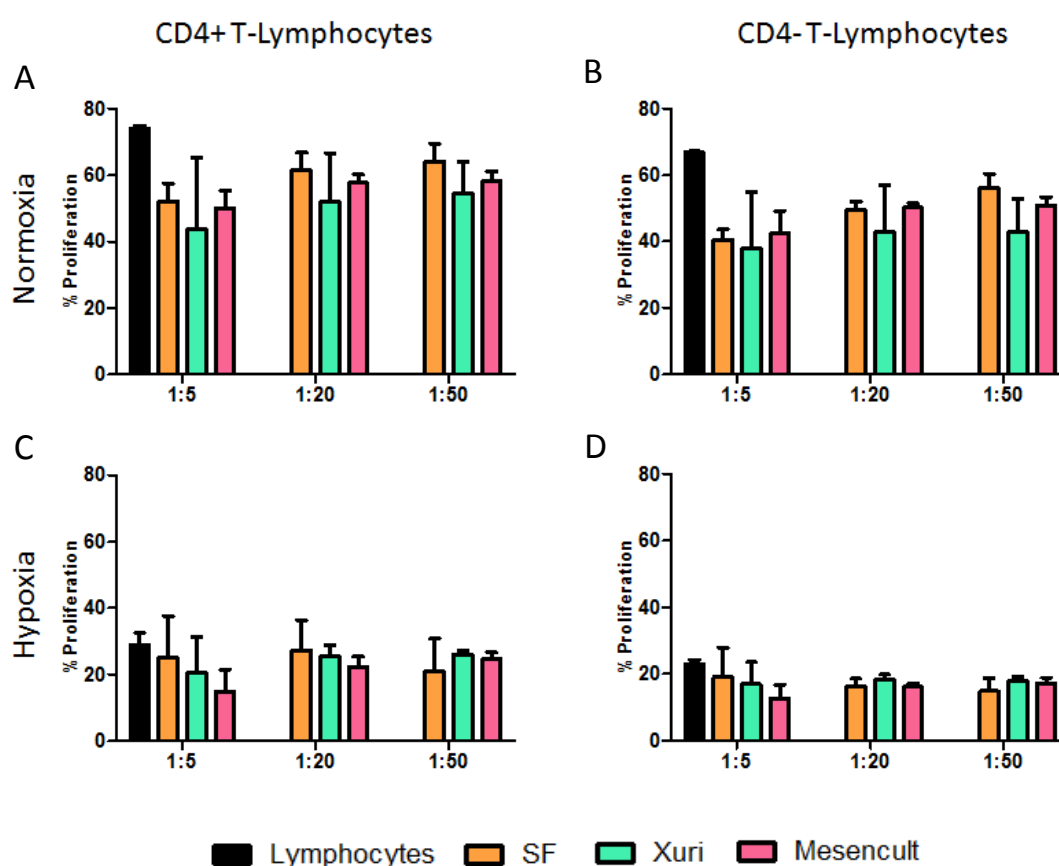


**Figure 6.3.10: Immunosuppressive effect of MSCs on CD28/CD3 stimulated peripheral blood T-lymphocytes.** Percentage proliferation of CD3/CD28 stimulated T-lymphocytes compared to unstimulated T-lymphocytes (Black), non-immunosuppressed T-lymphocytes (Orange); co-culture of SF-cultured MSCs with stimulated T-lymphocytes (Green); co-culture of Xuri-cultured MSCs with stimulated T-lymphocytes (Pink); co-culture of MC-cultured MSCs with stimulated T-lymphocytes. Effect of normoxia (A) and hypoxia (C) cultured MSCs on CD4+ T-lymphocytes at various ratios of MSC: T-lymphocyte. Effect of normoxia (B) and

*hypoxia (D) cultured MSCs on CD4<sup>-</sup> T-lymphocytes at various ratios of MSC: T-lymphocyte. Results are presented as the mean  $\pm$  standard deviation (SD) of 3 biological replicates with 3 technical replicates. No statistical differences were observed.*

### **6.3.11 Immunogenicity of MSCs cultured in SF and commercial media**

To demonstrate the immunogenic nature of MSCs cultured in SF, Xuri and MC medium in hypoxia and normoxia, PBMCs were isolated from healthy volunteers as outlined in sections 2.12.1-4 in an identical experimental setup as described above in section 6.3.11. PBMCs were labelled with CFSE and co-cultured with various ratios of MSCs to PBMCs for 5 days as reported in figure 6.3.12. Stimulated T-lymphocytes (black) were activated to proliferate by the addition of CD3 and CD28 antibodies. T-lymphocytes in MSC groups (Orange, green and pink) were not stimulated to proliferate by CD3 and CD28 antibody stimulation. MSCs were co-cultured with T-lymphocytes to assess the ability to activate proliferation and thus an immune response. Proliferation of cells was measured by flow cytometric analysis of CFSE expression (Figure 6.3.11). Figures 6.3.12a-b report the immunogenic effect of CD4<sup>+</sup> and CD4<sup>-</sup> T-lymphocytes respectively at 1:5, 1:20 and 1:50 ratios of MSC: T-lymphocyte with MSCs cultured in normoxia. No difference was observed in the CD4<sup>-</sup> group (Figure 6.3.12b) at any ratio. At the 1:50 ratio in CD4<sup>+</sup> group (Figure 6.3.12a) a statistically significant increase in T-lymphocyte activation by SF MSCs was observed. At 1:5 and 1:20 ratios, no difference was observed. Figures 6.3.12c-d report the immunogenic effect of CD4<sup>+</sup> and CD4<sup>-</sup> T-lymphocytes respectively at 1:5, 1:20 and 1:50 ratios of MSC: T-lymphocyte with MSCs cultured in hypoxia. Mirroring the immunosuppressive assay (Figure 6.3.10), assessment of the immunogenic effect of hypoxia cultured T-lymphocytes is not possible in low oxygen levels due to insufficient proliferation of T-lymphocytes. Results are presented as the mean  $\pm$  standard deviation (SD) of 3 biological replicates. Statistical analysis was performed using one-way ANOVA and Bonferroni's multiple comparisons post-test.

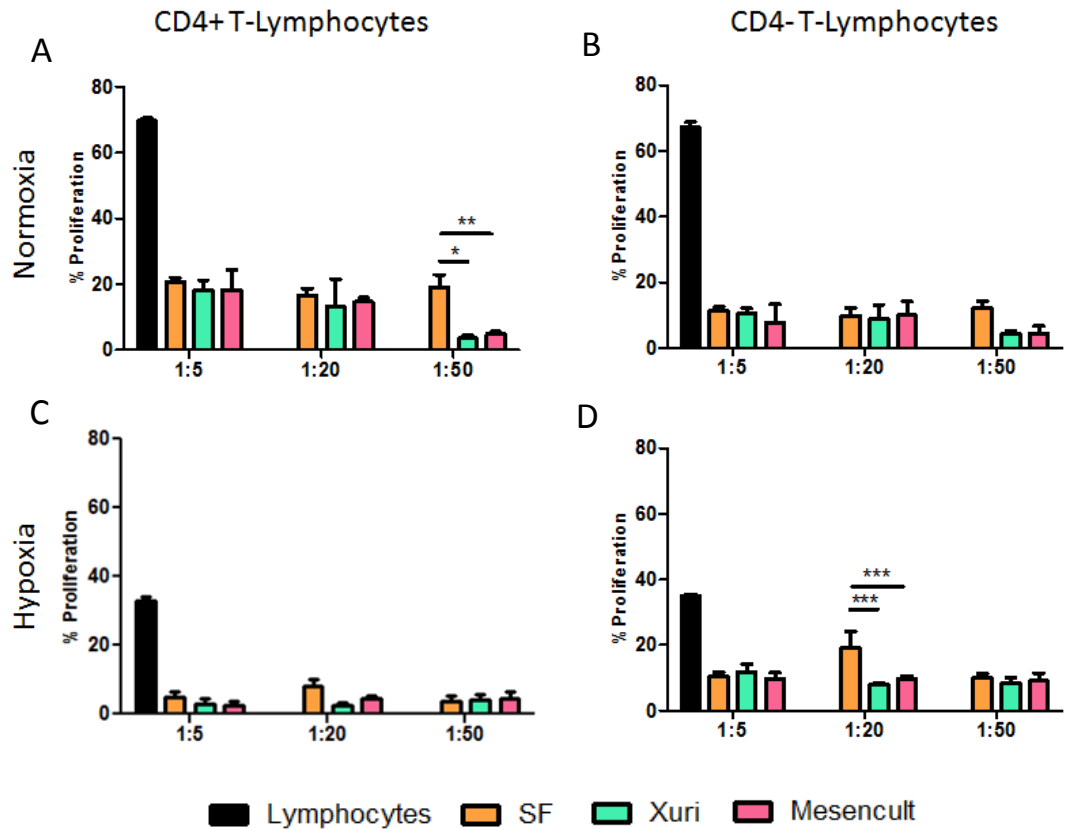


**Figure 6.3.11: Immunogenic potential of MSCs on unstimulated peripheral blood T-lymphocytes.** Percentage proliferation of CD3/CD28 stimulated T-lymphocytes compared to unstimulated T-lymphocytes. (Black) Stimulated T-lymphocytes alone; (Orange) Co-culture of SF-cultured MSCs with unstimulated T-lymphocytes; (Green) Co-culture of Xuri-cultured MSCs with unstimulated T-lymphocytes; (Pink) Co-culture of MC-cultured MSCs with unstimulated T-lymphocytes. Effect of normoxia (A) and hypoxia (C) cultured MSCs on CD4+ T-lymphocytes at various ratios of MSC: T-lymphocyte. Effect of normoxia (B) and hypoxia (D) cultured MSCs on CD4- T-lymphocytes at various ratios of MSC: T-lymphocyte. Results are presented as the mean  $\pm$  standard deviation (SD) of 3 biological replicates with 3 technical replicates. \* $p \leq 0.05$ , \*\* $p \leq 0.01$ , as determined using one-way ANOVA and Bonferroni's multiple comparisons post-test.

## 6.4 Discussion

The aim of this chapter was to compare the REMEDI serum-free medium with commercially available media and determine the commercial competitiveness of the serum-free medium against market leaders. This was done by isolating MSCs from bone marrow from healthy volunteers directly into four commercially available media. These media included DXF (Promocell), Therapeak (Lonza), Xuri (GE Healthcare) and Mesencult (Stemcell Technologies) and were compared to the current in-house serum-free medium. Initially, Mosaic MSC medium (BD) was also included in the study but was taken off the market immediately prior to carrying out this study. An initial study assessing the ability of the four commercial media listed above was performed. This involved isolation of bone marrow derived MSCs in the various media with and without the addition of 2% FBS to the media. At the time of the study, these media were described solely for the proliferation of MSCs and did not claim the ability to directly isolate MSCs from tissue sources. Data sheets of some of the media recommended the addition of 2% FBS to facilitate the isolation of MSCs in the presence of the commercial media. This study indicated that Therapeak and DXF were not capable of isolation of MSCs from bone marrow in the presence or absence of 2% FBS (Figure 6.3.1). For this reason, these media were excluded from all future studies. Subsequent studies aimed to assess the effect of isolating and culturing BM-MSCs in the serum-free medium, Xuri and Mesencult in both hypoxia and normoxia to determine if these cells behave differently under these conditions.

MSCs were isolated from three human bone marrow donors and CFU-fs were assessed (Figure 6.3.2). The morphology of the CFU-f was distinct to the media used. The SF medium generated many low density CFU-fs which were small in size and consisted of cells which were also small and round in shape. In contrast, MSCs isolated in Xuri medium were densely packed and larger in size. Oxygen tension didn't appear to have a noticeable effect on MSCs isolated in either of these media. Mesencult CFU-fs were extremely large and densely packed in normoxia. Cells of various morphologies were also observed. Conversely in hypoxia, mesencult CFU-fs consisted of uniform cells with an even distribution similar to that of SF MSCs.

When assessing CFU-f number, SF medium had increased CFU-f numbers compared to the commercially media but these were typically much smaller in size and with a lower cell number. While it is difficult to suggest a reason for these as the media formulations of these media are not available, what is clear is that based on CFU-fs alone, these media seem to alter the phenotype of MSCs at the time of isolation from bone marrow. The morphology of the cells was subsequently assessed during culture at P3 (Figure 6.3.4). No noticeable differences were observed between the cells at this point indicating that the differences in morphology may be a temporary artefact of the isolation process. Overall, cells exposed to all media groups assumed a more uniform phenotype after numerous passages in culture. Similarly growth kinetics of MSCs in culture were also assessed (Figure 6.3.3). Growth kinetics, based on population doublings of the cells, indicated equivalent growth of all media groups in both hypoxia and normoxia.

As previously discussed, tri-lineage differentiation is a trademark characteristic of MSCs (Krampera et al., 2013, Dominici et al., 2006a) and thus was assessed in this study. Mesencult does offer a range of supplements to be added to their medium to carry out tri-lineage differentiation assays. In the interest of maintaining uniformity throughout the study, standard tri-lineage assays were performed as previously outlined in sections 2.7-2.9. Osteogenesis was assessed by Alizarin red and quantitative assessment of calcium levels (Figure 6.3.5). Low levels of Alizarin red staining was observed in all groups except for MC in hypoxia. Based on Alizarin red staining, MC MSCs in hypoxia produced large dense regions of mineralisation. This Alizarin red staining is in conflict with calcium levels observed by these cells which were typically high in both Xuri and MC groups. The reason for this is unclear as typically an increase in one correlates with an increase in the other. Regardless, all MSC groups maintained their osteogenic ability. The levels observed in SF group were atypically low here. The reason for this is unclear. One noticeable difference is the lack of fibronectin during the culture of SF MSCs here which may be having an effect on osteogenesis compared to levels reported in chapter 3. In normoxia, Xuri MSCs produced high levels of calcium and was highly reproducible between donors. Similarly MC MSCs also produced high levels of calcium but this result was highly

variable between donors. In hypoxia, a reduction of calcium levels was seen in Xuri medium, although this was not statistically significant. MC MSCs in hypoxia maintained their high levels of calcium. This is in conflict with the current literature on the effect of hypoxia on MSC differentiation (Yang et al., 2011, Fehrer et al., 2007, Holzwarth et al., 2010a, Lee and Kemp, 2006). It is likely this maintained osteogenic potential of MC MSCs in hypoxia is due to a component in the media at the time of culture that has made these cells resistant to hypoxia-induced inhibition of osteogenesis. As the components of the medium are not commercially available, it is not possible to suggest which components of the medium may result in this effect.

Adipogenic assays were also performed assessing adipogenesis by Oil red O staining and quantification of that staining (Figure 6.3.6). All media groups maintained their adipogenic potential in normoxia and this was reduced in hypoxia for all media groups which indicates MSCs isolated in all media respond as predicted to hypoxia (Yun et al., 2002, Kim et al., 2005, Lin et al., 2006). In normoxia, Xuri-cultured MSCs produced the highest levels of fat vesicles as identified by Oil red O staining. This was significantly higher than both MC and SF media.

Similarly, the chondrogenic potential of MSCs was assessed after 21 days of induction in chondrogenic medium supplemented with TGF- $\beta$ 3. Chondrogenesis was assessed by Safranin O staining of sGAG levels and quantification of sGAG levels normalised to cell number (Figure 6.3.7). Safranin O staining indicated that all MSCs maintained their chondrogenic potential irrespective of the medium used except for the SF in normoxia which had very low GAG levels. In hypoxia, MC-cultured MSCs demonstrated high levels of sGAG levels compared to other groups and pellets were much larger in size. A reduction of the pellet size and sGAG levels was observed in Xuri-cultured MSCs and a further reduction was sGAG levels and size was seen in SF-cultured MSCs. The results were more variable in normoxia with all media groups seeing a reduction in Safranin O staining indicating a reduction in chondrogenesis. Quantification of sGAG levels by DMMB assay correlate with Safranin O staining of hypoxia differentiated groups. Results from the DMMB assay indicates improved chondrogenesis in hypoxia. As the DMMB assay measures the

total levels of sGAG in the pellet, it is reasonable to assume this result is more representative of the chondrogenic potential of MSCs and correlates with current literature on the effect of hypoxia on MSCs (Kanichai et al., 2008, Khan et al., 2007a, Schipani, 2005). Here we observe a reduction in chondrogenic potential of SF MSCs compared to chapter 3. No differences in media formulation were made between these studies except for the removal of fibronectin as an attachment factor. Further investigation is required to assess how this affects the tri-lineage differentiation potential of these cells.

Based on these tri-lineage differentiation data, the Xuri medium produces the highest levels of tri-lineage differentiation while also responding to environmental cues such as hypoxia in a similar manner as reported in current literature (Yang et al., 2011, Kim et al., 2005).

MSCs were also assessed for their maintenance of the minimum MSC surface marker profile as outlined by the ISCT (Dominici et al., 2006a). Both Xuri and SF media maintained positive expression of MSC markers above 95% while maintaining low levels of negative markers in both hypoxia and normoxia. Although the MC media maintained positive expression levels of all the MSC markers, HLA-DR expression of approximately 20% was observed in MC cultured cells in both hypoxia and normoxia. This constitutes a failure of MC MSCs to be classified as such according to the minimum criteria as set out by the ISCT. A possible reason for the increase in HLA-DR expression in MC MSCs may be due to high levels of mitogenic factors such as FGF-2 and platelet-derived growth factor BB (PDGF-BB) in the medium, which have been previously reported to induce HLA-DR expression in adult human MSCs (Bocelli-Tyndall et al., 2010a) and thus increase the immunogenic phenotype of these MSCs. However, it should be noted that an increase in immunogenicity in these cells was not observed when co-cultured with human peripheral blood isolated T-lymphocytes (Figure 6.3.12). Similarly, no difference was observed in the immunogenic profile of these cells in comparison to the other media (Figure 6.3.11).

Finally, the production of paracrine factors by MSCs cultured in the various media

was assessed. Conditioned medium from all media groups resulted in the formation of tubules by HUVEC cells (Figure 6.3.9) with a significant increase in the number of tubules when cultured with SF conditioned medium from normoxia cultured cells in comparison to other media groups. A similar trend was observed in hypoxia, although this was not significant. The basal media were also tested for their ability to induce tubule formation in a HUVEC assay. Significantly higher levels of tubules were formed in MC media group indicating higher levels of pro-angiogenic factors than the SF and Xuri media. This data is in support of the hypothesis that increased levels of growth factors resulted in increased HLA-DR expression, as discussed above.

In this chapter, a detailed *in vitro* comparison of SF medium was performed in comparison to two commercially available serum-free media. The data outlined above indicates that all three media are broadly capable of maintaining the MSC phenotype of bone marrow derived MSCs when isolated in hypoxia and normoxia. There were noticeable differences in these media which included the size and consistency of the CFU-fs, although this did not have an effect on the population doublings of the MSCs. Tri-lineage differentiation potential was superior in the commercially available media when compared to SF medium. Although, the tri-lineage differentiation potential of the SF medium has been reported to be higher in previous studies, as seen in chapter 3 (Figure 3.3.4), the results here would indicate variability in the SF MSCs ability to undergo tri-lineage differentiation and may require further development of the culture medium. However, higher levels of paracrine factors may be produced in the SF media as indicated by the HUVEC assay. This may highlight a role for varying the use of the media depending on the therapeutic target of the MSCs. From a clinical point of view, the progression of a number of serum-free media that are chemically defined indicates the potential to move away from the use of FBS to a more standardised product. From a research prospective, progress in this area may continue to be slow due to the proprietary nature of this work, typically being performed in commercial entities. Continuing comparison studies will need to be performed as new media formulations emerge and older formulations are developed.

# Chapter 7

To determine the feasibility of the serum-free medium in a three dimensional (3D) culture system for the scalable production of MSCs

### 7.1 Introduction

The progression of MSC-based therapies towards the clinic increases pressure to address the current limitations of MSCs and their large-scale production for therapeutic use. Simply put, it is not practical or cost effective to manually culture large batches of MSCs for widespread clinical use. Scalable systems with the ability to produce large batches of MSCs reproducibly at a relatively low cost will be essential for the advancement of cell therapies. Additionally much of the heterogeneity observed in the literature regarding the culture expansion of MSCs may be due to variations in culture conditions, that no matter how small, may have significant effects on the final cell product (Rafiq et al., 2013). Typical MSC culture is performed on 2D tissue culture plastic under static conditions in the presence of a medium containing FBS typically. These MSCs may have been isolated from different sources, directly plated or selected with a number of different antibodies reviewed elsewhere (Lv et al., 2014), seeded into a medium containing different batches of FBS typically and grown in different oxygen tensions. It is reasonable to assume that all these factors contribute to the heterogeneity of MSC preps. A number of factors can potentially reduce this heterogeneity, including the use of an antibody-selected seeding MSC, growth in a chemically defined medium and the use of an automated system to reduce variability introduced to the culture system due to user and system variation. Culture systems would also need to be scalable for large-scale manufacture. This upward scaling of 2D culture has been attempted with the use of T-flask stacks, which are now available up to 40 stacks high providing a surface area of over 25,000cm<sup>2</sup> in a single unit (Corning *HYPERFlask*). Although this addresses the issue of upscaling the process, these stacks are difficult to manipulate and cells in the majority of layers are not visible making in-process assessment of cells difficult. To overcome this, much research and development has gone into the development of 3D non-static culture systems with microcarriers which can ultimately be increased in sized to generate larger batches of MSCs without increasing manual handling (Eibes et al., 2010, Hewitt et al., 2011, Santos et al., 2011, Schop et al., 2010). Large-scale production of MSCs is particularly important in the context of allogeneic cell therapy where cell banks would be

required to reach target production of millions of cells to for many recipients (Dos Santos et al., 2014).

This issue is not specific to the MSC field and the same challenges are being faced in the production of other cell types in 3D systems such as HSCs (Cabral, 2001, Song et al., 2010), iPSCs (Olmer et al., 2012, Shafa et al., 2012), ESCs (Fernandes-Platzgummer et al., 2011) and neural stem cells (Rodrigues et al., 2011). Systems are currently being developed for the proliferation of these cells in an undifferentiated state but also to direct cell differentiation (Bardy et al., 2013). General requirements to be considered with the use of bioreactors for cell manufacturing include pH, temperature, dissolved oxygen levels and metabolism of the cells (dos Santos et al., 2013). Moreover, there are cell-specific considerations which need to be taken into account including how cells are isolated and cultured, whether they are adherent or in suspension and how these cells will be marketed e.g. autologous versus allogeneic which may impact bioreactor size and handling. Of course, the entire process must be GMP-compliant which will require in process quality assurances steps. Isolation of MSCs varies depending on tissue source and processes usually require multiple steps which can be challenging for bioreactor systems to incorporate in an automated setting (dos Santos et al., 2013). Similarly proliferation of specific cells can also be challenging. MSCs are an anchorage-dependent cell type and so microcarriers which facilitate the attachment of these cells in large-scale stirrer tanks are required to provide support. Biomechanical and biochemical stimuli to the cells are also key issues for concern and may often be cell-specific. Agitation rate and duration may also need to be evaluated as insufficient rotation may fail to adequately mix cells/microcarriers and may create pockets with different CO<sub>2</sub> levels and nutrient availability. Conversely, excessive agitation may result in cell damage due to shear stress (Stolberg and McCloskey, 2009). Additionally, constant versus intermittent stirring may be required. Although the 3D environment created by growing cells on microcarriers in a bioreactor is a closer approximation of the *in vivo* environment in which the cells originated, stirring of cells is not and may result in adverse effects. This negative effect may not be merely due to shear stress caused by the stirring but also due to collision of

cell-loaded microcarriers with other microcarriers or bioreactor parts such as the propeller (Cherry and Papoutsakis, 1988).

While there are a number of outstanding questions regarding the use of 3D culture systems for the culture of MSCs, the beneficial effects of a standardised 3D culture system may be overshadowed by the inherent heterogeneity of an undefined cell product. This chapter aims to assess the ability of MSCs cultured in a novel serum-free medium to propagate in a closed stirrer tank system on a novel 3D macrocarrier which allows in-process visualisation of cells.

### **7.2 Methods**

In collaboration with GE healthcare, The Xuri stirrer bioreactor with macrocarrier 'waffles' was evaluated for its ability to facilitate MSC proliferation. To determine the ability of the GE Xuri bioreactor system's ability to expand MSCs, previously isolated in SF and SC medium, cells previously cultured until the end of P1 in standard 2D culture were re-plated on standard TC plastic or in Xuri bioreactor for two subsequent passages for 7 days each (See sections 2.4 and 2.6). Cells were assessed for their ability to proliferate on the bioreactor waffles based on cell counts and visual assessment of MSCs at days 4 and 7. MSCs were also assessed for their ability to undergo tri-lineage differentiation using conventional methods as previously described (sections 2.7-2.9). In addition, MSCs cultured in the bioreactor were assessed for their ability to undergo tri-lineage differentiation on the macrocarrier waffles which could ultimately provide an easy means for in-process validation of MSCs during the manufacturing process (sections 2.7.3, 2.8.3, 2.9.4). Additionally, conditioned medium was harvested from bioreactors and assessed for its ability to promote angiogenesis of HUVEC cells cultured on Matrigel (section 2.13). A schematic representation of the experimental design is presented in figure 7.2.1.

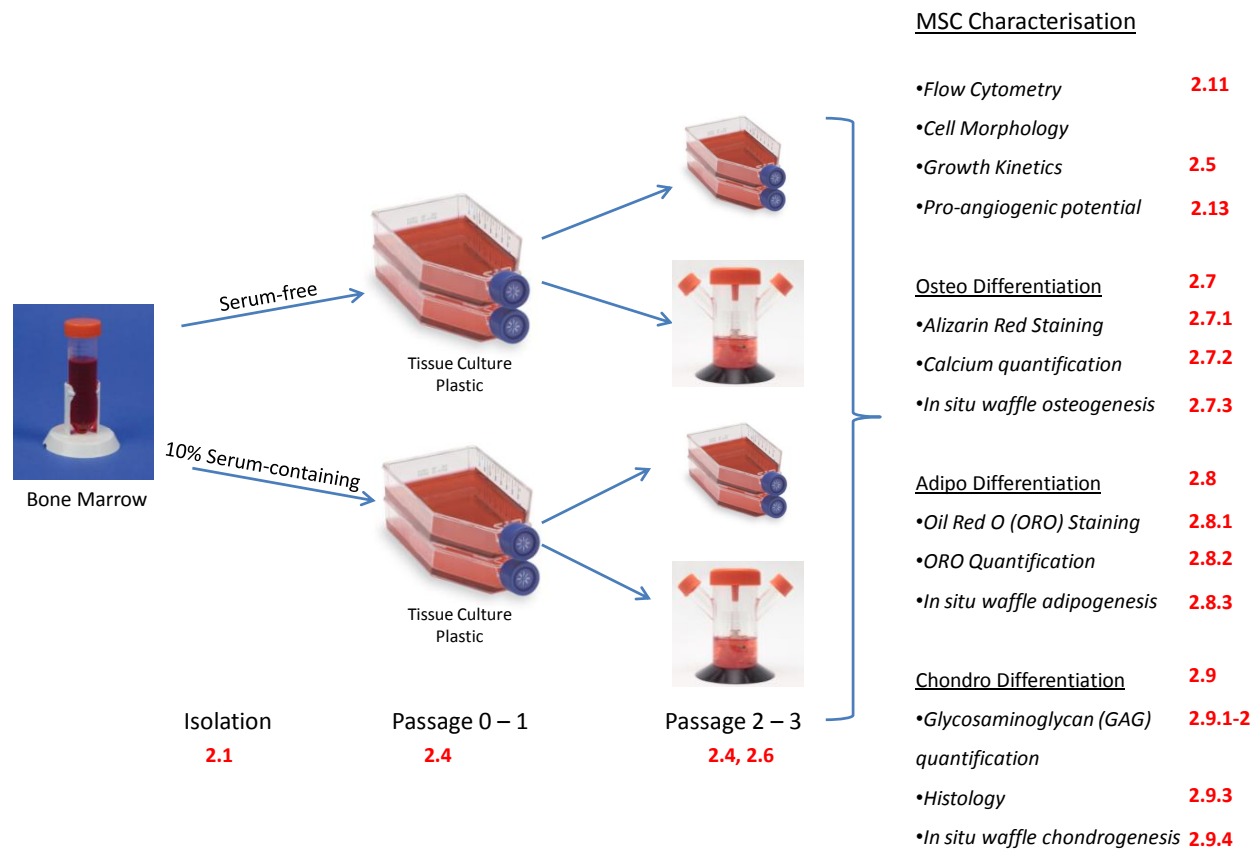


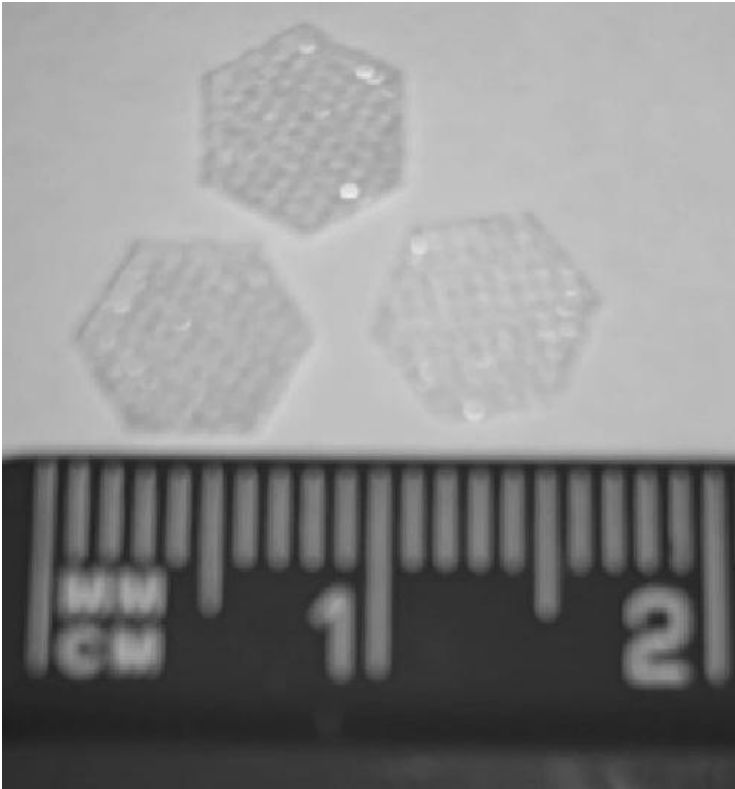
**Figure 7.2.1 Schematic representation of the approach taken to assess the ability of serum-free (SF) and serum-containing (SC) MSCs to proliferate and differentiate in the Xuri scalable bioreactor. Specific methods (as described in chapter 2) are indicated by the associated number in red.**

### 7.3 Results

#### 7.3.1 Growth kinetics of SF and SC MSCs cultured in a 3D Bioreactor with Xuri microcarriers (“Waffles”)

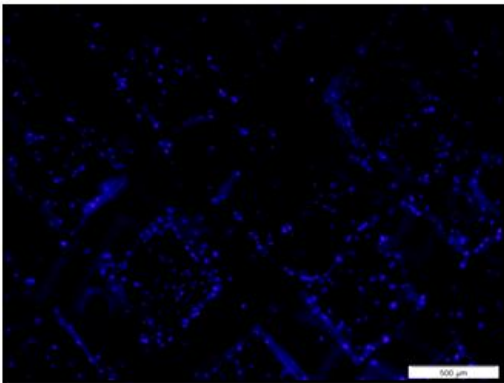
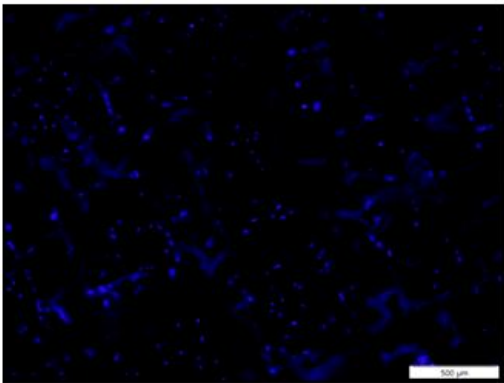
Growth kinetics of SF and SC MSCs, previously isolated and cultured up to the end of P1, were assessed after seeding  $2 \times 10^6$  cells into the Xuri bioreactor system. MSCs were grown in the bioreactor for 2 passages. Data is presented as population doublings based on cell counts at the end of each passage. Data indicates superior growth of SF cells in the bioreactor system compared to SC cells. However, SF cells in 2D standard culture on TC plastic demonstrated superior growth compared to the bioreactor (Figure 7.3.1). SC MSC proliferation appeared was low in the bioreactor indicating reduced proliferation compared to SC MSCs cultured on tissue culture plastic. With increased passage number, this difference may become significant. Predicted yield calculations indicate a significant reduction in proliferation of MSCs in the Xuri bioreactor system.

A

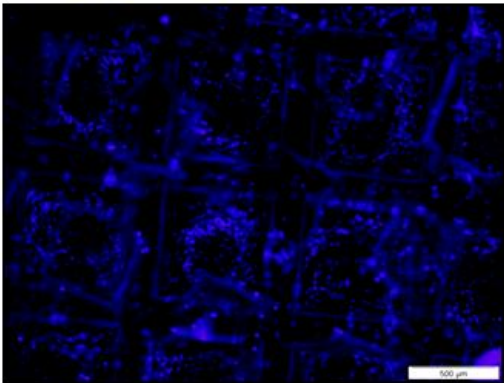
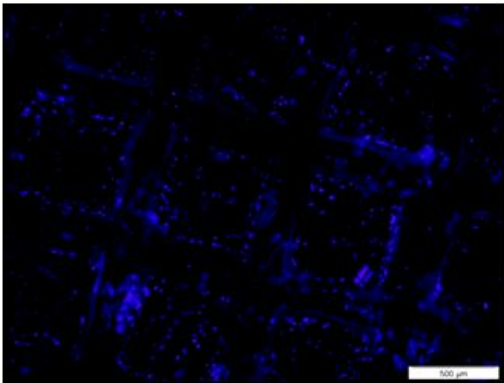


B

Serum



Serum-free



Day 4

Day 7

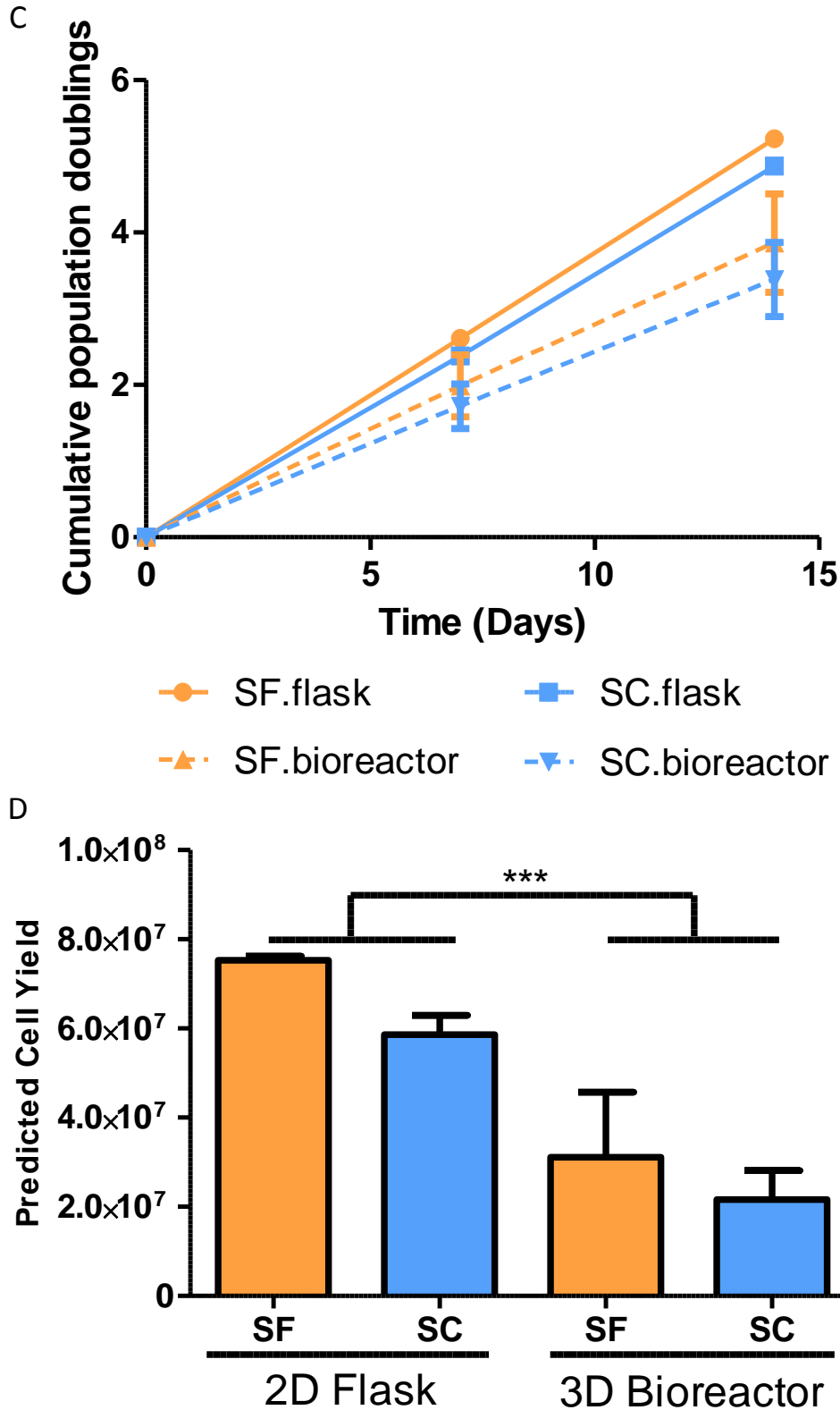


**Figure 7.3.1: Growth kinetics of serum-free (SF) and serum-containing (SC) cultured in Xuri bioreactor and in 2D culture (A) Representative image of waffles. Scale bar: 500µm. (B) Nuclear DAPI staining of waffles at day 4 and day 7 of culture in P3. Increased DAPI staining with time indicated cell proliferation of MSCs on**

waffles. (C) Representative growth kinetics of 3 biological replicates of SF and SC MSCs cultured in the Xuri bioreactor versus standard 2D culture. Data representative of mean CPD of 3 biological replicates  $\pm$  SD. No significant changes in growth rate of MSCs were seen in the bioreactor compared to 2D culture. (D) Predicted cell yields from  $2 \times 10^6$  MSCs cultured for 2 passages in the various conditions indicating a significant reduction in cell yield when MSCs are cultured in the bioreactor. Data is representative of 3 biological replicated  $\pm$  SD. \*\*\* $p \leq 0.001$  as determined using two-way ANOVA and Bonferroni's multiple comparisons post-test.

### 7.3.2 Morphology of MSCs is altered when cultured on Xuri Waffles

To visualise the MSCs on GE waffles, Waffles were selected at random from the Xuri bioreactor and washed twice in D-PBS. Waffles were then fixed in formalin for 30mins and stained with crystal violet for 5mins. Waffles were washed twice with D-PBS and visualised using microscopy. Figure 7.3.2 demonstrated representative images of waffles seeded with SF or SC MSCs at 4x and 10x magnification. Morphology of MSCs indicates a more rounded, less elongated MSC morphology indicative of a stressed phenotype of MSCs in the bioreactor.

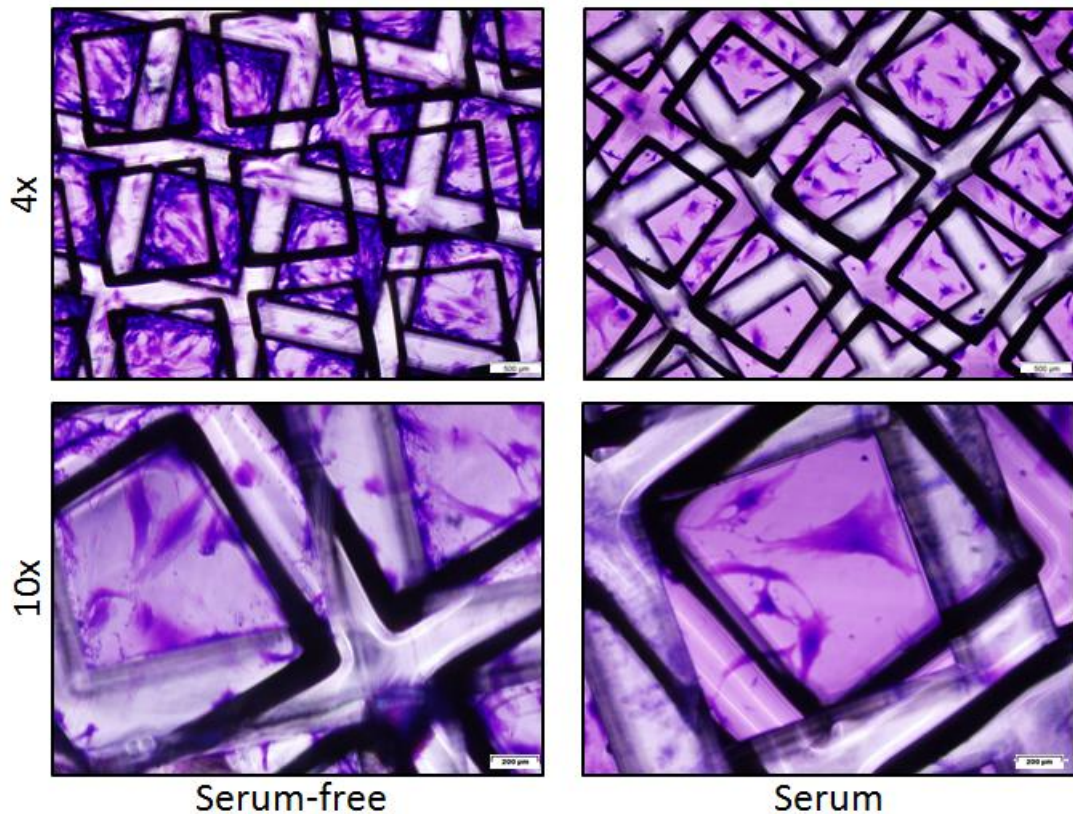
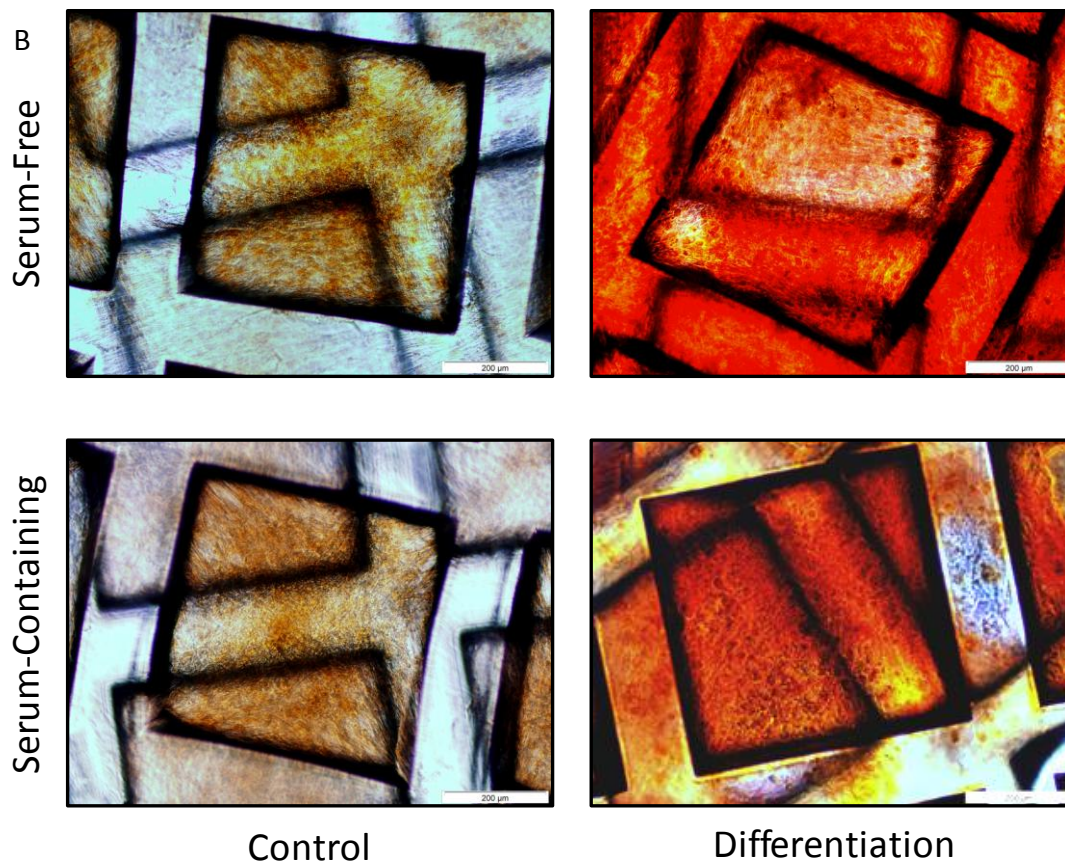
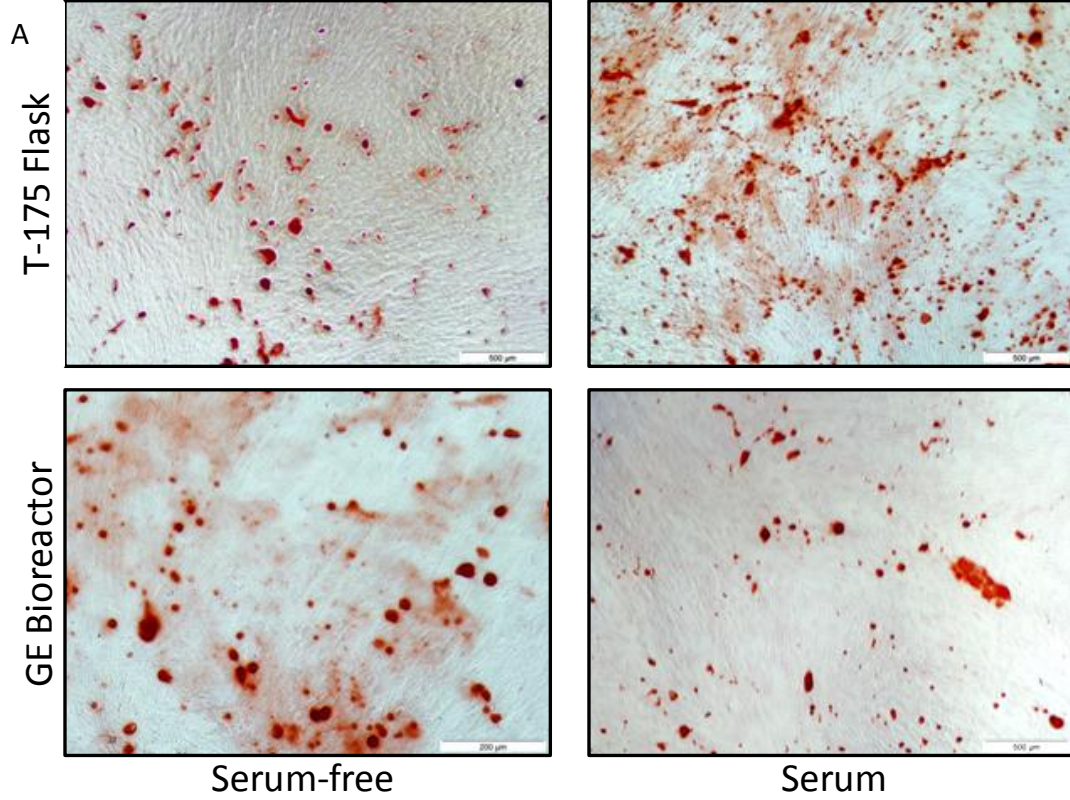


**Figure 7.3.2 Morphology of MSCs on Waffles is more rounded indicating stress**

### **7.3.3 Culture of MSCs in Xuri bioreactor increases their osteogenic potential**

To assess the effect of culturing MSCs in the Xuri bioreactor system on their osteogenic potential, MSCs harvested from the Xuri bioreactor were seeded into 24-well plates and standard osteogenic assays were carried out. These cells were assessed for their osteogenic potential in parallel to the same cell maintained in 2D culture on TC plastic. Prior to harvesting cells from bioreactor waffles, five waffles were selected at random from the bioreactor and placed directly into osteogenic induction medium. All MSC groups were cultured for 14 days in osteogenic medium prior to harvesting. Of the groups differentiated using standard MSC differentiation protocols in 2D, one well of each assay was taken to measure DNA levels using the Picogreen kit, 3 wells were assessed for calcium levels and one well was stained using Alizarin red. Similarly, of the 5 waffles harvested, 1 was assessed for DNA content, 3 for calcium levels and 1 for alizarin red staining. Figure 7.3.3a demonstrates representative alizarin red images of MSCs from 2D standard culture and 3D bioreactor culture after undergoing osteogenic differentiation. Alizarin red staining is evident in all groups with no noticeable difference observed between groups. Figure 7.3.3b represents Alizarin red staining of MSCs directly on Xuri waffles. Low levels of background staining were observed on control waffles, maintained in standard SC MSC culture medium. Highly increased levels of Alizarin red staining were observed in both SC and SF differentiation waffles. Positive staining is seen predominantly within squares of waffles in the SC group and over the entire surface of the waffles in the SF group indicating higher levels of osteogenesis in the SF group on waffles. Quantification of calcium levels was also assessed (Figure 7.3.3c). However, no differences were observed between SF and SC MSCs within any of the groups. MSCs cultured in the bioreactor showed significantly higher levels of calcium when differentiated on 2D plastic in standard osteogenesis assays and on Xuri waffles indicating culture of MSCs in the Xuri 3D system increases the osteogenic potential of MSCs compared to 2D culture. This increase in osteogenesis was further significantly increased when cells were differentiated on Xuri waffles. All data is presented as calcium levels normalised to

DNA content due to differences in cell number on the waffle compared to a 24-well plate well. Total calcium levels (Figure 7.3.3d) and total DNA levels (Figure 7.3.3e) are also presented separately. No difference in DNA levels is observed in the 2D osteogenesis assay with higher levels of calcium observed in cells harvested from bioreactor. Significantly lower levels of DNA are observed on Xuri waffles indicating a reduced number of cells. Despite this, these cells demonstrate increased calcium levels compared to approximately twice as many cells in cells cultured in 2D TC conditions.



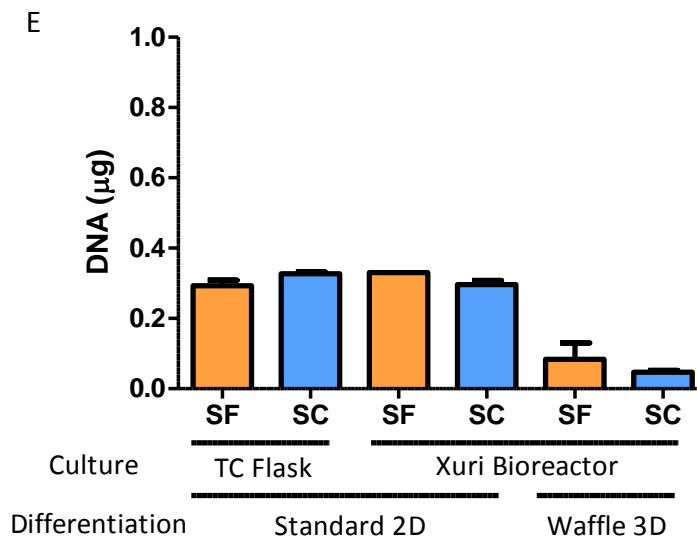
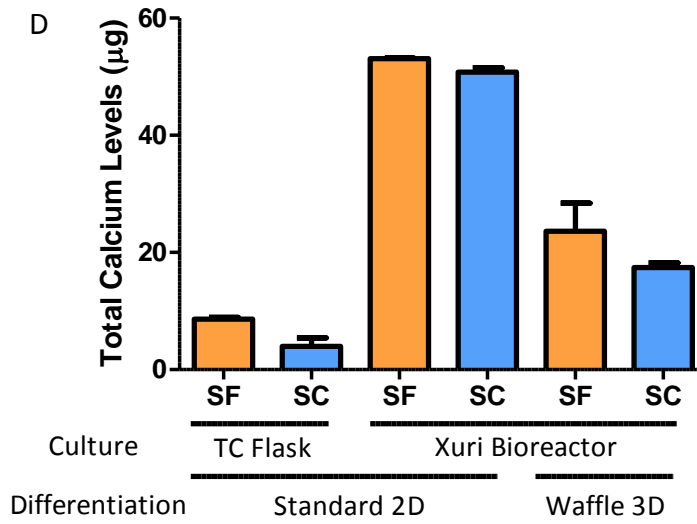
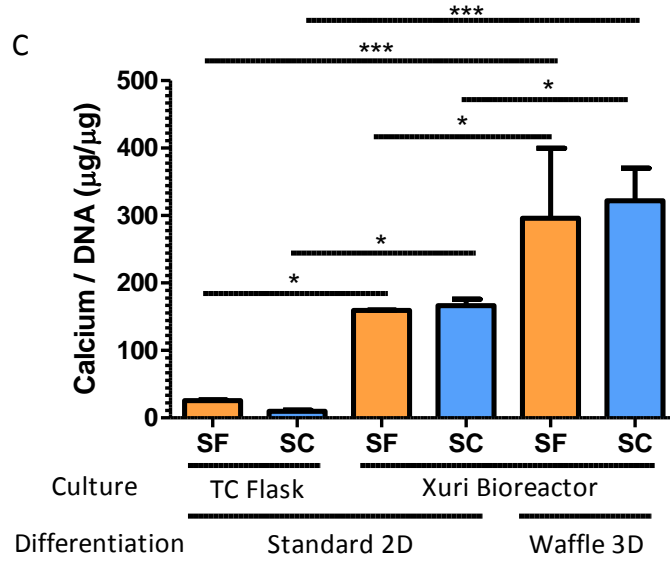
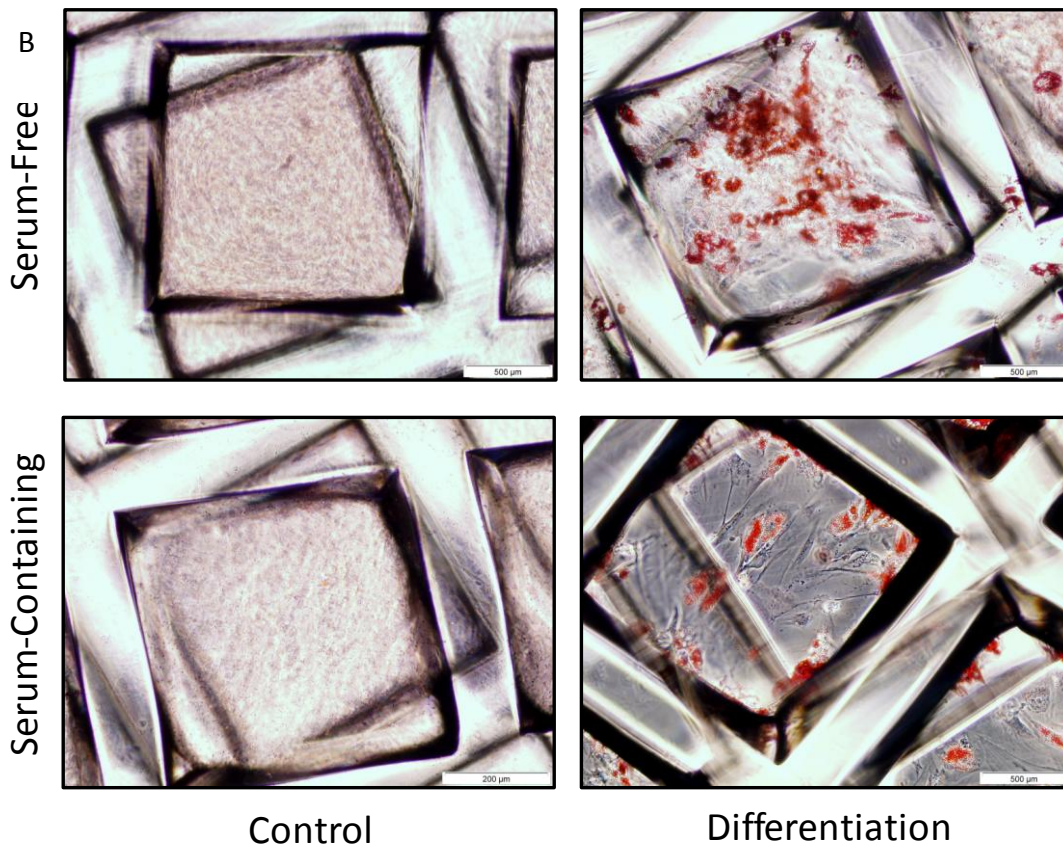
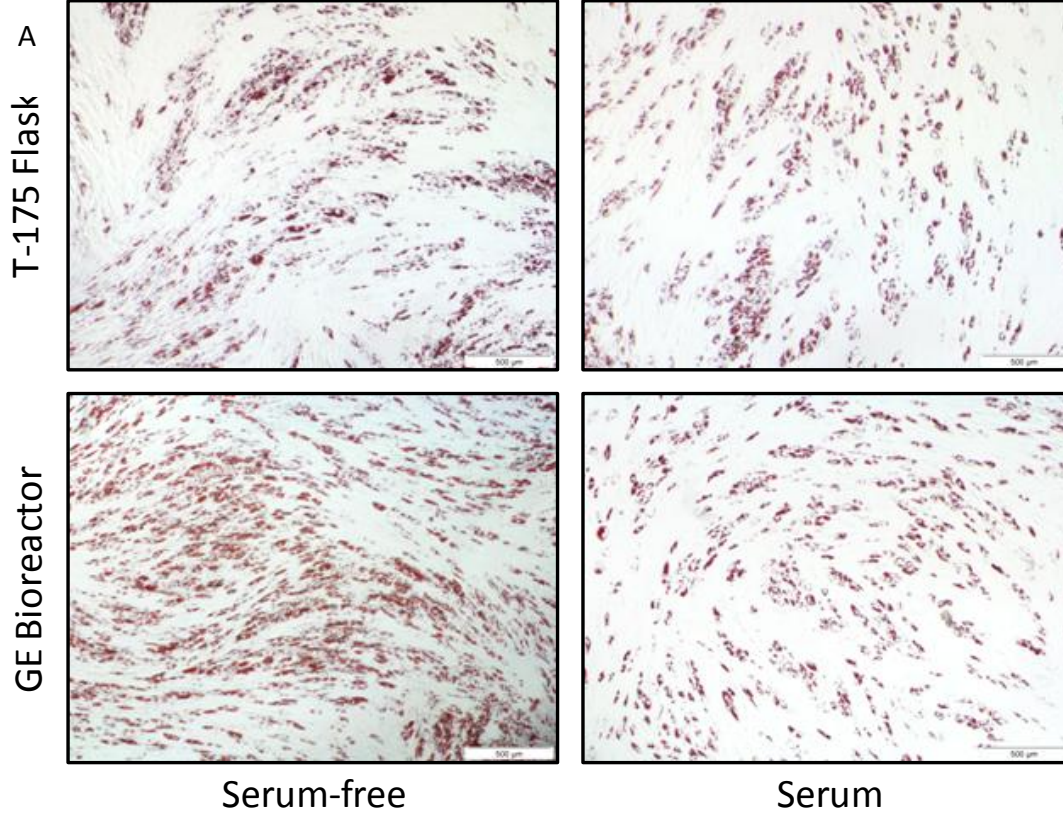


**Figure 7.3.3: Osteogenic potential of SF and SC MSCs cultured on 2D TC plastic and the 3D bioreactor system.** (A) Representative alizarin red staining of SF and SC cells from a 2D osteogenesis assay, previously cultured on 2D TC plastic or the 3D bioreactor system indicating positive alizarin red staining in all groups. (B) Representative alizarin red staining of SF and SC cells cultured and differentiated on the 3D bioreactor macrocarrier ‘waffle’ and undifferentiated control waffles as a staining control. Low levels of background staining were evident in control groups with high alizarin red staining evident in the differentiated groups. (C) Quantitative calcium levels normalised to DNA content of SF and SC MSCs from either 2D or 3D culture, differentiated in either 2D or 3D conditions. Data indicates significantly increased levels of calcium/DNA levels of all MSC groups previously cultured in the Xuri bioreactor with highest levels of calcium observed in MSCs cultured and differentiated on the bioreactor. (D) Absolute calcium levels of SF and SC MSCs from either 2D or 3D culture, differentiated in either 2D or 3D conditions. Increased levels of total calcium levels were observed in all MSC groups previously cultured in the Xuri bioreactor regardless of whether 2D or 3D osteogenesis was performed. (E) Absolute DNA levels of SF and SC MSCs from either 2D or 3D culture, differentiated in either 2D or 3D conditions. Comparable levels of DNA were observed in all MSC groups in 2D assays with a reduction in DNA levels of MSC groups on the waffles. Results are presented as the mean  $\pm$  standard deviation (SD) of 3 biological replicates, \* $p \leq 0.05$ , \*\*\* $p \leq 0.001$  as determined using two-way ANOVA and Bonferroni’s multiple comparisons post-test. Scale bar: 500 $\mu\text{m}$  (Figure 7.3.3a), 200 $\mu\text{m}$  (Figure 7.3.3b)

#### 7.3.4 Culture of MSCs on bioreactor increases adipogenic potential of MSCs

To assess the effect of culturing MSCs in the Xuri bioreactor system on their adipogenic potential, MSCs harvested from the Xuri bioreactor were seeded into 24-well plates and standard adipogenic assays were carried out. These cells were assessed for their adipogenic potential in parallel to the same cells maintained in 2D culture on TC plastic. Prior to harvesting cells from bioreactor waffles, four waffles were selected at random from the bioreactor and placed directly into adipogenic induction medium. All MSCs groups were cultured for 15 days alternating between adipogenic induction medium and adipogenic maintenance medium prior to harvesting. Of the groups differentiated using standard MSC differentiation protocols in 2D, one well of assay was taken to measure DNA levels using the Picogreen kit, 3 wells were assessed for Oil red O staining and subsequent

quantification. Similarly, of the 4 waffles harvested, 1 was assessed for DNA content, 3 for ORO staining and quantification. Figure 7.3.4a demonstrates representative Oil red O images of MSCs from 2D standard culture and 3D bioreactor culture after undergoing adipogenic differentiation using standard 2D adipogenic assays. Oil red O staining was evident in all groups with significantly higher levels observed in SF MSCs cultured in the bioreactor. Figure 7.3.4b represents Oil red O staining of MSCs directly on Xuri waffles. No background staining was observed on control waffles. Oil red O staining of fat formation was visible in both SF and SC groups differentiated on GE waffles. Quantification of Oil red O levels was also assessed and normalised to DNA levels (Figure 7.3.4c). SF MSCs cultured in the bioreactor showered significantly higher levels of Oil red O when differentiated on 2D plastic in standard adipogenesis assays and on Xuri waffles indicating culture of SF MSCs in Xuri 3D system increases the adipogenic potential of MSCs compared to 2D culture. No difference in 2D differentiation of SC MSCs was observed. SC MSCs cultured and differentiated on Xuri waffles demonstrated significantly higher adipogenic potential indicating that the Xuri bioreactor system promotes the adipogenic potential of MSCs. All data is presented as Oil red O levels normalised to DNA content due to differences in cell number on the waffle and in a 24-well plate. Absolute Oil red O (Figure 7.3.4d) and total DNA levels (Figure 7.3.4e) are also presented separately. A small variation in DNA levels is observed in the 2D adipogenesis assays. Lower levels of DNA are observed on the Xuri waffles indicating a reduced number of cells. Despite this, these cells demonstrate increased adipogenic potential to the same cells differentiated in 2D assays.



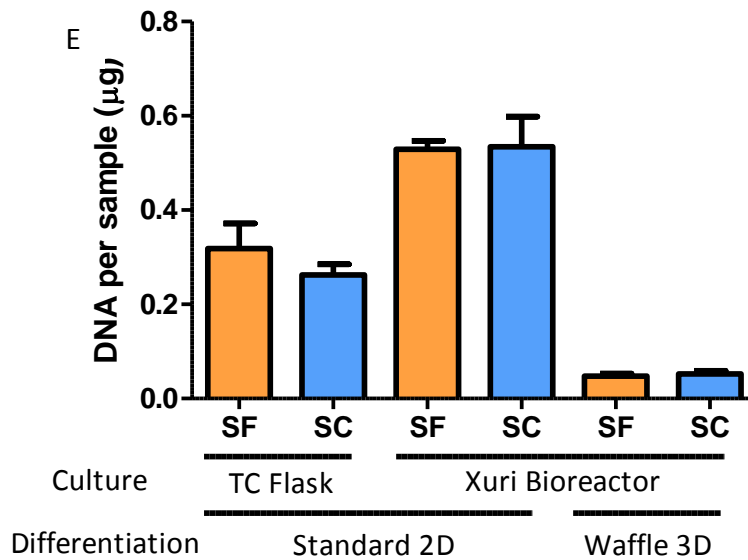
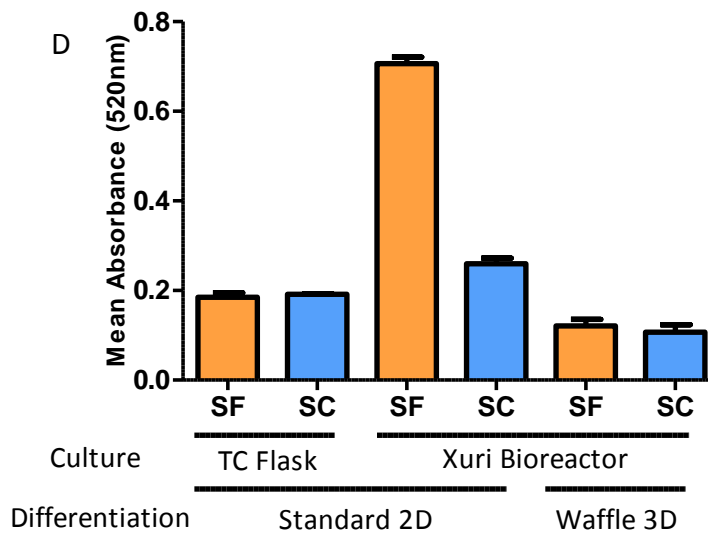
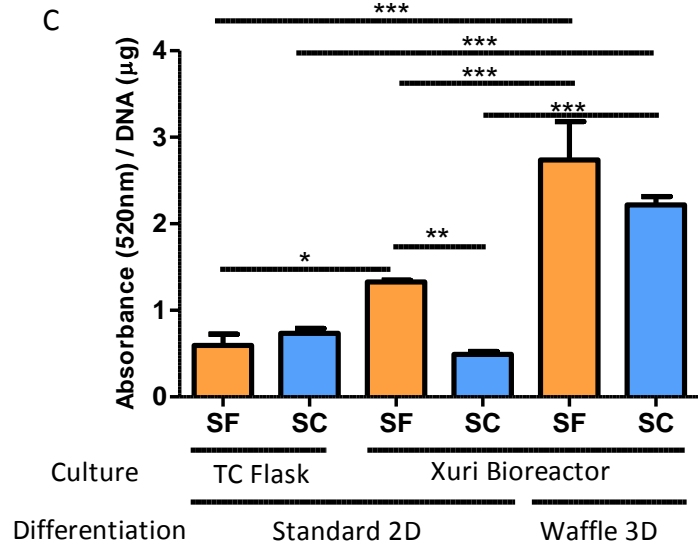
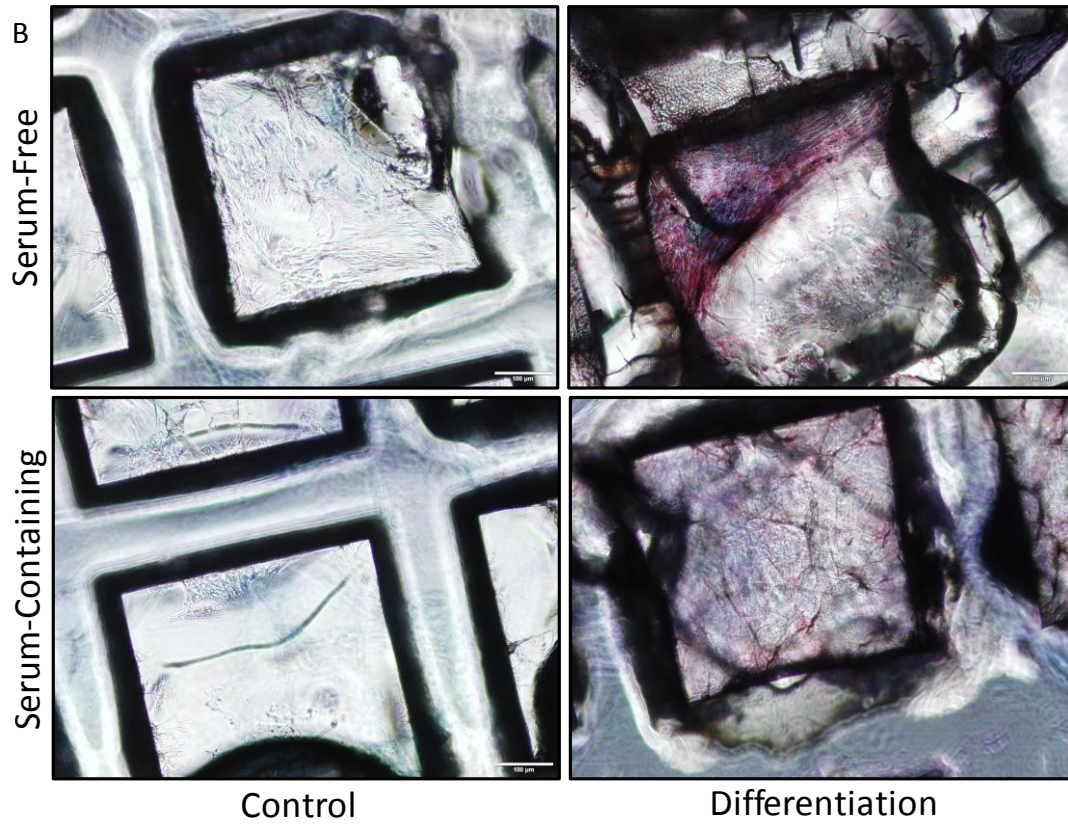
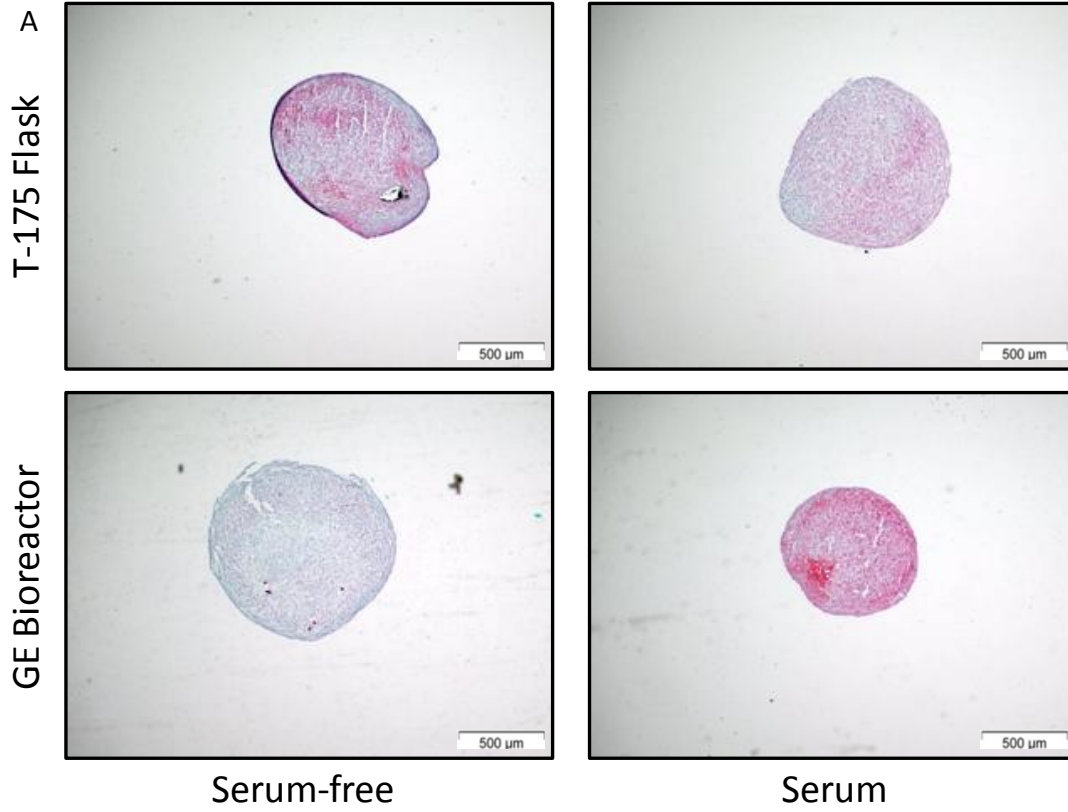


**Figure 7.3.4: Adipogenic potential of SF and SC MSCs was enhanced when differentiated on bioreactor waffles** (A) Representative ORO staining of SF and SC cells from a 2D adipogenesis assay, previously cultured on 2D TC plastic or the 3D bioreactor system indicating positive ORO staining in all groups. Increased levels were observed in the SF group, previously cultured in the bioreactor. (B) Representative ORO staining of SF and SC cells cultured and differentiated on 3D bioreactor macrocarrier 'waffles' and undifferentiated control waffles as a staining control. ORO staining was seen in differentiated samples and absent in staining controls. (C) Semi-quantitative ORO levels normalised to DNA content of SF and SC MSCs from either 2D or 3D cultures, differentiated in either 2D or 3D conditions. Data indicates significantly increased levels of ORO per DNA levels in cells differentiated on bioreactor waffles. (D) Absolute absorbance levels of ORO of SF and SC MSCs from either 2D or 3D culture, differentiated in either 2D or 3D conditions. Increased levels of ORO levels observed in SF MSC groups previously cultured in Xuri bioreactor regardless of whether 2D or 3D osteogenesis assay is performed. (E) Absolute DNA levels of SF and SC MSCs from either 2D or 3D culture, differentiated in either 2D or 3D conditions. Reduction of DNA levels of MSCs cultured on Xuri waffles indicating reduced cell number. Results are presented as the mean  $\pm$  standard deviation (SD) of 3 biological replicates, \* $p \leq 0.05$ , \*\* $p \leq 0.01$ , \*\*\* $p \leq 0.001$  as determined using two-way ANOVA and Bonferroni's multiple comparisons post-test. Scale bar: 500 $\mu$ m.

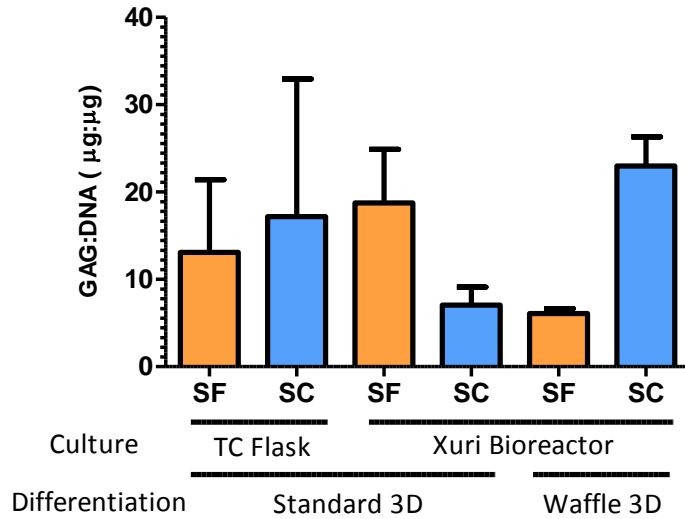
### 7.3.5 Chondrogenic potential of MSCs cultured on the Xuri bioreactor

To assess the effect of culturing MSCs in the Xuri bioreactor system on their chondrogenic potential, MSCs harvested from the bioreactor were set up in standard 3D chondrogenic assays as previously described in section 2.9. These cells were assessed for their chondrogenic potential in parallel to the same cells that were maintained in 2D culture on TC plastic prior to chondrogenesis assays being performed. Prior to harvesting cells from the bioreactor waffles, four waffles were selected at random from the bioreactor and placed directly into complete chondrogenic medium. Differentiation controls were cultured in incomplete chondrogenic medium which lacks TGF- $\beta$ 3. All MSCs groups were cultured for 21 days prior to harvesting. Of the groups differentiated using standard MSC differentiation protocols, 3 pellets were harvested to measure GAG and DNA levels and one pellet was fixed in formalin for subsequent Safranin O staining. Similarly, of the 4 waffles harvested, 3 were assessed for DNA and GAG levels and 1 was

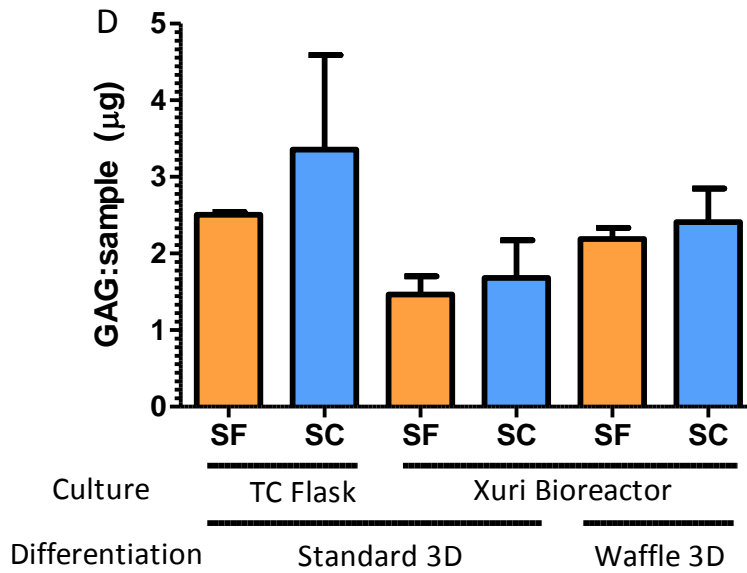
assessed for Safranin O staining. Figure 7.3.5a demonstrates representative Safranin O stained images of MSCs from standard 2D culture and 3D bioreactor culture after undergoing differentiation in standard chondrogenesis assays. Safranin O levels detected in all groups excluding the SF MSCs cultured in bioreactor. Based on Safranin O staining, the chondrogenic potential of SF MSCs is reduced by culture of cells in the bioreactor. Conversely, the chondrogenic potential of SC cells is increased by culture in the bioreactor. Figure 7.3.5b represents Safranin O staining of MSCs differentiated directly on Xuri waffles. No background staining was observed on control waffles, maintained in ICM culture medium. Low levels of Safranin O staining were observed in the SF or SC groups on waffles. Quantification of GAG levels, normalised to DNA content was also assessed (Figure 7.3.5c). No statistical differences were observed between any of the groups. High donor variability is observed in the case of MSCs cultured on TC plastic. A trend towards an increase in GAG levels is observed in SF MSCs harvested from the bioreactor but is not significantly different to the SC group. Conversely, there is a trend towards an increase in chondrogenesis of SC MSCs differentiated directly on waffles compared to the SF group but these data are also not statistically significant. These data overall indicate no difference in chondrogenic potential of MSCs when cultured on 2D TC plastic or in the 3D bioreactor. Similarly, differentiation potential may not be affected by performing chondrogenic differentiation assays directly on bioreactor waffle. Total GAG (Figure 7.3.5d) and DNA (Figure 7.3.5e) were also assessed. No statistical difference observed between any of the groups. High variation between biological donors was evident.



C



D



E

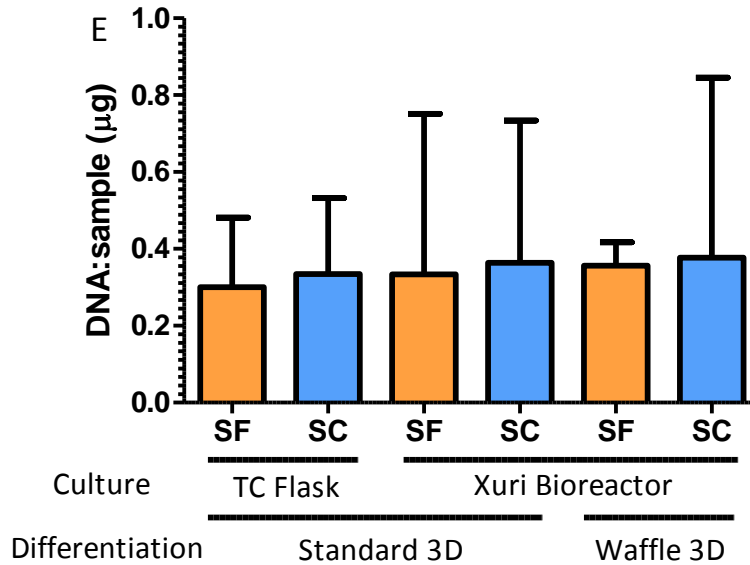


**Figure 7.3.5: Chondrogenic potential of SF and SC MSCs was unaltered by culture or differentiation on bioreactor waffles** (A) Representative Safranin O staining of SF and SC cells post-chondrogenesis, previously cultured on 2D TC plastic or the 3D bioreactor system indicating a reduction of GAG levels in SF MSCs cultured in bioreactor compared to 2D culture. (B) Representative Safranin O staining of SF and SC cells cultured and differentiated on the 3D bioreactor macrocarrier 'waffle' and undifferentiated control waffles as a staining control. Low levels of staining were present in differentiated samples and absent in staining controls. (C) GAG levels normalised to DNA content of SF and SC MSCs from either 2D or 3D culture, differentiated in either standard chondrogenesis or directly differentiated on waffles. High inter-donor variation were seen in GAG: DNA levels with no statistical differences observed. (D) Absolute GAG levels of SF and SC MSCs from either 2D or 3D culture, differentiated in either standard chondrogenic pellets on waffles. No difference in GAG levels was observed. (E) Absolute DNA levels of SF and SC MSCs from the various groups. High levels of variability in DNA levels were observed between groups. Results are presented as the mean  $\pm$  standard deviation (SD) of 3 biological replicates, Statistical analysis determined using two-way ANOVA and Bonferroni's multiple comparisons post-test. Scale bar: 500 $\mu$ m.

### **7.3.6 Surface marker phenotype of SF and SC MSCs is unaffected by culture in the Xuri bioreactor**

To assess whether the MSCs cultured in SF medium satisfied the ISCT criteria for definition as MSCs, SF and SC MSCs isolated and cultured on TC plastic and in the Xuri bioreactor system were assessed at the end of P3 for expression of the markers reported in figures 7.3.6a&b. No changes in surface marker expression were observed in either SF or SC MSCs due to being cultured in either system. SF MSCs maintained  $\geq 95\%$  expression of MSC markers CD105, CD73 and CD90 in both 2D and 3D culture. Equivalent expression profiles were observed for the SC MSCs in both conditions also. In addition to the ISCT panel, expression of CD271 and CD146 was also assessed. SF isolated and expanded MSCs maintained expression of CD271 in both 2D (figure 7.3.6a) and 3D (figure 7.3.6b) with no difference in expression levels. Expression of CD271 was not observed in SC MSCs in either culture conditions. Expression of CD146 was maintained in a subpopulation of SC MSCs in both culture conditions. This expression is mirrored in the SF cells but with a higher subpopulation of the cells maintaining this expression.

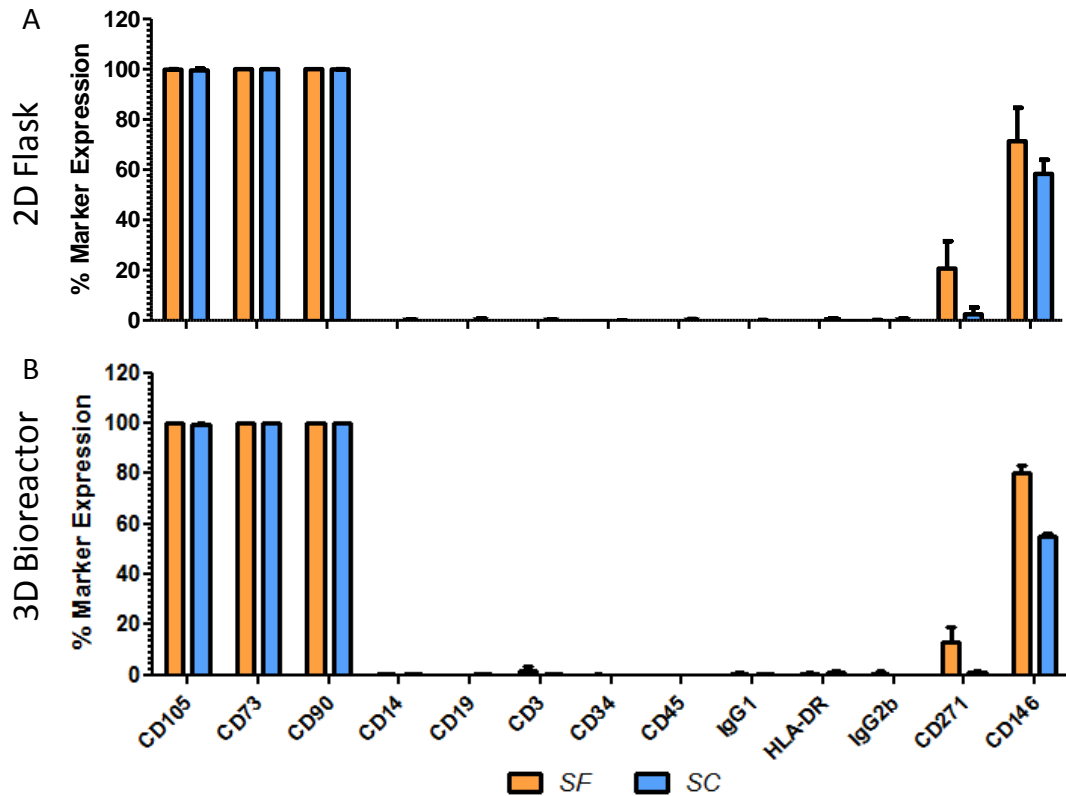


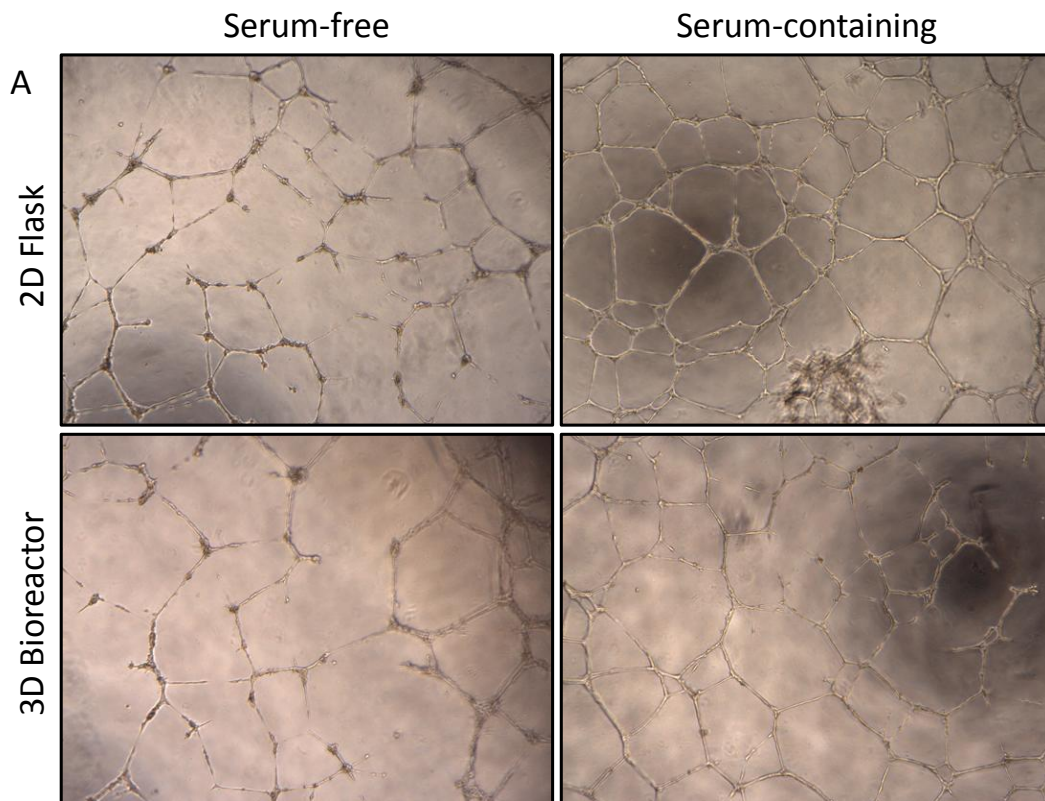
**Figure 7.3.6: Surface marker characterisation of bone marrow-derived MSCs.** (A) Quantitative marker expression of SF (orange) and SC (blue) MSCs cultured on standard 2D TC plastic. (B) Quantitative marker expression of SF and SC MSCs cultured in 3D Xuri bioreactor. Results are presented as the mean  $\pm$  standard deviation (SD) of 3 biological replicates.

### 7.3.7 Production of pro-angiogenic factors by MSCs is unaffected by culture in the Xuri bioreactor

The pro-angiogenic effect of MSC conditioned media was assessed by co-culturing of human umbilical cord vein epithelial cells (HUVECs) with conditioned medium from MSCs in SF and SC medium cultured in standard 2D TC plastic and 3D Xuri bioreactor. Details of the experimental setup are outlined in section 2.13. Briefly, to standardise collection of medium, samples were collected at time of passaging MSCs from TC plastic and the Xuri bioreactor. Conditioned media was harvested and centrifuged at 400xg for 5mins to remove any cells/debris present, and was then stored at  $-80^{\circ}\text{C}$  until use. To discriminate between the effect of the medium itself and the cells, unconditioned medium (not exposed to cells) was prepared in T-

## Chapter Seven

175 flasks in conjunction with conditioned media. Media samples were co-cultured with HUVEC cells for 18hrs and tubule numbers per well were determined. Tubules were defined as any fully formed tube joining two or more bridging points. All groups resulted in the formation of tubules. Culture on the bioreactor had no effect on either SF or SC groups. SF media groups demonstrated a significantly greater fold increase in tubule formation compared to the medium control and compared to SC media groups in both 2D and 3D cultured cells.



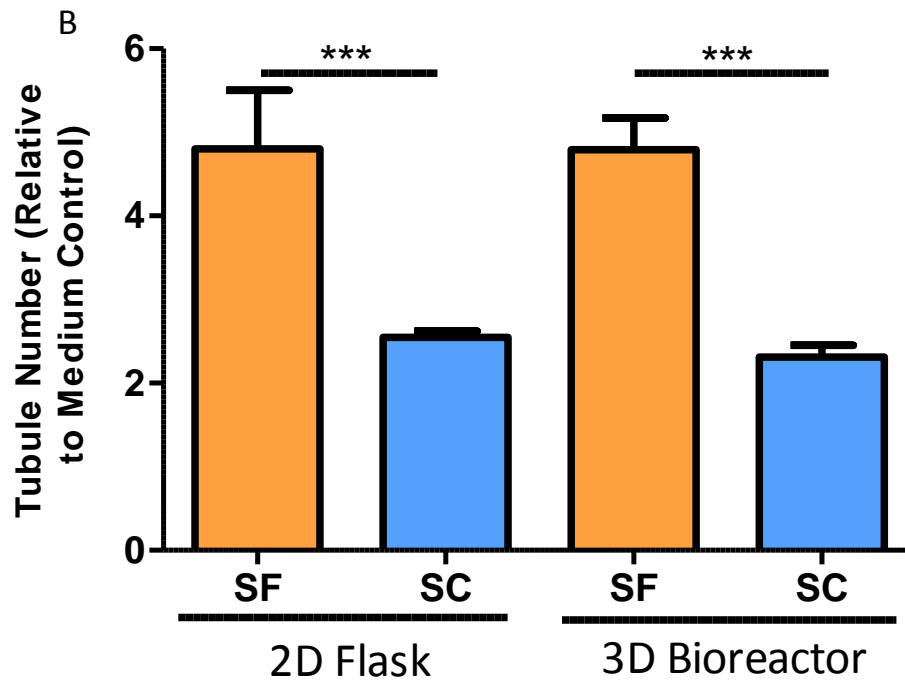


**Figure 7.3.7: Angiogenic potential of human umbilical vein epithelial cells (HUVEC) cells cultured in the presence of MSC conditioned medium from SF and SC MSCs cultured on 2D TC plastic and in 3D Xuri bioreactor. (A) Representative images of HUVEC-derived tubules 18hrs post culture in the presence of MSC conditioned media on Matrigel. (B) Quantitative analysis of tubule number formed after co-culture of SF and SC MSC conditioned medium from either 2D or 3D culture. Three biological replicates were assessed with three technical replicates. Five random fields were selected in each well and tubules identified as a complete connection of tubule between at least two bridging points. Tubule number is represented as a fold change from unconditioned basal medium appropriate to each cell group. No statistical differences were observed between MSCs cultured in either 2D or 3D systems. A statistical increase was seen in SF compared to SC groups. Results are presented as the mean  $\pm$  standard deviation (SD) of 3 biological replicates, \*\*\* $p \leq 0.001$  using two-way ANOVA and Bonferroni's multiple comparisons post-test.**

### 7.4 Discussion

With the progression of cell therapies towards large-scale clinical use, a new focus needs to be placed on technologies to ensure supply meets demand regarding cell availability. This will require not only up-scaling of systems for large-scale manufacturing but also out-scaling technologies that can deliver cell therapies from multiple centres in parallel. Indeed the long-term success of cell therapies will not only depend on efficacy during the clinical trial stage but also through demonstrating a reasonable cost-benefit ratio. For this to occur, the costly, labour intensive current practice of operators manually manufacturing cells cannot continue. Automated systems that provide reproducibility of process with a reduction in cost and labour hours are essential to achieving this. Of course, with the upscaling of any process, there are issues that arise due to changes in process. In the case of MSCs, one such issue may be changes in the phenotypic properties of the MSCs as they are translated from one process to another. The aim of this work was to determine if culturing MSCs in a small-scale 3D bioreactor model, which can ultimately be scaled up, alters the phenotype of the cells.

MSCs previously isolated and cultured in SF or SC medium were seeded into the GE Xuri Bioreactor system and cultured for 7 days for two passages. At this point, MSCs were characterised and compared to their counterparts who were maintained entirely in standard 2D culture. Comparable growth kinetics of MSCs were observed in the 3D system and 2D culture indicating the suitability of the bioreactor for the proliferation of MSCs that have previously been isolated using conventional 2D plastic adherence. What is unclear and will require future work is the assessment of the bioreactor for its ability to isolate MSCs directly from bone marrow and ultimately other tissue sources. Interestingly, differences were observed in the osteogenic and adipogenic potential of MSCs cultured in the bioreactor. MSCs were harvested from the bioreactor and standard osteogenic and adipogenic assays were set up. The idea of being able to harvest waffles directly from the bioreactor and placed directly into assays provides a means for in process assessment of a cell product. To determine if this was possible, immediately prior to disassociating MSCs from waffles, waffles were transferred from the bioreactor and placed in

differentiation medium. These assays were carried out in parallel to standard assays in 2D. A significant increase in osteogenic potential was observed in cells cultured in the bioreactor. This effect was seen in cells both cultured or cultured and differentiated on the waffles with a further increase in differentiation potential observed in cells differentiated on waffles. This suggests that the culture of MSCs on these waffles is increasing their osteogenic potential. One possible reason for this may be due to the mechanical strain exerted on the cells as they stretch to bind to the walls of the waffles. This effect is commonly reported in the literature and has been reported to increase expression of a number of pro-osteogenic genes including Runx2, TGF $\beta$  and ALP with an associated increase in matrix deposition (Qi et al., 2008, Huang et al., 2009, Luu et al., 2009, Qi et al., 2009). MSCs have previously been reported to recognise mechanical stimulation by primary cilia on the surface of MSCs (Hoey et al., 2012) which can regulate osteogenesis via regulation of the Wnt pathway (Tummala et al., 2010). Further studies would be required to investigate this further. However, a similar effect was also observed in adipogenic assays although to a lesser degree. An increase in adipogenic potential of MSCs was observed in cells differentiated on waffles. These data is in conflict with the current literature which reports a reduction of the adipogenic potential of MSCs under mechanical strain (Sen et al., 2008, Luu et al., 2009, Cristancho and Lazar, 2011). The same process that promotes osteogenesis has also been reported to inhibit adipogenesis via the Wnt canonical pathway and stabilisation of  $\beta$ -catenin (Sen et al., 2008, Luu et al., 2009, Cristancho and Lazar, 2011). This process has been reported to act as a switch in determining MSC fate by directing the cells towards either lineage. An alternative theory is that the geometric shape forced upon the cells by being cultured on the waffles may alter their differentiation potential and even paracrine factors produced by the cells (Kilian et al., 2010). This theory would also require further evaluation but no differences was observed in the angiogenesis assay when comparing MSCs cultured in either 2D or 3D culture indicating that paracrine factors produced by the cells was not altered based on their culture conditions. Similarly the surface marker phenotype of the cells was unaffected by culture in the 3D system. The SF cells continued to maintain a subpopulation of CD271 and CD146 positive cells and CD271 expression was absent

## Chapter Seven

on the SC cells. Overall these data suggest the suitability of the Xuri bioreactor system for the expansion of MSCs. Future work should be focussed on the development of a fully 3D system for the isolation and expansion of bone marrow MSCs to determine if this affects the phenotype of the cells. Understanding this will determine the suitability of such a system for large-scale manufacturing of MSCs and will facilitate making the leap from small scale 2D cell culture to large-scale 3D manufacturing of MSCs.

# **Chapter 8**

## **Discussion**

## Chapter Eight

It may well be that the future of medicine is regenerative medicine. Such a broad term that encompasses anything used to replace or regenerate human tissue which ultimately encompasses medical devices, small molecules, biomaterials and of course cell based therapies. However there are still major hurdles to be overcome with the transition of cell therapies from theoretical therapeutics to practical medicinal products. These include a number of issues such as poorly defined mechanisms of action, limitations in our understanding of basic biology and a clear route for the large scale manufacturing of cell therapies, moving from bench to bedside. These issues are more prominent with MSC-based therapies where high levels of heterogeneity in how we process (Phinney, 2012), handle and identify an MSC have resulted in many populations of cells being classed as MSCs with reported variability with efficacy limiting the progression of these cells to the clinic. Although attempts to standardise the definition of MSCs has been made (Dominici et al., 2006b), these have been insufficient and MSC populations continue to be heterogeneous in nature. Overcoming this issue requires the identification of MSC specific markers. However, this may not be possible in a population of MSCs constantly changing in response to environmental and biochemical cues. A number of markers have been identified which do appear to accurately identify the *in vivo* MSC, such as CD271 and CD146 (Jones et al., 2002, Sacchetti et al., 2007a). However, these are not MSC specific markers and the expression levels change during the *in vitro* culture of MSCs. This may not be a criticism of these markers but in fact the means in which we culture these MSCs, namely the use of poorly defined products.

Ultimately progression within the field of cell therapies will require a highly reproducible process for the manufacture of cell products to ensure efficacy and reproducibility. Currently this is not the case, with poorly understood products such as FBS still remaining the gold standard for the culture of many cell types today (Brindley et al., 2012). High variation within batches of FBS is to a degree that serum screens are often required to identify the most suitable FBS for the specific cell type. This is unacceptable for cell-based therapies, especially when therapies propose the administration of a cell type on which there is still a limited

understanding of its mechanism of action. While this limitation in MSC biology should not grind the translation to clinical use to a halt, it is important to recognise that standardisation of what can be controlled should be addressed. Therefore defining the production process should be a major focus. Moreover, once MSC therapies reach clinical use, we must ensure that adequate supply and delivery of these cells can be achieved. For these reasons, FBS is not suitable for the production of clinical MSCs as supply is not guaranteed, nor is its' safety (Brindley et al., 2012, Hodgson, 1995). This has long been realised but progression away from the use of FBS has been slow to say the least. A number of alternatives have been developed with the aim of replacing FBS and providing a safer product for the use of MSCs. These include humanised products such as human platelet lysate and autologous or allogeneic human serum (Burnouf et al., 2016). Efficacy with these has indeed been shown, however there are also limitations. The use of autologous serum may not always be possible dependent on the health status of the patient. Furthermore it limits the scale of cells that can be produced. This can be overcome with the use of pooled allogeneic serum or human platelet lysate. In the context of the allogeneic use of these human products, safety concerns relating to pooling multiple donors, each with a potential risk of disease transmission are a concern of regulators. Furthermore, the same batch variability issues still pertain to these products, although to a lesser extent, as they are not chemically defined. Thus the use of a truly xeno-free, chemically defined medium is essential for the large scale production for cellular therapy.

This thesis focussed on evaluation of a novel xeno-free, chemically defined medium for the production of MSCs. This medium formulation was assessed in comparison to the current gold standard use of FBS for culture of MSCs in chapter three. Here the ability of the medium to isolate and propagate MSCs *in vitro* was demonstrated. In addition, cells isolated in this medium formulation maintained the phenotypic characterisation of MSCs, namely tri-lineage differentiation potential and surface marker expression of MSC markers CD105, CD73 and CD90. This demonstrated the potential use of this medium as an alternative to the use of FBS. It is worth noting that, prior to this study, the FBS used was selected after serum screening multiple

## Chapter Eight

sera and identified as the most optimal FBS for use in the isolation and characterisation of MSCs. In addition to maintaining the MSC phenotype of these cells, maintenance of CD271 and CD146 on the SF MSCs above that observed in the SC MSCs indicates the potential of the SF medium to maintain a more native, truer representative of the *in vivo* MSCs *in vitro* or alternatively the absence of components of FBS that suppress the expression of these markers. The effect of oxygen tension on MSCs in culture was also determined assessing how culturing MSCs in either hypoxia or normoxia could affect their phenotype. This was done ultimately in an attempt to optimise culture conditions that would suitably prime MSCs to repair bone *in vivo*. This was inspired by the pro-angiogenic potential of MSCs observed in chapter 3 in both hypoxia and normoxia. Interestingly, what we observed was the changes in differentiation potential of MSCs in either hypoxia or normoxia, namely the pro-osteogenic phenotype of MSCs when cultured in normoxia and the pro-chondrogenic potential of MSCs cultured in hypoxia. This raised the hypothesis that MSCs cultured in either hypoxia or normoxia may repair bone via alternate mechanisms i.e. either in the form of direct bone repair by intramembranous ossification or by indirect bone repair via endochondral ossification. This was assessed in two models of bone regeneration, ectopically in the subcutaneous implantation of MSCs on BMCP+ into immunocompromised mice in chapter four and orthotopically in immunocompromised rats in chapter five.

With over 600,000 non-healing fractures in the United States alone requiring bone grafting, there is major potential for the use of MSCs in this field (Lane et al., 1999, Bucholz, 2002). While currently used biologically inert biomaterials and growth factors have shown efficacy, neither sufficiently recapitulate normal bone repair (Branemark et al., 2001). Thus we assessed the ability of SF MSCs to repair bone after being cultured in either hypoxia or normoxia. In the subcutaneous model, CD1 nude mice were implanted with MBP+ granules and  $2 \times 10^6$  MSCs and implanted for 8 weeks. Bone, cartilage and bone marrow were identified in all implants indicating bone repair. However, similar levels were also observed in the vehicle control which was not loaded with any MSCs. This indicates that the bone repair that did occur in this study was due to recruitment of endogenous MSCs to the implants and

subsequent differentiation of these cells. This indicates the efficacy of the MBCP+ granules as a means to stimulate bone repair. However this study did not accurately describe the bone forming ability of the MSCs. Subsequently the MSCs were also assessed in an immunocompromised rat femoral bone critical size defect model for 8 weeks. Here  $1 \times 10^6$  MSCs was loaded onto the same MBCP+ granules encapsulated in fibrin as reported in the mouse model in chapter four. In this model no healing of the empty defect control or the vehicle control groups was identified indicating the model as incapable of self repair. Also, distinct differences were observed between SC and SF MSCs, previously cultured in both hypoxia and normoxia. The SF MSCs cultured in normoxia reported essentially no bone repair indicated by the absence of bone or cartilage tissue. An increase in the capability of SF MSCs previously cultured in hypoxia was observed. This was observed as bridging of bone outside of the defect region with no bone present within the implant region. This would indicate that SF MSCs may be recruiting endogenous progenitors to the defect site which are repairing bone. These data is in stark contrast to the repair observed in the SC groups. The SC MSCs cultured in normoxia formed a cartilage tissue throughout a large portion of the defect region indicating the direct differentiation of these MSCs within the defect site. Furthermore it indicates these cells are capable of bone repair via endochondral ossification. Unlike their normoxic counterparts, the hypoxia-cultured SC MSCs appear to have repaired bone via intramembranous bone formation indicated by bone staining throughout the implant region and lack of cartilage. These data are in contrast to the *in vitro* phenotype of the MSCs and current literature which report an increase in chondrogenic potential of MSCs in hypoxia and increase in osteogenesis in normoxia (Sheehy et al., 2012). This would indicate that the *in vitro* differentiation potential of these cells is not representative of their *in vivo* bone repair potential. Additionally, this would indicate further development of the SF medium would be required to maintain *in vivo* osteochondral potential. Also worth exploring is the paracrine profile of the SF MSCs compared to SC MSCs in both hypoxia and normoxia. Differences here may indicate alternative models where SF MSCs may be more effective such as wound healing models where MSCs have previously shown therapeutic efficacy by recruitment of endogenous progenitors (Shin and Peterson,

2013). Similarly MSCs have been shown to stimulate endogenous cardiomyocyte progenitors to promote cardiac repair (Loffredo et al., 2011). Overall this data indicate the SF medium as being suitable for the isolation and proliferation of MSCs from bone marrow while maintaining the *in vitro* phenotype of the cell.

Although the SF medium was able to compete with SC medium *in vitro*, commercialisation of any new medium formulation would require a comparison with other commercially available SF media which was performed in chapter six. There are a number of serum-free media for MSC expansion and even isolation currently commercially available. The media selected for this study were those that were reported to be xeno-free, chemically defined and didn't require the use of FBS for any part of the isolation process. Five media were initially tested for their ability to isolate MSCs from bone marrow but two of the media failed to isolate CFU-fs. Subsequent studies focused on the Xuri medium produced by GE healthcare and Mesencult medium produced by Stemcell Technologies. These media were characterised for their ability to isolate and maintain bone marrow MSCs in both hypoxia and normoxia. Equivalent growth rates and morphology were observed in all three media. Significant differences were observed in the tri-lineage differentiation potential of MSCs in these media with both media performing better than the SF medium. The SF medium not only performed poorly in this comparison but also in terms of chondrogenic potential compared to SF MSCs expanded using the same medium in chapter 3. The only difference we identified in the preparation of these cells the lack of fibronectin-coating for selection of MSCs from bone marrow and expansion. Future work is required to explore if culturing MSCs on fibronectin maintains a population with superior differentiation potential. The commercially available media require an attachment substrate, although its specific active component is not disclosed. The SF MSCs also maintained lower levels of CD271 than previously reported in chapter 3. Again, it is unclear if this is a consequence of the lack of a fibronectin coating. The Xuri medium met the ISCT panel for surface marker expression whereas the Mesencult medium had higher levels of HLA-DR expression. This may be due to high levels of FGF-2 and/or PDGF-BB in the medium which have been reported in the literature to increase HLA-DR

expression in human MSCs (Bocelli-Tyndall et al., 2010b). This raises concerns regarding the immunogenic potential of MSCs cultured in Mesencult, although no differences were observed in T-cell assays. An improvement in the pro-angiogenic potential of SF MSCs was observed compared to the commercially available media. Together this data would indicate that the current SF formulation isolates and maintains an MSC with a pro-angiogenic potential whose differentiation potential is reduced, possibly by the lack of an attachment factor.

Whiles current data indicate that the current SF medium formulation is a chemically defined, xeno-free medium capable of competing with FBS and commercially available SF media formulations *in vitro*, the ability of the SF medium to function in a scalable process that could ultimately be used for large scale production of MSCs needed to be evaluated. In chapter seven, the SF medium was assessed in a 3D spinner flask bioreactor as a proof of concept study to assess the scalability of manufacturing MSCs in a 3D system. Here MSCs previously isolated in normoxia in either SF or SC medium were seeded at the end of passage 1 into the 3D Xuri bioreactor system for two passages. MSCs grown in the bioreactor maintained growth rates that were not statistically different over two passages. However, a reduction in proliferation was observed in the MSCs cultured in the bioreactor which may be become significant over multiple passages. This issue may be overcome by the use of fibronectin which may facilitate attachment. The culture of MSCs on macrocarriers within this system provided a unique opportunity to harvest MSCs with minimal effort at any point during the culture process by selecting individual macrocarrier 'waffles' and placing directly into assays of interest; in this instance, tri-lineage differentiation assays. What this study reported was a simpler means to perform these assays during the manufacturing process with minimal disruption to production of the cell therapy ultimately. Similarly the bioreactor maintained the pro-angiogenic phenotype of the MSCs and surface marker expression profile set out by ISCT. Overall this data indicates the suitability of the SF medium for a scalable process for the manufacture of MSCs.

Based on this work, the SF medium is currently being explored for an entirely closed, automated process from donor to patient called "Autostem" (Rafiq et al.,

## Chapter Eight

2016). Autostem aims to meet a number of the key issues outlined in this research by developing a fully automated, reproducible, GMP-compliant platform for the production of antibody selected MSCs in a chemically defined xeno-free medium in a highly reproducible system. Hopefully, this will limit some of the heterogeneity in MSC batches and ultimately will provide a vehicle for the efficient delivery of safe, regulatory compliant GMP-grade MSCs, a concept that will greatly benefit the advancement of cell therapies.

# **Appendix I**

## **Publications and Achievements**

Book Chapter;

1. The modulation of osteogenic differentiation in MSCs for “The biology and therapeutic application of mesenchymal stem cells” – In press

Patents (Filed and Ongoing);

1. European patent publication number WO2015121471 A1 – “serum-free medium” – approved 20<sup>th</sup> August 2015
2. Invention disclosure form filed – “Phrenoshell – a device for cardiothoracic surgery” – filed February 2016

Publications

1. Kilcup, N., Gaynard, S., Welner-Zwanziger, U., Tonkopi, E., Hayes, J., Boyd, D. Stimulation of apoptotic pathways in liver cancer cells: An alternative perspective on the biocompatibility and the utility of biomedical glasses. Journal of Biomaterials Applications, 2015.

Conference Papers published in Proceedings

1. Zafar H, Gaynard S, Ó Flatharta C, Doroshenkova T, Devine D, Sharif F, Barry F, Hayes J, Murphy JM, Leahy MJ. To assess the reparative ability of differentiated mesenchymal stem cells in a rat critical size bone repair defect model using high frequency co-registered photoacoustic/ultrasound imaging and micro computed tomography ", Proc. SPIE 9708, Photons Plus Ultrasound: Imaging and Sensing 2016, 970853 (March 15, 2016); doi:10.1117/12.2211382.
2. J Hayes, S Gaynard, D Devine, M Murphy. Validation of a stable bioactive Poly-(ether-ether) ketone surface for improved cell attachment. Journal of Tissue Engineering and Regenerative Medicine 8, 224-224, 2014.

3. S Gaynard, E Mooney, G Shaw, V Barron, J Hayes, F Barry, M Murphy. The effects of oxygen tension on growth kinetics and differentiation of bone marrow-derived MSCs isolated and expanded using a novel serum/xeno-free medium. *Journal of Tissue Engineering and Regenerative Medicine* 8, 115-116, 2014.

Conference Abstracts:

1. Zafar, H., Gaynard S\*, Ó Flatharta, C., Doroshenkova, T., Devine, D., Sharif, F., Barry, F., Hayes, J., Murphy, JM. Leahy, MJ. Optimisation of High Frequency Co-Registered Photoacoustic/Ultrasound Imaging &  $\mu$ -Computed Tomography Analysis of Mesenchymal Stem Cell Induced Neovascularisation *In vivo*. Microcirculation and Angiogenesis Symposium, Galway, September 2015 **(Best Poster Award)** \*Presenting
2. S. Horie, D. O'Toole, S. Gaynard, M. Murphy, F. Barry, J. G. Laffey. Enhancing the Efficacy of Mesenchymal Stromal Cell Therapy for ARDS. American Thoracic Society Conference San Francisco, May 2016. **(Poster)**
3. S Gaynard, E Mooney, G Shaw, V Barron, JS Hayes, F Barry, JM Murphy. "Effect of Hypoxia on Growth Kinetics and Differentiation of MSCs Cultured in a Novel Serum/Xeno-Free Culture System." Gordon Research Seminar, Andover, New Hampshire, August 2014. **(Poster)**
4. S Gaynard, E Mooney, G Shaw, V Barron, JS Hayes, F Barry, JM Murphy. "Development & *In vitro* Characterisation of A Novel Serum/Xeno-Free Culture system for human bone Marrow-Derived MSCs." Gordon Research Conference, Andover, New Hampshire, August 2014. **(Oral)**
5. S Gaynard, E Mooney, G Shaw, V Barron, T Doroshenkova, JS Hayes, F Barry, JM Murphy. "Development of a Serum/Xeno-free Culture System for

## Appendix I

Manufacture of Bone Marrow Derived Mesenchymal Stem Cells” Matrix  
Biology Ireland, Galway, Ireland **(Best Poster Award)**

6. S Gaynard, JS Hayes, T Doroshenkova, E Mooney, G Shaw, V Barron, F Barry, JM Murphy. “A Novel Serum/Xeno-free Medium for Manufacturing of Human Bone Marrow Derived MSCs” Stem Cell conference 2014, Galway Ireland. **(Oral)**
7. Gaynard SG, Mooney E, Shaw G, Barron V, Hayes JS, Barry F, Murphy M. Oxygen Tension Regulates Mesenchymal Phenotype in Novel Serum/Xeno-Free Culture Medium. NUI Galway College of Medicine, nursing & Health Sciences Postgraduate research Day, June 2014. **(Poster)**
8. S Gaynard, E Mooney, G Shaw, V Barron, JS Hayes, F Barry, JM Murphy, Oxygen Tension Regulates Mesenchymal Phenotype in Novel Serum/Xeno-Free Culture Medium. College of Medicine, Nursing & Health Sciences Postgraduate Research Day, NUI Galway, 2014 **(Poster)**
9. S Gaynard, E Mooney, G Shaw, V Barron, JS Hayes, F Barry, JM Murphy, Characterisation of a novel, clinically compliant, serum-free culture system for bone marrow derived mesenchymal stem cells, eCM XIV: Stem & Progenitor Cells for Musculoskeletal Regeneration, Davos, Switzerland, June 2013. **(Oral)**
10. S Gaynard, E Mooney, G Shaw, V Barron, JS Hayes, F Barry, JM Murphy, Characterisation of a novel, clinically compliant, serum-free culture system for bone marrow derived mesenchymal stem cells, BMERM Annual Research Meeting, September 2013. **(Oral)**.

# **Appendix II**

## **Permissions**

## Appendix II

### ELSEVIER LICENSE TERMS AND CONDITIONS

Aug 29, 2016

---

This Agreement between Sean Gaynard ("You") and Elsevier ("Elsevier") consists of your license details and the terms and conditions provided by Elsevier and Copyright Clearance Center.

License Number	3938131076433
License date	Aug 29, 2016
Licensed Content Publisher	Elsevier
Licensed Content Publication	Journal of Controlled Release
Licensed Content Title	Cell delivery and tissue regeneration
Licensed Content Author	Arnold I. Caplan
Licensed Content Date	January 1990
Licensed Content Volume Number	11
Licensed Content Issue Number	1-3
Licensed Content Pages	9
Start Page	157
End Page	165
Type of Use	reuse in a thesis/dissertation
Portion	figures/tables/illustrations
Number of figures/tables/illustrations	1
Format	both print and electronic
Are you the author of this Elsevier article?	No
Will you be translating?	No
Order reference number	
Original figure numbers	Mesengensis figure
Title of your thesis/dissertation	In Vitro, Pre-Clinical & Commercial Evaluation of a Novel Xeno & Serum-free Culture System for the Production of Human Bone Marrow Derived Mesenchymal Stem Cells for Bone Regeneration
Expected completion date	Sep 2016
Estimated size (number of pages)	300
Elsevier VAT number	GB 494 6272 12
Requestor Location	Sean Gaynard REMEDI, Bioscience building National University of Ireland, Galway  Galway, G00 Ireland Attn: Sean Gaynard

## Appendix II

### ELSEVIER LICENSE TERMS AND CONDITIONS

Aug 29, 2016

---

This Agreement between Sean Gaynard ("You") and Elsevier ("Elsevier") consists of your license details and the terms and conditions provided by Elsevier and Copyright Clearance Center.

License Number	3938140314032
License date	Aug 29, 2016
Licensed Content Publisher	Elsevier
Licensed Content Publication	Biomaterials
Licensed Content Title	Human platelet lysate: Replacing fetal bovine serum as a gold standard for human cell propagation?
Licensed Content Author	Thierry Burnouf,Dirk Strunk,Mickey B.C. Koh,Katharina Schallmoser
Licensed Content Date	January 2016
Licensed Content Volume Number	76
Licensed Content Issue Number	n/a
Licensed Content Pages	17
Start Page	371
End Page	387
Type of Use	reuse in a thesis/dissertation
Intended publisher of new work	other
Portion	figures/tables/illustrations
Number of figures/tables/illustrations	1
Format	both print and electronic
Are you the author of this Elsevier article?	No
Will you be translating?	No
Order reference number	
Original figure numbers	figure 1
Title of your thesis/dissertation	In Vitro, Pre-Clinical & Commercial Evaluation of a Novel Xeno & Serum-free Culture System for the Production of Human Bone Marrow Derived Mesenchymal Stem Cells for Bone Regeneration
Expected completion date	Sep 2016
Estimated size (number of pages)	300
Elsevier VAT number	GB 494 6272 12
Requestor Location	Sean Gaynard REMEDI, Bioscience building National University of Ireland, Galway

## Appendix II

### JOHN WILEY AND SONS LICENSE TERMS AND CONDITIONS

Aug 29, 2016

This Agreement between Sean Gaynard ("You") and John Wiley and Sons ("John Wiley and Sons") consists of your license details and the terms and conditions provided by John Wiley and Sons and Copyright Clearance Center.

License Number	3938150697036
License date	Aug 29, 2016
Licensed Content Publisher	John Wiley and Sons
Licensed Content Publication	Stem Cells
Licensed Content Title	Mesenchymal Stem Cells Transmigrate Between and Directly Through Tumor Necrosis Factor- $\alpha$ -Activated Endothelial Cells Via Both Leukocyte-Like and Novel Mechanisms
Licensed Content Author	Grace S. L. Teo,James A. Ankrum,Roberta Martinelli,Sarah E. Boetto,Kayla Simms,Tracey E. Sciuto,Ann M. Dvorak,Jeffrey M. Karp,Christopher V. Carman
Licensed Content Date	Oct 22, 2012
Licensed Content Pages	15
Type of use	Dissertation/Thesis
Requestor type	University/Academic
Format	Print and electronic
Portion	Figure/table
Number of figures/tables	1
Original Wiley figure/table number(s)	figure 6
Will you be translating?	No
Title of your thesis / dissertation	In Vitro, Pre-Clinical & Commercial Evaluation of a Novel Xeno & Serum-free Culture System for the Production of Human Bone Marrow Derived Mesenchymal Stem Cells for Bone Regeneration
Expected completion date	Sep 2016
Expected size (number of pages)	300
Requestor Location	Sean Gaynard REMEDI, Bioscience building National University of Ireland, Galway  Galway, G00 Ireland Attn: Sean Gaynard
Publisher Tax ID	EU826007151
Billing Type	Invoice
Billing Address	Sean Gaynard REMEDI, Bioscience building National University of Ireland, Galway

## Appendix II

### ELSEVIER LICENSE TERMS AND CONDITIONS

Sep 03, 2016

This Agreement between Sean Gaynard ("You") and Elsevier ("Elsevier") consists of your license details and the terms and conditions provided by Elsevier and Copyright Clearance Center.

License Number	3941420717622
License date	Sep 03, 2016
Licensed Content Publisher	Elsevier
Licensed Content Publication	Toxicology in Vitro
Licensed Content Title	Optimization of chemically defined cell culture media – Replacing fetal bovine serum in mammalian in vitro methods
Licensed Content Author	J. van der Valk,D. Brunner,K. De Smet,Å. Fex Svenningsen,P. Honegger,L.E. Knudsen,T. Lindl,J. Noraberg,A. Price,M.L. Scarino,G. Gstraunthaler
Licensed Content Date	June 2010
Licensed Content Volume Number	24
Licensed Content Issue Number	4
Licensed Content Pages	11
Start Page	1053
End Page	1063
Type of Use	reuse in a thesis/dissertation
Portion	figures/tables/illustrations
Number of figures/tables/illustrations	1
Format	both print and electronic
Are you the author of this Elsevier article?	No
Will you be translating?	No
Order reference number	
Original figure numbers	1. hierarchial
Title of your thesis/dissertation	In Vitro, Pre-Clinical & Commercial Evaluation of a Novel Xeno & Serum-free Culture System for the Production of Human Bone Marrow Derived Mesenchymal Stem Cells for Bone Regeneration
Expected completion date	Sep 2016
Estimated size (number of pages)	300
Elsevier VAT number	GB 494 6272 12
Requestor Location	Sean Gaynard REMEDI, Bioscience building National University of Ireland, Galway  Galway, G00 Ireland Attn: Sean Gaynard
Total	0.00 EUR
Terms and Conditions	



# **Appendix III**

# **Bibliography**

## Links

1. [HTTP://WWW.EMA.EUROPA.EU/DOCS/EN\\_GB/DOCUMENT\\_LIBRARY/SCIENTIFIC\\_GUIDELINE/2013/06/WC500143930.PDF](http://www.ema.europa.eu/docs/en_GB/document_library/scientific_guideline/2013/06/wc500143930.pdf)
2. [HTTPS://WWW.LAW.CORNELL.EDU/CFR/TEXT/9/PART-53](https://www.law.cornell.edu/cfr/text/9/part-53)
3. [HTTP://EUR-LEX.EUROPA.EU/LEXURISERV/LEXURISERV.DO?URI=OJ:L:2013:098:0001:0057:EN:PDF](http://eur-lex.europa.eu/lexuriserv/lexuriserv.do?uri=OJ:L:2013:098:0001:0057:EN:PDF)

## References

- ABAD, M., MOSTEIRO, L., PANTOJA, C., CANAMERO, M., RAYON, T., ORS, I., GRANA, O., MEGIAS, D., DOMINGUEZ, O., MARTINEZ, D., MANZANARES, M., ORTEGA, S. & SERRANO, M. 2013. Reprogramming in vivo produces teratomas and iPS cells with totipotency features. *Nature*, 502, 340-5.
- ABBOTT, J. D., HUANG, Y., LIU, D., HICKEY, R., KRAUSE, D. S. & GIORDANO, F. J. 2004. Stromal cell-derived factor-1alpha plays a critical role in stem cell recruitment to the heart after myocardial infarction but is not sufficient to induce homing in the absence of injury. *Circulation*, 110, 3300-5.
- ABDELRAZIK, H., SPAGGIARI, G. M., CHIOSSONE, L. & MORETTA, L. 2011. Mesenchymal stem cells expanded in human platelet lysate display a decreased inhibitory capacity on T- and NK-cell proliferation and function. *Eur J Immunol*, 41, 3281-90.
- ADESIDA, A. B., MULET-SIERRA, A. & JOMHA, N. M. 2012. Hypoxia mediated isolation and expansion enhances the chondrogenic capacity of bone marrow mesenchymal stromal cells. *Stem Cell Research & Therapy*, 3, 1-13.
- AGATA, H., ASAHINA, I., WATANABE, N., ISHII, Y., KUBO, N., OHSHIMA, S., YAMAZAKI, M., TOJO, A. & KAGAMI, H. 2010. Characteristic change and loss of in vivo osteogenic abilities of human bone marrow stromal cells during passage. *Tissue Eng Part A*, 16, 663-73.
- AGATA, H., WATANABE, N., ISHII, Y., KUBO, N., OHSHIMA, S., YAMAZAKI, M., TOJO, A. & KAGAMI, H. 2009. Feasibility and efficacy of bone tissue engineering using human bone marrow stromal cells cultivated in serum-free conditions. *Biochemical and Biophysical Research Communications*, 382, 353-358.
- AGGARWAL, S. & PITTENGER, M. F. 2005. Human mesenchymal stem cells modulate allogeneic immune cell responses. *Blood*, 105, 1815-22.
- AI-AQL, Z. S., ALAGL, A. S., GRAVES, D. T., GERSTENFELD, L. C. & EINHORN, T. A. 2008. Molecular mechanisms controlling bone formation during fracture healing and distraction osteogenesis. *Journal of Dental Research*, 87, 107-118.
- AL-SAQI, S. H., SALIEM, M., QUEZADA, H. C., EKBLAD, A., JONASSON, A. F., HOVATTA, O. & GOTHERSTROM, C. 2015. Defined serum- and xeno-

- free cryopreservation of mesenchymal stem cells. *Cell Tissue Bank*, 16, 181-93.
- ALON, R., KASSNER, P. D., CARR, M. W., FINGER, E. B., HEMLER, M. E. & SPRINGER, T. A. 1995. The integrin VLA-4 supports tethering and rolling in flow on VCAM-1. *J Cell Biol*, 128, 1243-53.
- AMINI, A. R., LAURENCIN, C. T. & NUKAVARAPU, S. P. 2012. Bone tissue engineering: recent advances and challenges. *Crit Rev Biomed Eng*, 40, 363-408.
- ARINZEH, T. L., TRAN, T., MCALARY, J. & DACULSI, G. 2005. A comparative study of biphasic calcium phosphate ceramics for human mesenchymal stem-cell-induced bone formation. *Biomaterials*, 26, 3631-3638.
- ARUFE, M. C., DE LA FUENTE, A., FUENTES, I., DE TORO, F. J. & BLANCO, F. J. 2010. Chondrogenic potential of subpopulations of cells expressing mesenchymal stem cell markers derived from human synovial membranes. *Journal of Cellular Biochemistry*, 111, 834-45.
- AZIZ, M. T. A., ATTA, H. M., MAHFOUZ, S., FOUAD, H. H., ROSHDY, N. K., AHMED, H. H., RASHED, L. A., SABRY, D., HASSOUNA, A. A. & HASAN, N. M. 2007. Therapeutic potential of bone marrow-derived mesenchymal stem cells on experimental liver fibrosis. *Clinical Biochemistry*, 40, 893-899.
- BAILLY-MAITRE, B., DE SOUSA, G., BOULUKOS, K., GUGENHEIM, J. & RAHMANI, R. 2001. Dexamethasone inhibits spontaneous apoptosis in primary cultures of human and rat hepatocytes via Bcl-2 and Bcl-xL induction. *Cell Death Differ*, 8, 279-88.
- BAJADA, S., MAZAKOVA, I., RICHARDSON, J. B. & ASHAMMAKHI, N. 2008. Updates on stem cells and their applications in regenerative medicine. *J Tissue Eng Regen Med*, 2, 169-83.
- BANG, O. Y., LEE, J. S., LEE, P. H. & LEE, G. 2005. Autologous mesenchymal stem cell transplantation in stroke patients. *Annals of Neurology*, 57, 874-882.
- BARDY, J., CHEN, A. K., LIM, Y. M., WU, S., WEI, S., WEIPING, H., CHAN, K., REUVENY, S. & OH, S. K. 2013. Microcarrier suspension cultures for high-density expansion and differentiation of human pluripotent stem cells to neural progenitor cells. *Tissue Eng Part C Methods*, 19, 166-80.
- BARNES, D. & SATO, G. 1980. Serum-free cell culture: a unifying approach. *Cell*, 22, 649-55.
- BARRADAS, A. M. C., YUAN, H. P., VAN BLITTERSWIJK, C. A. & HABIBOVIC, P. 2011. Osteoinductive Biomaterials: Current Knowledge of Properties, Experimental Models and Biological Mechanisms. *European Cells & Materials*, 21, 407-429.
- BARRY, F. & MURPHY, M. 2013. Mesenchymal stem cells in joint disease and repair. *Nat Rev Rheumatol*, 9, 584-594.
- BARRY, F. P., MOONEY, E. J., MURPHY, J. M., SHAW, G. M. & GAYNARD, S. P. 2015. Serum-free medium. Google Patents.
- BARTHOLOMEW, A., STURGEON, C., SIATSKAS, M., FERRER, K., MCINTOSH, K., PATIL, S., HARDY, W., DEVINE, S., UCKER, D., DEANS, R., MOSELEY, A. & HOFFMAN, R. 2002. Mesenchymal stem cells suppress lymphocyte proliferation in vitro and prolong skin graft survival in vivo. *Experimental Hematology*, 30, 42-48.

- BAXTER, M. A., WYNN, R. F., JOWITT, S. N., WRAITH, J. E., FAIRBAIRN, L. J. & BELLANTUONO, I. 2004. Study of Telomere Length Reveals Rapid Aging of Human Marrow Stromal Cells following In Vitro Expansion. *Stem Cells*, 22, 675-682.
- BEGGS, K. J., LYUBIMOV, A., BORNEMAN, J. N., BARTHOLOMEW, A., MOSELEY, A., DODDS, R., ARCHAMBAULT, M. P., SMITH, A. K. & MCINTOSH, K. R. 2006. Immunologic consequences of multiple, high-dose administration of allogeneic mesenchymal stem cells to baboons. *Cell Transplantation*, 15, 711-721.
- BENSIDHOUM, M., CHAPEL, A., FRANCOIS, S., DEMARQUAY, C., MAZURIER, C., FOUILLARD, L., BOUCHET, S., BERTHO, J. M., GOURMELON, P., AIGUEPERSE, J., CHARBORD, P., GORIN, N. C., THIERRY, D. & LOPEZ, M. 2004. Homing of in vitro expanded Stro-1- or Stro-1+ human mesenchymal stem cells into the NOD/SCID mouse and their role in supporting human CD34 cell engraftment. *Blood*, 103, 3313-9.
- BEYTH, S., BOROVSKY, Z., MEVORACH, D., LIEBERGALL, M., GAZIT, Z., ASLAN, H., GALUN, E. & RACHMILEWITZ, J. 2005. Human mesenchymal stem cells alter antigen-presenting cell maturation and induce T-cell unresponsiveness. *Blood*, 105, 2214-9.
- BIANCO, P., ROBEY, P. G. & SIMMONS, P. J. 2008. Mesenchymal stem cells: revisiting history, concepts, and assays. *Cell Stem Cell*, 2, 313-9.
- BIEBACK, K. 2013. Platelet lysate as replacement for fetal bovine serum in mesenchymal stromal cell cultures. *Transfus Med Hemother*, 40, 326-35.
- BIEBACK, K., HECKER, A., SCHLECHTER, T., HOFMANN, I., BROUSOS, N., REDMER, T., BESSER, D., KLUTER, H., MULLER, A. M. & BECKER, M. 2012. Replicative aging and differentiation potential of human adipose tissue-derived mesenchymal stromal cells expanded in pooled human or fetal bovine serum. *Cytotherapy*, 14, 570-83.
- BIEBACK, K., KERN, S., KLUTER, H. & EICHLER, H. 2004. Critical parameters for the isolation of mesenchymal stem cells from umbilical cord blood. *Stem Cells*, 22, 625-34.
- BJARE, U. 1992. Serum-free cell culture. *Pharmacol Ther*, 53, 355-74.
- BOBIS-WOZOWICZ, S., MIEKUS, K., WYBIERALSKA, E., JAROCHA, D., ZAWISZ, A., MADEJA, Z. & MAJKA, M. 2011. Genetically modified adipose tissue-derived mesenchymal stem cells overexpressing CXCR4 display increased motility, invasiveness, and homing to bone marrow of NOD/SCID mice. *Experimental Hematology*, 39, 686-696.e4.
- BOCELLI-TYNDALL, C., ZAJAC, P., DI MAGGIO, N., TRELLA, E., BENVENUTO, F., IEZZI, G., SCHERBERICH, A., BARBERO, A., SCHAEREN, S., PISTOIA, V., SPAGNOLI, G., VUKCEVIC, M., MARTIN, I. & TYNDALL, A. 2010a. Fibroblast growth factor 2 and platelet-derived growth factor, but not platelet lysate, induce proliferation-dependent, functional class II major histocompatibility complex antigen in human mesenchymal stem cells. *Arthritis & Rheumatism*, 62, 3815-3825.
- BOCELLI-TYNDALL, C., ZAJAC, P., DI MAGGIO, N., TRELLA, E., BENVENUTO, F., IEZZI, G., SCHERBERICH, A., BARBERO, A., SCHAEREN, S., PISTOIA, V., SPAGNOLI, G., VUKCEVIC, M., MARTIN, I. & TYNDALL, A. 2010b. Fibroblast growth factor 2 and platelet-derived growth factor, but not platelet lysate, induce proliferation-

- dependent, functional class II major histocompatibility complex antigen in human mesenchymal stem cells. *Arthritis Rheum*, 62, 3815-25.
- BONAB, M. M., ALIMOGHADDAM, K., TALEBIAN, F., GHAFFARI, S. H., GHAVAMZADEH, A. & NIKBIN, B. 2006. Aging of mesenchymal stem cell in vitro. *BMC Cell Biol*, 7, 14.
- BOSCH, P., MUSGRAVE, D. S., LEE, J. Y., CUMMINS, J., SHULER, F., GHIVIZZANI, S. C., EVANS, C., ROBBINS, P. D. & HUARD, J. 2000. Osteoprogenitor cells within skeletal muscle. *Journal of Orthopaedic Research*, 18, 933-944.
- BOXALL, S. A. & JONES, E. 2012. Markers for characterization of bone marrow multipotential stromal cells. *Stem Cells Int*, 2012, 975871.
- BRACCINI, A., WENDT, D., JAQUIERY, C., JAKOB, M., HEBERER, M., KENINS, L., WODNAR-FILIPOWICZ, A., QUARTO, R. & MARTIN, I. 2005. Three-Dimensional Perfusion Culture of Human Bone Marrow Cells and Generation of Osteoinductive Grafts. *Stem Cells*, 23, 1066-1072.
- BRAGDON, B., BONOR, J., SHULTZ, K. L., BEAMER, W. G., ROSEN, C. J. & NOHE, A. 2012. Bone morphogenetic protein receptor type Ia localization causes increased BMP2 signaling in mice exhibiting increased peak bone mass phenotype. *Journal of Cellular Physiology*, 227, 2870-2879.
- BRANEMARK, R., BRANEMARK, P. I., RYDEVIK, B. & MYERS, R. R. 2001. Osseointegration in skeletal reconstruction and rehabilitation: A review. *Journal of Rehabilitation Research and Development*, 38, 175-181.
- BRINDLEY, D. A., DAVIE, N. L., CULME-SEYMOUR, E. J., MASON, C., SMITH, D. W. & ROWLEY, J. A. 2012. Peak serum: implications of serum supply for cell therapy manufacturing. *Regen Med*, 7, 7-13.
- BUCHOLZ, R. W. 2002. Nonallograft osteoconductive bone graft substitutes. *Clin Orthop Relat Res*, 44-52.
- BUJAN, J., PASCUAL, G., CORRALES, C., GOMEZ-GIL, V., GARCIA-HONDUVILLA, N. & BELLON, J. M. 2006. Muscle-derived stem cells used to treat skin defects prevent wound contraction and expedite reepithelialization. *Wound Repair Regen*, 14, 216-23.
- BURA, A., PLANAT-BENARD, V., BOURIN, P., SILVESTRE, J.-S., GROSS, F., GROLLEAU, J.-L., SAINT-LEBESE, B., PEYRAFITTE, J.-A., FLEURY, S., GADELORGE, M., TAURAND, M., DUPUIS-CORONAS, S., LEOBON, B. & CASTEILLA, L. 2014. Phase I trial: the use of autologous cultured adipose-derived stroma/stem cells to treat patients with non-revascularizable critical limb ischemia. *Cytotherapy*, 16, 245-257.
- BURGE, R., DAWSON-HUGHES, B., SOLOMON, D. H., WONG, J. B., KING, A. & TOSTESON, A. 2007. Incidence and economic burden of osteoporosis-related fractures in the United States, 2005-2025. *J Bone Miner Res*, 22, 465-75.
- BURNOUF, T., STRUNK, D., KOH, M. B. C. & SCHALLMOSER, K. 2016. Human platelet lysate: Replacing fetal bovine serum as a gold standard for human cell propagation? *Biomaterials*, 76, 371-387.
- CABRAL, J. M. S. 2001. Ex vivo expansion of hematopoietic stem cells in bioreactors. *Biotechnology Letters*, 23, 741-751.
- CAI, S., CHAN, Y. S. & SHUM, D. K. 2014. Induced pluripotent stem cells and neurological disease models. *Sheng Li Xue Bao*, 66, 55-66.
- CALORI, G. M., TAGLIABUE, L., GALA, L., D'IMPORZANO, M., PERETTI, G. & ALBISETTI, W. 2008. Application of rhBMP-7 and platelet-rich plasma

- in the treatment of long bone non-unions: A prospective randomised clinical study on 120 patients. *Injury*, 39, 1391-1402.
- CAPLAN, A. I. 1990. Cell delivery and tissue regeneration. *Journal of Controlled Release*, 11, 157-165.
- CHANG, H. & KNOTHE TATE, M. L. 2012. Concise Review: The Periosteum: Tapping into a Reservoir of Clinically Useful Progenitor Cells. *Stem Cells Translational Medicine*, 1, 480-491.
- CHEN, B., SUN, H. H., WANG, H. G., KONG, H., CHEN, F. M. & YU, Q. 2012a. The effects of human platelet lysate on dental pulp stem cells derived from impacted human third molars. *Biomaterials*, 33, 5023-35.
- CHEN, G., DENG, C. & LI, Y. P. 2012b. TGF-beta and BMP signaling in osteoblast differentiation and bone formation. *Int J Biol Sci*, 8, 272-88.
- CHEN, Y., XIANG, L. X., SHAO, J. Z., PAN, R. L., WANG, Y. X., DONG, X. J. & ZHANG, G. R. 2010. Recruitment of endogenous bone marrow mesenchymal stem cells towards injured liver. *J Cell Mol Med*, 14, 1494-508.
- CHEN, Z. Y., WU, H. Z., ZHU, P. & FENG, X. B. 2015. Postoperative Changes in Hemoglobin and Hematocrit in Patients Undergoing Primary Total Hip and Knee Arthroplasty. *Chin Med J (Engl)*, 128, 1977-9.
- CHENG, H., JIANG, W., PHILLIPS, F. M., HAYDON, R. C., PENG, Y., ZHOU, L., LUU, H. H., AN, N., BREYER, B., VANICHAKARN, P., SZATKOWSKI, J. P., PARK, J. Y. & HE, T. C. 2003. Osteogenic activity of the fourteen types of human bone morphogenetic proteins (BMPs). *J Bone Joint Surg Am*, 85-A, 1544-52.
- CHENG, Z., OU, L., ZHOU, X., LI, F., JIA, X., ZHANG, Y., LIU, X., LI, Y., WARD, C. A., MELO, L. G. & KONG, D. 2008. Targeted Migration of Mesenchymal Stem Cells Modified With CXCR4 Gene to Infarcted Myocardium Improves Cardiac Performance. *Mol Ther*, 16, 571-579.
- CHERRY, R. S. & PAPOUTSAKIS, E. T. 1988. Physical-Mechanisms of Cell-Damage in Microcarrier Cell-Culture Bioreactors. *Biotechnology and Bioengineering*, 32, 1001-1014.
- CHO, T. J., GERSTENFELD, L. C. & EINHORN, T. A. 2002. Differential temporal expression of members of the transforming growth factor beta superfamily during murine fracture healing. *J Bone Miner Res*, 17, 513-20.
- CHUNG, H. M., WON, C. H. & SUNG, J. H. 2009. Responses of adipose-derived stem cells during hypoxia: enhanced skin-regenerative potential. *Expert Opin Biol Ther*, 9, 1499-508.
- CHURCHMAN, S. M., PONCHEL, F., BOXALL, S. A., CUTHBERT, R., KOUROUPIS, D., ROSHDY, T., GIANNOUDIS, P. V., EMERY, P., MCGONAGLE, D. & JONES, E. A. 2012. Transcriptional profile of native CD271+ multipotential stromal cells: evidence for multiple fates, with prominent osteogenic and Wnt pathway signaling activity. *Arthritis Rheum*, 64, 2632-43.
- COHEN, M. M., JR. 2000. Merging the old skeletal biology with the new. I. Intramembranous ossification, endochondral ossification, ectopic bone, secondary cartilage, and pathologic considerations. *J Craniofac Genet Dev Biol*, 20, 84-93.
- COLTER, D. C., SEKIYA, I. & PROCKOP, D. J. 2001. Identification of a subpopulation of rapidly self-renewing and multipotential adult stem cells in

- colonies of human marrow stromal cells. *Proc Natl Acad Sci U S A*, 98, 7841-5.
- CONNELLY, J. T., GARCIA, A. J. & LEVENSTON, M. E. 2007. Inhibition of in vitro chondrogenesis in RGD-modified three-dimensional alginate gels. *Biomaterials*, 28, 1071-83.
- CONNELLY, J. T., PETRIE, T. A., GARCIA, A. J. & LEVENSTON, M. E. 2011. Fibronectin- and collagen-mimetic ligands regulate bone marrow stromal cell chondrogenesis in three-dimensional hydrogels. *Eur Cell Mater*, 22, 168-76; discussion 176-7.
- COX, G., BOXALL, S. A., GIANNOUDIS, P. V., BUCKLEY, C. T., ROSHDY, T., CHURCHMAN, S. M., MCGONAGLE, D. & JONES, E. 2012. High abundance of CD271(+) multipotential stromal cells (MSCs) in intramedullary cavities of long bones. *Bone*, 50, 510-7.
- CRAPNELL, K., BLAESIUS, R., HASTINGS, A., LENNON, D. P., CAPLAN, A. I. & BRUDER, S. P. 2013. Growth, differentiation capacity, and function of mesenchymal stem cells expanded in serum-free medium developed via combinatorial screening. *Exp Cell Res*, 319, 1409-18.
- CRESPO-DIAZ, R., BEHFAR, A., BUTLER, G. W., PADLEY, D. J., SARR, M. G., BARTUNEK, J., DIETZ, A. B. & TERZIC, A. 2011. Platelet lysate consisting of a natural repair proteome supports human mesenchymal stem cell proliferation and chromosomal stability. *Cell Transplant*, 20, 797-811.
- CRISAN, M., YAP, S., CASTEILLA, L., CHEN, C. W., CORSELLI, M., PARK, T. S., ANDRIOLO, G., SUN, B., ZHENG, B., ZHANG, L., NOROTTE, C., TENG, P. N., TRAAS, J., SCHUGAR, R., DEASY, B. M., BADYLAK, S., BUHRING, H. J., GIACOBINO, J. P., LAZZARI, L., HUARD, J. & PEAULT, B. 2008. A perivascular origin for mesenchymal stem cells in multiple human organs. *Cell Stem Cell*, 3, 301-13.
- CRISTANCHO, A. G. & LAZAR, M. A. 2011. Forming functional fat: a growing understanding of adipocyte differentiation. *Nat Rev Mol Cell Biol*, 12, 722-34.
- CUNHA, B., AGUIAR, T., SILVA, M. M., SILVA, R. J. S., SOUSA, M. F. Q., PINEDA, E., PEIXOTO, C., CARRONDO, M. J. T., SERRA, M. & ALVES, P. M. 2015. Exploring continuous and integrated strategies for the up- and downstream processing of human mesenchymal stem cells. *Journal of Biotechnology*, 213, 97-108.
- CUTHBERT, R., BOXALL, S. A., TAN, H. B., GIANNOUDIS, P. V., MCGONAGLE, D. & JONES, E. 2012. Single-platform quality control assay to quantify multipotential stromal cells in bone marrow aspirates prior to bulk manufacture or direct therapeutic use. *Cytotherapy*, 14, 431-40.
- CUTHBERT, R. J., GIANNOUDIS, P. V., WANG, X. N., NICHOLSON, L., PAWSON, D., LUBENKO, A., TAN, H. B., DICKINSON, A., MCGONAGLE, D. & JONES, E. 2015. Examining the feasibility of clinical grade CD271+ enrichment of mesenchymal stromal cells for bone regeneration. *PLoS One*, 10, e0117855.
- CZEKANSKA, E. M., STODDART, M. J., RICHARDS, R. G. & HAYES, J. S. 2012. In Search of an Osteoblast Cell Model for in Vitro Research. *European Cells & Materials*, 24, 1-17.
- DA SILVA MEIRELLES, L., CAPLAN, A. I. & NARDI, N. B. 2008. In search of the in vivo identity of mesenchymal stem cells. *Stem Cells*, 26, 2287-99.

- DAHABREH, Z., DIMITRIOU, R. & GIANNOUDIS, P. V. 2007. Health economics: A cost analysis of treatment of persistent fracture non-unions using bone morphogenetic protein-7. *Injury-International Journal of the Care of the Injured*, 38, 371-377.
- DAI, W., HALE, S. L., MARTIN, B. J., KUANG, J.-Q., DOW, J. S., WOLD, L. E. & KLONER, R. A. 2005. Allogeneic Mesenchymal Stem Cell Transplantation in Postinfarcted Rat Myocardium: Short- and Long-Term Effects. *Circulation*, 112, 214-223.
- DE BARI, C., DELL'ACCIO, F. & LUYTEN, F. P. 2001a. Human periosteum-derived cells maintain phenotypic stability and chondrogenic potential throughout expansion regardless of donor age. *Arthritis Rheum*, 44, 85-95.
- DE BARI, C., DELL'ACCIO, F., TYLZANOWSKI, P. & LUYTEN, F. P. 2001b. Multipotent mesenchymal stem cells from adult human synovial membrane. *Arthritis Rheum*, 44, 1928-42.
- DE UGARTE, D. A., ALFONSO, Z., ZUK, P. A., ELBARBARY, A., ZHU, M., ASHJIAN, P., BENHAIM, P., HEDRICK, M. H. & FRASER, J. K. 2003. Differential expression of stem cell mobilization-associated molecules on multi-lineage cells from adipose tissue and bone marrow. *Immunol Lett*, 89, 267-70.
- DENNIS, J. E., KONSTANTAKOS, E. K., ARM, D. & CAPLAN, A. I. 1998. In vivo osteogenesis assay: a rapid method for quantitative analysis. *Biomaterials*, 19, 1323-8.
- DESAI, S. S., DUNCAN, B. S. & SLOAN, A. S. 2003. The cost of treating osteoporosis in a managed health care organization. *J Manag Care Pharm*, 9, 142-9.
- DEVINE, S. M., PETER, S., MARTIN, B. J., BARRY, F. & MCINTOSH, K. R. 2001. Mesenchymal stem cells: stealth and suppression. *Cancer J*, 7 Suppl 2, S76-82.
- DIMARAKIS, I. & LEVICAR, N. 2006. Cell culture medium composition and translational adult bone marrow-derived stem cell research. *Stem Cells*, 24, 1407-8.
- DIMITRIOU, R., JONES, E., MCGONAGLE, D. & GIANNOUDIS, P. V. 2011. Bone regeneration: current concepts and future directions. *BMC Med*, 9, 66.
- DJOUAD, F., BONY, C., HAUPL, T., UZE, G., LAHLOU, N., LOUIS-PLENCE, P., APPARAILLY, F., CANOVAS, F., REME, T., SANY, J., JORGENSEN, C. & NOEL, D. 2005. Transcriptional profiles discriminate bone marrow-derived and synovium-derived mesenchymal stem cells. *Arthritis Res Ther*, 7, R1304-15.
- DOMINICI, M., LE BLANC, K., MUELLER, I., SLAPER-CORTENBACH, I., MARINI, F., KRAUSE, D., DEANS, R., KEATING, A., PROCKOP, D. & HORWITZ, E. 2006a. Minimal criteria for defining multipotent mesenchymal stromal cells. The International Society for Cellular Therapy position statement. *Cytotherapy*, 8, 315-7.
- DOMINICI, M., LE BLANC, K., MÜLLER, I., SLAPER-CORTENBACH, I., MARINI, F., KRAUSE, D., DEANS, R., KEATING, A., PROCKOP, D. & HORWITZ, E. 2006b. Minimal criteria for defining multipotent mesenchymal stromal cells. The International Society for Cellular Therapy position statement. *Cytotherapy*, 8.
- DOS SANTOS, F., ANDRADE, P. Z., BOURA, J. S., ABECASIS, M. M., DA SILVA, C. L. & CABRAL, J. M. S. 2010. Ex vivo expansion of human

- mesenchymal stem cells: A more effective cell proliferation kinetics and metabolism under hypoxia. *Journal of Cellular Physiology*, 223, 27-35.
- DOS SANTOS, F., CAMPBELL, A., FERNANDES-PLATZGUMMER, A., ANDRADE, P. Z., GIMBLE, J. M., WEN, Y., BOUCHER, S., VEMURI, M. C., DA SILVA, C. L. & CABRAL, J. M. 2014. A xenogeneic-free bioreactor system for the clinical-scale expansion of human mesenchymal stem/stromal cells. *Biotechnol Bioeng*, 111, 1116-27.
- DOS SANTOS, F. F., ANDRADE, P. Z., DA SILVA, C. L. & CABRAL, J. M. S. 2013. Bioreactor design for clinical-grade expansion of stem cells. *Biotechnology Journal*, 8, 644-654.
- DOUCET, C., ERNOU, I., ZHANG, Y., LLENSE, J. R., BEGOT, L., HOLY, X. & LATAILLADE, J. J. 2005. Platelet lysates promote mesenchymal stem cell expansion: a safety substitute for animal serum in cell-based therapy applications. *J Cell Physiol*, 205, 228-36.
- DUFFY, M. M., PINDJAKOVA, J., HANLEY, S. A., MCCARTHY, C., WEIDHOFER, G. A., SWEENEY, E. M., ENGLISH, K., SHAW, G., MURPHY, J. M., BARRY, F. P., MAHON, B. P., BELTON, O., CEREDIG, R. & GRIFFIN, M. D. 2011. Mesenchymal stem cell inhibition of T-helper 17 cell- differentiation is triggered by cell-cell contact and mediated by prostaglandin E2 via the EP4 receptor. *Eur J Immunol*, 41, 2840-51.
- EAGLE, H. 1955. Nutrition needs of mammalian cells in tissue culture. *Science*, 122, 501-14.
- EIBES, G., DOS SANTOS, F., ANDRADE, P. Z., BOURA, J. S., ABECASIS, M. M. A., DA SILVA, C. L. & CABRAL, J. M. S. 2010. Maximizing the ex vivo expansion of human mesenchymal stem cells using a microcarrier-based stirred culture system. *Journal of Biotechnology*, 146, 194-197.
- ELABD, C., CHIELLINI, C., MASSOUDI, A., COCHET, O., ZARAGOSI, L.-E., TROJANI, C., MICHIELS, J.-F., WEISS, P., CARLE, G., ROCHET, N., DECHESSNE, C. A., AILHAUD, G., DANI, C. & AMRI, E.-Z. 2007. Human adipose tissue-derived multipotent stem cells differentiate in vitro and in vivo into osteocyte-like cells. *Biochemical and Biophysical Research Communications*, 361, 342-348.
- ELY, L. K., BURROWS, S. R., PURCELL, A. W., ROSSJOHN, J. & MCCLUSKEY, J. 2008. T-cells behaving badly: structural insights into alloreactivity and autoimmunity. *Current Opinion in Immunology*, 20, 575-580.
- EMADEDIN, M., AGHDAMI, N., TAGHIYAR, L., FAZELI, R., MOGHADASALI, R., JAHANGIR, S., FARJAD, R. & BAGHABAN ESLAMINEJAD, M. 2012. Intra-articular injection of autologous mesenchymal stem cells in six patients with knee osteoarthritis. *Arch Iran Med*, 15, 422-8.
- ERICKSON, G. A., BOLIN, S. R. & LANDGRAF, J. G. 1991. Viral contamination of fetal bovine serum used for tissue culture: risks and concerns. *Dev Biol Stand*, 75, 173-5.
- ESTRADA, J. C., ALBO, C., BENGURIA, A., DOPAZO, A., LOPEZ-ROMERO, P., CARRERA-QUINTANAR, L., ROCHE, E., CLEMENTE, E. P., ENRIQUEZ, J. A., BERNAD, A. & SAMPER, E. 2012. Culture of human mesenchymal stem cells at low oxygen tension improves growth and genetic stability by activating glycolysis. *Cell Death and Differentiation*, 19, 743-755.

- EVANS, C. H., GHIVIZZANI, S. C. & ROBBINS, P. D. 2008. Orthopedic Gene Therapy in 2008. *Mol Ther*, 17, 231-244.
- EVANS, M. J. & KAUFMAN, M. H. 1981. Establishment in culture of pluripotential cells from mouse embryos. *Nature*, 292, 154-6.
- FARRELL, E., BOTH, S. K., ODORFER, K. I., KOEVOET, W., KOPS, N., O'BRIEN, F. J., DE JONG, R. J. B., VERHAAR, J. A., CUIJPERS, V., JANSEN, J., ERBEN, R. G. & VAN OSCH, G. J. V. M. 2011. In-vivo generation of bone via endochondral ossification by in-vitro chondrogenic priming of adult human and rat mesenchymal stem cells. *Bmc Musculoskeletal Disorders*, 12.
- FARRELL, E., VAN DER JAGT, O. P., KOEVOET, W., KOPS, N., VAN MANEN, C. J., HELLINGMAN, C. A., JAHR, H., O'BRIEN, F. J., VERHAAR, J. A., WEINANS, H. & VAN OSCH, G. J. 2009. Chondrogenic priming of human bone marrow stromal cells: a better route to bone repair? *Tissue Eng Part C Methods*, 15, 285-95.
- FEHRER, C., BRUNAUER, R., LASCHOBBER, G., UNTERLUGGAUER, H., REITINGER, S., KLOSS, F., GULLY, C., GASSNER, R. & LEPPERDINGER, G. 2007. Reduced oxygen tension attenuates differentiation capacity of human mesenchymal stem cells and prolongs their lifespan. *Aging Cell*, 6, 745-757.
- FERNANDES-PLATZGUMMER, A., DIOGO, M. M., BAPTISTA, R. P., DA SILVA, C. L. & CABRAL, J. M. S. 2011. Scale-Up of Mouse Embryonic Stem Cell Expansion in Stirred Bioreactors. *Biotechnology Progress*, 27, 1421-1432.
- FESTEN, R. 2007. Understanding Animal Sera: Considerations for Use in the Production of Biological Therapeutics. *Medicines from Animal Cell Culture*. John Wiley & Sons, Ltd.
- FINK, T., ABILDTRUP, L., FOGD, K., ABDALLAH, B. M., KASSEM, M., EBBESEN, P. & ZACHAR, V. 2004. Induction of adipocyte-like phenotype in human mesenchymal stem cells by hypoxia. *Stem Cells*, 22, 1346-55.
- FONG, E. L., CHAN, C. K. & GOODMAN, S. B. 2011. Stem cell homing in musculoskeletal injury. *Biomaterials*, 32, 395-409.
- FORD, C. E., HAMERTON, J. L., BARNES, D. W. & LOUITIT, J. F. 1956. Cytological identification of radiation-chimaeras. *Nature*, 177, 452-4.
- FOTIA, C., MASSA, A., BORIANI, F., BALDINI, N. & GRANCHI, D. 2015. Hypoxia enhances proliferation and stemness of human adipose-derived mesenchymal stem cells. *Cytotechnology*, 67, 1073-84.
- FRIEDENS.AJ, PIATETZK.II & PETRAKOV.KV 1966. Osteogenesis in Transplants of Bone Marrow Cells. *Journal of Embryology and Experimental Morphology*, 16, 381-&.
- FRIEDENSTEIN, A. J., GORSKAJA, U. F. & KULAGINA, N. N. 1976. Fibroblast Precursors in Normal and Irradiated Mouse Hematopoietic Organs. *Experimental Hematology*, 4, 267-274.
- FU, X., HAN, B., CAI, S., LEI, Y., SUN, T. & SHENG, Z. 2009. Migration of bone marrow-derived mesenchymal stem cells induced by tumor necrosis factor- $\alpha$  and its possible role in wound healing. *Wound Repair and Regeneration*, 17, 185-191.
- FUGERE, F., OWEN, H., ILSLEY, A. H., PLUMMER, J. L. & HAWKINS, D. J. 1994. Changes in oxygen saturation in the 72 hours after hip surgery: the effect of oxygen therapy. *Anaesth Intensive Care*, 22, 724-8.

- GARCÍA-OLMO, D., GARCÍA-ARRANZ, M., HERREROS, D., PASCUAL, I., PEIRO, C. & RODRÍGUEZ-MONTES, A. J. 2005. A Phase I Clinical Trial of the Treatment of Crohn's Fistula by Adipose Mesenchymal Stem Cell Transplantation. *Diseases of the Colon & Rectum*, 48, 1416-1423.
- GAUTHIER, O., GOYENVALLE, E., BOULER, J. M., GUICHEUX, J., PILET, P., WEISS, P. & DACULSI, G. 2001. Macroporous biphasic calcium phosphate ceramics versus injectable bone substitute: a comparative study 3 and 8 weeks after implantation in rabbit bone. *Journal of Materials Science: Materials in Medicine*, 12, 385-390.
- GERSTENFELD, L. C. & EINHORN, T. A. 2003. Developmental aspects of fracture healing and the use of pharmacological agents to alter healing. *J Musculoskelet Neuronal Interact*, 3, 297-303; discussion 320-1.
- GEY, G. O. & THALHIMER, W. 1924. Observations on the effects of insulin introduced into the medium of tissue cultures. *Journal of the American Medical Association*, 82, 1609-1609.
- GIANNOUDIS, P. V., EINHORN, T. A. & MARSH, D. 2007. Fracture healing: the diamond concept. *Injury*, 38 Suppl 4, S3-6.
- GOTTIPAMULA, S., MUTTIGI, M. S., CHAANSA, S., ASHWIN, K. M., PRIYA, N., KOLKUNDKAR, U., SUNDARRAJ, S., MAJUMDAR, A. S. & SEETHARAM, R. N. 2016. Large-scale expansion of pre-isolated bone marrow mesenchymal stromal cells in serum-free conditions. *J Tissue Eng Regen Med*, 10, 108-19.
- GOVENDER, S., CSIMMA, C., GENANT, H. K., VALENTIN-OPRAN, A., AMIT, Y., ARBEL, R., ARO, H., ATAR, D., BISHAY, M., BORNER, M. G., CHIRON, P., CHOONG, P., CINATS, J., COURTENAY, B., FEIBEL, R., GEULETTE, B., GOVENDER, S., GRAVEL, C., HAAS, N., RASCHKE, M., HAMMACHER, E., VAN DER VELDE, D., HARDY, P., HOLT, M., JOSTEN, C., KETTERL, R. L., LINDEQUE, B., LOB, G., MATHEVON, H., MCCOY, G., MARSH, D., MILLER, R., MUNTING, E., OEVRE, S., NORDSLETTEN, L., PATEL, A., POHL, A., RENNIE, W., REYNDERS, P., ROMMENS, P. M., RONDIA, J., ROSSOUW, W. C., DANEEL, P. J., RUFF, S., RUTER, A., SANTAVIRTA, S., SCHILDHAUER, T. A., GEKLE, C., SCHNETTLER, R., SEGAL, D., SEILER, H., SNOWDOWNE, R. B., STAPERT, J., TAGLANG, G., VERDONK, R., VOGELS, L., WECKBACH, A., WENTZENSEN, A., WISNIEWSKI, T. & GRP, B. S. 2002. Recombinant human bone morphogenetic protein-2 for treatment of open tibial fractures - A prospective, controlled, randomized study of four hundred and fifty patients. *Journal of Bone and Joint Surgery-American Volume*, 84A, 2123-2134.
- GRANERO-MOLTO, F., WEIS, J. A., MIGA, M. I., LANDIS, B., MYERS, T. J., O'REAR, L., LONGOBARDI, L., JANSEN, E. D., MORTLOCK, D. P. & SPAGNOLI, A. 2009. Regenerative effects of transplanted mesenchymal stem cells in fracture healing. *Stem Cells*, 27, 1887-98.
- GRAYSON, W. L., ZHAO, F., BUNNELL, B. & MA, T. 2007a. Hypoxia enhances proliferation and tissue formation of human mesenchymal stem cells. *Biochemical and Biophysical Research Communications*, 358, 948-953.
- GRAYSON, W. L., ZHAO, F., BUNNELL, B. & MA, T. 2007b. Hypoxia enhances proliferation and tissue formation of human mesenchymal stem cells. *Biochem Biophys Res Commun*, 358, 948-53.

- GRAYSON, W. L., ZHAO, F., IZADPANA, R., BUNNELL, B. & MA, T. 2006. Effects of hypoxia on human mesenchymal stem cell expansion and plasticity in 3D constructs. *Journal of Cellular Physiology*, 207, 331-339.
- GRIFFIN, M. D., RITTER, T. & MAHON, B. P. 2010. Immunological aspects of allogeneic mesenchymal stem cell therapies. *Hum Gene Ther*, 21, 1641-55.
- GRUBER, R., KARRETH, F., KANDLER, B., FUERST, G., ROT, A., FISCHER, M. B. & WATZEK, G. 2004. Platelet-released supernatants increase migration and proliferation, and decrease osteogenic differentiation of bone marrow-derived mesenchymal progenitor cells under in vitro conditions. *Platelets*, 15, 29-35.
- GUSTAFSSON, M. V., ZHENG, X., PEREIRA, T., GRADIN, K., JIN, S., LUNDKVIST, J., RUAS, J. L., POELLINGER, L., LENDAHL, U. & BONDESSON, M. 2005. Hypoxia requires notch signaling to maintain the undifferentiated cell state. *Dev Cell*, 9, 617-28.
- HARWOOD, P. J. & FERGUSON, D. O. 2015. (ii) An update on fracture healing and non-union. *Orthopaedics and Trauma*, 29, 228-242.
- HAUSSLER, B., GOTHE, H., GOL, D., GLAESKE, G., PIENKA, L. & FELSEBERG, D. 2007. Epidemiology, treatment and costs of osteoporosis in Germany--the BoneEVA Study. *Osteoporos Int*, 18, 77-84.
- HAWKES, P. W. 2015. Fetal bovine serum: geographic origin and regulatory relevance of viral contamination. *Bioresources and Bioprocessing*, 2, 1-5.
- HEATHMAN, T. R. J., RAFIQ, Q. A., CHAN, A. K. C., COOPMAN, K., NIENOW, A. W., KARA, B. & HEWITT, C. J. 2016. Characterization of human mesenchymal stem cells from multiple donors and the implications for large scale bioprocess development. *Biochemical Engineering Journal*, 108, 14-23.
- HEATHMAN, T. R. J., STOLZING, A., FABIAN, C., RAFIQ, Q. A., COOPMAN, K., NIENOW, A. W., KARA, B. & HEWITT, C. J. 2015. Serum-free process development: improving the yield and consistency of human mesenchymal stromal cell production. *Cytotherapy*, 17, 1524-1535.
- HEISKANEN, A., SATOMAA, T., TIITINEN, S., LAITINEN, A., MANNELIN, S., IMPOLA, U., MIKKOLA, M., OLSSON, C., MILLER-PODRAZA, H., BLOMQVIST, M., OLONEN, A., SALO, H., LEHENKARI, P., TUURI, T., OTONKOSKI, T., NATUNEN, J., SAARINEN, J. & LAINE, J. 2007. N-glycolylneuraminic acid xenoantigen contamination of human embryonic and mesenchymal stem cells is substantially reversible. *Stem Cells*, 25, 197-202.
- HELMY, M. H., ISMAIL, S. S., FAYED, H. & EL-BASSIOUNI, E. A. 2000. Effect of selenium supplementation on the activities of glutathione metabolizing enzymes in human hepatoma Hep G2 cell line. *Toxicology*, 144, 57-61.
- HERBST, R. S. 2004. Review of epidermal growth factor receptor biology. *International Journal of Radiation Oncology\*Biophysics\*Physics*, 59, S21-S26.
- HEWITT, C. J., LEE, K., NIENOW, A. W., THOMAS, R. J., SMITH, M. & THOMAS, C. R. 2011. Expansion of human mesenchymal stem cells on microcarriers. *Biotechnol Lett*, 33, 2325-35.
- HICOK, K. C., DU LANEY, T. V., ZHOU, Y. S., HALVORSEN, Y. D., HITT, D. C., COOPER, L. F. & GIMBLE, J. M. 2004. Human adipose-derived adult stem cells produce osteoid in vivo. *Tissue Eng*, 10, 371-80.
- HING, K. A. 2004. Bone repair in the twenty-first century: biology, chemistry or engineering? *Philos Transact A Math Phys Eng Sci*, 362, 2821-50.

- HODGSON, J. 1995. To treat or not to treat: that is the question for serum. *Biotechnology (N Y)*, 13, 333-4, 337-8, 342-3.
- HOEY, D. A., TORMEY, S., RAMCHARAN, S., O'BRIEN, F. J. & JACOBS, C. R. 2012. Primary cilia-mediated mechanotransduction in human mesenchymal stem cells. *Stem Cells*, 30, 2561-70.
- HOLLINGER, J. O. & KLEINSCHMIDT, J. C. 1990. The Critical Size Defect as an Experimental Model To Test Bone Repair Materials. *Journal of Craniofacial Surgery*, 1, 60-68.
- HOLZWARTH, C., VAEGLER, M., GIESEKE, F., PFISTER, S. M., HANDGRETINGER, R., KERST, G. & MULLER, I. 2010a. Low physiologic oxygen tensions reduce proliferation and differentiation of human multipotent mesenchymal stromal cells. *BMC Cell Biol*, 11, 11.
- HOLZWARTH, C., VAEGLER, M., GIESEKE, F., PFISTER, S. M., HANDGRETINGER, R., KERST, G. & MÜLLER, I. 2010b. Low physiologic oxygen tensions reduce proliferation and differentiation of human multipotent mesenchymal stromal cells. *BMC Cell Biology*, 11, 1-11.
- HONEGGER, P. & LENOIR, D. 1982. Nerve growth factor (NGF) stimulation of cholinergic telencephalic neurons in aggregating cell cultures. *Developmental Brain Research*, 3, 229-238.
- HONN, K. V., SINGLEY, J. A. & CHAVIN, W. 1975. Fetal Bovine Serum: A Multivariate Standard. *Experimental Biology and Medicine*, 149, 344-347.
- HU, X., YU, S. P., FRASER, J. L., LU, Z., OGLE, M. E., WANG, J. A. & WEI, L. 2008. Transplantation of hypoxia-preconditioned mesenchymal stem cells improves infarcted heart function via enhanced survival of implanted cells and angiogenesis. *J Thorac Cardiovasc Surg*, 135, 799-808.
- HUANG, C. H., CHEN, M. H., YOUNG, T. H., JENG, J. H. & CHEN, Y. J. 2009. Interactive effects of mechanical stretching and extracellular matrix proteins on initiating osteogenic differentiation of human mesenchymal stem cells. *Journal of Cellular Biochemistry*, 108, 1263-73.
- HUNG, S.-P., HO, J. H., SHIH, Y.-R. V., LO, T. & LEE, O. K. 2012a. Hypoxia promotes proliferation and osteogenic differentiation potentials of human mesenchymal stem cells. *Journal of Orthopaedic Research*, 30, 260-266.
- HUNG, S. P., HO, J. H., SHIH, Y. R. V., LO, T. & LEE, O. K. 2012b. Hypoxia promotes proliferation and osteogenic differentiation potentials of human mesenchymal stem cells. *Journal of Orthopaedic Research*, 30, 260-266.
- IIDA, K., TAKEDA-KAWAGUCHI, T., TEZUKA, Y., KUNISADA, T., SHIBATA, T. & TEZUKA, K. 2010. Hypoxia enhances colony formation and proliferation but inhibits differentiation of human dental pulp cells. *Arch Oral Biol*, 55, 648-54.
- ISHIKAWA, I., SAWADA, R., KATO, Y., TSUJI, K., SHAO, J., YAMADA, T., KATO, R. & TSUCHIYA, T. 2009. [Effectivity of the novel serum-free medium STK2 for proliferating human mesenchymal stem cells]. *Yakugaku Zasshi*, 129, 381-4.
- ISO, Y., YAMAYA, S., SATO, T., POOLE, C. N., ISOYAMA, K., MIMURA, M., KOBAYASHI, Y., TAKEYAMA, Y., SPEES, J. L. & SUZUKI, H. 2012. Distinct mobilization of circulating CD271+ mesenchymal progenitors from hematopoietic progenitors during aging and after myocardial infarction. *Stem Cells Transl Med*, 1, 462-8.
- IUDICONE, P., FIORAVANTI, D., BONANNO, G., MICELI, M., LAVORINO, C., TOTTA, P., FRATI, L., NUTI, M. & PIERELLI, L. 2014. Pathogen-free,

- plasma-poor platelet lysate and expansion of human mesenchymal stem cells. *J Transl Med*, 12, 28.
- JANICKI, P., BOEUF, S., STECK, E., EGERMANN, M., KASTEN, P. & RICHTER, W. 2011. Prediction of in vivo bone forming potency of bone marrow-derived human mesenchymal stem cells. *Eur Cell Mater*, 21, 488-507.
- JANICKI, P., KASTEN, P., KLEINSCHMIDT, K., LUGINBUEHL, R. & RICHTER, W. 2010. Chondrogenic pre-induction of human mesenchymal stem cells on beta-TCP: enhanced bone quality by endochondral heterotopic bone formation. *Acta Biomater*, 6, 3292-301.
- JAQUIÉRY, C., SCHAEREN, S., FARHADI, J., MAINIL-VARLET, P., KUNZ, C., ZEILHOFER, H.-F., HEBERER, M. & MARTIN, I. 2005. In Vitro Osteogenic Differentiation and In Vivo Bone-Forming Capacity of Human Isogenic Jaw Periosteal Cells and Bone Marrow Stromal Cells. *Annals of Surgery*, 242, 859-868.
- JAYME, D. W. & SMITH, S. R. 2000. Media formulation options and manufacturing process controls to safeguard against introduction of animal origin contaminants in animal cell culture. *Cytotechnology*, 33, 27-36.
- JI, J. F., HE, B. P., DHEEN, S. T. & TAY, S. S. 2004. Interactions of chemokines and chemokine receptors mediate the migration of mesenchymal stem cells to the impaired site in the brain after hypoglossal nerve injury. *Stem Cells*, 22, 415-27.
- JIANG, Y., JAHAGIRDAR, B. N., REINHARDT, R. L., SCHWARTZ, R. E., KEENE, C. D., ORTIZ-GONZALEZ, X. R., REYES, M., LENVIK, T., LUND, T., BLACKSTAD, M., DU, J., ALDRICH, S., LISBERG, A., LOW, W. C., LARGAESPADA, D. A. & VERFAILLIE, C. M. 2002. Pluripotency of mesenchymal stem cells derived from adult marrow. *Nature*, 418, 41-9.
- JOHNSTONE, B., HERING, T. M., CAPLAN, A. I., GOLDBERG, V. M. & YOO, J. U. 1998. In Vitro Chondrogenesis of Bone Marrow-Derived Mesenchymal Progenitor Cells. *Experimental Cell Research*, 238, 265-272.
- JONES, E. A., KINSEY, S. E., ENGLISH, A., JONES, R. A., STRASZYNSKI, L., MEREDITH, D. M., MARKHAM, A. F., JACK, A., EMERY, P. & MCGONAGLE, D. 2002. Isolation and characterization of bone marrow multipotential mesenchymal progenitor cells. *Arthritis Rheum*, 46, 3349-60.
- JONES, G. N., MOSCHIDOU, D., LAY, K., ABDULRAZZAK, H., VANLEENE, M., SHEFELBINE, S. J., POLAK, J., DE COPPI, P., FISK, N. M. & GUILLOT, P. V. 2012. Upregulating CXCR4 in Human Fetal Mesenchymal Stem Cells Enhances Engraftment and Bone Mechanics in a Mouse Model of Osteogenesis Imperfecta. *Stem Cells Translational Medicine*, 1, 70-78.
- JUNG, S., PANCHALINGAM, K. M., ROSENBERG, L. & BEHIE, L. A. 2012. Ex vivo expansion of human mesenchymal stem cells in defined serum-free media. *Stem Cells Int*, 2012, 123030.
- KADIYALA, S., JAISWAL, N. & BRUDER, S. P. 1997. Culture-expanded, bone marrow-derived mesenchymal stem cells can regenerate a critical-sized segmental bone defect. *Tissue Engineering*, 3, 173-185.
- KAJJA, I., BIMENYA, G. S., EINDHOVEN, B., JAN TEN DUIS, H. & SIBINGA, C. T. 2010. Blood loss and contributing factors in femoral fracture surgery. *Afr Health Sci*, 10, 18-25.

- KAKUDO, N., MORIMOTO, N., OGAWA, T., TAKETANI, S. & KUSUMOTO, K. 2015. Hypoxia Enhances Proliferation of Human Adipose-Derived Stem Cells via HIF-1 $\alpha$  Activation. *PLoS One*, 10, e0139890.
- KANICHAJ, M., FERGUSON, D., PRENDERGAST, P. J. & CAMPBELL, V. A. 2008. Hypoxia promotes chondrogenesis in rat mesenchymal stem cells: A role for AKT and hypoxia-inducible factor (HIF)-1 $\alpha$ . *Journal of Cellular Physiology*, 216, 708-715.
- KANIS, J. A. 2007. Assessment of osteoporosis at the primary health care level. *WHO Scientific Group Technical Report*.
- KANIS, J. A. & JOHNELL, O. 2005. Requirements for DXA for the management of osteoporosis in Europe. *Osteoporos Int*, 16, 229-38.
- KEYSER, K. A., BEAGLES, K. E. & KIEM, H. P. 2007. Comparison of mesenchymal stem cells from different tissues to suppress T-cell activation. *Cell Transplant*, 16, 555-62.
- KHAN, W. S., ADESIDA, A. B. & HARDINGHAM, T. E. 2007a. Hypoxic conditions increase hypoxia-inducible transcription factor 2 $\alpha$  and enhance chondrogenesis in stem cells from the infrapatellar fat pad of osteoarthritis patients. *Arthritis Res Ther*, 9.
- KHAN, W. S., ADESIDA, A. B. & HARDINGHAM, T. E. 2007b. Hypoxic conditions increase hypoxia-inducible transcription factor 2 $\alpha$  and enhance chondrogenesis in stem cells from the infrapatellar fat pad of osteoarthritis patients. *Arthritis Res Ther*, 9, R55.
- KILIAN, K. A., BUGARIJA, B., LAHN, B. T. & MRKSICH, M. 2010. Geometric cues for directing the differentiation of mesenchymal stem cells. *Proc Natl Acad Sci U S A*, 107, 4872-7.
- KILIAN, O., FLESCH, I., WENISCH, S., TABORSKI, B., JORK, A., SCHNETTLER, R. & JONULEIT, T. 2004. Effects of platelet growth factors on human mesenchymal stem cells and human endothelial cells in vitro. *Eur J Med Res*, 9, 337-44.
- KIM, K. H., SONG, M. J., CHUNG, J., PARK, H. & KIM, J. B. 2005. Hypoxia inhibits adipocyte differentiation in a HDAC-independent manner. *Biochemical and Biophysical Research Communications*, 333, 1178-1184.
- KITAORI, T., ITO, H., SCHWARZ, E. A., TSUTSUMI, R., YOSHITOMI, H., OISHI, S., NAKANO, M., FUJII, N., NAGASAWA, T. & NAKAMURA, T. 2009a. Stromal Cell-Derived Factor 1/CXCR4 Signaling Is Critical for the Recruitment of Mesenchymal Stem Cells to the Fracture Site During Skeletal Repair in a Mouse Model. *Arthritis and Rheumatism*, 60, 813-823.
- KITAORI, T., ITO, H., SCHWARZ, E. M., TSUTSUMI, R., YOSHITOMI, H., OISHI, S., NAKANO, M., FUJII, N., NAGASAWA, T. & NAKAMURA, T. 2009b. Stromal cell-derived factor 1/CXCR4 signaling is critical for the recruitment of mesenchymal stem cells to the fracture site during skeletal repair in a mouse model. *Arthritis & Rheumatism*, 60, 813-823.
- KOKABU, S., GAMER, L., COX, K., LOWERY, J., TSUJI, K., RAZ, R., ECONOMIDES, A., KATAGIRI, T. & ROSEN, V. 2012. BMP3 suppresses osteoblast differentiation of bone marrow stromal cells via interaction with Acvr2b. *Mol Endocrinol*, 26, 87-94.
- KRAMPERA, M., GALIPEAU, J., SHI, Y., TARTE, K. & SENSEBE, L. 2013. Immunological characterization of multipotent mesenchymal stromal cells--The International Society for Cellular Therapy (ISCT) working proposal. *Cytotherapy*, 15, 1054-61.

- KREBSBACH, P. H., KUZNETSOV, S. A., SATOMURA, K., EMMONS, R. V., ROWE, D. W. & ROBEY, P. G. 1997. Bone formation in vivo: comparison of osteogenesis by transplanted mouse and human marrow stromal fibroblasts. *Transplantation*, 63, 1059-69.
- KUCI, S., KUCI, Z., KREYENBERG, H., DEAK, E., PUTSCH, K., HUENECKE, S., AMARA, C., KOLLER, S., RETTINGER, E., GREZ, M., KOEHL, U., LATIFI-PUPOVCI, H., HENSCHLER, R., TONN, T., VON LAER, D., KLINGEBIEL, T. & BADER, P. 2010. CD271 antigen defines a subset of multipotent stromal cells with immunosuppressive and lymphohematopoietic engraftment-promoting properties. *Haematologica*, 95, 651-9.
- KUMAGAI, K., VASANJI, A., DRAZBA, J. A., BUTLER, R. S. & MUSCHLER, G. F. 2008. Circulating cells with osteogenic potential are physiologically mobilized into the fracture healing site in the parabiotic mice model. *J Orthop Res*, 26, 165-75.
- KURODA, Y., KITADA, M., WAKAO, S., NISHIKAWA, K., TANIMURA, Y., MAKINOSHIMA, H., GODA, M., AKASHI, H., INUTSUKA, A., NIWA, A., SHIGEMOTO, T., NABESHIMA, Y., NAKAHATA, T., FUJIYOSHI, Y. & DEZAWA, M. 2010. Unique multipotent cells in adult human mesenchymal cell populations. *Proc Natl Acad Sci U S A*, 107, 8639-43.
- KUZNETSOV, S. A., FRIEDENSTEIN, A. J. & ROBEY, P. G. 1997. Factors required for bone marrow stromal fibroblast colony formation in vitro. *Br J Haematol*, 97, 561-70.
- KUZNETSOV, S. A., MANKANI, M. H. & ROBEY, P. G. 2000. Effect of serum on human bone marrow stromal cells: ex vivo expansion and in vivo bone formation. *Transplantation*, 70, 1780-7.
- LAKHKAR, N. J., M DAY, R., KIM, H.-W., LUDKA, K., MORDAN, N. J., SALIH, V. & KNOWLES, J. C. 2015. Titanium phosphate glass microcarriers induce enhanced osteogenic cell proliferation and human mesenchymal stem cell protein expression. *Journal of Tissue Engineering*, 6.
- LANE, J. M., TOMIN, E. & BOSTROM, M. P. 1999. Biosynthetic bone grafting. *Clin Orthop Relat Res*, S107-17.
- LANE, S. W., WILLIAMS, D. A. & WATT, F. M. 2014. Modulating the stem cell niche for tissue regeneration. *Nat Biotechnol*, 32, 795-803.
- LE BLANC, K., FRASSONI, F., BALL, L., LOCATELLI, F., ROELOFS, H., LEWIS, I., LANINO, E., SUNDBERG, B., BERNARDO, M. E., REMBERGER, M., DINI, G., EGELER, R. M., BACIGALUPO, A., FIBBE, W. & RINGDÉN, O. Mesenchymal stem cells for treatment of steroid-resistant, severe, acute graft-versus-host disease: a phase II study. *The Lancet*, 371, 1579-1586.
- LE BLANC, K. & RINGDEN, O. 2005. Immunobiology of human mesenchymal stem cells and future use in hematopoietic stem cell transplantation. *Biol Blood Marrow Transplant*, 11, 321-34.
- LE BLANC, K., TAMMIK, C., ROSENDAHL, K., ZETTERBERG, E. & RINGDEN, O. 2003. HLA expression and immunologic properties of differentiated and undifferentiated mesenchymal stem cells. *Exp Hematol*, 31, 890-6.
- LE GUEHENNEC, L., GOYENVALLE, E., AGUADO, E., PILET, P., D'ARC, M. B., BILBAN, M., SPAETHE, R. & DACULSI, G. 2005. MBCP® biphasic calcium phosphate granules and tissucol® fibrin sealant in rabbit femoral

- defects: The effect of fibrin on bone ingrowth. *Journal of Materials Science: Materials in Medicine*, 16, 29-35.
- LE NIHOUANEN, D., DACULSI, G., SAFFARZADEH, A., GAUTHIER, O., DELPLACE, S., PILET, P. & LAYROLLE, P. 2005. Ectopic bone formation by microporous calcium phosphate ceramic particles in sheep muscles. *Bone*, 36, 1086-1093.
- LEE, J. H. & KEMP, D. M. 2006. Human adipose-derived stem cells display myogenic potential and perturbed function in hypoxic conditions. *Biochem Biophys Res Commun*, 341, 882-8.
- LEE, R. H., HSU, S. C., MUNOZ, J., JUNG, J. S., LEE, N. R., POCHAMPALLY, R. & PROCKOP, D. J. 2006. A subset of human rapidly self-renewing marrow stromal cells preferentially engraft in mice. *Blood*, 107, 2153-61.
- LEE, S. W., PADMANABHAN, P., RAY, P., GAMBHIR, S. S., DOYLE, T., CONTAG, C., GOODMAN, S. B. & BISWAL, S. 2009. Stem cell-mediated accelerated bone healing observed with in vivo molecular and small animal imaging technologies in a model of skeletal injury. *J Orthop Res*, 27, 295-302.
- LEVINGS, R. L. & WESSMAN, S. J. 1991. Bovine viral diarrhea virus contamination of nutrient serum, cell cultures and viral vaccines. *Dev Biol Stand*, 75, 177-81.
- LIN, Q., LEE, Y. J. & YUN, Z. 2006. Differentiation arrest by hypoxia. *J Biol Chem*, 281, 30678-83.
- LINDROOS, B., BOUCHER, S., CHASE, L., KUOKKANEN, H., HUHTALA, H., HAATAJA, R., VEMURI, M., SUURONEN, R. & MIETTINEN, S. 2009. Serum-free, xeno-free culture media maintain the proliferation rate and multipotentiality of adipose stem cells in vitro. *Cytotherapy*, 11, 958-72.
- LIU, J., HAO, H., XIA, L., TI, D., HUANG, H., DONG, L., TONG, C., HOU, Q., ZHAO, Y., LIU, H., FU, X. & HAN, W. 2015. Hypoxia Pretreatment of Bone Marrow Mesenchymal Stem Cells Facilitates Angiogenesis by Improving the Function of Endothelial Cells in Diabetic Rats with Lower Ischemia. *PLoS One*, 10, e0126715.
- LIU, X., DUAN, B., CHENG, Z., JIA, X., MAO, L., FU, H., CHE, Y., OU, L., LIU, L. & KONG, D. 2011. SDF-1/CXCR4 axis modulates bone marrow mesenchymal stem cell apoptosis, migration and cytokine secretion. *Protein & Cell*, 2, 845-854.
- LOFFREDO, F. S., STEINHAUSER, M. L., GANNON, J. & LEE, R. T. 2011. Bone Marrow-Derived Cell Therapy Stimulates Endogenous Cardiomyocyte Progenitors and Promotes Cardiac Repair. *Cell Stem Cell*, 8, 389-398.
- LU, C., ROLLINS, M., HOU, H., SWARTZ, H. M., HOPF, H., MICLAU, T. & MARCUCIO, R. S. 2008. Tibial Fracture Decreases Oxygen Levels at the Site of Injury. *The Iowa Orthopaedic Journal*, 28, 14-21.
- LUU, Y. K., CAPILLA, E., ROSEN, C. J., GILSANZ, V., PESSIN, J. E., JUDEX, S. & RUBIN, C. T. 2009. Mechanical stimulation of mesenchymal stem cell proliferation and differentiation promotes osteogenesis while preventing dietary-induced obesity. *J Bone Miner Res*, 24, 50-61.
- LV, F. J., TUAN, R. S., CHEUNG, K. M. & LEUNG, V. Y. 2014. Concise review: the surface markers and identity of human mesenchymal stem cells. *Stem Cells*, 32, 1408-19.
- MABUCHI, Y., MORIKAWA, S., HARADA, S., NIIBE, K., SUZUKI, S., RENAULT-MIHARA, F., HOULIHAN, D. D., AKAZAWA, C., OKANO,

- H. & MATSUZAKI, Y. 2013. LNGFR(+)THY-1(+)VCAM-1(hi+) cells reveal functionally distinct subpopulations in mesenchymal stem cells. *Stem Cell Reports*, 1, 152-65.
- MACKAY, A. M., BECK, S. C., MURPHY, J. M., BARRY, F. P., CHICHESTER, C. O. & PITTENGER, M. F. 1998. Chondrogenic differentiation of cultured human mesenchymal stem cells from marrow. *Tissue Eng*, 4, 415-28.
- MALARD, O., GUICHEUX, J., BOULER, J.-M., GAUTHIER, O., BEAUVILLAIN DE MONTREUIL, C., AGUADO, E., PILET, P., LEGEROS, R. & DACULSI, G. 2005. Calcium phosphate scaffold and bone marrow for bone reconstruction in irradiated area: a dog study. *Bone*, 36, 323-330.
- MALLADI, P., XU, Y., CHIOU, M., GIACCIA, A. J. & LONGAKER, M. T. 2006. Effect of reduced oxygen tension on chondrogenesis and osteogenesis in adipose-derived mesenchymal cells. *American Journal of Physiology-Cell Physiology*, 290, C1139-C1145.
- MANKANI, M. H., KUZNETSOV, S. A., FOWLER, B., KINGMAN, A. & ROBEY, P. G. 2001. In vivo bone formation by human bone marrow stromal cells: effect of carrier particle size and shape. *Biotechnol Bioeng*, 72, 96-107.
- MANKANI, M. H., KUZNETSOV, S. A., MARSHALL, G. W. & ROBEY, P. G. 2008. Creation of new bone by the percutaneous injection of human bone marrow stromal cell and HA/TCP suspensions. *Tissue Eng Part A*, 14, 1949-58.
- MARKEY, K. L. 1987. Stress fractures. *Clin Sports Med*, 6, 405-25.
- MARTIN, G. R. 1981. Isolation of a pluripotent cell line from early mouse embryos cultured in medium conditioned by teratocarcinoma stem cells. *Proc Natl Acad Sci U S A*, 78, 7634-8.
- MARTIN, I., MURAGLIA, A., CAMPANILE, G., CANCEDDA, R. & QUARTO, R. 1997. Fibroblast growth factor-2 supports ex vivo expansion and maintenance of osteogenic precursors from human bone marrow. *Endocrinology*, 138, 4456-62.
- MATSUNOBU, T., TORIGOE, K., ISHIKAWA, M., DE VEGA, S., KULKARNI, A. B., IWAMOTO, Y. & YAMADA, Y. 2009. Critical roles of the TGF- $\beta$  type I receptor ALK5 in perichondrial formation and function, cartilage integrity, and osteoblast differentiation during growth plate development. *Developmental Biology*, 332, 325-338.
- MEISEL, H. J., SCHNORING, M., HOHAUS, C., MINKUS, Y., BEIER, A., GANEY, T. & MANSMANN, U. 2008. Posterior lumbar interbody fusion using rhBMP-2. *European Spine Journal*, 17, 1735-1744.
- MENDICINO, M., BAILEY, A. M., WONNACOTT, K., PURI, R. K. & BAUER, S. R. 2014. MSC-based product characterization for clinical trials: an FDA perspective. *Cell Stem Cell*, 14, 141-5.
- MEYER, E. G., BUCKLEY, C. T., THORPE, S. D. & KELLY, D. J. 2010. Low oxygen tension is a more potent promoter of chondrogenic differentiation than dynamic compression. *Journal of Biomechanics*, 43, 2516-2523.
- MIFUNE, Y., MATSUMOTO, T., MURASAWA, S., KAWAMOTO, A., KURODA, R., SHOJI, T., KURODA, T., FUKUI, T., KAWAKAMI, Y., KUROSAKA, M. & ASAHARA, T. 2013. Therapeutic superiority for cartilage repair by CD271-positive marrow stromal cell transplantation. *Cell Transplant*, 22, 1201-11.

- MIRABELLA, T., POGGI, A., SCARANARI, M., MOGNI, M., LITUANIA, M., BALDO, C., CANCEDDA, R. & GENTILI, C. 2011. Recruitment of host's progenitor cells to sites of human amniotic fluid stem cells implantation. *Biomaterials*, 32, 4218-27.
- MIRAMOND, T., CORRE, P., BORGET, P., MOREAU, F., GUICHEUX, J., DACULSI, G. & WEISS, P. 2014. Osteoinduction of biphasic calcium phosphate scaffolds in a nude mouse model. *J Biomater Appl*, 29, 595-604.
- MITSIADIS, T. A., BARRANDON, O., ROCHAT, A., BARRANDON, Y. & DE BARI, C. 2007. Stem cell niches in mammals. *Exp Cell Res*, 313, 3377-85.
- MIWA, H., HASHIMOTO, Y., TENSHO, K., WAKITANI, S. & TAKAGI, M. 2012. Xeno-free proliferation of human bone marrow mesenchymal stem cells. *Cytotechnology*, 64, 301-8.
- MIZRAHI, O., SHEYN, D., TAWACKOLI, W., KALLAI, I., OH, A., SU, S., DA, X., ZARRINI, P., COOK-WIENS, G., GAZIT, D. & GAZIT, Z. 2013. BMP-6 is more efficient in bone formation than BMP-2 when overexpressed in mesenchymal stem cells. *Gene Ther*, 20, 370-377.
- MO, M., WANG, S., ZHOU, Y., LI, H. & WU, Y. 2016. Mesenchymal stem cell subpopulations: phenotype, property and therapeutic potential. *Cell Mol Life Sci*.
- MOHYELDIN, A., GARZON-MUVDI, T. & QUINONES-HINOJOSA, A. 2010. Oxygen in stem cell biology: a critical component of the stem cell niche. *Cell Stem Cell*, 7, 150-61.
- MOORE, G. E., GERNER, R. E. & FRANKLIN, H. A. 1967. Culture of normal human leukocytes. *JAMA*, 199, 519-24.
- MULLER-SIEBURG, C. E., CHO, R. H., THOMAN, M., ADKINS, B. & SIEBURG, H. B. 2002. Deterministic regulation of hematopoietic stem cell self-renewal and differentiation. *Blood*, 100, 1302-9.
- MURAGLIA, A., MARTIN, I., CANCEDDA, R. & QUARTO, R. 1998. A nude mouse model for human bone formation in unloaded conditions. *Bone*, 22, 131S-134S.
- MURAO, H., YAMAMOTO, K., MATSUDA, S. & AKIYAMA, H. 2013. Periosteal cells are a major source of soft callus in bone fracture. *J Bone Miner Metab*, 31, 390-8.
- NAKAHARA, H., GOLDBERG, V. M. & CAPLAN, A. I. 1991. Culture-expanded human periosteal-derived cells exhibit osteochondral potential in vivo. *J Orthop Res*, 9, 465-76.
- NAUTA, A. J. & FIBBE, W. E. 2007. Immunomodulatory properties of mesenchymal stromal cells. *Blood*, 110, 3499-506.
- NEKANTI, U., DASTIDAR, S., VENUGOPAL, P., TOTEY, S. & TA, M. 2010. Increased proliferation and analysis of differential gene expression in human Wharton's jelly-derived mesenchymal stromal cells under hypoxia. *Int J Biol Sci*, 6, 499-512.
- NING, H., LIN, G., LUE, T. F. & LIN, C. S. 2011. Mesenchymal stem cell marker Stro-1 is a 75 kd endothelial antigen. *Biochem Biophys Res Commun*, 413, 353-7.
- NOORT, W. A., OERLEMANS, M. I., ROZEMULLER, H., FEYEN, D., JAKSANI, S., STECHER, D., NAAJKENS, B., MARTENS, A. C., BUHRING, H. J., DOEVENDANS, P. A. & SLUIJTER, J. P. 2012. Human versus porcine mesenchymal stromal cells: phenotype, differentiation

- potential, immunomodulation and cardiac improvement after transplantation. *J Cell Mol Med*, 16, 1827-39.
- OEST, M. E., DUPONT, K. M., KONG, H. J., MOONEY, D. J. & GULDBERG, R. E. 2007. Quantitative assessment of scaffold and growth factor-mediated repair of critically sized bone defects. *Journal of Orthopaedic Research*, 25, 941-950.
- OLMER, R., LANGE, A., SELZER, S., KASPER, C., HAVERICH, A., MARTIN, U. & ZWEIGERDT, R. 2012. Suspension Culture of Human Pluripotent Stem Cells in Controlled, Stirred Bioreactors. *Tissue Engineering Part C-Methods*, 18, 772-784.
- ORTIZ, L. A., GAMBELLI, F., MCBRIDE, C., GAUPP, D., BADDOO, M., KAMINSKI, N. & PHINNEY, D. G. 2003. Mesenchymal stem cell engraftment in lung is enhanced in response to bleomycin exposure and ameliorates its fibrotic effects. *Proc Natl Acad Sci U S A*, 100, 8407-11.
- OZAKI, Y., NISHIMURA, M., SEKIYA, K., SUEHIRO, F., KANAWA, M., NIKAWA, H., HAMADA, T. & KATO, Y. 2007. Comprehensive analysis of chemotactic factors for bone marrow mesenchymal stem cells. *Stem Cells Dev*, 16, 119-29.
- PAL, R., HANWATE, M., JAN, M. & TOTTEY, S. 2009. Phenotypic and functional comparison of optimum culture conditions for upscaling of bone marrow-derived mesenchymal stem cells. *J Tissue Eng Regen Med*, 3, 163-74.
- PARK, RYU, KIM, LIM, JEONG, JUN, OH & JEUN 2011. CXCR4-transfected human umbilical cord blood-derived mesenchymal stem cells exhibit enhanced migratory capacity toward gliomas. *International Journal of Oncology*, 38, 97-103.
- PARKER, M. J., RAGHAVAN, R. & GURUSAMY, K. 2007. Incidence of fracture-healing complications after femoral neck fractures. *Clinical Orthopaedics and Related Research*, 175-179.
- PERS, Y.-M., RACKWITZ, L., FERREIRA, R., PULLIG, O., DELFOUR, C., BARRY, F., SENSEBE, L., CASTEILLA, L., FLEURY, S., BOURIN, P., NOËL, D., CANOVAS, F., CYTEVAL, C., LISIGNOLI, G., SCHRAUTH, J., HADDAD, D., DOMERGUE, S., NOETH, U., JORGENSEN, C. & CONSORTIUM, O. B. O. T. A. 2016. Adipose Mesenchymal Stromal Cell-Based Therapy for Severe Osteoarthritis of the Knee: A Phase I Dose-Escalation Trial. *Stem Cells Translational Medicine*.
- PETERSON, B., ZHANG, J., IGLESIAS, R., KABO, M., HEDRICK, M., BENHAIM, P. & LIEBERMAN, J. R. 2005. Healing of critically sized femoral defects, using genetically modified mesenchymal stem cells from human adipose tissue. *Tissue Engineering*, 11, 120-129.
- PHINNEY, D. G. 2012. Functional heterogeneity of mesenchymal stem cells: implications for cell therapy. *Journal of Cellular Biochemistry*, 113, 2806-12.
- PICINICH, S. C., MISHRA, P. J., MISHRA, P. J., GLOD, J. & BANERJEE, D. 2007. The therapeutic potential of mesenchymal stem cells. *Expert Opinion on Biological Therapy*, 7, 965-973.
- PILGAARD, L., LUND, P., DUROUX, M., LOCKSTONE, H., TAYLOR, J., EMMERSEN, J., FINK, T., RAGOISSIS, J. & ZACHAR, V. 2009. Transcriptional signature of human adipose tissue-derived stem cells (hASCs) preconditioned for chondrogenesis in hypoxic conditions. *Experimental Cell Research*, 315, 1937-1952.

- PRATHER, W. R., TOREN, A., MEIRON, M., OFIR, R., TSCHOPE, C. & HORWITZ, E. M. 2009. The role of placental-derived adherent stromal cell (PLX-PAD) in the treatment of critical limb ischemia. *Cytotherapy*, 11, 427-34.
- PROCKOP, D. J. 1998. Marrow stromal cells as stem cells for continual renewal of nonhematopoietic tissues and as potential vectors for gene therapy. *Journal of Cellular Biochemistry*, 284-285.
- PROCKOP, D. J., SEKIYA, I. & COLTER, D. C. 2001. Isolation and characterization of rapidly self-renewing stem cells from cultures of human marrow stromal cells. *Cytotherapy*, 3, 393-6.
- PSALTIS, P. J., PATON, S., SEE, F., ARTHUR, A., MARTIN, S., ITESCU, S., WORTHLEY, S. G., GRONTHOS, S. & ZANNETTINO, A. C. 2010. Enrichment for STRO-1 expression enhances the cardiovascular paracrine activity of human bone marrow-derived mesenchymal cell populations. *J Cell Physiol*, 223, 530-40.
- QI, M. C., HU, J., ZOU, S. J., CHEN, H. Q., ZHOU, H. X. & HAN, L. C. 2008. Mechanical strain induces osteogenic differentiation: Cbfa1 and Ets-1 expression in stretched rat mesenchymal stem cells. *International Journal of Oral and Maxillofacial Surgery*, 37, 453-458.
- QI, M. C., ZOU, S. J., HAN, L. C., ZHOU, H. X. & HU, J. 2009. Expression of bone-related genes in bone marrow MSCs after cyclic mechanical strain: implications for distraction osteogenesis. *Int J Oral Sci*, 1, 143-50.
- QU, Z. H., ZHANG, X. L., TANG, T. T. & DAI, K. R. 2008. Promotion of osteogenesis through beta-catenin signaling by desferrioxamine. *Biochemical and Biophysical Research Communications*, 370, 332-337.
- RAAYMAKERS, E. L. 2006. Fractures of the femoral neck: a review and personal statement. *Acta Chir Orthop Traumatol Cech*, 73, 45-59.
- RAFIQ, Q. A., COOPMAN, K., NIENOW, A. W. & HEWITT, C. J. 2013. A quantitative approach for understanding small-scale human mesenchymal stem cell culture - implications for large-scale bioprocess development. *Biotechnol J*, 8, 459-71.
- RAFIQ, Q. A., TWOMEY, K., KULIK, M., LESCHKE, C., O'DEA, J., CALLENS, S., GENTILI, C., BARRY, F. P. & MURPHY, M. 2016. Developing an automated robotic factory for novel stem cell therapy production. *Regenerative medicine*, 11, 351-354.
- RAJARAMAN, G., WHITE, J., TAN, K. S., ULRICH, D., ROSAMILIA, A., WERKMEISTER, J. & GARGETT, C. E. 2013. Optimization and scale-up culture of human endometrial multipotent mesenchymal stromal cells: potential for clinical application. *Tissue Eng Part C Methods*, 19, 80-92.
- RASMUSSEN, J. G., FROBERT, O., PILGAARD, L., KASTRUP, J., SIMONSEN, U., ZACHAR, V. & FINK, T. 2011. Prolonged hypoxic culture and trypsinization increase the pro-angiogenic potential of human adipose tissue-derived stem cells. *Cytotherapy*, 13, 318-28.
- RENNERT, R. C., SORKIN, M., GARG, R. K. & GURTNER, G. C. 2012. Stem cell recruitment after injury: lessons for regenerative medicine. *Regenerative medicine*, 7, 833-850.
- ROBERTSON, J. A. 2001. Human embryonic stem cell research: ethical and legal issues. *Nat Rev Genet*, 2, 74-8.
- ROCHFORT, G. Y., DELORME, B., LOPEZ, A., HÉRAULT, O., BONNET, P., CHARBORD, P., EDER, V. & DOMENECH, J. 2006. Multipotential

- Mesenchymal Stem Cells Are Mobilized into Peripheral Blood by Hypoxia. *Stem Cells*, 24, 2202-2208.
- RODRIGUES, C. A. V., DIOGO, M. M., DA SILVA, C. L. & CABRAL, J. M. S. 2011. Microcarrier expansion of mouse embryonic stem cell-derived neural stem cells in stirred bioreactors. *Biotechnology and Applied Biochemistry*, 58, 231-242.
- ROSTOVSKAYA, M. & ANASTASSIADIS, K. 2012. Differential expression of surface markers in mouse bone marrow mesenchymal stromal cell subpopulations with distinct lineage commitment. *PLoS One*, 7, e51221.
- SACCHETTI, B., FUNARI, A., MICHENZI, S., CESARE, S., PIERSANTI, S. & SAGGIO, I. 2007a. Self-renewing osteoprogenitors in bone marrow sinusoids can organize a hematopoietic microenvironment. *Cell*, 131.
- SACCHETTI, B., FUNARI, A., MICHENZI, S., DI CESARE, S., PIERSANTI, S., SAGGIO, I., TAGLIAFICO, E., FERRARI, S., ROBEY, P. G., RIMINUCCI, M. & BIANCO, P. 2007b. Self-renewing osteoprogenitors in bone marrow sinusoids can organize a hematopoietic microenvironment. *Cell*, 131, 324-36.
- SAKAGUCHI, Y., SEKIYA, I., YAGISHITA, K. & MUNETA, T. 2005. Comparison of human stem cells derived from various mesenchymal tissues: Superiority of synovium as a cell source. *Arthritis & Rheumatism*, 52, 2521-2529.
- SANTOS, F., ANDRADE, P. Z., ABECASIS, M. M., GIMBLE, J. M., CHASE, L. G., CAMPBELL, A. M., BOUCHER, S., VEMURI, M. C., SILVA, C. L. & CABRAL, J. M. 2011. Toward a clinical-grade expansion of mesenchymal stem cells from human sources: a microcarrier-based culture system under xeno-free conditions. *Tissue Eng Part C Methods*, 17, 1201-10.
- SASAKI, M., ABE, R., FUJITA, Y., ANDO, S., INOKUMA, D. & SHIMIZU, H. 2008. Mesenchymal stem cells are recruited into wounded skin and contribute to wound repair by transdifferentiation into multiple skin cell type. *Journal of Immunology*, 180, 2581-2587.
- SAWADA, R., YAMADA, T., TSUCHIYA, T. & MATSUOKA, A. 2010. [Microarray analysis of the effects of serum-free medium on gene expression changes in human mesenchymal stem cells during the in vitro culture]. *Yakugaku Zasshi*, 130, 1387-93.
- SCHAFFLER, A. & BUCHLER, C. 2007. Concise review: adipose tissue-derived stromal cells--basic and clinical implications for novel cell-based therapies. *Stem Cells*, 25, 818-27.
- SCHALLMOSER, K., BARTMANN, C., ROHDE, E., REINISCH, A., KASHOFER, K., STADELMEYER, E., DREXLER, C., LANZER, G., LINKESCH, W. & STRUNK, D. 2007. Human platelet lysate can replace fetal bovine serum for clinical-scale expansion of functional mesenchymal stromal cells. *Transfusion*, 47, 1436-1446.
- SCHENK, S., MAL, N., FINAN, A., ZHANG, M., KIEDROWSKI, M., POPOVIC, Z., MCCARTHY, P. M. & PENN, M. S. 2007. Monocyte chemotactic protein-3 is a myocardial mesenchymal stem cell homing factor. *Stem Cells*, 25, 245-51.
- SCHIPANI, E. 2005. Hypoxia and HIF-1 $\alpha$  in chondrogenesis. *Seminars in Cell & Developmental Biology*, 16, 539-546.
- SCHMIDT-BLEEK, K., SCHELL, H., LIENAU, J., SCHULZ, N., HOFF, P., PFAFF, M., SCHMIDT, G., MARTIN, C., PERKA, C., BUTTGEREIT, F.,

- VOLK, H. D. & DUDA, G. 2014. Initial immune reaction and angiogenesis in bone healing. *Journal of Tissue Engineering and Regenerative Medicine*, 8, 120-130.
- SCHOP, D., VAN DIJKHUIZEN-RADERSMA, R., BORGART, E., JANSSEN, F. W., ROZEMULLER, H., PRINS, H. J. & DE BRUIJN, J. D. 2010. Expansion of human mesenchymal stromal cells on microcarriers: growth and metabolism. *J Tissue Eng Regen Med*, 4, 131-40.
- SCHOPPER, C., MOSER, D., SPASSOVA, E., GORIWODA, W., LAGOIANNIS, G., HOERING, B., EWERS, R. & REDL, H. 2008. Bone regeneration using a naturally grown HA/TCP carrier loaded with rhBMP-2 is independent of barrier-membrane effects. *Journal of Biomedical Materials Research Part A*, 85A, 954-963.
- SCOLARO, J. A., SCHENKER, M. L., YANNASCOLI, S., BALDWIN, K., MEHTA, S. & AHN, J. 2014. Cigarette Smoking Increases Complications Following Fracture. *Journal of Bone and Joint Surgery-American Volume*, 96A, 674-681.
- SEN, B., XIE, Z., CASE, N., MA, M., RUBIN, C. & RUBIN, J. 2008. Mechanical strain inhibits adipogenesis in mesenchymal stem cells by stimulating a durable beta-catenin signal. *Endocrinology*, 149, 6065-75.
- SHAFI, M., SJONNESEN, K., YAMASHITA, A., LIU, S. Y., MICHALAK, M., KALLOS, M. S. & RANCOURT, D. E. 2012. Expansion and long-term maintenance of induced pluripotent stem cells in stirred suspension bioreactors. *Journal of Tissue Engineering and Regenerative Medicine*, 6, 462-472.
- SHAHDADFAR, A., FRONSDAL, K., HAUG, T., REINHOLT, F. P. & BRINCHMANN, J. E. 2005. In vitro expansion of human mesenchymal stem cells: choice of serum is a determinant of cell proliferation, differentiation, gene expression, and transcriptome stability. *Stem Cells*, 23, 1357-66.
- SHEEHY, E. J., BUCKLEY, C. T. & KELLY, D. J. 2012. Oxygen tension regulates the osteogenic, chondrogenic and endochondral phenotype of bone marrow derived mesenchymal stem cells. *Biochem Biophys Res Commun*, 417, 305-10.
- SHI, S. & GRONTHOS, S. 2003. Perivascular Niche of Postnatal Mesenchymal Stem Cells in Human Bone Marrow and Dental Pulp. *Journal of Bone and Mineral Research*, 18, 696-704.
- SHIHABUDDIN, L. S., RAY, J. & GAGE, F. H. 1997. FGF-2 is sufficient to isolate progenitors found in the adult mammalian spinal cord. *Experimental Neurology*, 148, 577-586.
- SHIN, L. & PETERSON, D. A. 2013. Human Mesenchymal Stem Cell Grafts Enhance Normal and Impaired Wound Healing by Recruiting Existing Endogenous Tissue Stem/Progenitor Cells. *Stem Cells Translational Medicine*, 2, 33-42.
- SHOOTER, R. A. & GEY, G. O. 1952. Studies of the mineral requirements of mammalian cells. *Br J Exp Pathol*, 33, 98-103.
- SI, Y. L., ZHAO, Y. L., HAO, H. J., FU, X. B. & HAN, W. D. 2011. MSCs: Biological characteristics, clinical applications and their outstanding concerns. *Ageing Research Reviews*, 10, 93-103.
- SIEGEL W, F. 2013. Fetal bovine serum the impact of geography *BioProcessing*, 12.

- SIMMONS, P. & TOROK-STORB, B. 1991. Identification of stromal cell precursors in human bone marrow by a novel monoclonal antibody, STRO-1. *Blood*, 78, 55-62.
- SIMOES, I. N., BOURA, J. S., DOS SANTOS, F., ANDRADE, P. Z., CARDOSO, C. M., GIMBLE, J. M., DA SILVA, C. L. & CABRAL, J. M. 2013. Human mesenchymal stem cells from the umbilical cord matrix: successful isolation and ex vivo expansion using serum-/xeno-free culture media. *Biotechnol J*, 8, 448-58.
- SINGER, N. G. & CAPLAN, A. I. 2011. Mesenchymal stem cells: mechanisms of inflammation. *Annu Rev Pathol*, 6, 457-78.
- SMITH, A. G., HEATH, J. K., DONALDSON, D. D., WONG, G. G., MOREAU, J., STAHL, M. & ROGERS, D. 1988. Inhibition of pluripotential embryonic stem cell differentiation by purified polypeptides. *Nature*, 336, 688-90.
- SONG, K. D., FAN, X. B., LIU, T. Q., MACEDO, H. M., JIANG, L. L., FANG, M. Y., SHI, F. X., MA, X. H. & CUI, Z. F. 2010. Simultaneous expansion and harvest of hematopoietic stem cells and mesenchymal stem cells derived from umbilical cord blood. *Journal of Materials Science-Materials in Medicine*, 21, 3183-3193.
- SQUATRITO, R. C., CONNOR, J. P. & BULLER, R. E. 1995. Comparison of a novel redox dye cell growth assay to the ATP bioluminescence assay. *Gynecol Oncol*, 58, 101-5.
- STEINERT, A. F., RACKWITZ, L., GILBERT, F., NOTH, U. & TUAN, R. S. 2012. Concise Review: The Clinical Application of Mesenchymal Stem Cells for Musculoskeletal Regeneration: Current Status and Perspectives. *Stem Cells Translational Medicine*, 1, 237-247.
- STEWART, A., GUAN, H. Y. & YANG, K. P. 2010. BMP-3 Promotes Mesenchymal Stem Cell Proliferation Through the TGF-beta/Activin Signaling Pathway. *Journal of Cellular Physiology*, 223, 658-666.
- STOLBERG, S. & MCCLOSKEY, K. E. 2009. Can Shear Stress Direct Stem Cell Fate? *Biotechnology Progress*, 25, 10-19.
- STUTE, N., HOLTZ, K., BUBENHEIM, M., LANGE, C., BLAKE, F. & ZANDER, A. R. 2004. Autologous serum for isolation and expansion of human mesenchymal stem cells for clinical use. *Experimental Hematology*, 32, 1212-1225.
- TAKAHASHI, K. & YAMANAKA, S. 2006. Induction of pluripotent stem cells from mouse embryonic and adult fibroblast cultures by defined factors. *Cell*, 126, 663-76.
- TANG, Y. L., ZHAO, Q., ZHANG, Y. C., CHENG, L., LIU, M., SHI, J., YANG, Y. Z., PAN, C., GE, J. & PHILLIPS, M. I. 2004. Autologous mesenchymal stem cell transplantation induce VEGF and neovascularization in ischemic myocardium. *Regulatory Peptides*, 117, 3-10.
- TEKKATTE, C., GUNASINGH, G. P., CHERIAN, K. M. & SANKARANARAYANAN, K. 2011. "Humanized" stem cell culture techniques: the animal serum controversy. *Stem Cells Int*, 2011, 504723.
- TEO, G. S., ANKRUM, J. A., MARTINELLI, R., BOETTO, S. E., SIMMS, K., SCIUTO, T. E., DVORAK, A. M., KARP, J. M. & CARMAN, C. V. 2012. Mesenchymal stem cells transmigrate between and directly through tumor necrosis factor-alpha-activated endothelial cells via both leukocyte-like and novel mechanisms. *Stem Cells*, 30, 2472-86.

- TORMIN, A., BRUNE, J. C., OLSSON, E., VALCICH, J., NEUMAN, U., OLOFSSON, T., JACOBSEN, S. E. & SCHEDING, S. 2009. Characterization of bone marrow-derived mesenchymal stromal cells (MSC) based on gene expression profiling of functionally defined MSC subsets. *Cytotherapy*, 11, 114-28.
- TORMIN, A., LI, O., BRUNE, J. C., WALSH, S., SCHUTZ, B., EHINGER, M., DITZEL, N., KASSEM, M. & SCHEDING, S. 2011a. CD146 expression on primary nonhematopoietic bone marrow stem cells is correlated with in situ localization. *Blood*, 117, 5067-77.
- TORMIN, A., LI, O., BRUNE, J. C., WALSH, S., SCHÜTZ, B., EHINGER, M., DITZEL, N., KASSEM, M. & SCHEDING, S. 2011b. CD146 expression on primary nonhematopoietic bone marrow stem cells is correlated with in situ localization. *Blood*, 117, 5067-5077.
- TORTELLI, F., TASSO, R., LOIACONO, F. & CANCEDDA, R. 2010. The development of tissue-engineered bone of different origin through endochondral and intramembranous ossification following the implantation of mesenchymal stem cells and osteoblasts in a murine model. *Biomaterials*, 31, 242-249.
- TSAI, C.-C., YEW, T.-L., YANG, D.-C., HUANG, W.-H. & HUNG, S.-C. 2012. Benefits of hypoxic culture on bone marrow multipotent stromal cells. *American Journal of Blood Research*, 2, 148-159.
- TSANG, W. P., SHU, Y. L., KWOK, P. L., ZHANG, F. J., LEE, K. K. H., TANG, M. K., LI, G., CHAN, K. M., CHAN, W. Y. & WAN, C. 2013. CD146(+) Human Umbilical Cord Perivascular Cells Maintain Stemness under Hypoxia and as a Cell Source for Skeletal Regeneration. *PLoS One*, 8.
- TSUJI, K., COX, K., GAMER, L., GRAF, D., ECONOMIDES, A. & ROSEN, V. 2010. Conditional deletion of BMP7 from the limb skeleton does not affect bone formation or fracture repair. *J Orthop Res*, 28, 384-9.
- TUMMALA, P., ARNSDORF, E. J. & JACOBS, C. R. 2010. The Role of Primary Cilia in Mesenchymal Stem Cell Differentiation: A Pivotal Switch in Guiding Lineage Commitment. *Cell Mol Bioeng*, 3, 207-212.
- UCCELLI, A., MORETTA, L. & PISTOIA, V. 2006. Immunoregulatory function of mesenchymal stem cells. *Eur J Immunol*, 36, 2566-73.
- VALORANI, M. G., MONTELATICI, E., GERMANI, A., BIDDLE, A., D'ALESSANDRO, D., STROLLO, R., PATRIZI, M. P., LAZZARI, L., NYE, E., OTTO, W. R., POZZILLI, P. & ALISON, M. R. 2012. Pre-culturing human adipose tissue mesenchymal stem cells under hypoxia increases their adipogenic and osteogenic differentiation potentials. *Cell Proliferation*, 45, 225-238.
- VAN DER STOK, J., KOOLEN, M. K., JAHR, H., KOPS, N., WAARSING, J. H., WEINANS, H. & VAN DER JAGT, O. P. 2014a. Chondrogenically differentiated mesenchymal stromal cell pellets stimulate endochondral bone regeneration in critical-sized bone defects. *Eur Cell Mater*, 27, 137-48; discussion 148.
- VAN DER STOK, J., KOOLEN, M. K. E., JAHR, H., KOPS, N., WAARSING, J. H., WEINANS, H. & VAN DER JAGT, O. P. 2014b. Chondrogenically Differentiated Mesenchymal Stromal Cell Pellets Stimulate Endochondral Bone Regeneration in Critical-Sized Bone Defects. *European Cells & Materials*, 27, 137-148.

- VAN DER VALK, J., BRUNNER, D., DE SMET, K., FEX SVENNINGSSEN, A., HONEGGER, P., KNUDSEN, L. E., LINDL, T., NORABERG, J., PRICE, A., SCARINO, M. L. & GSTRAUNTHALER, G. 2010. Optimization of chemically defined cell culture media--replacing fetal bovine serum in mammalian in vitro methods. *Toxicol In Vitro*, 24, 1053-63.
- VAN DER VALK, J., MELLOR, D., BRANDS, R., FISCHER, R., GRUBER, F., GSTRAUNTHALER, G., HELLEBREKERS, L., HYLLNER, J., JONKER, F. H., PRIETO, P., THALEN, M. & BAUMANS, V. 2004. The humane collection of fetal bovine serum and possibilities for serum-free cell and tissue culture. *Toxicol In Vitro*, 18, 1-12.
- VESTERGAARD, P., REINMARK, L. & MOSEKILDE, L. 2007. Increased mortality in patients with a hip fracture - Effect of pre-morbid conditions and post-fracture complications. *Journal of Bone and Mineral Research*, 22, S14-S14.
- VOYTIK-HARBIN, S. L., BRIGHTMAN, A. O., WAISNER, B., LAMAR, C. H. & BADYLAK, S. F. 1998. Application and evaluation of the alamarBlue assay for cell growth and survival of fibroblasts. *In Vitro Cell Dev Biol Anim*, 34, 239-46.
- WAGEGG, M., GABER, T., LOHANATHA, F. L., HAHNE, M., STREHL, C., FANGRADT, M., TRAN, C. L., SCHONBECK, K., HOFF, P., ODE, A., PERKA, C., DUDA, G. N. & BUTTGEREIT, F. 2012. Hypoxia Promotes Osteogenesis but Suppresses Adipogenesis of Human Mesenchymal Stromal Cells in a Hypoxia-Inducible Factor-1 Dependent Manner. *PLoS One*, 7.
- WAGNER, W., WEIN, F., SECKINGER, A., FRANKHAUSER, M., WIRKNER, U., KRAUSE, U., BLAKE, J., SCHWAGER, C., ECKSTEIN, V., ANSORGE, W. & HO, A. D. 2005. Comparative characteristics of mesenchymal stem cells from human bone marrow, adipose tissue, and umbilical cord blood. *Experimental Hematology*, 33, 1402-1416.
- WALENDA, G., HEMEDA, H., SCHNEIDER, R. K., MERKEL, R., HOFFMANN, B. & WAGNER, W. 2012. Human platelet lysate gel provides a novel three dimensional-matrix for enhanced culture expansion of mesenchymal stromal cells. *Tissue Eng Part C Methods*, 18, 924-34.
- WAN, M., LI, C., ZHEN, G., JIAO, K., HE, W., JIA, X., WANG, W., SHI, C., XING, Q., CHEN, Y.-F., JAN DE BEUR, S., YU, B. & CAO, X. 2012. Injury-Activated TGF $\beta$  Controls Mobilization of MSCs for Tissue Remodeling. *Stem cells (Dayton, Ohio)*, 30, 2498-2511.
- WANG, C.-J., CHEN, H.-S., CHEN, C.-E. & YANG, K. D. 2001. Treatment of Nonunions of Long Bone Fractures With Shock Waves. *Clinical Orthopaedics and Related Research*, 387, 95-101.
- WANG, Y., DENG, Y. & ZHOU, G.-Q. 2008. SDF-1 $\alpha$ /CXCR4-mediated migration of systemically transplanted bone marrow stromal cells towards ischemic brain lesion in a rat model. *Brain Research*, 1195, 104-112.
- WHITE, A. P., VACCARO, A. R., HALL, J. A., WHANG, P. G., FRIEL, B. C. & MCKEE, M. D. 2007. Clinical applications of BMP-7/OP-1 in fractures, nonunions and spinal fusion. *Int Orthop*, 31, 735-41.
- WILLIAMS, R. L., HILTON, D. J., PEASE, S., WILLSON, T. A., STEWART, C. L., GEARING, D. P., WAGNER, E. F., METCALF, D., NICOLA, N. A. & GOUGH, N. M. 1988. Myeloid leukaemia inhibitory factor maintains the developmental potential of embryonic stem cells. *Nature*, 336, 684-7.

- WU, C. C., LIU, F. L., SYTWU, H. K., TSAI, C. Y. & CHANG, D. M. 2016. CD146+ mesenchymal stem cells display greater therapeutic potential than CD146- cells for treating collagen-induced arthritis in mice. *Stem Cell Res Ther*, 7, 23.
- WU, X., SHI, W. & CAO, X. 2007. Multiplicity of BMP signaling in skeletal development. *Ann N Y Acad Sci*, 1116, 29-49.
- WUCHTER, P., VETTER, M., SAFFRICH, R., DIEHLMANN, A., BIEBACK, K., HO, A. D. & HORN, P. 2016. Evaluation of GMP-compliant culture media for in vitro expansion of human bone marrow mesenchymal stromal cells. *Experimental Hematology*, 44, 508-518.
- XU, N. R., LIU, H., QU, F., FAN, J., MAO, K. Z., YIN, Y., LIU, J. H., GENG, Z. Y. & WANG, Y. 2013. Hypoxia inhibits the differentiation of mesenchymal stem cells into osteoblasts by activation of Notch signaling. *Experimental and Molecular Pathology*, 94, 33-39.
- XU, Y., MALLADI, P., CHIOU, M., BEKERMAN, E., GIACCIA, A. J. & LONGAKER, M. T. 2007. In vitro expansion of adipose-derived adult stromal cells in hypoxia enhances early chondrogenesis. *Tissue Eng*, 13, 2981-93.
- YANG, D. C., YANG, M. H., TSAI, C. C., HUANG, T. F., CHEN, Y. H. & HUNG, S. C. 2011. Hypoxia Inhibits Osteogenesis in Human Mesenchymal Stem Cells through Direct Regulation of RUNX2 by TWIST. *PLoS One*, 6.
- YANG, S., PILGAARD, L., CHASE, L. G., BOUCHER, S., VEMURI, M. C., FINK, T. & ZACHAR, V. 2012a. Defined xenogeneic-free and hypoxic environment provides superior conditions for long-term expansion of human adipose-derived stem cells. *Tissue Eng Part C Methods*, 18, 593-602.
- YANG, T., CHEN, G. H., XUE, S. L., QIAO, M., LIU, H. W., TIAN, H., QIAO, S. M., CHEN, F., CHEN, Z. Z., SUN, A. N. & WU, D. P. 2012b. [Comparison of the biological characteristics of serum-free and fetal bovine serum-contained medium cultured umbilical cord-derived mesenchymal stem cells]. *Zhonghua Xue Ye Xue Za Zhi*, 33, 715-9.
- YANG, W., YANG, F., WANG, Y., BOTH, S. K. & JANSEN, J. A. 2013a. In vivo bone generation via the endochondral pathway on three-dimensional electrospun fibers. *Acta Biomater*, 9, 4505-12.
- YANG, Z. X., HAN, Z. B., JI, Y. R., WANG, Y. W., LIANG, L., CHI, Y., YANG, S. G., LI, L. N., LUO, W. F., LI, J. P., CHEN, D. D., DU, W. J., CAO, X. C., ZHUO, G. S., WANG, T. & HAN, Z. C. 2013b. CD106 identifies a subpopulation of mesenchymal stem cells with unique immunomodulatory properties. *PLoS One*, 8, e59354.
- YOSHIMURA, H., MUNETA, T., NIMURA, A., YOKOYAMA, A., KOGA, H. & SEKIYA, I. 2007. Comparison of rat mesenchymal stem cells derived from bone marrow, synovium, periosteum, adipose tissue, and muscle. *Cell Tissue Res*, 327, 449-62.
- YOUNG, S., PATEL, Z. S., KRETLOW, J. D., MURPHY, M. B., MOUNTZIARIS, P. M., BAGGETT, L. S., UEDA, H., TABATA, Y., JANSEN, J. A., WONG, M. & MIKOS, A. G. 2009. Dose effect of dual delivery of vascular endothelial growth factor and bone morphogenetic protein-2 on bone regeneration in a rat critical-size defect model. *Tissue Eng Part A*, 15, 2347-62.
- YU, X., CHEN, D., ZHANG, Y., WU, X., HUANG, Z., ZHOU, H., ZHANG, Y. & ZHANG, Z. 2012. Overexpression of CXCR4 in mesenchymal stem cells

### Appendix III

- promotes migration, neuroprotection and angiogenesis in a rat model of stroke. *Journal of the Neurological Sciences*, 316, 141-149.
- YUN, Z., MAECKER, H. L., JOHNSON, R. S. & GIACCIA, A. J. 2002. Inhibition of PPAR $\gamma$ 2 Gene Expression by the HIF-1-Regulated Gene DEC1/Stra13: A Mechanism for Regulation of Adipogenesis by Hypoxia. *Developmental Cell*, 2, 331-341.
- ZHANG, Y. E. 2009. Non-Smad pathways in TGF-beta signaling. *Cell Res*, 19, 128-39.
- ZHAO, L., WEIR, M. D. & XU, H. H. K. 2010. An injectable calcium phosphate-alginate hydrogel-umbilical cord mesenchymal stem cell paste for bone tissue engineering. *Biomaterials*, 31, 6502-6510.
- ZHOU, S. H., LECHPAMMER, S., GREENBERGER, J. S. & GLOWACKI, J. 2005. Hypoxia inhibition of adipocytogenesis in human bone marrow stromal cells requires transforming growth factor-beta/Smad3 signaling. *Journal of Biological Chemistry*, 280, 22688-22696.
- ZIMMERMANN, G. & MOGHADDAM, A. 2011. Allograft bone matrix versus synthetic bone graft substitutes. *Injury*, 42, Supplement 2, S16-S21.